Nicotinamide Mononucleotide Supplementation: A Potential Treatment of Vascular Cognitive Impairment and Dementia

PhD Thesis

Tamas Kiss, MD

Supervisor:
Zoltán Ungvári, MD, PhD

University of Szeged
University of Oklahoma Health Sciences Center

Szeged, 2020

PUBLICATIONS

I. **Nicotinamide Mononucleotide (NMN) Treatment Attenuates Oxidative Stress and Rescues Angiogenic Capacity in Aged Cerebromicrovascular Endothelial Cells: A Potential Mechanism for the Prevention of Vascular Cognitive Impairment;** Tamas Kiss, Priya Balasubramanian, Marta Noa Valcarcel-Ares, Stefano Tarantini, Andriy Yabluchanskiy, Tamas Csipo, Agnes Lipecz, Dora Reglodi, Xin A Zhang, Ferenc Bari, Eszter Farkas, Anna Csiszar, Zoltan Ungvari; *Geroscience, 41 (5): 619-630, Oct 2019*

II. **Nicotinamide Mononucleotide (NMN) Supplementation Rescues Cerebromicrovascular Endothelial Function and Neurovascular Coupling Responses and Improves Cognitive Function in Aged Mice;** Stefano Tarantini, Marta Noa Valcarcel-Ares, Peter Toth, Andriy Yabluchanskiy, Zsuzsanna Tucsek, Tamas Kiss, Peter Hertelendy, Michael Kinter, Praveen Ballabh, Zoltán Süle, Eszter Farkas, Joseph A Baur, David A Sinclair, Anna Csiszar, Zoltan Ungvari; *Redox Biology, 24: 101192, Jun 2019*

III. **Nicotinamide Mononucleotide (NMN) Supplementation Promotes Anti-Aging miRNA Expression Profile in the Aorta of Aged Mice, Predicting Epigenetic Rejuvenation and Anti-Atherogenic Effects;** Tamas Kiss, Cory B Giles, Stefano Tarantini, Andriy Yabluchanskiy, Priya Balasubramanian, Tripti Gautam, Tamas Csipo, Ádám Nyúl-Tóth, Agnes Lipecz, Csaba Szabo, Eszter Farkas, Jonathan D Wren, Anna Csiszar, Zoltan Ungvari; *Geroscience, 41 (4): 419-439, Aug 2019*

IV. **Nicotinamide Mononucleotide (NMN) Supplementation Promotes Neurovascular Rejuvenation in Aged Mice: Transcriptional Footprint of SIRT1 Activation, Mitochondrial Protection, Anti-Inflammatory, and Anti-Apoptotic Effects;** Tamas Kiss, Ádám Nyúl-Tóth, Priya Balasubramanian, Stefano Tarantini, Chetan Ahire, Andriy Yabluchanskiy, Tamas Csipo, Eszter Farkas, Jonathan D. Wren, Lori Garman, Anna Csiszar, Zoltan Ungvari; *Geroscience, 42 (2): 527-546, Feb 2020*

Table of Contents

ABBREVIATIONS

CBF	cerebral blood flow
CFSE	carboxyfluorescein diacetate succinimidyl ester
CM-H_2DCFDA	5(and 6)-chloromethyl-2′,7′-dichlorodihydrofluorescein diacetate-acetyl ester
CMVEC	cerebromicrovascular endothelial cells
ECIS	Electric Cell-substrate Impedance Sensing technology
GO	Gene Ontology
IRIDESCENT	Identification by in-Silico Construction of an Entity-based Network from Text
l-NAME	Nω-Nitro-l-arginine methyl ester
miRNA	microRNA
mtROS	mitochondrial production of reactive oxygen species
NAD^+	nicotinamide adenine dinucleotide
NMN	nicotinamide mononucleotide
NVC	neurovascular coupling
OCR	oxygen consumption rate
PCA	principle components analysis
ROS	reactive oxygen species
shRNA	short hairpin RNA
SIRT1	selective sirtuin 1
VCI	vascular cognitive impairment
VEGF	vascular endothelial growth factor

ABSTRACT

Vascular cognitive impairment (VCI) is a major cause of dementia among elderly individuals. Understanding molecular mechanisms behind vascular aging is essential to develop novel interventional strategies for the treatment and prevention of VCI. Recent studies have provided critical evidence that vascular aging is characterized by cellular NAD^+ depletion. In our studies we systematically investigated the effects of boosting cellular NAD^+ levels by the use of nicotinamide mononucleotide (NMN), an intermediate of NAD^+ metabolism. First, we conducted in vitro examination of cultured cerebromicrovascular endothelial cells (CMVEC) isolated from young and aged F344xBN rats. We have shown that NMN treatment attenuates oxidative stress and rescues angiogenic capacity in aged CMVEC. Next, in vivo aged C57BL/6 mice were treated daily with NMN for 14 days. NMN treatment rescued cognitive performance, motor function and neurovascular coupling in aged animals. To understand the fundamental gene regulation underlying the beneficial effects of NMN treatment, we generated a miRNA profile from the aorta and a gene expression profile from isolated brain endothelial cells. Bioinformatic analysis revealed that the effects of NMN treatment were mediated by the sirtuin pathway and induced gene expression changes associated with mitochondrial rejuvenation, anti-inflammatory and anti-apoptotic pathways.

INTRODUCTION

In recent years, it has been recognized that the health of the cerebral microcirculation is critical for the brain health during aging[1,2]. It is now known that aging is associated with structural and functional impairments of cerebral microvasculature which substantially contribute to the pathogenesis of age-related cognitive decline[3]. Vascular cognitive impairment and dementia is the second most common cause of dementia[4] and up to 75% of all patients with dementia have evidence of vascular pathology at autopsy[5]. Due to the rapidly aging population of Europe, it is increasingly important to explore potential drugs which could prevent or delay cognitive impairment and dementia in the elderly.

Maintenance of cerebral homeostasis requires a tightly controlled supply of oxygen and nutrients as well as washout of harmful metabolites. The brain has limited energy reserves and cerebral oxygen content, so the neuronal function can be sustained only for a short period of time if cerebral blood flow (CBF) decreases[6]. Both structural and functional impairment of the cerebromicrovasculature can damage the fine structure of the neuronal network causing deterioration of cognitive and motor performance in patients. The dynamic balance between angiogenesis and microvascular regression is critical for the maintenance of a healthy cerebral microcirculatory network. Previous studies showed that advanced aging is associated with a significant impairment of endothelial angiogenic processes[7] resulting in cerebromicrovascular rarefaction in the aged brain. Microvascular rarefaction contributes to a decline in cerebral blood flow compromising oxygen and nutrient delivery to the active neurons[8,9] and leading to the formation of ischemic foci, neuronal dysfunction and demyelination[10,11]. In addition to being essential for the structural integrity in the brain, complex spatial regulation of CBF is needed for a healthy brain. Intense neuronal activity requires rapid adjustment of regional oxygen and glucose delivery. This is provided by an evolutionarily conserved physiological mechanism known as neurovascular coupling (NVC). NVC is achieved through orchestrated, tightly controlled intercellular communication between activated neurons, astrocytes, vascular endothelial cells, pericytes and smooth muscle cells. Impairment of functional hyperemia (‘neurovascular uncoupling’) has been described in a wide spectrum of pathophysiologic conditions associated with aging, including hypertension, obesity, cognitive impairment and Alzheimer’s disease[12,13].

Nicotinamide adenine dinucleotide (NAD^+) acts as an important, rate-limiting coenzyme in multiple electron transfer reactions. NAD^+ is a donor of ADP-ribose moieties in ADP-ribosylation reactions, precursor of the second messenger molecule cyclic ADP-ribose, and substrate for the longevity assurance factor sirtuin enzymes[14]. Maintenance of NAD^+ level is critical for normal cellular proliferation and function, regulation of mitochondrial metabolism and cellular bioenergetics, adaptive stress responses, and normal activation of pro-survival, anti-aging pathways. With advanced age, there is decreased availability of cellular NAD^+[15,16], which has been proposed to be a critical driving force of aging processes. Aging-induced NAD^+ depletion has been suggested to contribute to a wide range of chronic diseases and pathological conditions associated with old age[17,18,2019], including endothelial dysfunction[20]. There is strong preclinical evidence that restoration of cellular NAD^+ levels in aged rodents by administration of NAD^+ precursors exerts potent anti-aging effects, reversing age-related organ dysfunction[21,22] and increasing mouse lifespan[23]. Nicotinamide mononucleotide (NMN) is an example of an intracellular NAD-boosting molecule, and is a precursor of NAD^+ biosynthesis. Cells take up NMN with great efficiency, however the underlying mechanism is unknown. Intracellularly, NMN is converted to NAD^+ through the NAD^+ salvage pathway by nicotinamide mononucleotide adenylyl transferase enzymes. Furthermore, NMN has great pharmacokinetics in humans giving it great therapeutic potential[24].

MicroRNAs (miRNA) are short, endogenous, non-coding transcripts that repress gene expression at post-transcriptional level in both physiological and pathological conditions. Strong evidence suggests that miRNAs have a role in regulation of lifespan in mammalian[25]. Importantly, miRNAs were also reported to regulate several important aspects of endothelial biology and vascular function[26,27]. Furthermore, several studies have demonstrated that age-related miRNA dysregulation contributes to the development of vascular aging phenotypes[2428,29]. Despite these advances, fundamental cellular and molecular processes of aging that are responsible for dysregulation of vascular miRNA expression have not been elucidated.

The present study was designed to test the hypothesis that restoration of cellular NAD^+ level with the supplementation of NMN can improve the health of cerebromicrovasculature in aging. Our hypothesis was tested in an array of in vitro and in vivo studies.

MATERIALS AND METHODS

Primary Cerebromicrovascular Endothelial Cell Cultures

We used Fischer 344 x Brown Norway (F344xBN) rats as a model of aging. In F344xBN rats the primary effects of aging can be studied without complications caused by age-related pathology[30]. 3 and 24-month-old, male F344xBN rats were obtained from the National Institute on Aging. The rats were housed in an environmentally controlled vivarium under pathogen-free conditions with unlimited access to food and water and a controlled photoperiod (12 hours light:12 hours dark). All experimental animals were maintained according to National Institutes of Health guidelines, and all animal use protocols were approved by the Institutional Animal Care and Use Committees of the participating institutions.

The animals were euthanized with CO_2. The brains were rapidly dissected to establish primary cerebromicrovascular endothelial cell (CMVEC) cultures[31,32]. Briefly, after the harvested tissue was mechanically and enzymatically dissociated the endothelial cell–enriched fraction was collected using an OptiPrep gradient solution (Axi-Shield, PoC, Norway) according to the manufacturer's guidelines. Next, the enriched fraction was incubated with anti-CD31/PE and anti-MCAM/FITC antibodies (BD Biosciences, San Jose, CA, USA). After washing, anti-FITC and anti-PE magnetic bead labeled secondary antibodies were used. Endothelial cells were collected using the MACS LD magnetic separation columns according to the manufacturer's guidelines (Milltenyi Biotech, Cambridge, MA, USA). The endothelial fraction was cultured on fibronectin coated plates in Endothelial Growth Medium (Cell Application, San Diego, CA, USA) with reduced nicotinamide concentration (11.04 μM) for 10 days.

Endothelial cells were phenotypically characterized by flow cytometry (Guava EasyCyte 8HT, Merck Millipore, Billerica, MA, USA) using antibodies against endothelial specific markers (anti-CD31-PE, anti-EPOR-APC, anti-VEGF/R2-PerCP, anti-ICAM-fluorescein, anti-CD146-PE). All antibodies were manufactured by R&D Systems (R&D Systems, Minneapolis, MN, USA).

Since the results of assays investigating mitochondrial reactive oxygen species, mitochondrial function and ATP concentration are affected by the number of viable cells, cell viability of each population was determined.

To assess the direct effects of NMN on endothelial mitochondrial function primary CMVECs derived from young and aged rats were treated with NMN in vitro in 5×10^{-4} mol/L concentration for 5 days.

Assessment of Angiogenic Processes in CMVECs

Cell Proliferation Assay: Cell proliferation capacity was assessed in CMVECs using the flow cytometry–based Guava CellGrowth assay (Guava Technologies, Hayward, CA, USA). Cells were collected, resuspended in PBS containing 0.1% BSA, and stained with 16 μmol/L carboxyfluorescein diacetate succinimidyl ester (CFSE) for 15 minutes at 37°C. This dye diffuses into cells and is cleaved by intracellular esterases to form an amine-reactive product that produces a detectable fluorescence and binds covalently to intracellular lysine residues and other amine sources. Upon cell division, CFSE divides equally into the daughter cells halving the CFSE concentration of the mother cell; therefore, there is an inverse correlation between the fluorescence intensity and the proliferation capacity of the cells. After incubation, unbound dye was quenched with serum-containing medium. Cells were washed three times and incubated for 24 hours with 100 ng/mL vascular endothelial growth factor (VEGF). Finally, cells were collected, washed, stained with propidium iodide (to gate out dead cells), and analyzed with a flow cytometer (Guava EasyCyte 8HT, Merck Millipore, Billerica, MA, USA).

Wound-healing and Cell Migration Assay: Electric Cell-substrate Impedance Sensing technology (ECIS, 96W1E) was used to monitor the migration of CMVECs in a wound-healing assay[33] (Applied BioPhysics, Troy, NY, USA). Briefly, CMVECs (2.5×105 cells/well) were seeded in 96-well array culture dishes and placed in an incubator (37°C), and changes in resistance and impedance were continuously monitored. When impedance reached a plateau, cells in each well were subjected to an elevated field pulse ("wounding") of 5 mA applied for 20 seconds at 100 kHz, which killed the cells present on the small active electrode due to severe electroporation. The detachment of the dead cells was immediately evident as a sudden drop in resistance (monitored at 4000 Hz) and a parallel increase in conductance. VEGF (100 ng/mL) was immediately added to each well. CMVECs surrounding the active electrode that had not been subjected to the wounding then migrated inward to replace the detached dead cells resulting in resistance recovery (continuously monitored at 4000 Hz for up to 24 hours). The time to reach 50% resistance recovery (corresponding to 50% confluence on the active electrode) was determined for cells in each

experimental group, and this parameter and the known physical dimensions of the electrode were used to calculate the migration rate (expressed as μm/h).

Tube Formation Assay: To assess tube formation, CMVECs were plated on Geltrex Reduced Growth Factor Basement Membrane Matrix in Medium 200PRF (Invitrogen, Carlsbad, CA, USA). Half of the aged control cells and NMN-treated aged cells were pre-treated with EX-527[34] (Active Motif, Carlsbad, CA, USA), a potent and selective sirtuin 1 (SIRT1) inhibitor (IC50 38 nM). 150μL/well of Geltrex was distributed in ice-cold 24-well plates. The gel was allowed to solidify while incubating the plates for 30 minutes at 37°C. CMVECs were then seeded at a density of 5×10^4 cells/well and placed in the incubator for 24 hours. Microscopic images were captured using a Nikon Eclipse Ti microscope. The extent of tube formation was quantified by measuring total tube length in five random fields per well using NIS-Elements microscope imaging software (Nikon Instruments, Melville, NY, USA). The mean of the total tube length per total area imaged (μm tube/mm^2) was calculated for each well. Experiments were run in quadruplicates.

Assessment of Cellular H_2O_2 Production in CMVECs

To assess cellular peroxide production, we used the cell-permeant oxidative fluorescent indicator dye CM-H_2DCFDA (5 (and 6)-chloromethyl-2′,7′-dichlorodihydrofluorescein diacetate-acetyl ester, Invitrogen, Carlsbad, CA, USA). Cells were washed with warm PBS and incubated with CM-H_2DCFDA (10 μM), at 37°C, for 30 minutes. CM-H_2DCFDA fluorescence was assessed by flow cytometry (Guava EasyCyte 8HT, Merck Millipore, Billerica, MA, USA).

SIRT1 and SIRT2 shRNA Transfection of CMVECs

To determine the role of sirtuin signaling in the endothelial effects of NMN treatment, the downregulation of SIRT1 and SIRT2, key anti-aging proteins whose activity is regulated by NAD^+ levels, in CMVECs was achieved by RNA interference using proprietary, tested SIRT1 and SIRT2 short hairpin RNA (shRNA) sequences (GeneCopoeia, Rockville, MD, USA). CMVECs were transfected using the electroporation-based Amaxa Nucleofector technology (Amaxa, Gaithersburg, MD, USA), as we have previously reported[35,36]. Experiments were performed on day 2 after the transfection.

Assessment of Mitochondrial Function in CMVECs

Mitochondrial ROS Production: To assess the effect of NMN treatment on age-related mitochondrial oxidative stress, mitochondrial production of reactive oxygen species (mtROS) in CMVECs was measured using MitoSOX Red (Thermo Fisher Scientific, Waltham, MA, USA), a mitochondrion-specific hydroethidine-derivative fluorescent dye[37,38]. In brief, cells were incubated with MitoSOX (5×10^{-6} mol/L) for 30 minutes, at 37°C, in the dark. The cells were then washed with PBS and MitoSOX fluorescence was measured by flow cytometry (Guava EasyCyte 8HT, Merck Millipore, Billerica, MA, USA).

Mitochondrial Membrane Potential: To elucidate the effects of NMN on mitochondrial membrane potential in CMVECs we used the mitochondrial membrane potential indicator fluorescent dye JC-1 (Guava Technologies, Hayward, CA, USA). JC-1 is a cationic carbocyanine dye that accumulates in energized mitochondria. When it is present in its monomer form in the mitochondria at low concentrations (low mitochondrial potential), the dye exhibits green fluorescence. When it accumulates in the energized mitochondria and forms J-aggregates at higher concentrations (high mitochondrial potential), it exhibits red fluorescence. A decrease in the aggregate red fluorescence and an increase in monomer green fluorescence is indicative of depolarization whereas an increase in the aggregate red fluorescence and a decrease in monomer green fluorescence is indicative of hyperpolarization. Cells were labeled with JC-1 for 30 minutes at 37 °C and fluorescence was analyzed with flow cytometry. The red/green fluorescence ratio was calculated as an indicator of mitochondrial membrane potential.

Mitochondrial Bioenergetics Assay: To substantiate the endothelium-protective effect of NMN, we performed real-time measurements of the oxygen consumption rate (OCR) as a marker of oxidative phosphorylation in young and aged CMVECs after treatment with NMN using a Seahorse XF96 extracellular flux analyzer (Agilent, Palo Alto, CA, USA). CMVECs were seeded into XF96 cell culture microplates in Seahorse XF-Assay media supplemented with 25 mM glucose and 1 mM sodium pyruvate (pH 7.4) the day before the assay. Plates were maintained for 45 minutes at 37 °C in 0% CO_2 prior to the measurement. Basal respiration, coupling efficiency, and spare respiratory capacity were compared using the Mito Stress Test Kit following the manufacturer's protocol. OCR was monitored before and after the addition of the electron transport inhibitors oligomycin (1.0 μM) and FCCP (1.0 μM), an ionophore that is a mobile ion carrier, and a mixture of antimycin-A (1.0 μM) (which is a complex III inhibitor) and rotenone (1.0 μM), a

mitochondrial inhibitor that prevents the transfer of electrons from the Fe–S center in complex I to ubiquinone. Basal respiration (baseline respiration minus antimycin-A post injection respiration), ATP synthesis coupled respiration (baseline respiration minus oligomycin post injection respiration), maximal respiratory capacity (FCCP stimulated respiration minus antimycin-A post injection respiration) and reserve respiratory capacity (FCCP stimulated respiration minus baseline respiration) were calculated. Sample protein content was used for normalization purposes[39].

Measurement of Cellular NO Release in CMVECs

To assess the effect of NMN treatment on age-related decline in NO release, in separate experiments the production of NO in CMVECs was measured using the fluorescent indicator DAF-FM (4-amino-5-methylamino- 2′,7′-difluorescein; Thermo Fisher Scientific, Waltham, MA, USA). After incubation with 5 μmol/L DAF-FM for 30 minutes at 37°C the cells were washed with PBS and the DAF-FM fluorescence was measured by flow cytometry (GUAVA 8HT, Merck Millipore, Billerica, MA, USA).

Measurement of Cellular ATP Levels in CMVECs

To correlate changes in OCR with directly to ATP production, we also measured cellular ATP concentration in CMVECs. ATP levels in endothelial cells were assessed using the ENLITEN ATP bioluminescent assay (Promega, Madison, WI, USA). First, CMVECs were seeded in 96-well plates. For ATP determination the cells were homogenized in Passive Lysis Buffer (Promega, Madison, WI, USA). The samples were diluted 1:10 and mixed with an equal volume of the luciferase reagent. The plates were incubated at room temperature for 10 min and the luminescence signal was detected with a Tecan Infinite M200 plate reader. ATP quantification was carried out from a standard curve using ATP disodium salt hydrate. BCA protein determination was performed for normalization purposes. Cell viability in each population was determined by flow cytometry (Guava EasyCyte 8HT, Merck Millipore, Billerica, MA, USA) to ensure similar viability of CMVECs in each group in a parallel experiment using the ViaCount Assay (Guava Technologies, Hayward, CA, USA).

In vivo Animal Model

Young (3 months) and aged (24 months) male C57BL/6 mice were obtained from the aging colony maintained by the National Institute on Aging at Charles River Laboratories (Wilmington, MA, USA). The biological age of 24 month old mice corresponds to that of ~ 70-year old humans[40]. Animals were housed under specific pathogen-free barrier conditions in the Rodent Barrier Facility at University of Oklahoma Health Sciences Center under a controlled photoperiod (12-12 hours light/dark) with unlimited access to water and were fed a standard AIN-93G diet (ad libitum). Mice in the aged cohort were assigned to two groups. One group of the aged mice was injected daily with NMN (i.p. injections of 500 mg NMN/kg body weight per day) or the equivalent volume of PBS for 14 consecutive days at 6 PM and 8 AM. On day 14 animals were sacrificed 4 hours after last injection. Similar dosages of NMN have been shown to exert potent anti-aging effects on mouse health span[19]. All procedures were approved by the Institutional Animal Use and Care Committees of the University of Oklahoma Health Sciences Center.

To confirm efficiency of NMN treatment, NAD^+ levels were measured in snap frozen aortas from young and aged mice using a bioluminescent assay (NAD/NADH-Glo Assay; Promega, Madison, WI, USA), according to the manufacturer's instructions.

Animal Behavior Testing

Radial arms water maze test: Spatial learning and memory in each group of mice were tested by the radial arms water maze test[41,42]. The maze consisted of eight, 9 cm wide arms that radiated out from an open central area. Paint was added into the water to make it opaque. At the end of one arm there was a submerged escape platform. The maze was surrounded by privacy blinds and intra- and extra-maze clues were provided to help the animals during the experiment. The mice were monitored by a video tracking system from above the maze and parameters were measured using Ethovision software (Noldus Information Technology, Leesburg, VA, USA). During the learning period mice were given the opportunity to learn the location of the submerged platform during two sessions each consisting of four consecutive acquisition trials. On each trial, the mouse was started in one arm not containing the platform and allowed to wade for up to one minute to find the escape platform. All mice spent 30 seconds on the platform following each trial before beginning the next trial. The platform was located in the same arm on each trial. Over the three days of training, mice in the young control group gradually improved performance as they

learned the procedural aspects of the task. Upon entering an incorrect arm (all four paws within the distal half of the arm) or failing to select an arm after 15 seconds the mouse was charged an error. Learning capability was assessed by comparing performance on days 2 and 3 of the learning period.

Elevated plus maze, learning protocol: Mice were also assessed for learning capacity using an elevated plus maze-based learning protocol[43]. Two open arms (25 × 5 cm) and two (25 × 5 cm) closed arms were attached at right angles to a central platform (5 × 5 cm). The apparatus was 40 cm above the floor. Mice were placed individually at the end of an open arm. The time for mice to cross a line halfway along one of the closed arms was measured (transfer latency) on day 1 and day 2. Mice had to have their body and each paw on the other side of the line. If a mouse had not crossed the line after 120 seconds, it was placed beyond it. Learning was defined as reduced transfer latency on day 2 compared to day 1. Higher relative difference in transfer latency on day 1 and day 2 indicates superior hippocampal function.

Novel object recognition test: The novel object recognition task was also performed to characterize the effect of NMN on learning and memory[44,45]. The test consists of a habituation phase, acquisition (familiarization) phase and trial phase. During the habituation phase the animals explored the empty open-field arena for 5 minutes. Then, in the acquisition phase the mice explore two identical objects for 2 minutes. After a 4 hours delay, a trial phase occurred. During this period animals explored the familiar object and a novel object for 2 minutes. Exploration of the objects was defined as directing the nose at a distance less than 2 cm to the object. For data collection and analysis Ethovision software (Noldus Information Technology, Leesburg, VA, USA) was used. A percent of time spent exploring the novel object relative to the total time spent exploring both objects was used as a measure of novel object recognition. The Recognition Index (RI, representing the time spent investigating the novel object $Tnovel$ relative to the total object investigation) was used as the main index of retention, which was calculated according to the following formula: $RI = \frac{Tnovel}{Tnovel + Tfamiliar}$.

Rotarod performance: Motor coordination was assessed in each group of mice by using an automated four-lane rotarod device (Columbus Instruments, Columbus, OH, USA)[44]. Mice were pre-trained by placing them on the moving rotarod at 10 rounds per minute (rpm) until they performed at this speed for 120 seconds. The test phase consisted of 3 trials. The testing apparatus was set to accelerate from 4 to 40 rpm in 300 seconds. One mouse was then placed on each lane.

The rotational velocity was set to increase every 10 seconds and the latency to fall was recorded. Latency to fall was recorded in by an infrared beam across the fall path along with the max rpm sustained by each mouse[46].

Grip strength test: Maximal muscle strength of forelimbs of the mice[44] were measured by a grip strength meter (Ametek, Brooklyn, NY, USA). The strength measurements of each group of mice were repeated three times by the same investigator. The maximum grip strength values were used for subsequent analysis.

Analysis of gait function: To determine how aging and NMN treatment affect gait coordination, we tested the animals using an automated computer assisted method (CatWalk; Noldus Information Technology, Leesburg, VA) as described[41,42]. Using the CatWalk system, the detection of paw print size, pressure and pattern during volunteer running on an illuminated glass walkway by a camera placed under the glass surface provides an automated analysis of gait function and the spatial and temporal aspects of interlimb coordinationp[44]. Animals were tested in three consecutive runs. Data were averaged across ten runs in which the animal maintained a constant speed across the walkway. After labeling of each footprint, spatial and temporal indices of gait were calculated.

Assessment of Neurovascular Coupling

After behavioral testing the neurovascular coupling of 5 to 8 animals from each group animal was assessed[12]. Animals were anesthetized with isoflurane (4% induction and 1% maintenance), endotracheally intubated and ventilated (MousVent G500; Kent Scientific Co, Torrington, CT, USA). A thermostatic heating pad (Kent Scientific Co, Torrington, CT, USA) was used to maintain body temperature. Arterial blood pressure was measured via femoral artery catheter (Living Systems Instrumentations, Burlington, VT, USA). Mice were placed on a stereotaxic frame (Leica Microsystems, Buffalo Grove, IL, USA) and were equipped with an open cranial window. Changes in CBF were assessed above the left barrel cortex using a laser Doppler probe (Transonic Systems, Ithaca, NY, USA). The cranial window was filled with artificial cerebrospinal fluid. The right whisker pad was stimulated by a bipolar stimulating electrode. The stimulation protocol used to investigate neurovascular coupling consisted of 10 stimulation presentation trials with an intertrial interval of 70 seconds, each delivering a 30 second train of electrical pulses (2 Hz, 0.2 mA, intensity, and 0.3 milliseconds pulse width) to the mystacial pad.

Changes in CBF were expressed as percent increase from the baseline value. To assess the role of NO mediation, CBF responses to whisker stimulation were repeated in the presence of the nitric oxide synthase inhibitor Nω-Nitro-l-arginine methyl ester (l-NAME; 3×10^{-4} mol/L, 20 min). To assess microvascular endothelial function, CBF responses to topical administration of acetylcholine (ACh; 10−5 mol/L) were obtained before and after topical administration of the mitochondrial antioxidant mitoTEMPO (10−5 mol/L). Cortex and aorta of these animals were harvested for the following experiments.

Assessment of Oxidative Stress in the Cortex

To characterize the effect of NMN treatment on cellular redox homeostasis in aging, 3-nitrotyrosine, a marker for peroxynitrite activity, was assessed in homogenates of cortical samples using OxiSelect Protein Nitrotyrosine ELISA Kits (Cell Biolabs, San Diego, CA, USA), according to the manufacturer's guidelines[31]. In the microcirculation of aged rodents' endothelium-derived NO was shown to react with O_2^- forming $ONOO^-$ thus decreasing the bioavailability of NO[47].

Endothelial Function in the Aorta

To assess the specific effect of NMN treatment on endothelial function we used isolated aorta rings[48]. Aortas were cut into ring segments 1.5 mm in length and mounted in myographs chambers (Danish Myo Technology A/S, Denmark) for measurement of isometric tension. The vessels were superfused with Krebs buffer solution. After an equilibration period of 1 hour during which an optimal passive tension was applied to the rings (as determined from the vascular length-tension relationship), they were pre-contracted with 10^{-6} M phenylephrine and relaxation in response to acetylcholine was measured.

Quantitative Real-time RT-PCR and miRNA Expression Profiling

A quantitative real time RT-PCR technique was used to analyze miRNA expression profiles in the aortas of mice from each experimental group[32,49]. Total RNA was isolated with a mirVana™ miRNA Isolation Kit (Thermo Fisher Scientific, Waltham, MA, USA) and was reverse transcribed using TaqMan® MicroRNA Reverse Transcription Kit[32,49]. The expression profile of mouse miRNAs in aortas was analyzed using the TaqMan Array Rodent MicroRNA A+B Cards Set v3.0 (Thermo Fisher Scientific, Waltham, MA, USA). The qPCR data were quantified using

the ΔΔCt method[50]. Predicted and experimentally validated microRNA targets were obtained from the TargetScan database[51], and Gene Ontology enrichment analysis was performed on differentially expressed microRNA targets using Fisher's exact test between TargetScan targets and annotations from the Gene Ontology database[52]. To identify relationships between miRNA targets and terms in the biomedical literature, we utilized the Implicit Relationship IDEntification by in-Silico Construction of an Entity-based Network from Text (IRIDESCENT) system[53]. IRIDESCENT processes all available MEDLINE abstracts and uses a unique statistical model to determine whether each upstream regulator co-occurs with a term of interest more frequently than would be expected by chance, and quantifies this in terms of the mutual information measure.

mRNA-sequencing of Isolated CMVECs

Animals from a separate cohort were killed and transcardially perfused with PBS. From the mechanically and enzymatically dissociated tissue the endothelial cell–enriched fraction was collected using an OptiPrep gradient solution (Axi-Shield, PoC, Norway) according to the manufacturer's guidelines. The neurovascular unit–enriched fraction was incubated with anti-CD31/PE and anti-MCAM/FITC antibodies (BD Biosciences, San Jose, CA, USA). After washing, the cells twice with MACS Buffer (Milltenyi Biotech, Cambridge, MA, USA) anti-FITC and anti-PE magnetic bead labeled secondary antibodies were used. The endothelial/neurovascular (endothelial cells with attached astrocytes and pericytes were collected) enriched fraction was collected by magnetic separation using the MACS LD magnetic separation columns (Milltenyi Biotech, Cambridge, MA, USA).

RNA isolation and next generation sequencing: RNA was isolated from the samples using AllPrep DNA/RNA Mini Kit (QIAGEN, Venlo, Netherlands)[54]. RNA quantity and quality were measured using the RNA 6000 Nano Assay with an Agilent 2100 Bioanalyzer (Agilent, Palo Alto, CA, USA). Using 1μg RNA, cDNA was synthesized from purified RNA using ABI High-capacity cDNA Reverse Transcription Kit (Applied Biosystems, Foster City, CA, USA). Library construction was performed in a stranded manner. The mature mRNA was enriched via pull down by beads coated with oligo-dT homopolymers. The mRNA molecules were then chemically fragmented, and the first strand of cDNA was generated using random primers. Following RNase digestion, the second strand of cDNA was generated, replacing dTTP in the reaction mix with dUTP. Double stranded cDNA then underwent adenylation of 3′ends following ligation of Illumina

adapter sequences. Subsequent PCR enrichment of ligated products was further selected for those strands not incorporating dUTP, leading to strand-specific sequencing libraries. Final libraries for each sample were assayed on the Agilent Tapestation for size and quantity. Libraries were then pooled in equimolar amounts as ascertained via fluorometric analyses. Final pools were absolutely quantified using qPCR on a Roche LightCycler 480 instrument with Kapa Biosystems Illumina Library Quantification reagents. Sequencing was performed on an Illumina NovaSeq 6000 instrument with paired-end 50 base pairs reads.

Data Analysis: Raw sequencing reads were trimmed of their Illumina TruSeq adapter sequences using Trimmomatic v0.35[55] then aligned to the mouse genome version GRCm38 using Kallisto v0.43.03[56]. Samples were checked for outliers and separation by principle components analysis (PCA) with the R function prcomp. Raw expression counts were summarized at the gene level to transcript-length adjusted, library-size scaled counts per million with the R package tximport[57]. Differential expression analysis was performed using the empirical Bayes approach implemented in the R/Bioconductor package DESeq2[58]. Genes were considered differentially expressed if the absolute value of the fold-change ≥ 1.5 and the False Discovery Rate p-value adjusted ≤ 0.05.

The org.Mm.eg.db v3.8.2 R/Bioconductor package was used to collect Gene Ontology (GO) terms associated with differentially expressed genes. The hypergeometric test implemented in GOstats v2.51.0. R/Bioconductor package was used to calculate enrichment of the GO terms[59].

We used the Upstream Regulator Analysis[60] algorithm in the Ingenuity Pathway Analysis (QIAGEN, Venlo, Netherlands) software to find upstream regulators that potentially explain the observed gene expression changes in our samples. The IPA software uses a manually curated database (Ingenuity Knowledge Base) to calculate enrichment score (Fisher's exact test p value), measures the overlap of observed and predicted regulated gene sets, and a z-score assessing the match of observed and predicted up/downregulation patterns.

RESULTS

NMN Supplementation Rescue Angiogenic Processes

Proliferation represents a key step in angiogenesis. The proliferative capacity of young and aged CMVECs was compared after incubation with VEGF for 24 hours. We found that CFSE fluorescence measured by flow cytometry was significantly increased in aged CMVECs as compared with young CMVECs, indicating that proliferation capacity is impaired by aging. NMN treatment rescued the proliferative capacity of aged CMVECs (Fig. 1A).

The migratory capability of vascular endothelial cells has a pivotal role in the maintenance of microvascular integrity and angiogenesis. An ECIS-based wound-healing assay was used to assess the effect of NMN treatment on the migratory capability of CMVECs. We found that aged CMVECs exhibited impaired migratory capability compared to young CMVECs. In contrast, the migration rate of aged CMVECs with NMN treatment did not differ significantly from that of young CMVECs (Fig. 1B).

When seeded onto Geltrex matrices, young CMVECs form elaborated capillary networks[32,49]. Compared with young cells, formation of capillary-like structures in aged CMVECs was significantly impaired. However, treatment with NMN significantly improved formation of capillary-like structures in aged CMVECs. This finding suggests that age-related NAD^+ deficiency is causally linked to the impaired angiogenic capacity of aged endothelial cells. We found that pharmacological inhibition of SIRT1 significantly inhibited the formation of capillary-like structures in NMN-treated aged CMVECs (Fig. 1D-H).

Age-related oxidative stress has been implicated in endothelial angiogenic dysfunction. ROS production in young and aged CMVECs was compared by assessing CM-H_2DCFDA fluorescence. We found that CM-H_2DCFDA fluorescence was significantly increased in aged CMVECs compared to young CMVECs, consistent with the view that endothelial cells in the aged cerebral microcirculation exhibit increased oxidative stress. NMN treatment resulted in dramatic attenuation of H_2O_2 production in aged CMVECs (Fig. 1C).

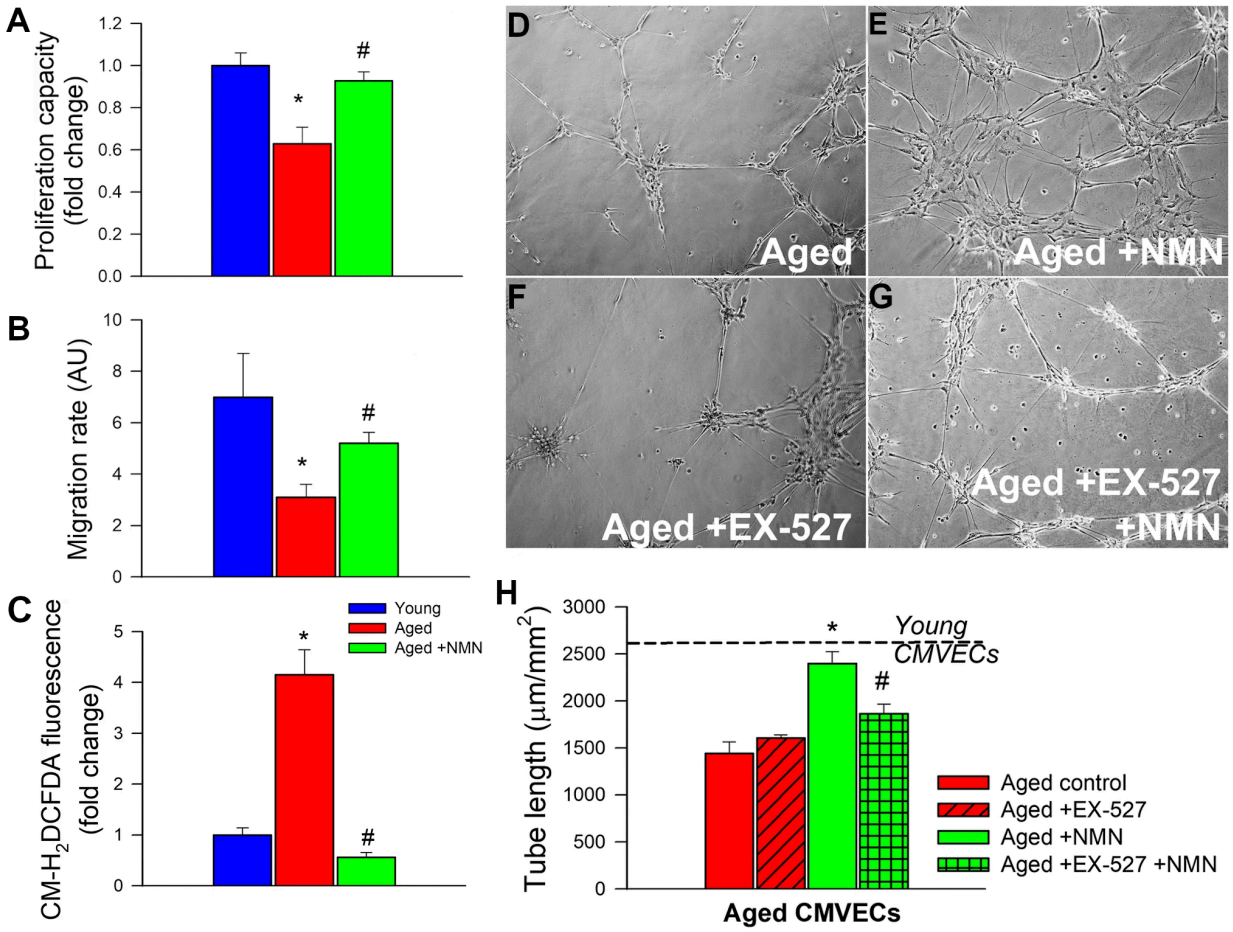

Figure 1: NMN supplementation rescue angiogenic capacity and attenuates oxidative stress in aged CMVECs: **A)** Cell proliferation capacity was assessed in primary CMVECs stimulated with VEGF (100 ng/mL) using the flow cytometry–based Guava CellGrowth assay. NMN treatment significantly increased proliferation capacity of aged CMVECs. **B)** VEGF (100 ng/mL)-stimulated cell migration was monitored by electric cell-substrate impedance sensing (ECIS) technology in a wound-healing assay. NMN treatment significantly increased migration capacity of aged CMVECs. **C)** Cellular peroxide production was assessed by measuring CM-H_2DCFDA fluorescence using EasyCyte 8HT flow cytometer. NMN treatment significantly attenuated oxidative stress in aged CMVECs. **D-H)** CMVECs were plated on Geltrex matrix–coated wells, and tube formation was induced by treating cells with VEGF (100 ng/mL, for 24 h). Representative examples of capillary-like structures are shown on panels D, E, F, G. Summary data, expressed as total tube length per total area scanned (μm tube/mm^2), are shown in panel H. NMN treatment significantly improved the tube formation ability of aged CMVECs.

Data are plotted as means ± S.E.M.; N = 6 in each group; *p < 0.05 vs. control, #p < 0.05 vs. aged; one-way ANOVA with post-hoc Tukey's test.

Effects of NMN Supplementation on the Mitochondrial Function of Endothelial Cells

To substantiate the endothelial protective effects of NMN in vitro, we assessed the effects of NMN on mtROS production in CMVECs derived from aged animals using the MitoSOX fluorescence method. First, we demonstrated that NAD^+ content in aged CMVECs was significantly decreased, whereas it was normalized by treatment with NMN (Fig. 2A). We found that in aged CMVECs mtROS production was significantly increased as compared to that in CMVECs derived from young animals (Fig. 2B and C). This increased mtROS production was associated with a decreased production of NO assessed by DAF fluorescence (Fig. 2D), as well as impaired mitochondrial membrane potential (Fig. 2E), and decreased ATP levels (Fig. 2F). NMN treatment attenuated mtROS generation (Fig. 2B and C), increased NO production (Fig. 2D), rescued mitochondrial membrane potential (Fig. 2E) and restored cellular ATP content (Fig. 2E) in aged CMVECs, eliminating the difference between young vs. aged cells. Attenuation of mtROS production in NMN-treated aged CMVECs was associated with significant improvement in both basal and maximal mitochondrial respiration (Fig. 2G–H) measured by the Seahorse instrument. Combined shRNA knockdown of SIRT1/SIRT2 prevented the beneficial effects of NMN on mtROS (Fig. 2C), NO production (Fig. 2D), mitochondrial membrane potential (Fig. 2E) and mitochondrial respiration (Fig. 2H) in aged CMVECs.

It is possible that mitochondrial protective effects of NMN are linked to promotion of mitochondrial biogenesis. However, we excluded this possibility by using electron microscopy and unbiased morphometric methods to assess mitochondrial morphology. We found that total mitochondrial volume and mitochondrial density in cerebromicrovascular endothelial cells were unaffected by NMN treatment. NMN treatment of aged mice also does not affect mitochondrial DNA content in cerebral arteries. Results obtained from cultured CMVECs showed unaltered mtDNA content after NMN treatment, thus extending the in vivo data. (methods and results are detailed in our original publication[II])

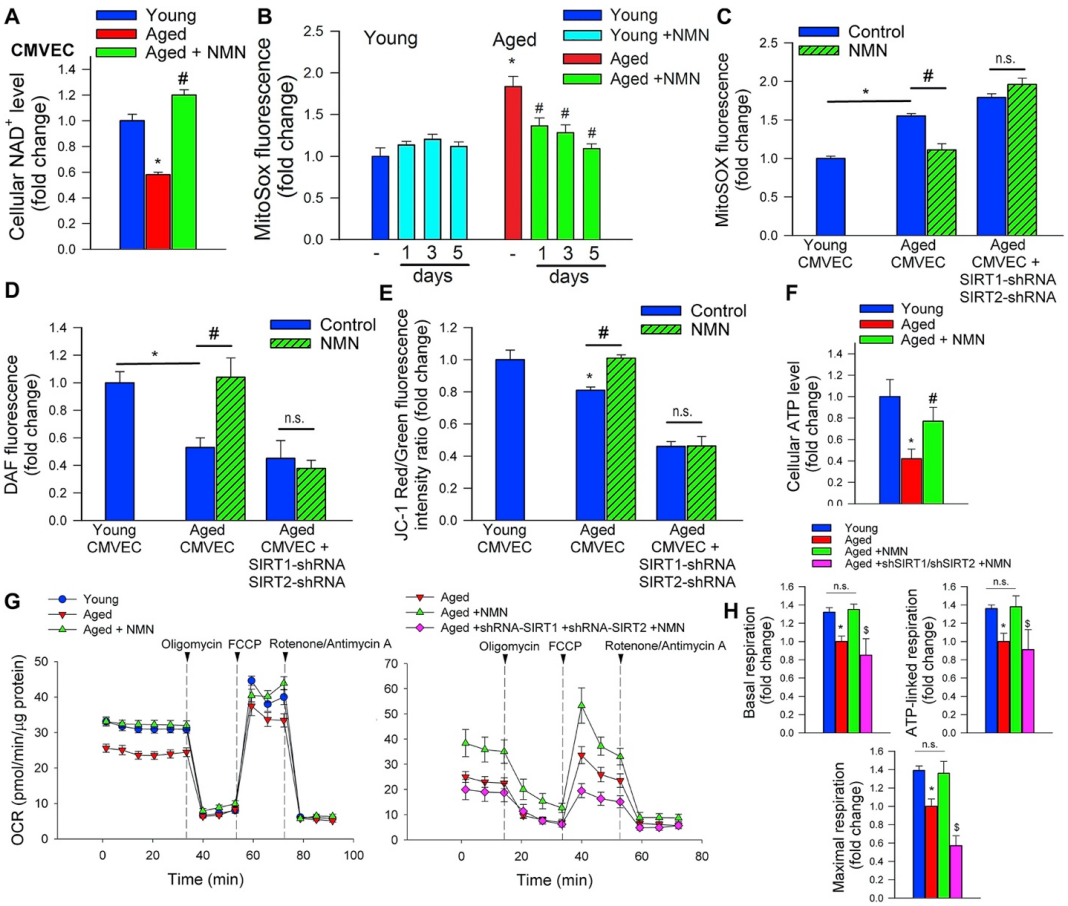

Figure 2: Treatment with NMN improved mitochondrial energetics and attenuated mitochondrial ROS production in CMVECs: A) Treatment with NMN restored NAD^+ levels in primary CMVECs derived from aged rats. **B)** Treatment with NMN attenuated age-related increases in mtROS production in CMVECs (MitoSOX, assessed by flow cytometry). **C)** shRNA knockdown of SIRT1/SIRT2 prevented NMN-induced attenuation of mtROS in aged CMVECs. **D)** NMN treatment rescued cellular NO production (DAF, assessed by flow cytometry) **E)** NMN treatment increased mitochondrial membrane potential (JC-1, assessed by flow cytometry). shRNA knockdown prevented the NMN effect. **F)** Treatment of aged CMVECs with NMN restored cellular ATP levels. **G)** Attenuation of mtROS production and improved mitochondrial membrane potential in NMN treated aged CMVECs were associated with improvement in OCR. OCR in untreated young and aged CMVECs is shown for reference. Marked NMN-induced increase in both basal and maximal respiration was seen in aged CMVECs. Right panel shows the effects of shRNA knockdown on NMN-induced changes in OCR in aged CMVECs. OCR in aged CMVECs transfected with scrambled shRNA is shown for reference. **H)** Summary data showing the effects of aging and NMN on basal respiration, ATP-linked respiration and maximal respiration.

Data are plotted as mean ± S.E.M.; N = 9 for each data point; *p < 0.05 vs. young; #p < 0.05 vs. aged. $p < 0.05 vs. aged + NMN; one-way ANOVA with post-hoc Tukey's test.

NMN Supplementation Improves Cognitive and Motor Performance in Aged Animals

Radial arm water maze test: To determine how rescue of cerebromicrovascular function by NMN supplementation impacts cognitive performance in aged mice, animals were tested in the radial arms water maze. We compared the learning performance of mice in each experimental group by analyzing the day-to-day changes in the combined error rate, working memory errors, successful escape rate, path length and time latency. During acquisition, mice from all groups showed a decrease in the combined error rate across days, indicating learning of the task. After the first day of learning, young mice consistently had lower combined error rates than aged mice. Decrease in the combined error rate induced by NMN supplementation in aged mice reached statistical significance by trial block 6. (Fig. 3A and B) To analyze working memory function (short-term memory that is involved in immediate conscious perception) we examined re-entries into incorrect arms (without hidden platform) that were previously attempted for escape during the trial. We found that working memory function was impaired in aged mice as compared to young controls. Aged mice supplemented with NMN supplementation showed significant restoration of working memory to levels comparable to young animals (Fig. 3C). Successful escape rate from the maze was assessed by measuring the percent of animals that could find the hidden platform within the 60 seconds allowed for each trial. During acquisition, mice from all groups showed an increase in successful escape rate consistent with the learning of the task. Young mice exhibited significantly better escape success than untreated aged mice. Although in aged mice NMN treatment tended to increase the successful escape rate, the differences did not reach statistical significance (Fig. 3D). We also compared path length and escape latency. During acquisition, mice from all groups displayed shorter path length (Fig. 3E) and lower escape latencies (Fig. 3F), indicating spatial learning. Young mice exhibited shorter path length and lower escape latency than untreated aged mice, differences which became pronounced by day 3. NMN supplementation did not significantly affect either path length or escape latencies. Analyses of noncognitive parameters revealed a slight age-related decline in swimming speed (Fig. 3G) and an age-dependent increase in non-exploratory behavior (Fig. 3H), which were partially rescued by NMN treatment.

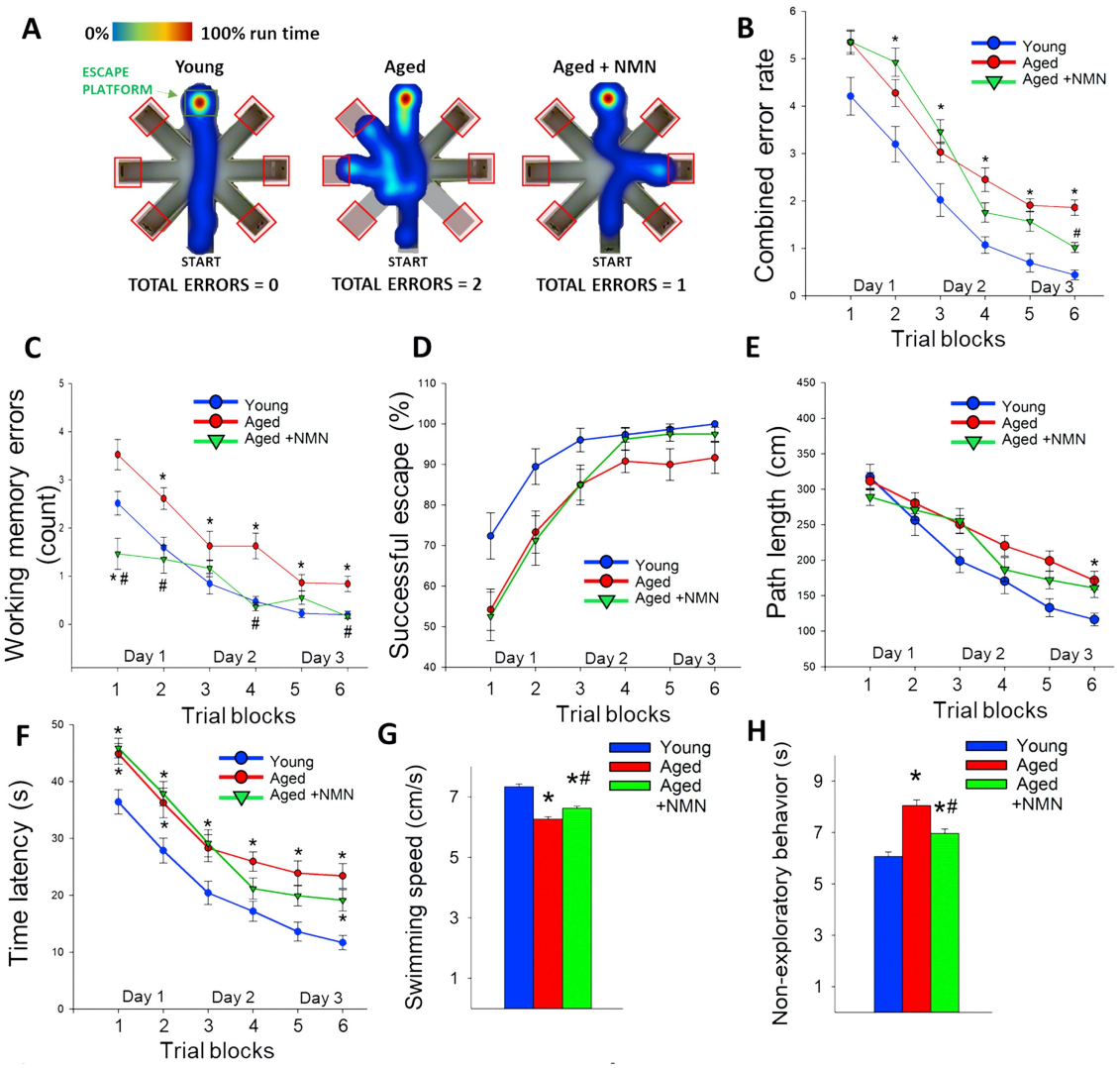

Figure 3: A) Heatmap represents the percentage of time spent in different locations in the maze for a randomly selected animal from each group during experimental day 3. **B)** Older animals had higher combined error rates through day 2 and 3 of the learning phase. **C)** NMN treated animals made fewer working memory errors as compared to aged, untreated animals. **D)** The ratio of successful escapes, averaged across trial blocks, is shown for each group. **E)** Shown are average path length and **(F)** escape latencies required to reach the hidden platform in the RAWM for trial blocks. Young mice found the hidden platform significantly sooner while swimming less than aged animals. In aged mice treated with NMN the escape latencies and the average path length required to reach the hidden platform did not differ from those in aged mice. **G)** NMN had only marginal effect on the swimming speed. **H)** Aged control mice exhibited longer non-exploratory behavior compared to young mice. Treatment with NMN partially reduced the non-exploratory time to young levels.

Data are plotted as mean ± S.E.M.; N = 20 in each group; *p < 0.05 vs. young; #p < 0.05 vs. aged; one-way ANOVA with Tukey's post-hoc test.

Elevated plus maze, learning protocol: We also evaluated hippocampal-dependent learning and memory by employing the elevated plus-maze. For young mice, transfer latency on day 2 was significantly decreased (by ~49%) compared to day 1, indicating intact learning processes. In contrast, for aged mice the transfer latency on day 1 and day 2 were similar, indicating impaired learning capability. NMN supplementation in aged mice restored learning performance (Fig. 4A).

Novel Object Recognition Test: Subsequently we tested the performance of mice in the novel object recognition test. We found no significant difference in the time that mice from each group spent exploring the two identical objects placed at the opposite ends of the arena during the acquisition phase, confirming that the location of the objects did not affect the exploratory behavior of mice. In the trial phase with two different objects (one novel, the other familiar), young mice explored the novel object for a significantly longer time period than aged mice, indicating that they remember the familiar object. In contrast, aged mice had a significantly lower calculated Recognition Index (RI). NMN supplementation in aged mice significantly improved their performance, which is consistent with improved hippocampal- and cortical-dependent recognition memory (Fig. 4B).

Rotarod: To investigate the effects of age and NMN treatment on motor performance we performed accelerating rotarod and grip strength measurements which evaluate muscle strength, balance, and endurance. NMN supplementation did not significantly affect age-related decreases in latency to fall from the rotarod (Fig. 4C) and did not reverse age-related decline in grip strength.

Gait Performance: Age-related deficiencies in NVC responses in human patients[61] and animal models of aging[42] have been linked to gait abnormalities. Recent studies also demonstrate that pharmacologically-induced neurovascular uncoupling associates with subclinical gait alterations in mice[62]. To identify age- and treatment-related systematic differences between mouse gait patterns, principal component analysis (PCA) was carried out on the correlation matrix of spatial and temporal indices of gait. This analysis identified three principal components that accounted for ~63% of the variance in the data. We plotted the position of each mouse against the PC1, PC2, and PC3 axis in three-dimensional space (Fig. 4D). The most conspicuous trend was that aged and young mice were well separated along the PC1 axis, whereas NMN treated aged mice were clustered together with young mice. Collectively, the aforementioned results support the view that rescue of NVC by NMN treatment is associated with improved gait performance in aged mice.

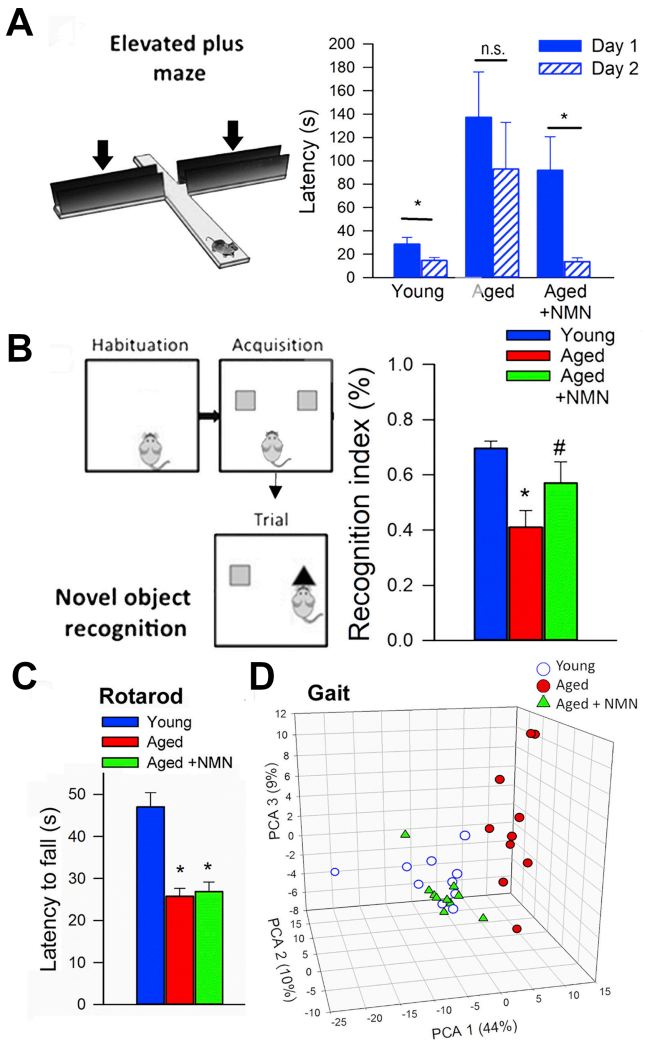

Figure. 4: NMN treatment improved cognitive performance in aged mice: A) NMN treatment improved learning ability in aged mice, as assessed using the elevated plus maze-based learning protocol. For young mice, transfer latency on day 2 was significantly decreased compared to day 1, indicating an intact learning effect. For aged mice the transfer latency on day 1 and day 2 were similar, indicating impaired learning capability. NMN supplementation in aged mice restored learning performance to that in young mice. **B)** NMN treatment restored recognition memory in aged mice as measured by the novel object recognition test. Recognition memory is expressed as a recognition index which is defined as the ratio of time spent exploring the novel object over the total time spent exploring both familiar and novel objects. **C)** NMN supplementation in aged mice does not affect mean latencies to fall from the rotarod.

All data are shown as mean ± SEM. (= 20 for each data point). Statistical significance was calculated using one-way ANOVA with Tukey's post hoc test to determine differences among groups. *p < 0.05 vs. young; #p < 0.05 vs. Aged control.

D) NMN supplementation improves gait performance in aged mice. Shown is the 3D triplot of first three principal components (PC) identified by PCA on the correlation matrix of spatial and temporal indices of gait. Each point represents an individual mouse. Note that mice in the same age groups clustered together. Differences between young and aged mouse gait were evident. NMN supplementation partially reverses age-related changes in mouse gait. Data are plotted as mean ± S.E.M.; N = 20 in each group; #p < 0.01 aged vs. aged treated; *p < 0.01 young vs. aged; MANOVA with Tukey's post-hoc test.

NMN Supplementation Beneficially Affect Neurovascular Coupling

CBF responses in the whisker barrel cortex elicited by contralateral whisker stimulation were significantly decreased in aged mice compared to young animals indicating impaired NVC in aging. We found that NMN treatment significantly increased CBF responses induced by contralateral whisker stimulation in aged mice, restoring NVC (Fig. 5A and B).

To test the involvement of endothelial cells we administrated a potent NO synthase inhibitor l-NAME. In young mice it significantly decreased NVC responses, eliminating the differences between the age groups. In NMN treated aged mice, l-NAME significantly decreased CBF responses elicited by whisker stimulation (Fig. 5A and B), suggesting that NMN treatment restored the NO mediation of NVC in aged animals. To further evaluate the ability of NMN to protect endothelial cells, endothelium-dependent vasodilator responses to acetylcholine were tested. In young mice topical administration of acetylcholine resulted in significant CBF increases, whereas these responses were significantly attenuated in aging mice. Treatment of aged mice with NMN significantly improved acetylcholine-induced vasodilation (Fig. 5C).

Furthermore, NMN supplementation decreased protein 3-nitrotyrosine content in the aged cortex, indicating decreased peroxynitrite formation (Fig. 5D) after treatment.

Effect of NMN Supplementation on the Aorta Function

Similar findings were obtained in aorta ring preparations from aged mice treated with NMN. After an equilibration period of 1 hour during which an optimal passive tension was applied to the rings, the relaxation response to acetylcholine was measured. The relaxation was significantly impaired in aged animal, which was restored by NMN treatment (Fig. 5E). These finding suggests that NMN significantly improves endothelial function in aged vessels, extending our recent findings[19]. Furthermore, efficiency of NMN treatment was confirmed by demonstration of increased aorta NAD^+ levels measured from snap frozen aorta rings by Promega NAD/NADH-Glo Assay (Fig. 5F).

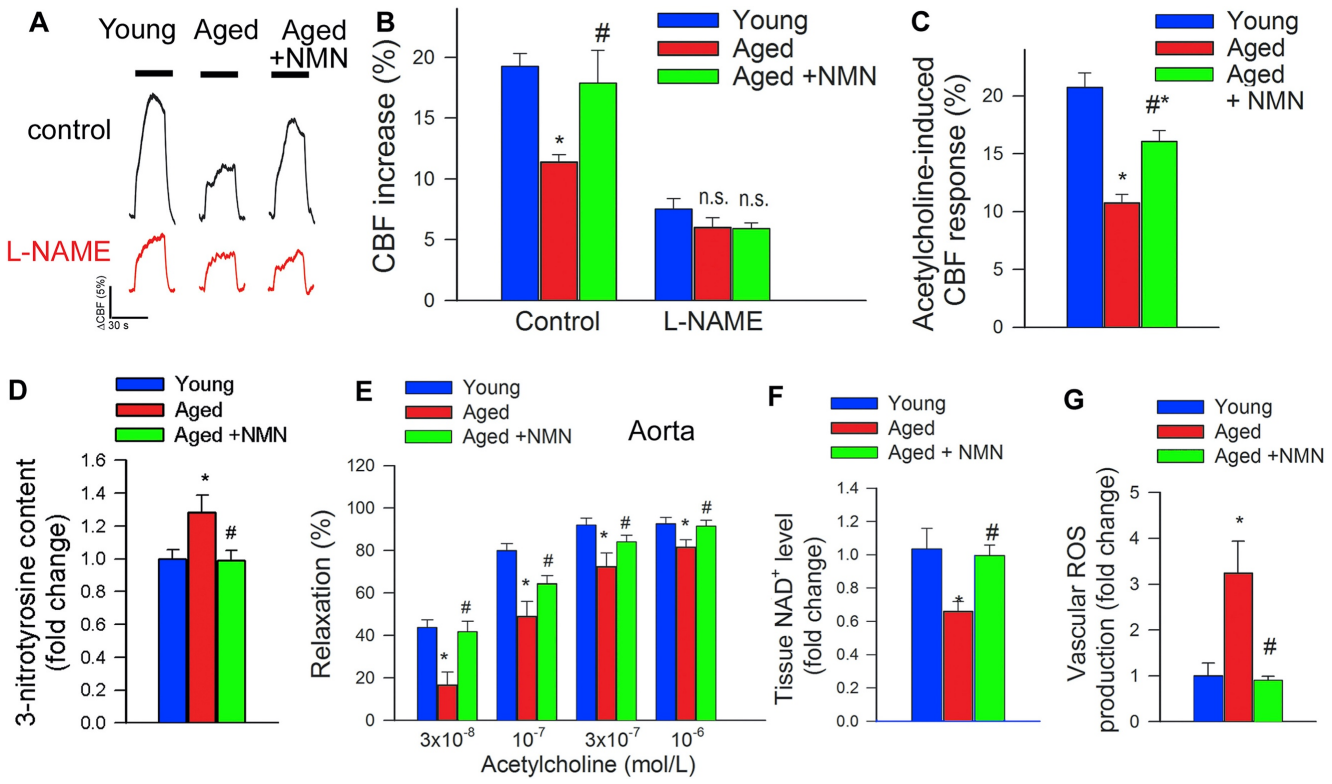

Figure 5: NMN supplementation improves microvascular endothelial function and rescues NO mediated neurovascular coupling responses in aged mice: A) Representative traces of cerebral blood flow (CBF; measured with a laser Doppler probe above the whisker barrel cortex) during contralateral whisker stimulation (30 seconds, 5 Hz) in the absence and presence of the NO synthase inhibitor l-NAME in young (3-month-old), aged (24-month-old) and NMN treated aged mice. **B)** Summary data showing that in aged mice NMN supplementation restored the NO-mediated component of NVC responses. **C)** In aged mice NMN supplementation improved endothelium-mediated CBF responses elicited by topical perfusion of acetylcholine. **D)** NMN supplementation decreased protein 3-nitrotyrosine content in the aged cortex, indicating decreased peroxynitrite formation. **E-G)** In aged mouse aortas NMN supplementation rescued acetylcholine-induced endothelium-mediated relaxation **(E)**, increased tissue NAD^+ levels **(F)** and attenuated oxidative stress (G; see Methods).

Data are plotted as mean ± S.E.M.; N = 5–8 for each data point; *p < 0.05 vs. young; #p < 0.05 vs. aged; one-way ANOVA with post-hoc Tukey's test; n.s.: not significant.

NMN Supplementation Alters miRNA Expression Profiles in the Aorta

We assessed changes in miRNA expression in aortas from aged, young and NMN treated aged mice. Hierarchical clustering (Fig. 6A) and principal component analysis (Fig. 6B) of miRNA expression showed a clear separation between the young and aged groups. Aged control mice and aged NMN-treated mice were also separated in the principal component analysis and hierarchical clustering. In contrast, miRNA expression in young mice and NMN-treated aged mice was similar and these groups did not separate well in the principal component analysis and hierarchical clustering. The Venn diagram (Fig. 6C) shows that expression of several miRNAs, which are differentially expressed in the aortas of young and aged mice, was restored to young levels in the aortas of NMN-treated aged mice. These data suggest that NAD^+ depletion has a critical role in age-related dysregulation of vascular miRNA expression.

Since the discovery of miRNA regulation of genes, several studies have focused on predicting the biologically relevant target genes for miRNAs. We identified several miRNAs whose expression levels were rescued by NMN-treatment and then used the TargetScan database to predict putative biological targets for these miRNAs (Table 1). GO terms enriched among the miRNAs that differentially expressed with age and whose expression was restored to the levels seen in aortas of young mice by NMN supplementation are shown in Table 2. Analysis of the differentially expressed miRNAs indicated that a statistically significant number of them had target sites within genes associated with pathways regulating intracellular signaling, protein homeostasis, and inflammation (Table 2). The results are consistent with the predicted anti-aging effects of NMN treatment.

We also attempted to predict the biological effects of the differentially expressed miRNAs by identifying relationships between miRNA targets and terms in the biomedical literature utilizing the IRIDESCENT system[53]. The results of this analysis suggest that NMN supplementation likely promotes epigenetic rejuvenation and confers anti-atherogenic effects (Table 3).

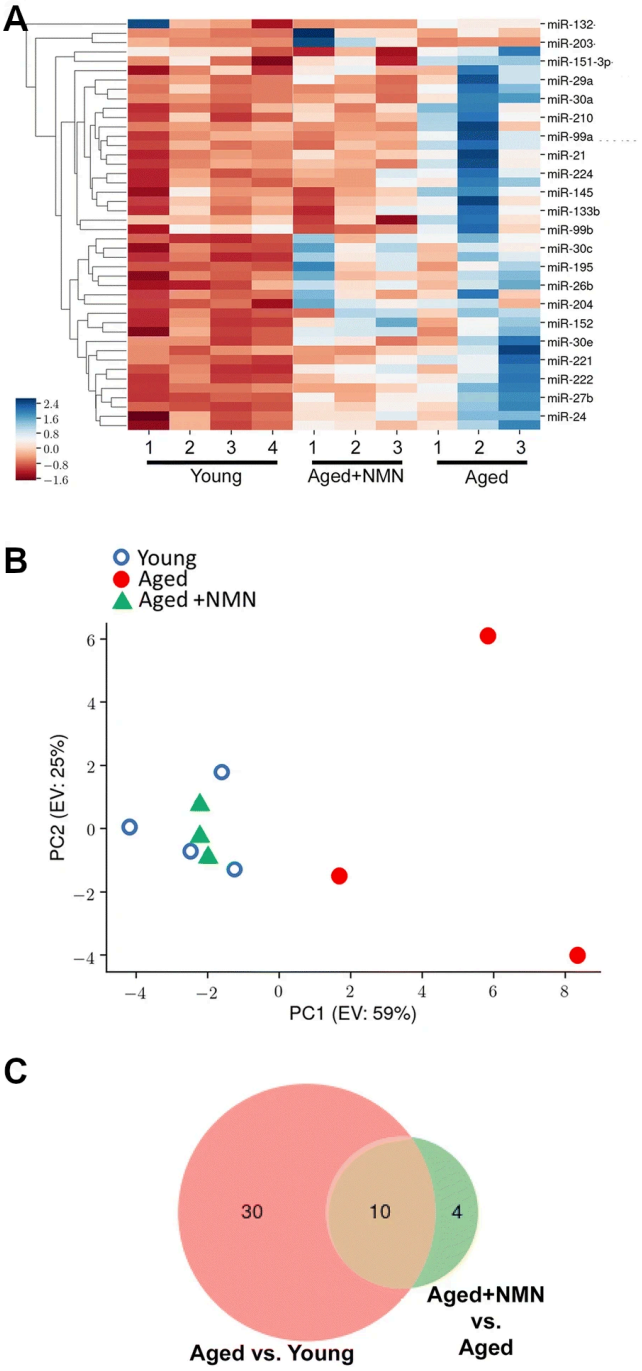

Figure 6: NMN treatment reversed age-related changes in miRNA expression profile in the mouse aorta: A) The heat map is a graphical representation of normalized miRNA expression values in aortas derived from young (3-month-old), aged (24-month-old), and NMN-treated aged mice. Hierarchical clustering analysis revealed the similarities in miRNA expression profiles of aortas from young and NMN-treated aged mice. **B)** Shown in a principal component analysis (PCA) plot of miRNA expression profiles from aortas derived from young, aged control, and NMN-treated aged mice. The profiles from aged mice (red dots) cluster separately from clusters representative of young mice (blue circles) and NMN-treated aged mice (green triangles). PC1 and PC2: Principal components 1 and 2, respectively. **C)** Venn diagram showing the differentially expressed miRNAs in each group, which are significantly up- or down-regulated in aortas from aged mice compared to those from young mice or aged NMN-treated mice.

PCR data were quantified with ΔΔCt method; one-way ANOVA with post-hoc Tukey's test; $p < 0.05$ were considered significant.

Gene symbol	NMN-induced significant miRNAs	AgeAtlas change	Cellular function	Role in vascular pathology
Sec62	4	− 0.0089	Component of the protein translocation apparatus	Single nucleotide polymorphism is associated with vulnerable plaque
Nbeal1	3	− 0.81	Vesicle trafficking, membrane dynamics, receptor signaling, pre-mRNA processing, and cytoskeleton assembly	Single nucleotide polymorphism is associated with early atherogenesis and development of ischemic white matter hyperintensities in stroke patients.
Fyn	2	− 0.31	Kinase	Genome-wide analysis of DNA methylation showed association with aortic atherosclerosis; in vitro overexpressed in activated smooth muscle cells.
Mef2a	2	− 0.094	Transcription factor	In vitro increased expression in senescence endothelial cell; increased plasma level in coronary artery disease patients.
Tet2	2	− 0.45	Epigenetic regulator	Contributes to the development of atherosclerosis by epigenetic modification.
Ptch1	2	− 0.0072	Hedgehog signaling pathway	Overexpressed in atherosclerotic plaque in mouse carotid artery.
Adra2b	2	− 0.061	Seven-pass transmembrane protein	It has a role in hypertension.
Abcg4	2	− 0.0038	ABC-transporter	Cholesterol transporter, strongly linked to atherosclerosis and other cardiovascular disease.
Epha6	2	− 0.59	Ephrin receptor	GenSalt and MESA studies: SNP variant associated with hypertension; in vitro activated in cells relevant for atherogenesis.
Atf2	2	− 0.34	Transcription factor	In mouse models participates in foam cells activation signaling; vascular smooth cell activation.
Homer2	2	− 0.31	Glutamate signaling pathway	Biomarker of atherosclerosis.
Kcnb1	3	− 0.21	Potassium channel subunit	Changed expression in arteries in rat model of hypertension
Rap1a	2	− 0.52	Ras signaling pathway	Potential role in carotid atherosclerosis
Fryl	2	− 0.71	Transcription factor; Notch signaling	Downregulated in hypertensive mouse aorta

Table 1: Selected genes whose expression changed with age and are predicted to be targeted by NMN-dependent differentially expressed miRNAs. Shown are the number of miRNAs targeting the gene whose expression is significantly changed my NMN treatment, relative age-dependent changes in gene expression, predicted by the AgeAtlas software, and cellular function of the protein encoded by the gene and its putative role in vascular pathologies.

GO term ID	Name of biological process/molecular function	N	Odds Ratio	SLPV
6886	Intracellular protein transport	20	3.17	3.26
7218	Neuropeptide signaling pathway	7	7.32	2.54
5198	Structural molecule activity	6	9.40	2.45
51082	Unfolded protein binding	7	5.49	2.20
45778	Positive regulation of ossification	6	6.27	2.07
50839	Cell adhesion molecule binding	10	3.49	1.92
15137	Citrate transmembrane transporter activity	3	inf	1.84
48227	Plasma membrane to endosome transport	3	inf	1.84
8188	Neuropeptide receptor activity	3	inf	1.84
7217	Tachykinin receptor signaling pathway	3	inf	1.84
42594	Response to starvation	3	inf	1.84
70536	Protein K63-linked deubiquitination	6	4.70	1.77
71108	Protein K48-linked deubiquitination	6	4.70	1.77
5102	Receptor binding	27	1.82	1.72
90630	Activation of GTPase activity	10	2.85	1.71
31338	Regulation of vesicle fusion	7	3.66	1.68
1664	G-protein coupled receptor binding	6	3.76	1.52
6631	Fatty acid metabolic process	6	3.76	1.52
45777	Positive regulation of blood pressure	4	6.25	1.47
32924	Activin receptor signaling pathway	4	6.25	1.47
70530	K63-linked polyubiquitin binding	4	6.25	1.47
10863	Positive regulation of phospholipase C activity	4	6.25	1.47
16579	Protein deubiquitination	8	3.13	1.47
18107	Peptidyl-threonine phosphorylation	9	2.57	1.42
48015	Phosphatidylinositol-mediated signaling	5	3.91	1.36
7200	Phospholipase C-activating G-protein coupled receptor signaling pathway	5	3.91	1.36
71837	HMG box domain binding	5	3.91	1.36
61578	Lys63-specific deubiquitinase activity	3	9.37	1.33
33674	Positive regulation of kinase activity	3	9.37	1.33
43122	Regulation of I-kappaB kinase/NF-kappaB signaling	3	9.37	1.33
50995	Negative regulation of lipid catabolic process	3	9.37	1.33

Table 2: Predicted regulatory effects of miRNAs whose expression is restored to young levels in aortas of aged mice treated with NMN. Shown are GO terms enriched among miRNAs differentially expressed with age in the aorta whose expression is significantly affected by NMN treatment. N = genes in each GO category, targeted by miRNAs that are differentially regulated in the aged mouse aorta. Significance was determined by Fisher's exact test; odds ratio: (observed to expected ratio); SLPV: signed log10 p value.

Literature associations	# shared relationships	Obs/exp	Score	Biological process/function
CTNNB1	63	2.25	139.9	Adherent junctions; Wnt/beta-catenin signaling in VSMCs contribute to Intimal thickening.
Wnt	56	2.02	110.8	Wnt signaling regulates atherogenesis.
PTEN	43	2.2	93	Regulates VSMC phenotype.
epithelial-mesenchymal transition	41	2.07	83.3	Endothelial to menesnchymal transition contributes to atherogenesis.
SMARCA4	22	3.73	81	Chromatin remodeling; genome wide association study showed its potential role in atherosclerosis.
FGFR1	28	2.63	72.3	Receptor; FGF receptor signaling regulates atherogenesis.
EP300	32	2.27	71.3	Transcriptional coactivator; VEGFA triggers changes in transcriptional activity of endothelial cells via epigenetic regulation with the help of EP300.
EZH2	25	2.78	68.6	Histone methyltransferase; epigenetic suppression of gene expression.
sumoylation	24	2.56	60.6	Sumolylation reactions play a role in atherogenesis.
RNA polymerase II	29	2.08	58.9	mRNA transcription
SOX2	27	2.15	57.7	Transcription factor, stem cell function; upregulated in aortic endothelial cells in atherosclerotic mice. Limiting Sox2 decreases calcification in aortas of ApoE(-/-) mice .
chromatin remodeling	29	2.03	57.3	
CDH2	27	2.11	55.5	Adherent junctions; neointima formation.
CDKN1A	27	2.02	53.3	Senescence; regulates atherogenesis and neointima formation.
KMT2D	15	3.6	53	Histone methyltransferase; epigenetic regulation of gene expression.

Table 3: Literature commonalities of the genes targeted by miRNAs whose expression is restored to young levels in aortas of aged mice treated with NMN. The IRIDESCENT literature-mining software was used to identify commonalities (e.g., genes, diseases, phenotypes, biological processes) of the genes predicted to be targeted by the miRNAs. A network of related objects was established by their co-occurrence within MEDLINE records, shared relationships were identified, and their statistical relevance was scored by comparing observed frequencies with what would be expected in a random network model. Number of shared relationships is the number of genes (out of the top 15 most significant) co-mentioned with the terms in the left-hand column. The observed to expected (obs/exp) ratio is the enrichment for the term. References and notes on how each relate to vascular pathophysiology of aging are shown in the rightmost column.

NMN Supplementation Alters Gene Expression Profile of Neurovascular Unit

We assessed transcriptomic changes in the NVU associated with aging and with NMN treatment. We performed unsupervised clustering of RNA-seq data from all samples using the topmost variably expressed genes across all samples. Biological replicates from the same group cluster together, and young samples segregated away from aged ones (Fig. 7A). PCA (Fig. 7B) of the transcriptomic data also showed a clear separation between the young and aged groups. Aged control mice and aged NMN-treated mice were also segregated in the PCA and hierarchical clustering. This finding indicated a clear difference between the transcriptome profiles of the two age groups. In contrast, mRNA expression in young mice and NMN-treated aged mice were similar, and these groups did not separate well in the PCA and hierarchical clustering.

We determined the number of genes that are significantly upregulated or downregulated (DE: fold-change ≥ 1.5 or ≤ -1.5; $p < 0.05$ adjusted for multiple comparisons) in the NVU by aging or by NMN treatment. We identified 590 differentially expressed genes in aged animals compared with young controls. We also identified 459 DE genes in the NMN-treated aged mice compared with the untreated aged controls (Fig. 7C). In Fig. 7D, a volcano plot shows statistical significance (p value) versus magnitude of age-related change in gene expression. Red symbols denote genes, whose expression levels differed in the aged phenotype, but have shifted back toward the young level by NMN treatment ("discordant DE genes").

In Fig. 7E, the magnitude of age-related changes in gene expression is plotted against the magnitude of NMN-induced changes in gene expression. Red symbols denote discordant DE genes, whose expression levels shifted back toward the young phenotype by NMN treatment with statistical significance. Genes which are DE only in one group but otherwise satisfy the other criteria are denoted by blue (DE in aging) and green (DE in NMN-treated) symbols. Using this approach, we have identified 466 discordant genes, which changed in opposite directions between the two comparisons (Fig. 7C). These data suggest that NAD^+ depletion has a critical role in age-related dysregulation of neurovascular gene expression.

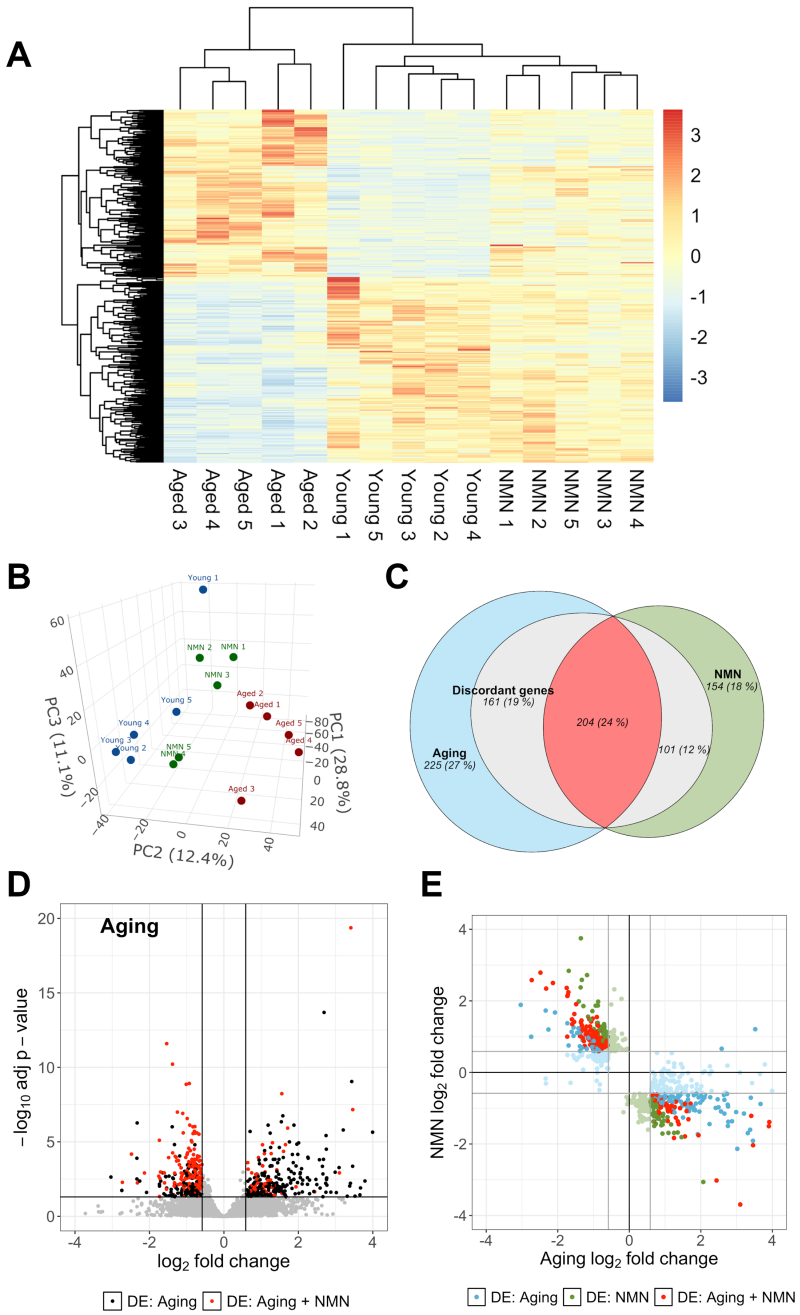

Figure 7: NMN treatment reverses age-related changes in neurovascular mRNA expression profile: A) The heat map shows normalized expression values of differentially expressed genes in neurovascular samples derived from young, aged and NMN-treated aged mice. Hierarchical clustering revealed similarities in neurovascular mRNA expression profiles in young and NMN-treated aged mice. **B)** Shown is a principal component analysis plot of neurovascular mRNA expression profiles in young, aged control, and NMN-treated aged mice. The profiles from aged mice (red) clustered separately from clusters representing young mice (blue) and NMN-treated aged mice (green). **C)** Venn diagrams sowing the numbers of differentially expressed in each group. The gray areas represent discordant genes, whose expression is changed by NMN treatment toward young levels, but the effect does not reach the cutoff for statistical significance. **D)** Volcano plot depicting differentially expressed genes comparing neurovascular samples derived from young and aged mice. Colored points refer to genes whose expression was significantly altered by NMN treatment. **E)** NMN-induced changes in gene expression were plotted against age-related changes in the neurovascular transcriptome. Red symbols indicate discordant differentially expressed genes with youthful shifts, whose expression significantly changes with age and is restored by NMN treatment toward young levels.

N = 5 in each group; differential gene expression assessed by the empirical Bayes approach implemented in the R/Bioconductor package DESeq2.

Previous studies suggested that restoration of NAD^+ levels in aged cells by NMN treatment activates the NAD^+ dependent histone deacetylase enzyme SIRT1[15]. To provide additional evidence that SIRT1 activation contributes to the neurovascular protective effects of NMN, we examined the neurovascular SIRT1 activation in NMN treated aged mice (Fig. 8).

Using the IPA upstream regulator analysis, we examined how many known targets of each transcriptional regulator were differentially expressed in our samples, and the direction of these gene expression changes were compared with what is expected from the literature. The results of the IPA upstream regulator analysis are presented in Fig. 8A. We also determined the link between the predicted upstream regulators activated by NMN and SIRT1 using IPA. We found that many of the predicted upstream regulators activated by NMN are known to be regulated by SIRT1-dependent pathways. In particular, the IPA upstream regulator analysis predicted that NMN-induced SIRT1 activation upregulates PGC-1α (PPARGC1A), FOXO3- and FOXO4-mediated pathways, whereas it inhibits HIF-1α-regulated pathways (Fig. 8B). We also attempted to predict NMN-activated, SIRT1-dependent regulatory networks by identifying relationships between SIRT1 and the predicted upstream regulators utilizing the IRIDESCENT system[53]. The results of this analysis provide additional support for the view that the predicted NMN-induced SIRT1 activation results in inhibition of HIF-1α and activation of PGC-1α and FOXO3-dependent pathways[63]. PGC-1α and FOXOs are known targets for SIRT1-mediated deacetylation (Fig. 8C).

In addition, we also intersected the list of differentially expressed genes in our dataset with the list of genes differentially expressed in the brains of $Sirt1^{-/-}$ mice (NCBI Gene Expression Omnibus: GSE28790).[64] A heat map showing the expression pattern of these SIRT1-sensitive genes is shown in Fig. 8D. Hierarchical clustering of the data showed a clear separation between the young and aged groups. Aged control mice and aged NMN-treated mice were clearly separated as well. In contrast, expression of SIRT1-sensitive genes in young mice and NMN-treated aged mice were similar, and these groups did not separate well in the hierarchical clustering, consistent with the idea that aging is associated with dysregulation of SIRT1-sensitive genes, which are rescued by NMN treatment (Fig. 8D).

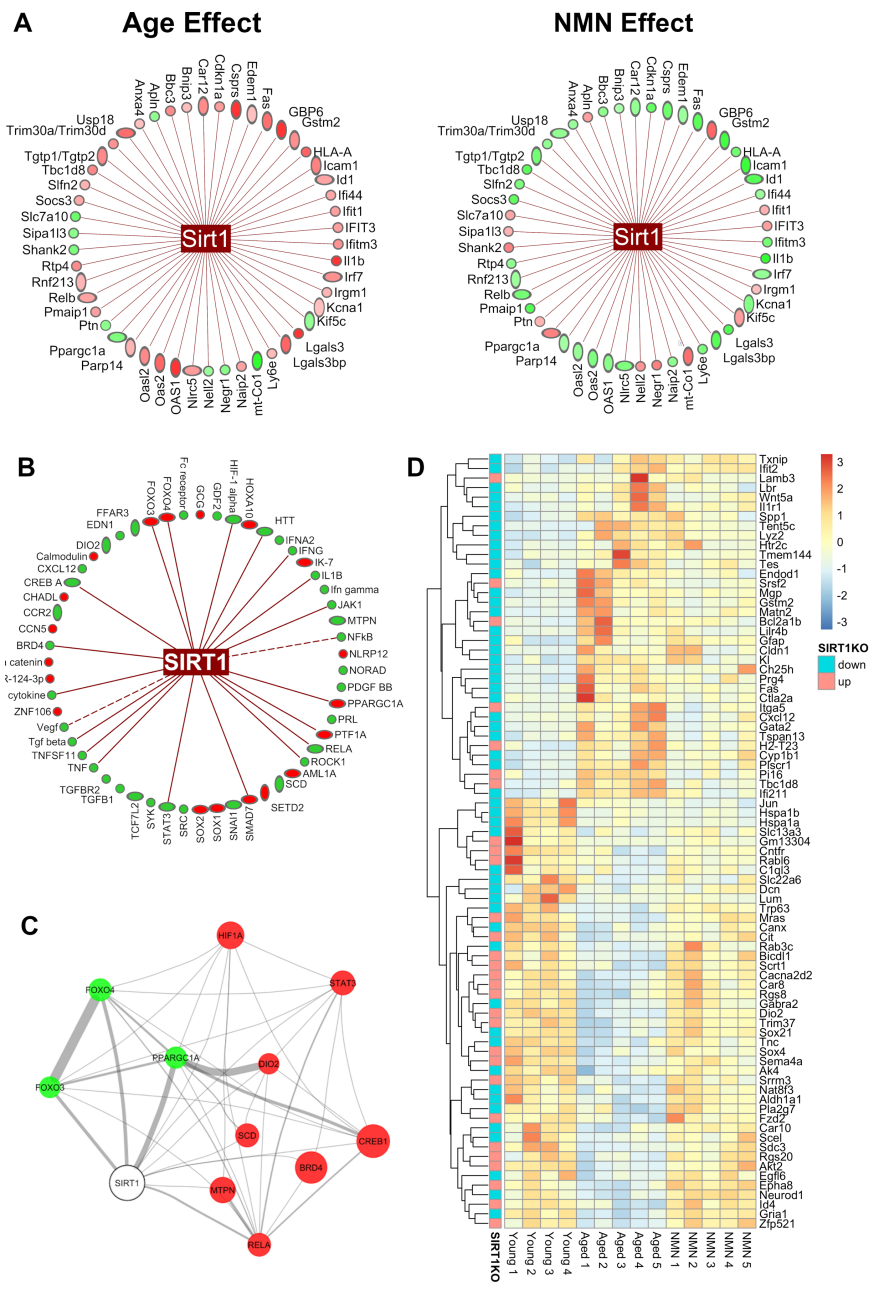

Figure 8: NMN reversed age-related changes in neurovascular expression of SIRT1-regulated genes: A) The Ingenuity Pathway Analysis results are showing age-related (left) and NMN-induced (right) changes in the expression of SIRT1-regulated genes. Green, downregulation; red, upregulation. **B)** Results of the IPA upstream regulator analysis. Shown are predicted upstream transcriptional regulators that may contribute to the observed NMN-induced transcriptomic changes in our dataset. Known links between the predicted upstream regulators activated by NMN and SIRT1 activity are indicated. **C)** Literature-based relationships with positive mutual information among the predicted upstream regulators. Node size correlates with the activation z-score from IPA, edge width correlates with the mutual information of the genes within the literature, green marks which are predicted activators and red marks predicted repressors. **D)** The heat map represents the normalized expression values of differentially expressed SIRT1-dependent genes in neurovascular samples derived from young, aged, and NMN-treated aged mice. Hierarchical clustering analysis revealed the similarities in neurovascular expression profiles of SIRT1-dependent genes in young and NMN-treated aged mice. SIRT1-dependent genes were identified based on their differential expression in the brain of Sirt1$^{-/-}$ mice.

N = 5 in each group; upstream regulators were predicted by the Ingenuity Pathway Analysis software.

GO enrichment analysis of discordant differentially expressed genes with young shifts identified functions in mitochondrial regulation and oxidative stress, apoptosis, inflammation, endothelial activation and transcriptional regulation (Fig. 9).

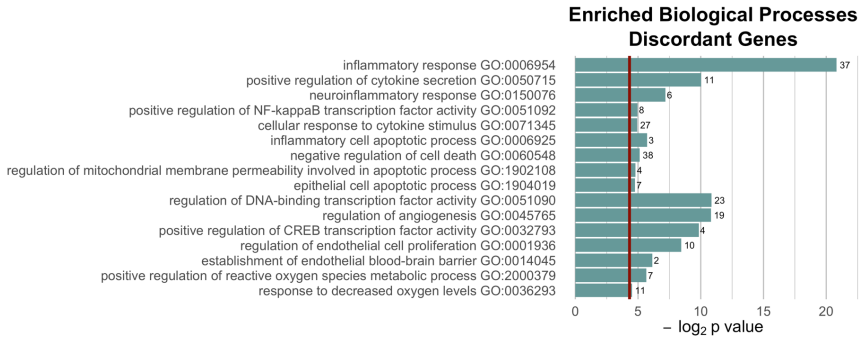

Figure 9: Most significantly enriched Gene Ontology (GO) terms for discordant genes: Note that NMN treatment is associated with transcriptional changes indicating multifaceted anti-inflammatory, anti-apoptotic, mitochondrial protective, and anti-oxidant effects. GO enrichment was calculated by hypergeometric test implemented in GOstats R/Bioconductor package.

To investigate whether mitochondria-related gene expression is altered in the aging NVU, we analyzed expression of nuclear- and mtDNA-encoded mitochondria-related genes (Fig. 10).

Heatmaps showing mtDNA-encoded genes are shown in Fig. 10A, respectively. The running enrichment scores increase when a gene is a member of the mtDNA-encoded ETC gene set and decrease when it is not. In aged mice running enrichment scores increased, indicating down-regulation of mtDNA encoded ETC genes by aging. In contrast, in NMN treated aged mice running enrichment scores increased predominantly on the left indicating up-regulation of mtDNA-encoded ETC genes by NMN treatment in aged mice (Fig. 10B).

Hierarchical clustering of the data showed a clear separation between the young and aged groups. Aged control mice and aged NMN treated mice were also separated. In contrast, expression of mitochondria-related genes in young mice and NMN treated aged mice were similar and these groups did not separate well in the hierarchical clustering, consistent with the idea that age-related dysregulation of mitochondria-related genes in the NVU is reversed, at least in part, by NMN treatment. We have used GO databases to compile a list of genes associated with mitochondria. (Fig. 10C)

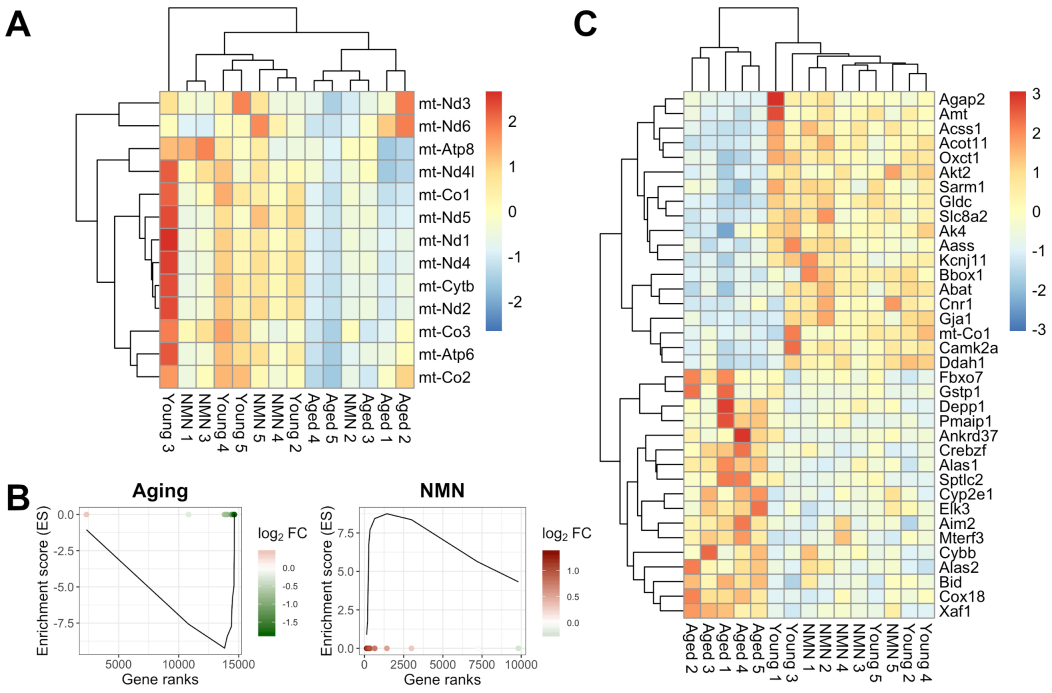

Figure 10: NMN treatment reversed age-related changes in neurovascular expression of mitochondria-related genes: A) The heat map shows normalized expression values of differentially expressed mtDNA-encoded electron transport chain (ETC) genes. **B)** Running enrichment score of mtDNA-endcoded subunits of ETC by comparing NVU samples derived from aged mice with NVU samples derived from young mice and NMN-treated aged NVU samples with untreated aged NVU samples. Note that in aged mice, enrichment scores increased predominantly on the right indicating downregulation of mtDNA-encoded ETC genes by aging. In contrast, in NMN-treated aged mice running enrichment scores increased predominantly on the left indicating upregulation of mtDNA-encoded ETC genes by NMN treatment in aged mice. **C)** The heat map shows normalized expression values of differentially expressed mtDNA-encoded genes. Hierarchical clustering revealed similarities in neurovascular expression profiles of mitochondria-related genes in young and NMN-treated aged mice. Mitochondria-related genes were identified on the basis of Gene Ontology database (GO:0005739). Note that one young sample was a statistical outlier and was therefore excluded from the mtDNA-encoded gene expression analysis.
N = 5 in each group; enrichment was calculated by the Running Enrichment Score method.

Previous studies suggested that endothelial cell apoptosis plays a critical role in age-related structural remodeling of cerebromicrovascular network by contributing to microvascular rarefaction[65]. To determine how NMN treatment alters apoptosis-related gene expression in the aging NVU, we analyzed expression of genes known to be involved in regulation of programmed cell death. Apoptosis-related genes were identified based on GO classification. Gene set enrichment score was calculated for pro-apoptotic genes. The result of this analysis suggested that aging is associated with upregulation of pro-apoptotic genes, which tends to be reversed by NMN treatment (Fig. 10B). A KEGG pathway map depicting age- and NMN treatment-related changes in the expression of genes in the apoptosis pathways is shown in Fig. 11A.

Chronic low-grade inflammation characterized by endothelial activation is a hallmark of vascular aging. To elucidate the putative anti-inflammatory effects of NMN treatment, we assessed NMN effect on the expression of endothelial activation–related genes. Endothelial activation–related genes were identified based on published microarray data (GEO database; GSE45880), showing mRNA expression changes after activation of cultured cerebromicrovascular endothelial cells (CMVECs) by 10 ng/mL TNFα and IFNγ[66]. Running enrichment score analysis showed that aging is associated with upregulation of endothelial activation–related genes in the NVU while NMN treatment exerts significant anti-inflammatory effects, downregulating endothelial activation–related genes in the NVU (Fig. 11C). The heat map shows the normalized expression values of differentially expressed endothelial activation–related genes in NVU samples derived from young, aged, and NMN-treated aged mice (Fig. 11D).

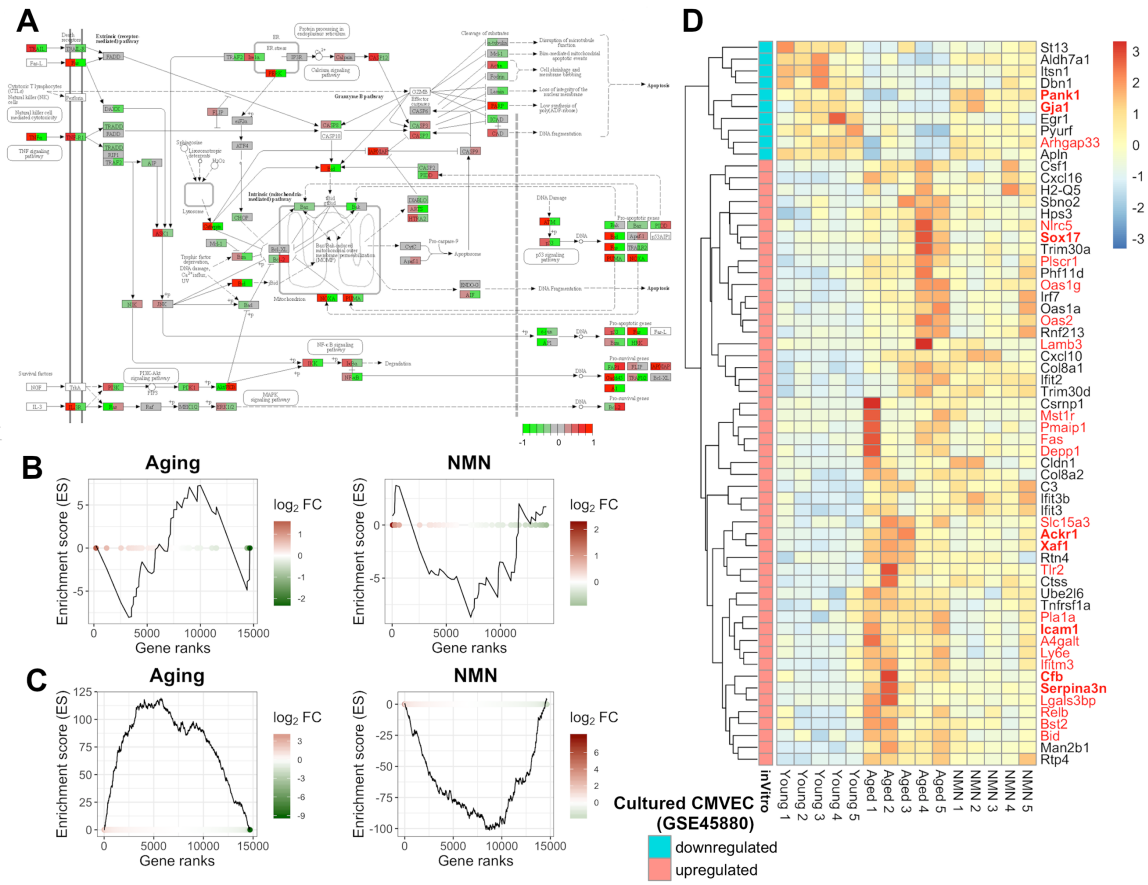

Figure 11: NMN treatment reverses age-related changes in neurovascular expression of apoptosis and endothelial activation-related genes: A) KEGG pathway map depicting age- and NMN treatment-related changes in the expression of genes in the apoptosis pathways. The rectangles are set to color by age-induced (left side) and NMN-induced (right side) changes in gene expression (fold-change). Red color indicates upregulation, green color indicates downregulation. **B)** Running enrichment score of the set of pro-apoptotic genes comparing NVU samples derived from aged mice with NVU samples derived from young mice and NMN-treated aged NVU samples with untreated aged NVU samples. **C)**. Running enrichment score of endothelial activation-related genes comparing NVU samples derived from aged mice and NMN-treated aged NVU samples with untreated aged NVU samples. **D)** The heat map shows the normalized expression values of endothelial activation–related genes in neurovascular samples derived from young, aged, and NMN-treated aged mice. Endothelial activation–related genes were identified based on published microarray data (GEO database; GSE45880), showing a distinct transcriptional signature of up and downregulated genes after activation of cultured cerebromicrovascular endothelial cells with 10 ng/mL TNFα and IFNγ (Lopez-Ramirez et al. 2013). Included in the figure are genes whose expression in aging changes similarly to the expressional changes observed in vitro upon cytokine stimulation. Discordant genes are shown in red font (bold, DE both in aging and NMN treated groups).

DISCUSSION

It is well accepted that aging is associated with structural and functional impairments of cerebral microvasculature which substantially contribute to the pathogenesis of vascular cognitive impairment and dementia[2,5]. Despite of its epidemiological importance, currently there isn't any available pharmacological intervention to prevent or treat this devastating disease[4].

Maintenance of intracellular NAD^+ level is critical for normal cellular proliferation, mitochondrial metabolism, cellular bioenergetics, adaptive stress responses, and normal activation of pro-survival pathways. With advanced age, there is decreased availability of intracellular NAD^+[15,16]. However, with small molecular drugs like NNM the level of intracellular NAD^+ can be boosted. The cellular uptake of NMN is very efficient and it is converted to NAD^+ through the NAD^+ salvage pathway. Furthermore, NMN has great pharmacokinetics in humans giving it great therapeutic potential[24]. Increased oxidative stress, cerebromicrovascular rarefaction and neurovascular uncoupling in animal models of aging as well as in clinical studies of older individuals has been linked to deterioration of high-level brain function, causing vascular cognitive impairment and dementia[67,68]. In our studies we performed a series of in vitro and in vivo experiments to systematically evaluate the effect of NMN treatment on these hallmarks of cerebromicrovascular aging and to assess the underlying gene expression changes of NMN treatment. To our knowledge, this is the most comprehensive study available in the literature investigating the effects of NMN on the aged cerebromicrovascular.

Previous studies showed that aging is characterized by mitochondrial dysfunction and increased free radical production[68]. The importance of the excessive free radicals in the cerebromicrovasculature were highlighted in some of our recent studies in which different inhibitors or scavengers of mitochondrial reactive oxygen species (SS-31, resveratrol or mitoTEMPO) could improve cognitive and gait function by rescuing NO mediated neurovascular coupling responses in aging[41]. In our current in vitro study based on cultured, aged cerebromicrovascular endothelial cells, we measured decreased mitochondrial membrane potential, decreased oxygen consumption and increased free radical production compared to cells isolated from young animals. In contrast, NMN treatment of aged cells significantly improved mitochondrial function characterized by increased mitochondrial membrane potential, increased oxygen consumption rate and decreased free radical production. Our in vitro findings were also

confirmed by our in vivo results. The 14 days NMN treatment of the aged mice significantly reduced the level of nitrogen free radical species in the cortex, which was indicated by the decreased level of modified proteins assessed by 3-nitrotyrosin staining.

Aging is also associated with cerebromicrovascular rarefaction due to declining VEGF-induced angiogenic processes. Previous studies showed that decreased capillary density significantly contributes to the pathogenesis of the aging-associated cognitive impairment and dementia[67]. Our in vitro results show that age-related decline in cellular NAD^+ levels are associated with impaired VEGF-induced angiogenic response in aged rat cerebromicrovascular endothelial cells. However, restoration of cellular NAD^+ levels with 14 days of NMN treatment significantly improved cell proliferation and rescued the increased migration and tube forming capacity of the aged cells.

According to our current understanding of aging associated vascular cognitive impairment, the dysfunction of the neurovascular unit ("neurovascular uncoupling") connects the subcellular processes to the organ level dysfucntion[6,69]. Here we provide data to confirm that aging associated cognitive impairment strongly correlates with neurovascular uncoupling, which was assessed in the barrel cortex after whisker stimulation. In aged animals, 14 days of NMN treatment was sufficient to successfully restore neurovascular coupling. Our finding strongly correlates with our in vitro results showing that NMN treatment successfully restored NO release in cultured aged cerebromicrovascular endothelial cells. In another set of ex vivo experiments, NMN supplementation also rescued endothelial NO-mediated vasodilation in the aortas of aged mice. In addition to vasoregulation endothelium-derived NO plays versatile biological roles.[47]. NO is a paracrine regulator of cellular metabolism and mitochondrial function, which modulates the function of dozens of proteins by promoting nitrosylation on their cysteine residues. This protein nitrosylation plays a role in platelet aggregation, smooth muscle cell proliferation and leukocyte adhesion, promotes stability of atherosclerotic plaques and exerts potent anti-inflammatory, anti-apoptotic and pro-angiogenic effects[47]. Thus, rescue of cerebromicrovascular NO bioavailability by treatment with NAD^+ precursors likely has clinical significance beyond restoration of neurovascular coupling.

Finally, to show the beneficial effect of NMN on the higher-level brain functions, including hippocampal learning, memory and cortical gait function were tested extensively in our animals. According to our results, aged mice had impaired learning and memory function, which were

successfully rescued by 14 days NMN treatment. NMN treated mice performed significantly better in multiple behavioral assays including radial arm water maze, elevated plus maze compared to age-matched counterparts. Neurovascular dysfunction in older adults as well as in preclinical models of aging has been linked to gait alterations as well[62]. Recent experimental studies in mouse models of pharmacologically-induced neurovascular uncoupling established a mechanistic link between impaired neurovascular coupling and gait abnormalities[44]. In our experiments, aging associated gait abnormalities were also reversed by the 14 days NMN treatment.

To understand the underlying gene expression changes of NMN treatment, high throughput gene expression assays were performed. Previous studies demonstrated that alterations in miRNA expression profiles are linked to the development of multiple cardiovascular diseases and the aging phenotypes[26,28]. Frist, miRNA profiling of aorta samples was performed by a TaqMan PCR Array. NMN treatment reversed aging associated changes in the miRNA expression profile. These findings raise the possibility that changes in post-transcriptional control of gene expression that encode critical targets for vascular health contribute to the beneficial effects of treatment with NAD^+ boosters. Furthermore, functional annotation of mRNA sequencing data, acquired from isolated neurovascular unit showed that NMN treatment in aged mice reversed, age-related, pro-inflammatory, pro-oxidative, pro-apoptotic, and endothelial-dysfunction-promoting transcriptional alterations. Analysis of the differential gene expression profile indicated that SIRT1 plays a critical role as upstream regulator in the development of the beneficial effects of NMN treatment. This finding strongly correlates both with the data available in the literature[15,16] and with our in vitro findings. In our cultured cerebromicrovascular endothelial cells originating from aged rats, shRNA knockdown of SIRT1 prevents the beneficial effects of NMN treatment.

In conclusion, we successfully demonstrated that NMN has a wide range of beneficial effects not only on the aged cerebromicrovascular endothelial cells but on the high-level of brain functions in the aged mice. Our study provides strong evidence that restoration of cellular NAD^+ level in the cerebromicrovascular endothelial cells by a small molecular booster NMN can provide a long-anticipated, efficient and safe intervention to prevent and/or treat aging-associated vascular cognitive impairment and dementia in elderly.

ACKNOWLEDGEMENT

I am especially thankful to my PhD mentors Zoltán Ungvári and Anna Csiszár for personal guidance, professional advice and continuous support of my work!

I am thankful to all my current and past colleges who has contributed to the presented research project: Stefano Tarantini, Ádám Nyúl-Tóth, Priya Balasubramanian, Andriy Yabluchanskiy, Cory B Giles, Jonathan D Wren, Lori Garman, Marta Noa Valcarcel-Ares, Péter Tóth, Tamás Csipő, Ágnes Lipecz, Eszter Farkas, Tripti Gautam, Zsuzsanna Tucsek! Thank you for your effort and the awesome teamwork!

This work was supported by grants from the American Heart Association (ST), the Oklahoma Center for the Advancement of Science and Technology (to AC, AY, ZU), the National Institute on Aging (R01-AG047879; R01-AG038747; R01-AG055395), the National Institute of Neurological Disorders and Stroke (NINDS; R01-NS056218 to AC, R01-NS100782 to ZU), the National Institute of General Medical Sciences Oklahoma Shared Clinical and Translational Resources (OSCTR) (GM104938, to AY and JW) and Molecular Mechanisms and Genetics of Autoimmunity COBRE (P30-GM110766, to LG), the Presbyterian Health Foundation (to ZU, AC, AY), the NIA-supported Geroscience Training Program in Oklahoma (T32AG052363), the Oklahoma Nathan Shock Center (P30AG050911), and the Cellular and Molecular GeroScience CoBRE (1P20GM125528, sub#5337). The funding sources had no role in the study design; in the collection, analysis, and interpretation of data; in the writing of the report; and in the decision to submit the article for publication.

Társszerzői lemondó nyilatkozat

Co-author certification

Alulírott Dr. Ungvári Zoltán (felelős társszerző) kijelentem, hogy Dr. Kiss Tamás (pályázó) PhD értekezésének tézispontjaiban bemutatott - közösen publikált - tudományos eredmények elérésében a pályázónak meghatározó szerepe volt, ezért ezeket a téziseket más a PhD fokozat megszerzését célzó minősítési eljárásban nem használta fel, illetve nem kívánja felhasználni.

Szeged, 2020.09.05.
dátum

Zoltán Ungvári
szerző

A pályázó tézispontjaiban érintett, közösen publikált közlemények:

I. Nicotinamide Mononucleotide (NMN) Treatment Attenuates Oxidative Stress and Rescues Angiogenic Capacity in Aged Cerebromicrovascular Endothelial Cells: A Potential Mechanism for the Prevention of Vascular Cognitive Impairment; Tamas Kiss, Priya Balasubramanian, Marta Noa Valcarcel-Ares, Stefano Tarantini, Andriy Yabluchanskiy, Tamas Csipo, Agnes Lipecz, Dora Reglodi, Xin A Zhang, Ferenc Bari, Eszter Farkas, Anna Csiszar, Zoltan Ungvari; Geroscience, 41 (5): 619-630, Oct 2019

II. Nicotinamide Mononucleotide (NMN) Supplementation Rescues Cerebromicrovascular Endothelial Function and Neurovascular Coupling Responses and Improves Cognitive Function in Aged Mice; Stefano Tarantini, Marta Noa Valcarcel-Ares, Peter Toth, Andriy Yabluchanskiy, Zsuzsanna Tucsek, Tamas Kiss, Peter Hertelendy, Michael Kinter, Praveen Ballabh, Zoltán Süle, Eszter Farkas, Joseph A Baur, David A Sinclair, Anna Csiszar, Zoltan Ungvari; Redox Biology, 24: 101192, Jun 2019

III. Nicotinamide Mononucleotide (NMN) Supplementation Promotes Anti-Aging miRNA Expression Profile in the Aorta of Aged Mice, Predicting Epigenetic Rejuvenation and Anti-Atherogenic Effects; Tamas Kiss, Cory B Giles, Stefano Tarantini, Andriy Yabluchanskiy, Priya Balasubramanian, Tripti Gautam, Tamas Csipo, Ádám Nyúl-Tóth, Agnes Lipecz, Csaba Szabo, Eszter Farkas, Jonathan D Wren, Anna Csiszar, Zoltan Ungvari; Geroscience, 41 (4): 419-439, Aug 2019

IV. Nicotinamide Mononucleotide (NMN) Supplementation Promotes Neurovascular Rejuvenation in Aged Mice: Transcriptional Footprint of SIRT1 Activation, Mitochondrial Protection, Anti-Inflammatory, and Anti-Apoptotic Effects; Tamas Kiss, Ádám Nyúl-Tóth, Priya Balasubramanian, Stefano Tarantini, Chetan Ahire, Andriy Yabluchanskiy, Tamas Csipo, Eszter Farkas, Jonathan D. Wren, Lori Garman, Anna Csiszar, Zoltan Ungvari; Geroscience, 42 (2): 527-546, Feb 2020

REFERENCES

1. Kisler K, Nelson AR, Montagne A, Zlokovic BV. Cerebral blood flow regulation and neurovascular dysfunction in Alzheimer disease. *Nat Rev Neurosci*. 2017;18(7):419-434. doi:10.1038/nrn.2017.48

2. Iadecola C. The Neurovascular Unit Coming of Age: A Journey through Neurovascular Coupling in Health and Disease. *Neuron*. 2017;96(1):17-42. doi:10.1016/j.neuron.2017.07.030

3. Zlokovic BV. Neurovascular pathways to neurodegeneration in Alzheimer's disease and other disorders. *Nat Rev Neurosci*. 2011;12(12):723-738. doi:10.1038/nrn3114

4. Goodman RA, Lochner KA, Thambisetty M, Wingo TS, Posner SF, Ling SM. Prevalence of dementia subtypes in United States Medicare fee-for-service beneficiaries, 2011-2013. *Alzheimers Dement J Alzheimers Assoc*. 2017;13(1):28-37. doi:10.1016/j.jalz.2016.04.002

5. Neuropathology Group. Medical Research Council Cognitive Function and Aging Study. Pathological correlates of late-onset dementia in a multicentre, community-based population in England and Wales. Neuropathology Group of the Medical Research Council Cognitive Function and Ageing Study (MRC CFAS). *Lancet Lond Engl*. 2001;357(9251):169-175. doi:10.1016/s0140-6736(00)03589-3

6. Toth P, Tarantini S, Csiszar A, Ungvari Z. Functional vascular contributions to cognitive impairment and dementia: mechanisms and consequences of cerebral autoregulatory dysfunction, endothelial impairment, and neurovascular uncoupling in aging. *Am J Physiol Heart Circ Physiol*. 2017;312(1):H1-H20. doi:10.1152/ajpheart.00581.2016

7. Murugesan N, Demarest TG, Madri JA, Pachter JS. Brain regional angiogenic potential at the neurovascular unit during normal aging. *Neurobiol Aging*. 2012;33(5):1004.e1-16. doi:10.1016/j.neurobiolaging.2011.09.022

8. Kawamura J, Terayama Y, Takashima S, et al. Leuko-araiosis and cerebral perfusion in normal aging. *Exp Aging Res*. 1993;19(3):225-240. doi:10.1080/03610739308253935

9. Sonntag WE, Lynch CD, Cooney PT, Hutchins PM. Decreases in cerebral microvasculature with age are associated with the decline in growth hormone and insulin-like growth factor 1. *Endocrinology*. 1997;138(8):3515-3520. doi:10.1210/endo.138.8.5330

10. Warrington JP, Csiszar A, Johnson DA, et al. Cerebral microvascular rarefaction induced by whole brain radiation is reversible by systemic hypoxia in mice. *Am J Physiol Heart Circ Physiol*. 2011;300(3):H736-744. doi:10.1152/ajpheart.01024.2010

11. Khan AS, Lynch CD, Sane DC, Willingham MC, Sonntag WE. Growth hormone increases regional coronary blood flow and capillary density in aged rats. *J Gerontol A Biol Sci Med Sci*. 2001;56(8):B364-371. doi:10.1093/gerona/56.8.b364

12. Kazama K, Anrather J, Zhou P, et al. Angiotensin II impairs neurovascular coupling in neocortex through NADPH oxidase-derived radicals. *Circ Res*. 2004;95(10):1019-1026. doi:10.1161/01.RES.0000148637.85595.c5

13. Tucsek Z, Toth P, Sosnowska D, et al. Obesity in aging exacerbates blood-brain barrier disruption, neuroinflammation, and oxidative stress in the mouse hippocampus: effects on expression of genes involved in beta-amyloid generation and Alzheimer's disease. *J Gerontol A Biol Sci Med Sci*. 2014;69(10):1212-1226. doi:10.1093/gerona/glt177

14. Das A, Huang GX, Bonkowski MS, et al. Impairment of an Endothelial NAD+-H2S Signaling Network Is a Reversible Cause of Vascular Aging. *Cell*. 2018;173(1):74-89.e20. doi:10.1016/j.cell.2018.02.008

15. Gomes AP, Price NL, Ling AJY, et al. Declining NAD(+) induces a pseudohypoxic state disrupting nuclear-mitochondrial communication during aging. *Cell*. 2013;155(7):1624-1638. doi:10.1016/j.cell.2013.11.037

16. Massudi H, Grant R, Braidy N, Guest J, Farnsworth B, Guillemin GJ. Age-associated changes in oxidative stress and NAD+ metabolism in human tissue. *PloS One*. 2012;7(7):e42357. doi:10.1371/journal.pone.0042357

17. Yang H, Yang T, Baur JA, et al. Nutrient-sensitive mitochondrial NAD+ levels dictate cell survival. *Cell*. 2007;130(6):1095-1107. doi:10.1016/j.cell.2007.07.035

18. Bonkowski MS, Sinclair DA. Slowing ageing by design: the rise of NAD+ and sirtuin-activating compounds. *Nat Rev Mol Cell Biol*. 2016;17(11):679-690. doi:10.1038/nrm.2016.93

19. de Picciotto NE, Gano LB, Johnson LC, et al. Nicotinamide mononucleotide supplementation reverses vascular dysfunction and oxidative stress with aging in mice. *Aging Cell*. 2016;15(3):522-530. doi:10.1111/acel.12461

20. Csiszar A, Tarantini S, Yabluchanskiy A, et al. Role of endothelial NAD+ deficiency in age-related vascular dysfunction. *Am J Physiol Heart Circ Physiol*. 2019;316(6):H1253-H1266. doi:10.1152/ajpheart.00039.2019

21. Johnson S, Wozniak DF, Imai S. CA1 Nampt knockdown recapitulates hippocampal cognitive phenotypes in old mice which nicotinamide mononucleotide improves. *NPJ Aging Mech Dis*. 2018;4:10. doi:10.1038/s41514-018-0029-z

22. Mills KF, Yoshida S, Stein LR, et al. Long-Term Administration of Nicotinamide Mononucleotide Mitigates Age-Associated Physiological Decline in Mice. *Cell Metab*. 2016;24(6):795-806. doi:10.1016/j.cmet.2016.09.013

23. Zhang H, Ryu D, Wu Y, et al. NAD^+ repletion improves mitochondrial and stem cell function and enhances life span in mice. *Science*. 2016;352(6292):1436-1443. doi:10.1126/science.aaf2693

24. Poddar SK, Sifat AE, Haque S, Nahid NA, Chowdhury S, Mehedi I. Nicotinamide Mononucleotide: Exploration of Diverse Therapeutic Applications of a Potential Molecule. *Biomolecules*. 2019;9(1). doi:10.3390/biom9010034

25. Inukai S, Slack F. MicroRNAs and the genetic network in aging. *J Mol Biol*. 2013;425(19):3601-3608. doi:10.1016/j.jmb.2013.01.023

26. Kuehbacher A, Urbich C, Zeiher AM, Dimmeler S. Role of Dicer and Drosha for endothelial microRNA expression and angiogenesis. *Circ Res*. 2007;101(1):59-68. doi:10.1161/CIRCRESAHA.107.153916

27. Hergenreider E, Heydt S, Tréguer K, et al. Atheroprotective communication between endothelial cells and smooth muscle cells through miRNAs. *Nat Cell Biol*. 2012;14(3):249-256. doi:10.1038/ncb2441

28. Guo Y, Li P, Gao L, et al. Kallistatin reduces vascular senescence and aging by regulating microRNA-34a-SIRT1 pathway. *Aging Cell*. 2017;16(4):837-846. doi:10.1111/acel.12615

29. Badi I, Mancinelli L, Polizzotto A, et al. miR-34a Promotes Vascular Smooth Muscle Cell Calcification by Downregulating SIRT1 (Sirtuin 1) and Axl (AXL Receptor Tyrosine Kinase). *Arterioscler Thromb Vasc Biol*. 2018;38(9):2079-2090. doi:10.1161/ATVBAHA.118.311298

30. Sprott RL. Development of animal models of aging at the National Institute of Aging. *Neurobiol Aging*. 1991;12(6):635-638. doi:10.1016/0197-4580(91)90113-x

31. Toth P, Tarantini S, Tucsek Z, et al. Resveratrol treatment rescues neurovascular coupling in aged mice: role of improved cerebromicrovascular endothelial function and downregulation of NADPH oxidase. *Am J Physiol Heart Circ Physiol*. 2014;306(3):H299-308. doi:10.1152/ajpheart.00744.2013

32. Ungvari Z, Tucsek Z, Sosnowska D, et al. Aging-induced dysregulation of dicer1-dependent microRNA expression impairs angiogenic capacity of rat cerebromicrovascular endothelial cells. *J Gerontol A Biol Sci Med Sci*. 2013;68(8):877-891. doi:10.1093/gerona/gls242

33. Keese CR, Wegener J, Walker SR, Giaever I. Electrical wound-healing assay for cells in vitro. *Proc Natl Acad Sci U S A*. 2004;101(6):1554-1559. doi:10.1073/pnas.0307588100

34. Napper AD, Hixon J, McDonagh T, et al. Discovery of indoles as potent and selective inhibitors of the deacetylase SIRT1. *J Med Chem*. 2005;48(25):8045-8054. doi:10.1021/jm050522v

35. Csiszar A, Labinskyy N, Jimenez R, et al. Anti-oxidative and anti-inflammatory vasoprotective effects of caloric restriction in aging: role of circulating factors and SIRT1. *Mech Ageing Dev*. 2009;130(8):518-527. doi:10.1016/j.mad.2009.06.004

36. Csiszar A, Labinskyy N, Podlutsky A, et al. Vasoprotective effects of resveratrol and SIRT1: attenuation of cigarette smoke-induced oxidative stress and proinflammatory phenotypic

alterations. *Am J Physiol Heart Circ Physiol*. 2008;294(6):H2721-2735. doi:10.1152/ajpheart.00235.2008

37. Springo Z, Tarantini S, Toth P, et al. Aging Exacerbates Pressure-Induced Mitochondrial Oxidative Stress in Mouse Cerebral Arteries. *J Gerontol A Biol Sci Med Sci*. 2015;70(11):1355-1359. doi:10.1093/gerona/glu244

38. Robinson KM, Janes MS, Beckman JS. The selective detection of mitochondrial superoxide by live cell imaging. *Nat Protoc*. 2008;3(6):941-947. doi:10.1038/nprot.2008.56

39. Divakaruni AS, Rogers GW, Murphy AN. Measuring Mitochondrial Function in Permeabilized Cells Using the Seahorse XF Analyzer or a Clark-Type Oxygen Electrode. *Curr Protoc Toxicol*. 2014;60:25.2.1-16. doi:10.1002/0471140856.tx2502s60

40. Dutta S, Sengupta P. Men and mice: Relating their ages. *Life Sci*. 2016;152:244-248. doi:10.1016/j.lfs.2015.10.025

41. Tarantini S, Valcarcel-Ares NM, Yabluchanskiy A, et al. Treatment with the mitochondrial-targeted antioxidant peptide SS-31 rescues neurovascular coupling responses and cerebrovascular endothelial function and improves cognition in aged mice. *Aging Cell*. 2018;17(2). doi:10.1111/acel.12731

42. Ungvari Z, Tarantini S, Hertelendy P, et al. Cerebromicrovascular dysfunction predicts cognitive decline and gait abnormalities in a mouse model of whole brain irradiation-induced accelerated brain senescence. *GeroScience*. 2017;39(1):33-42. doi:10.1007/s11357-017-9964-z

43. Toth P, Tucsek Z, Sosnowska D, et al. Age-related autoregulatory dysfunction and cerebromicrovascular injury in mice with angiotensin II-induced hypertension. *J Cereb Blood Flow Metab Off J Int Soc Cereb Blood Flow Metab*. 2013;33(11):1732-1742. doi:10.1038/jcbfm.2013.143

44. Tarantini S, Hertelendy P, Tucsek Z, et al. Pharmacologically-induced neurovascular uncoupling is associated with cognitive impairment in mice. *J Cereb Blood Flow Metab Off J Int Soc Cereb Blood Flow Metab*. 2015;35(11):1871-1881. doi:10.1038/jcbfm.2015.162

45. Csiszar A, Tucsek Z, Toth P, et al. Synergistic effects of hypertension and aging on cognitive function and hippocampal expression of genes involved in β-amyloid generation and Alzheimer's disease. *Am J Physiol Heart Circ Physiol*. 2013;305(8):H1120-1130. doi:10.1152/ajpheart.00288.2013

46. MacLaren DAA, Santini JA, Russell AL, Markovic T, Clark SD. Deficits in motor performance after pedunculopontine lesions in rats--impairment depends on demands of task. *Eur J Neurosci*. 2014;40(8):3224-3236. doi:10.1111/ejn.12666

47. Pacher P, Beckman JS, Liaudet L. Nitric oxide and peroxynitrite in health and disease. *Physiol Rev*. 2007;87(1):315-424. doi:10.1152/physrev.00029.2006

48. Pearson KJ, Baur JA, Lewis KN, et al. Resveratrol delays age-related deterioration and mimics transcriptional aspects of dietary restriction without extending life span. *Cell Metab*. 2008;8(2):157-168. doi:10.1016/j.cmet.2008.06.011

49. Csiszar A, Gautam T, Sosnowska D, et al. Caloric restriction confers persistent anti-oxidative, pro-angiogenic, and anti-inflammatory effects and promotes anti-aging miRNA expression profile in cerebromicrovascular endothelial cells of aged rats. *Am J Physiol Heart Circ Physiol*. 2014;307(3):H292-306. doi:10.1152/ajpheart.00307.2014

50. Livak KJ, Schmittgen TD. Analysis of relative gene expression data using real-time quantitative PCR and the 2(-Delta Delta C(T)) Method. *Methods San Diego Calif*. 2001;25(4):402-408. doi:10.1006/meth.2001.1262

51. Agarwal V, Bell GW, Nam J-W, Bartel DP. Predicting effective microRNA target sites in mammalian mRNAs. *eLife*. 2015;4. doi:10.7554/eLife.05005

52. Harris MA, Clark J, Ireland A, et al. The Gene Ontology (GO) database and informatics resource. *Nucleic Acids Res*. 2004;32(Database issue):D258-261. doi:10.1093/nar/gkh036

53. Wren JD, Garner HR. Shared relationship analysis: ranking set cohesion and commonalities within a literature-derived relationship network. *Bioinforma Oxf Engl*. 2004;20(2):191-198. doi:10.1093/bioinformatics/btg390

54. Valcarcel-Ares MN, Tucsek Z, Kiss T, et al. Obesity in Aging Exacerbates Neuroinflammation, Dysregulating Synaptic Function-Related Genes and Altering Eicosanoid Synthesis in the Mouse Hippocampus: Potential Role in Impaired Synaptic Plasticity and Cognitive Decline. *J Gerontol A Biol Sci Med Sci*. 2019;74(3):290-298. doi:10.1093/gerona/gly127

55. Bolger AM, Lohse M, Usadel B. Trimmomatic: a flexible trimmer for Illumina sequence data. *Bioinforma Oxf Engl*. 2014;30(15):2114-2120. doi:10.1093/bioinformatics/btu170

56. Bray NL, Pimentel H, Melsted P, Pachter L. Near-optimal probabilistic RNA-seq quantification. *Nat Biotechnol*. 2016;34(5):525-527. doi:10.1038/nbt.3519

57. Soneson C, Love MI, Robinson MD. Differential analyses for RNA-seq: transcript-level estimates improve gene-level inferences. *F1000Research*. 2015;4:1521. doi:10.12688/f1000research.7563.2

58. Love MI, Huber W, Anders S. Moderated estimation of fold change and dispersion for RNA-seq data with DESeq2. *Genome Biol*. 2014;15(12):550. doi:10.1186/s13059-014-0550-8

59. Falcon S, Gentleman R. Using GOstats to test gene lists for GO term association. *Bioinforma Oxf Engl*. 2007;23(2):257-258. doi:10.1093/bioinformatics/btl567

60. Krämer A, Green J, Pollard J, Tugendreich S. Causal analysis approaches in Ingenuity Pathway Analysis. *Bioinforma Oxf Engl*. 2014;30(4):523-530. doi:10.1093/bioinformatics/btt703

61. Sorond FA, Kiely DK, Galica A, et al. Neurovascular coupling is impaired in slow walkers: the MOBILIZE Boston Study. *Ann Neurol*. 2011;70(2):213-220. doi:10.1002/ana.22433

62. Tarantini S, Yabluchanksiy A, Fülöp GA, et al. Pharmacologically induced impairment of neurovascular coupling responses alters gait coordination in mice. *GeroScience*. 2017;39(5-6):601-614. doi:10.1007/s11357-017-0003-x

63. Hubbard BP, Gomes AP, Dai H, et al. Evidence for a common mechanism of SIRT1 regulation by allosteric activators. *Science*. 2013;339(6124):1216-1219. doi:10.1126/science.1231097

64. Libert S, Pointer K, Bell EL, et al. SIRT1 activates MAO-A in the brain to mediate anxiety and exploratory drive. *Cell*. 2011;147(7):1459-1472. doi:10.1016/j.cell.2011.10.054

65. Ungvari Z, Tarantini S, Kiss T, et al. Endothelial dysfunction and angiogenesis impairment in the ageing vasculature. *Nat Rev Cardiol*. 2018;15(9):555-565. doi:10.1038/s41569-018-0030-z

66. Lopez-Ramirez MA, Male DK, Wang C, Sharrack B, Wu D, Romero IA. Cytokine-induced changes in the gene expression profile of a human cerebral microvascular endothelial cell-line, hCMEC/D3. *Fluids Barriers CNS*. 2013;10(1):27. doi:10.1186/2045-8118-10-27

67. Tarantini S, Tucsek Z, Valcarcel-Ares MN, et al. Circulating IGF-1 deficiency exacerbates hypertension-induced microvascular rarefaction in the mouse hippocampus and retrosplenial cortex: implications for cerebromicrovascular and brain aging. *Age Dordr Neth*. 2016;38(4):273-289. doi:10.1007/s11357-016-9931-0

68. Tarantini S, Valcarcel-Ares MN, Yabluchanskiy A, et al. Nrf2 Deficiency Exacerbates Obesity-Induced Oxidative Stress, Neurovascular Dysfunction, Blood-Brain Barrier Disruption, Neuroinflammation, Amyloidogenic Gene Expression, and Cognitive Decline in Mice, Mimicking the Aging Phenotype. *J Gerontol A Biol Sci Med Sci*. 2018;73(7):853-863. doi:10.1093/gerona/glx177

69. Iadecola C, Gottesman RF. Neurovascular and Cognitive Dysfunction in Hypertension. *Circ Res*. 2019;124(7):1025-1044. doi:10.1161/CIRCRESAHA.118.313260

GeroScience (2019) 41:619–630
https://doi.org/10.1007/s11357-019-00074-2

ORIGINAL ARTICLE

Nicotinamide mononucleotide (NMN) treatment attenuates oxidative stress and rescues angiogenic capacity in aged cerebromicrovascular endothelial cells: a potential mechanism for the prevention of vascular cognitive impairment

Tamas Kiss · Priya Balasubramanian · Marta Noa Valcarcel-Ares · Stefano Tarantini · Andriy Yabluchanskiy · Tamas Csipo · Agnes Lipecz · Dora Reglodi · Xin A. Zhang · Ferenc Bari · Eszter Farkas · Anna Csiszar · Zoltan Ungvari

Received: 11 May 2019 / Accepted: 16 May 2019 / Published online: 29 May 2019

Abstract Age-related impairment of angiogenesis likely has a critical role in cerebromicrovascular rarefaction and development of vascular cognitive impairment and dementia (VCID) in the elderly. Recently, we demonstrated that aging is associated with NAD^+ depletion in the vasculature and that administration of NAD^+ precursors exerts potent anti-aging vascular effects, rescuing endothelium-mediated vasodilation in the cerebral circulation and improving cerebral blood supply. The present study was designed to elucidate how treatment with nicotinamide mononucleotide (NMN), a key NAD^+ intermediate, impacts age-related impairment of endothelial angiogenic processes. Using cerebromicrovascular endothelial cells (CMVECs) isolated from young and aged F344xBN rats, we demonstrated that compared with young cells, aged CMVECs exhibit impaired proliferation, cellular migration (measured by a wound-healing assay using electric cell-substrate impedance sensing [ECIS] technology), impaired ability to form capillary-like structures, and increased oxidative stress.

Tamas Kiss, Priya Balasubramanian, Marta Noa Valcarcel-Ares and Stefano Tarantini contributed equally to this work.

T. Kiss · P. Balasubramanian · M. N. Valcarcel-Ares · S. Tarantini · A. Yabluchanskiy · T. Csipo · A. Lipecz · A. Csiszar · Z. Ungvari (✉)
Vascular Cognitive Impairment and Neurodegeneration Program, Reynolds Oklahoma Center on Aging, Department of Geriatric Medicine, University of Oklahoma Health Sciences Center, 975 NE 10th Street, BRC 1311, Oklahoma City, OK 73104, USA
e-mail: zoltan-ungvari@ouhsc.edu

T. Kiss · T. Csipo · A. Lipecz · F. Bari · E. Farkas · A. Csiszar · Z. Ungvari
Department of Medical Physics and Informatics, University of Szeged, Szeged, Hungary

T. Kiss · F. Bari · E. Farkas · A. Csiszar · Z. Ungvari
Theoretical Medicine Doctoral School, University of Szeged, Szeged, Hungary

D. Reglodi
Department of Anatomy, MTA-PTE PACAP Research Team, University of Pecs Medical School, Pecs, Hungary
e-mail: dora.reglodi@aok.pte.hu

X. A. Zhang
Department of Physiology, University of Oklahoma Health Sciences Center, Oklahoma City, OK, USA

Z. Ungvari
Department of Public Health, Semmelweis University, Budapest, Hungary

Z. Ungvari
Department of Health Promotion Sciences, the Hudson College of Public Health, University of Oklahoma Health Sciences Center, Oklahoma City, OK, USA

NMN treatment in aged CMVECs significantly improved angiogenic processes and attenuated H_2O_2 production. We also found that pre-treatment with EX-527, a pharmacological inhibitor of SIRT1, prevented NMN-mediated restoration of angiogenic processes in aged CMVECs. Collectively, we find that normal cellular NAD^+ levels are essential for normal endothelial angiogenic processes, suggesting that age-related cellular NAD^+ depletion and consequential SIRT1 dysregulation may be a potentially reversible mechanism underlying impaired angiogenesis and cerebromicrovascular rarefaction in aging. We recommend that pro-angiogenic effects of NAD^+ boosters should be considered in both preclinical and clinical studies.

Keywords Senescence · Endothelial dysfunction · Vascular contributions to cognitive impairment and dementia · Microcirculation · NAD^+ precursor

Introduction

The brain is the most energy-demanding organ, yet, it lacks energy stores. Normal neuronal function is therefore critically dependent on adequate supply of nutrients and oxygen through a dense network of over 600 km of cerebral microvessels. In the brain, the number of endothelial cells is very similar to that of neurons (Garcia-Amado and Prensa 2012) and nearly every neuron is supplied by its own capillary, with an average distance of 8–20 μm between the neuron and the microvessels. Aging-induced functional and structural impairments of the cerebral microcirculatory network have a critical role in the pathogenesis of age-related cognitive decline (Zlokovic 2011; Toth et al. 2013, 2017; Tucsek et al. 2014a, 2014b; Tarantini et al. 2016; Csiszar et al. 2017).

The dynamic balance between angiogenesis (new capillary formation from pre-existing microvessels) and microvascular regression is critical for the maintenance of a healthy cerebral microcirculatory network. Advanced aging is associated with a progressive deterioration of cerebromicrovascular homeostasis, at least in part, due to a significant impairment of endothelial angiogenic processes (Ingraham et al. 2008; Murugesan et al. 2012; Ungvari et al. 2018a). This results in cerebromicrovascular rarefaction/decreased capillary density in the aged brain, which contributes to a decline in cerebral blood flow compromising oxygen and nutrient delivery to the active neurons (Hagstadius and Risberg 1989; Martin et al. 1991; Kawamura et al. 1993; Moeller et al. 1996; Sonntag et al. 1997; Krejza et al. 1999; Lynch et al. 1999; Schultz et al. 1999; Bentourkia et al. 2000; Farkas and Luiten 2001; Khan et al. 2001; Pagani et al. 2002; Riddle et al. 2003; Mitschelen et al. 2009) and the formation of ischemic foci, neuronal dysfunction, demyelination, and, ultimately, to neurodegeneration (Sonntag et al. 1997, 2000; Khan et al. 2001; Ingraham et al. 2008; Warrington et al. 2011, 2012).

Sprouting angiogenesis, which is initiated by VEGF in poorly perfused hypoxic areas of the brain, is critical to satisfy the metabolic requirements of the neuronal tissue. Previous ex vivo studies provide strong evidence that cell-autonomous mechanisms contribute to age-related impairment of sprouting angiogenesis, compromising cellular angiogenic processes induced in response to VEGF in cerebromicrovascular endothelial cells (including endothelial cell proliferation and directed migration, tubulogenesis) (Ungvari et al. 2013; Csiszar et al. 2014). However, the molecular mechanisms, by which aging impairs VEGF-induced endothelial angiogenic processes, remain elusive (Lahteenvuo and Rosenzweig 2012).

NAD^+ acts as a coenzyme in electron transfer reactions, as a donor of ADP-ribose moieties in ADP-ribosylation reactions, as a precursor of the second messenger molecule cyclic ADP-ribose, and as a substrate for the longevity assurance factor sirtuin enzymes. Maintenance of NAD^+ levels is critical for normal cellular proliferation and function, regulation of mitochondrial metabolism and cellular bioenergetics, adaptive stress responses, and normal activation of pro-survival, anti-aging pathways. With advanced age, there is decreased availability of cellular NAD^+ (Massudi et al. 2012; Gomes et al. 2013; Yoshino et al. 2018), which may be a fundamental, evolutionarily conserved contributor to aging processes across tissues. Aging-induced NAD^+ depletion was suggested to predispose to a wide range of chronic diseases and pathological conditions associated with old age (Yang et al. 2007; Garten et al. 2009; Bonkowski and Sinclair 2016; de Picciotto et al. 2016; Imai and Guarente 2016; Schultz and Sinclair 2016; Das et al. 2018; Csiszar et al. 2019), including endothelial dysfunction (Csiszar et al. 2019). There is strong preclinical evidence that restoration of cellular NAD^+ levels in aged rodents by administration of NAD^+ precursors exerts potent anti-aging effects, reversing age-related organ dysfunction (Gomes et al. 2013; Mills et al. 2016; Johnson et al. 2018) and increasing mouse lifespan

(Zhang et al. 2016). Recently, we demonstrated that treatment of old mice with nicotinamide mononucleotide (NMN), a key NAD^+ intermediate, restores vascular NAD^+ levels, rescues endothelium-mediated vasodilation in the cerebral circulation, and improves cerebral blood supply (Tarantini et al. 2019).

The present study was designed to elucidate how NMN treatment impacts age-related impairment of endothelial angiogenic processes. Using cerebromicrovascular endothelial cells (CMVECs) isolated from young and aged F344xBN rats, we tested the hypothesis that chronic treatment of aged endothelial cells with NMN improves angiogenic capacity, including proliferation, migration, and ability to form capillary-like structures.

Materials and methods

Animals and endothelial cell isolation

We used Fischer 344x Brown Norway (F344xBN) rats as a model of aging, since this strain has a lower incidence of age-specific pathology than other rats. In F344xBN rats, the primary effects of aging can be studied without complications caused by age-related pathology. Male, 3- and 24-month-old F344xBN rats were obtained from the National Institute on Aging. All animals were disease-free with no signs of systemic inflammation and/or neoplastic diseases. The rats were housed in an environmentally controlled vivarium under pathogen-free conditions with unlimited access to food and water and a controlled photoperiod (12 h light:12 h dark). All experimental animals were maintained according to National Institutes of Health guidelines, and all animal use protocols were approved by the Institutional Animal Care and Use Committees of the participating institutions. The animals were euthanized with CO_2. The brains were rapidly dissected to establish primary cerebromicrovascular endothelial cell (CMVEC) cultures as described.

Establishment and characterization of primary cerebromicrovascular endothelial cell cultures

To assess the effects of NMN on endothelial angiogenic capacity, we measured the effects of NMN on cell proliferation, migration, and tube formation ability in cultured primary CMVECs. The establishment and characterization of the CMVEC strains have been recently reported. In brief, to establish primary cultures of CMVECs, the brains of the 3- and 24-month-old F344xBN rats were removed aseptically, rinsed in ice cold PBS, and minced into ≈ 1 mm^2. The tissue was washed twice in ice cold 1X PBS by low-speed centrifugation (50*g*, 2–3 min). The diced tissue was digested in a solution of collagenase (800 U/g tissue), hyaluronidase (2.5 U/g tissue), and elastase (3 U/g tissue) in 1 mL PBS/100 mg tissue for 45 min at 37 °C in a rotating humid incubator. The digested tissue was passed through a 100-μm cell strainer. The single-cell lysate was centrifuged for 2 min at 70*g*. After removing the supernatant, the pellet was washed twice in cold PBS supplemented with 2.5% fetal calf serum (FCS), and the suspension was centrifuged at 300*g* for 5 min at 4 °C. To create an endothelial cell–enriched fraction, the cell suspension was centrifuged using an OptiPrep gradient solution (Axi-Shield, PoC, Norway). Briefly, the cell pellet was resuspended in Hanks' balanced salt solution (HBSS) and mixed with 40% iodixanol thoroughly (final concentration 17% (*v*/*v*) iodixanol solution; $\rho = 1.096$ g/mL). Two milliliters of HBSS was layered on top and centrifuged at 400*g* for 15 min at 20 °C. Endothelial cells, which banded at the interface between HBSS and the 17% iodixanol layer, were collected. The endothelial cell–enriched fraction was incubated for 30 min at 4 °C in the dark with anti-CD31/PE (BD Biosciences, San Jose, CA, USA) and anti-MCAM/FITC (BD Biosciences, San Jose, CA, USA). After washing, the cells twice with MACS Buffer (Milltenyi Biotech, Cambridge, MA, USA) anti-FITC and anti-PE magnetic bead labeled secondary antibodies were used for 15 min at room temperature. Endothelial cells were collected by magnetic separation using the MACS LD magnetic separation columns according to the manufacturer's guidelines (Milltenyi Biotech, Cambridge, MA, USA). The endothelial fraction was cultured on fibronectin coated plates in Endothelial Growth Medium (Cell Application, San Diego, CA, USA) for 10 days. Endothelial cells were phenotypically characterized by flow cytometry (GUAVA 8HT, Merck Millipore, Billerica, MA, USA). Briefly, antibodies against five different endothelial specific markers were used (anti-CD31-PE, anti-erythropoietin receptor-APC, anti-VEGF R2-PerCP, anti-ICAM-fluorescein, anti-CD146-PE), and isotype specific antibody

labeled fractions served as negative controls. Flow cytometric analysis showed that after the third cycle of immunomagnetic selection, there were virtually no $CD31^-$, $CD146^-$, $EpoR^-$, and $VEGFR2^-$ cells in the resultant cell populations. All antibodies were purchased from R&D Systems (R&D Systems, Minneapolis, MN, USA).

Primary CMVECs were cultured in custom-made Rat Brain Endothelial Cell Growth Medium (Cell Applications, Inc.) with reduced nicotinamide concentration (11.04 μM). Since the results of the assays investigating the endpoints used are affected by the number of viable cells, cell viability of each population was determined as described. To assess the direct effects of NMN on endothelial phenotype, primary CMVECs derived from aged rats were treated with NMN (Santa Cruz, Dallas, TX) in vitro (5×10^{-4} mol/L; for 1 to 5 days).

Cell proliferation assay

Cell proliferation capacity was assessed in CMVECs using the flow cytometry–based Guava CellGrowth assay (Guava Technologies, Inc., Hayward, CA) as previously reported. Briefly, cells were collected, resuspended in PBS containing 0.1% BSA, and stained with 16 μmol/L carboxyfluorescein diacetate succinimidyl ester (CFSE) for 15 min at 37 °C. This dye diffuses into cells and is cleaved by intracellular esterases to form an amine-reactive product that produces a detectable fluorescence and binds covalently to intracellular lysine residues and other amine sources. Upon cell division, CFSE divides equally into the daughter cells halving the CFSE concentration of the mother cell; therefore, there is an inverse correlation between the fluorescence intensity and the proliferation capacity of the cells. After incubation, unbound dye was quenched with serum-containing medium. Then, cells were washed three times and incubated for 24 h with 100 ng/mL VEGF. Finally, cells were collected, washed, stained with propidium iodide (to gate out dead cells), and analyzed with a flow cytometer (Guava EasyCyte 8HT; Millipore, Billerica, MA). The inverse of the fluorescence intensity was used as an index of proliferation.

Assessment of cell migration by ECIS-based wound-healing assay

Electric cell-substrate impedance sensing technology was used to monitor the migration of CMVECs in a wound-healing assay as reported (Applied BioPhysics Inc., Troy, NY). Briefly, CMVECs (2.5×10^5 cells/well) were seeded in 96-well array culture dishes (electric cell-substrate impedance sensing (ECIS), 96W1E) and placed in an incubator (37 °C), and changes in resistance and impedance were continuously monitored. When impedance reached a plateau, cells in each well were subjected to an elevated field pulse ("wounding") of 5 mA applied for 20 s at 100 kHz, which killed the cells present on the small active electrode due to severe electroporation. The detachment of the dead cells was immediately evident as a sudden drop in resistance (monitored at 4000 Hz) and a parallel increase in conductance. VEGF (100 ng/mL) was immediately added to each well. CMVECs surrounding the active electrode that had not been subjected to the wounding then migrated inward to replace the detached dead cells resulting in resistance recovery (continuously monitored at 4000 Hz for up to 24 h). The time to reach 50% resistance recovery (corresponding to 50% confluence on the active electrode) was determined for cells in each experimental group, and this parameter and the known physical dimensions of the electrode were used to calculate the migration rate (expressed as μm/h).

Tube formation assay

To investigate the influence of age and NMN on tube formation ability, young, aged, and NMN-treated aged CMVECs were plated on Geltrex Reduced Growth Factor Basement Membrane Matrix (Invitrogen, Carlsbad CA) in Medium 200PRF (Invitrogen, Carlsbad CA). To inhibit sirtuin activity, half of the aged control cells and NMN-treated aged cells were pre-treated with EX-527 (Active Motif Inc., Carlsbad, CA). EX-524 is a potent and selective sirtuin 1 (SIRT1) inhibitor (IC50 38 nM). Briefly, 150 μL/well of Geltrex was distributed in ice-cold 24-well plates. The gel was allowed to solidify while incubating the plates for 30 min at 37 °C. CMVECs were then seeded at a density of 5×10^4 cells/well and placed in the incubator for 24 h. Microscopic images were captured using a Nikon Eclipse Ti microscope equipped with a ×10 phase-contrast objective (Nikon Instruments Inc., Melville, NY). The extent of tube formation was quantified by measuring total tube length in five random fields per well using NIS-Elements microscope imaging software (Nikon Instruments Inc.), as recently reported. The mean of

the total tube length per total area imaged (μm tube/mm^2) was calculated for each well. Experiments were run in quadruplicates. The experimenter was blinded to the groups throughout the period of analysis.

Measurement of cellular H_2O_2 production

To assess cellular peroxide production, we used the cell-permeant oxidative fluorescent indicator dye CM-H_2DCFDA (5 (and 6)-chloromethyl-2′,7′-dichlorodihydrofluorescein diacetate-acetyl ester, Invitrogen, Carlsbad, CA) as we previously reported. Cells were washed with warm PBS and incubated with CM-H_2DCFDA (10 μM, at 37 °C, for 30 min). CM-H_2DCFDA fluorescence was assessed by flow cytometry.

Data analysis

Statistical analyses were performed using one-way ANOVA. $p < 0.05$ was considered statistically significant. Data are expressed as means ± S.E.M.

Results

NMN treatment improves proliferative capacity of aged CMVECs

Proliferation represents a key step in angiogenesis. Proliferative capacity of young and aged CMVECs was compared after incubation with VEGF for 24 h. We found that CFSE fluorescence was significantly increased in aged CMVECs as compared with young CMVECs, indicating that proliferation capacity is impaired by aging (Fig. 1). NMN treatment rescued proliferative capacity of aged CMVECs (Fig. 1).

NMN treatment improves migratory capability of aged CMVECs

The migratory capability of vascular endothelial cells has a pivotal role in the maintenance of microvascular integrity and angiogenesis. An ECIS-based wound-healing assay was used to assess the effect of NMN treatment on migratory capability of VEGF-treated CMVECs. We found that aged CMVECs exhibited impaired migratory capability as compared with young CMVECs (Fig. 2). In contrast, migration rate of aged CMVECs with NMN treatment did not differ significantly from that of young CMVECs (Fig. 2).

NMN treatment increases formation of capillary-like structures by aged CMVECs

When seeded onto Geltrex matrices, young CMVECs form elaborated capillary networks (Ungvari et al. 2013; Csiszar et al. 2014). Compared with young cells in aged CMVECs, formation of capillary-like structures was significantly impaired (Fig. 3a–e). The finding that treatment with NMN significantly improved formation of capillary-like structures by aged CMVECs (Fig. 3e)

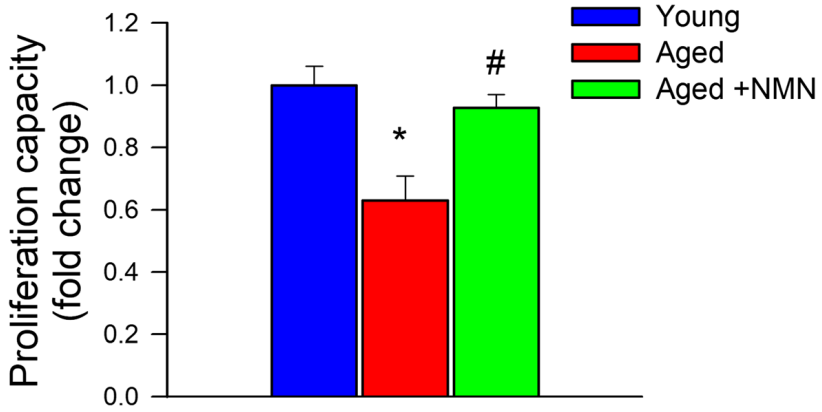

Fig. 1 NMN treatment significantly increases proliferation capacity of aged CMVECs. Cell proliferation capacity of CMVECs isolated from aged F344xBN rats is impaired as compared with that of cells isolated from young F344xBN rats, and it is significantly improved by treatment with NMN. Cell proliferation capacity was assessed in primary CMVECs stimulated with VEGF (100 ng/mL) using the flow cytometry–based *Guava CellGrowth* assay (see "Materials and Methods"). The inverse of the fluorescence intensity of the indicator dye CFSE was used as an index of proliferation capacity of the cells. Data are plotted as means ± S.E.M. ($n = 6$ in each group); *$p < 0.05$ vs. control, $^{\#}p < 0.05$ vs. aged

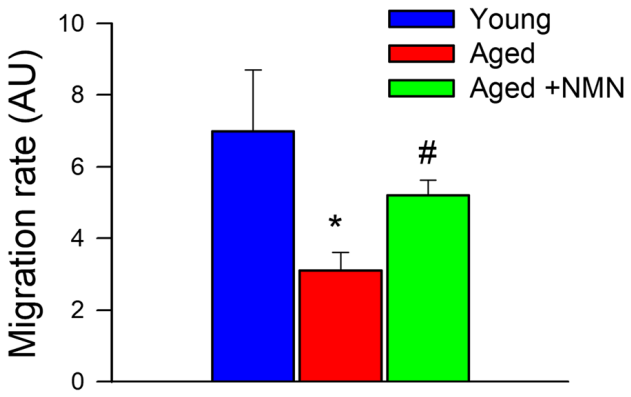

Fig. 2 NMN treatment significantly increases migration capacity of aged CMVECs. Migration capacity of CMVECs isolated from aged F344xBN rats is impaired as compared with that of cells isolated from young F344xBN rats, and it is significantly improved by treatment with NMN. VEGF (100 ng/mL)-stimulated cell migration was monitored by electric cell-substrate impedance sensing (ECIS) technology in a wound-healing assay (see "Materials and Methods"). In brief, time course of resistance recovery after wounding (electric pulse of 5 mA for 20 s at 60 kHz) was monitored at 4000 Hz. The time to reach 50% resistance recovery (corresponding to 50% confluence on the active electrode) was determined for each group, and this parameter and the known physical dimensions of the electrode were used to calculate the migration rate. Bar graph depicts the summary data for migration rate in each group. Data are plotted as means ± S.E.M. ($n = 5$ in each group); $^{*}p < 0.05$ vs. young control, $^{\#}p < 0.05$ vs. aged

suggests that age-related NAD^+ deficiency is causally linked to the impaired angiogenic capacity of aged endothelial cells. We found that pharmacological inhibition of SIRT1 significantly inhibited the formation of capillary-like structures by NMN-treated aged CMVECs (Fig. 3e).

NMN treatment attenuates oxidative stress in aged CMVECs

Age-related oxidative stress has been implicated in endothelial angiogenic dysfunction (Ungvari et al. 2013). ROS production in young and aged CMVECs was compared by assessing CM-H_2DCFDA fluorescence. We found that CM-H_2DCFDA fluorescence was significantly increased in aged CMVECs as compared with that in young CMVECs, consistent with the view that endothelial cells in the aged cerebral microcirculation exhibit increased oxidative stress (Fig. 4). NMN treatment resulted in dramatic attenuation of H_2O_2 production in aged CMVECs (Fig. 4). Recent developments in our understanding of mechanisms of aging (Deepa et al. 2017; Fang et al. 2017; Grant et al. 2017; Konopka et al. 2017; Podlutsky et al. 2017; Cunningham et al. 2018; Habermehl et al. 2018; Kim et al. 2018; Lewis et al. 2018; Masser et al. 2018; Nacarelli et al. 2018; Olecka et al. 2018; Reglodi et al. 2018) and vascular aging processes (Csiszar et al. 2017; Tarantini et al. 2017a, b; Tucsek et al. 2017; Ungvari et al. 2017a, b; Csipo et al. 2018; Fulop et al. 2018; Lee et al. 2018; Reglodi et al. 2018; Sure et al. 2018; Ungvari et al. 2018b, c) highlight the importance of in vitro screening assays that model complex physiological processes for the evaluation of the anti-aging effects of novel pharmacological interventions. The combination of the in vitro assays used in this study, based on rescue of age-related loss-of-function in endothelial cells, could correctly identify the anti-aging effects of caloric restriction (Csiszar et al. 2013, 2014) as well as neuroendocrine factors (Banki et al. 2015).

Discussion

The principal new findings of this study are that (1) age-related decline in cellular NAD^+ levels is associated with impaired angiogenic response in aged rat CMVECs, and that (2) restoration of cellular NAD^+ levels in aged CMVECs by treatment with NMN confers pro-angiogenic effects, counteracting, at least in part, the adverse effects of aging.

The formation of a new sprout growing out of existing vessels represents the first step in angiogenesis, which is mediated by VEGF-induced stalk cell proliferation and tip cell migration. VEGF also induces in endothelial cell branching and tubulogenesis to create microvascular networks. VEGF-induced proliferation and migration and tube forming capacity of CMVECs decline significantly with age, which are thought to contribute significantly to aging-induced impairment of angiogenesis and, consequentially, microvascular rarefaction (Valcarcel-Ares et al. 2012a, b; Ungvari et al. 2013; Csiszar et al. 2014; Ungvari et al. 2018a, b).

Recently, we demonstrated that age-related decline in NAD^+ levels in CMVECs can be reversed by treatment with the NAD^+ precursor NMN (Tarantini et al. 2019). This is the first study to demonstrate that treatment with NMN also improves proliferation and rescues migration and tube forming capacity of aged CMVECs. Our studies provide strong evidence that age-related NAD^+ depletion compromises endothelial angiogenic responses in the cerebromicrovasculature. Follow-up studies are needed to determine whether in vivo treatment of aged

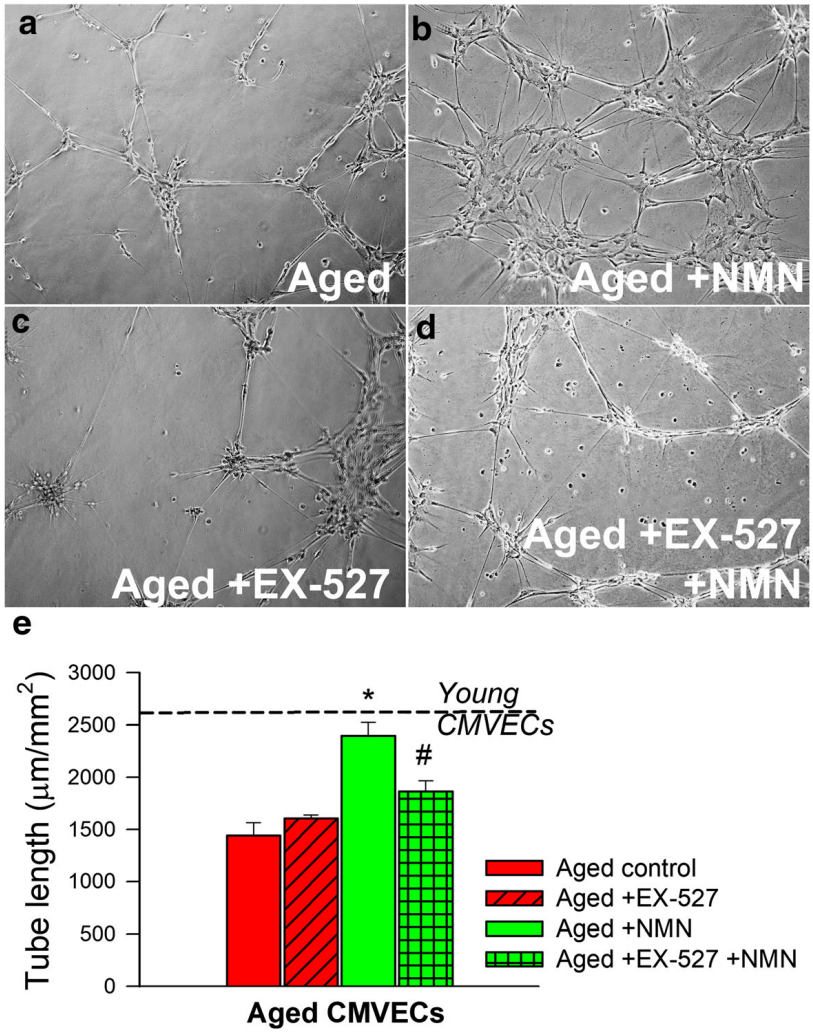

Fig. 3 NMN treatment significantly improves the tube formation ability of aged CMVECs. Tube formation ability of CMVECs isolated from aged F344xBN rats is impaired as compared with that of cells isolated from young F344xBN rats (dashed line), and it is significantly improved by NMN treatment. Inhibition of SIRT1 by EX-524 significantly impairs the ability of NMN-treated aged CMVECs to form capillary-like structures, suggesting that the protective effects of NMN are mediated by sirtuin activation. CMVECs were plated on Geltrex matrix–coated wells, and tube formation was induced by treating cells with VEGF (100 ng/mL, for 24 h). Representative examples of capillary-like structures are shown on panels **a**, **b**, **c**, **d**. Summary data, expressed as total tube length per total area scanned (μm tube/mm^2), are shown in panel **e**. Data are means ± S.E.M. ($n = 5$ in each group); $^*p < 0.05$ vs. aged control, $^\#p < 0.05$ vs. aged + NMN

rodents with NMN restores a youthful capillary density in brain regions important for learning and memory and whether NMN positively affects cerebral angiogenesis and/or collateral formation induced by physiological (e.g., exercise, local ischemia) or pharmacological stimuli. As the protective effect of NMN on formation of capillary-like structures by aged CMVECs is prevented by disruption of SIRT1 signaling, it is likely that restoration of NAD^+ levels activates sirtuins, which confer pro-angiogenic effects. This concept is supported also by the observation that treatment of aged mice with NMN improves skeletal muscle blood flow by promoting SIRT1-dependent increases in capillary density (Das et al. 2018).

Previous studies established a causal link among age-related oxidative stress, decreased bioavailability of NO, and impaired angiogenic capacity of aged endothelial cells (Koike et al. 2003; Sadoun and Reed 2003; Bach et al. 2005; Reed et al. 2005; Ungvari et al. 2013; Ungvari et al. 2018a, b). Our previous studies demonstrate that increased cellular H_2O_2 levels promote down-regulation of Dicer-dependent angiomirs (pro-angiogenic miRNAs) in aged CMVECs (Ungvari et al. 2013). Further, induction of oxidative stress by

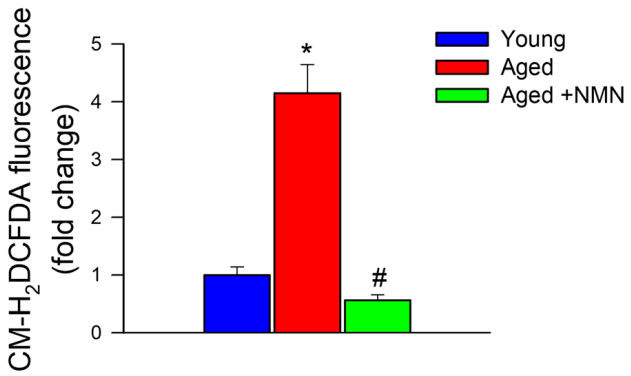

Fig. 4 NMN treatment significantly attenuates oxidative stress in aged CMVECs. Cellular peroxide production is significantly increased in cultured primary CMVECs derived from aged F344xBN rats as compared with cells isolated from young F344xBN rats, and it is significantly attenuated by treatment with NMN. Cellular peroxide production was assessed by measuring CM-H_2DCFDA fluorescence using a flow cytometry–based approach. Data are plotted as means ± S.E.M. ($n = 6$ in each group); $^{*}p < 0.05$ vs. control, $^{\#}p < 0.05$ vs. aged

downregulation of key antioxidant systems impairs angiogenic potential of endothelial cells (Valcarcel-Ares et al. 2012a, b). Here, we demonstrate that age-related increase in endothelial H_2O_2 production is effectively attenuated by NMN treatment. This observation extends the findings of our recent studies showing that in vivo treatment with NMN treatment also attenuates age-related mitochondrial oxidative stress in CMVECs restoring NO bioavailability and improving endothelium-mediated vasodilation, suggesting a key role for these mechanisms in NAD^+-mediated endothelial protection (Csiszar et al. 2019; Tarantini et al. 2019). Mitochondria-derived O_2^- is dismutated to H_2O_2 by manganese superoxide dismutase (MnSOD). H_2O_2 can readily penetrate the mitochondrial membrane, and its increased cytosolic level is likely responsible for the anti-angiogenic effects associated with mitochondrial oxidative stress. Previous studies provide additional support to this concept by showing that attenuation of mitochondrial oxidative stress using structurally different inhibitors/scavengers of mtROS production (resveratrol, mitoTEMPO) increases cerebral capillary density and/or restores angiogenic potential in aged rodents (Oomen et al. 2009; Miura et al. 2017). Our recent studies also demonstrate that attenuation of mitochondrial oxidative stress (Ungvari et al. 2009; Toth et al. 2014; Tarantini et al. 2018, 2019) also restores endothelium-mediated vasodilation in aged mice. The synergistic functional and structural microvascular protective effects of NMN and mitochondria-targeted antioxidants likely significantly improve cerebral blood flow in aging, contributing to their beneficial effects on cognitive function (Tarantini et al. 2018, 2019). Other age-related mechanisms, which may contribute to the induction of the anti-angiogenic phenotype in CMVECs exacerbating the effects of NAD^+ depletion, include age-related IGF-1 deficiency (Sonntag et al. 1997, 2012; Ungvari and Csiszar 2012) and Nrf2 dysfunction (Valcarcel-Ares et al. 2012a, b).

Significant data are available to support the efficacy and translational relevance of NMN and other related NAD^+ boosters (e.g., nicotinamide riboside treatment; Yoshino et al. 2018) (Csiszar et al. 2019). Studies are currently underway to determine whether chronic treatment with nicotinamide riboside improves cerebral blood flow (ClinicalTrials.gov Identifier: NCT03482167) in older adults with mild cognitive impairment. If these studies yield positive results, the effects of NMN treatment of organ capillarization in elderly patients should also be investigated.

Funding information This work was supported by grants from the American Heart Association (ST, MNVA), the Oklahoma Center for the Advancement of Science and Technology (to AC, AY, ZU), the National Institute on Aging (R01-AG047879; R01-AG038747; R01-AG055395), the National Institute of Neurological Disorders and Stroke (NINDS; R01-NS056218 to AC, R01-NS100782 to ZU), the Oklahoma Shared Clinical and Translational Resources (OSCTR) program funded by the National Institute of General Medical Sciences (GM104938, to AY), and the Presbyterian Health Foundation (to ZU, AC, AY).

Compliance with ethical standards

Disclaimer The funding sources had no role in the study design; in the collection, analysis, and interpretation of data; in the writing of the report; and in the decision to submit the article for publication.

References

Bach MH, Sadoun E, Reed MJ (2005) Defects in activation of nitric oxide synthases occur during delayed angiogenesis in aging. Mech Ageing Dev 126(4):467–473

Banki E, Sosnowska D, Tucsek Z, Gautam T, Toth P, Tarantini S, Tamas A, Helyes Z, Reglodi D, Sonntag WE, Csiszar A, Ungvari Z (2015) Age-related decline of autocrine pituitary adenylate cyclase-activating polypeptide impairs angiogenic capacity of rat cerebromicrovascular endothelial cells. J Gerontol A Biol Sci Med Sci 70(6):665–674

Bentourkia M, Bol A, Ivanoiu A, Labar D, Sibomana M, Coppens A, Michel C, Cosnard G, De Volder AG (2000) Comparison of regional cerebral blood flow and glucose metabolism in the normal brain: effect of aging. J Neurol Sci 181(1–2):19–28

Bonkowski MS, Sinclair DA (2016) Slowing ageing by design: the rise of NAD+ and sirtuin-activating compounds. Nat Rev Mol Cell Biol 17(11):679–690

Csipo T, Fulop GA, Lipecz A, Tarantini S, Kiss T, Balasubramanian P, Csiszar A, Ungvari Z, Yabluchanskiy A (2018) Short-term weight loss reverses obesity-induced microvascular endothelial dysfunction. Geroscience 40: 337–346

Csiszar A, Gautam T, Sosnowska D, Tarantini S, Banki E, Tucsek Z, Toth P, Losonczy G, Koller A, Reglodi D, Giles CB, Wren JD, Sonntag WE, Ungvari Z (2014) Caloric restriction confers persistent anti-oxidative, pro-angiogenic, and anti-inflammatory effects and promotes anti-aging miRNA expression profile in cerebromicrovascular endothelial cells of aged rats. Am J Physiol Heart Circ Physiol 307(3):H292–H306

Csiszar A, Sosnowska D, Tucsek Z, Gautam T, Toth P, Losonczy G, Colman RJ, Weindruch R, Anderson RM, Sonntag WE, Ungvari Z (2013) Circulating factors induced by caloric restriction in the nonhuman primate Macaca mulatta activate angiogenic processes in endothelial cells. J Gerontol A Biol Sci Med Sci 68(3):235–249

Csiszar A, Tarantini S, Fulop GA, Kiss T, Valcarcel-Ares MN, Galvan V, Ungvari Z, Yabluchanskiy A (2017) Hypertension impairs neurovascular coupling and promotes microvascular injury: role in exacerbation of Alzheimer's disease. Geroscience 39:359–372

Csiszar A, Tarantini S, Yabluchanskiy A, Balasubramanian P, Kiss T, Farkas E, Baur JA, Ungvari ZI (2019) Role of endothelial NAD+ deficiency in age-related vascular dysfunction. Am J Physiol Heart Circ Physiol: in press 316:H1253–H1266

Cunningham GM, Flores LC, Roman MG, Cheng C, Dube S, Allen C, Valentine JM, Hubbard GB, Bai Y, Saunders TL, Ikeno Y (2018) Thioredoxin overexpression in both the cytosol and mitochondria accelerates age-related disease and shortens lifespan in male C57BL/6 mice. Geroscience 40:453–468

Das A, Huang GX, Bonkowski MS, Longchamp A, Li C, Schultz MB, Kim LJ, Osborne B, Joshi S, Lu Y, Trevino-Villarreal JH, Kang MJ, Hung TT, Lee B, Williams EO, Igarashi M, Mitchell JR, Wu LE, Turner N, Arany Z, Guarente L, Sinclair DA (2018) Impairment of an endothelial NAD(+)-H2S signaling network is a reversible cause of vascular aging. Cell 173(1):74–89 e20

de Picciotto NE, Gano LB, Johnson LC, Martens CR, Sindler AL, Mills KF, Imai S, Seals DR (2016) Nicotinamide mononucleotide supplementation reverses vascular dysfunction and oxidative stress with aging in mice. Aging Cell 15(3):522–530

Deepa SS, Bhaskaran S, Espinoza S, Brooks SV, McArdle A, Jackson MJ, Van Remmen H, Richardson A (2017) A new mouse model of frailty: the Cu/Zn superoxide dismutase knockout mouse. Geroscience 39(2):187–198

Fang Y, McFadden S, Darcy J, Hill CM, Huber JA, Verhulst S, Kopchick JJ, Miller RA, Sun LY, Bartke A (2017) Differential effects of early-life nutrient restriction in long-lived GHR-KO and normal mice. Geroscience 39(3):347–356

Farkas E, Luiten PG (2001) Cerebral microvascular pathology in aging and Alzheimer's disease. Prog Neurobiol 64(6):575–611

Fulop GA, Kiss T, Tarantini S, Balasubramanian P, Yabluchanskiy A, Farkas E, Bari F, Ungvari Z, Csiszar A (2018) Nrf2 deficiency in aged mice exacerbates cellular senescence promoting cerebrovascular inflammation. Geroscience 40(5–6):513–521

Garcia-Amado M, Prensa L (2012) Stereological analysis of neuron, glial and endothelial cell numbers in the human amygdaloid complex. PLoS One 7(6):e38692

Garten A, Petzold S, Korner A, Imai S, Kiess W (2009) Nampt: linking NAD biology, metabolism and cancer. Trends Endocrinol Metab 20(3):130–138

Gomes AP, Price NL, Ling AJ, Moslehi JJ, Montgomery MK, Rajman L, White JP, Teodoro JS, Wrann CD, Hubbard BP, Mercken EM, Palmeira CM, de Cabo R, Rolo AP, Turner N, Bell EL, Sinclair DA (2013) Declining NAD(+) induces a pseudohypoxic state disrupting nuclear-mitochondrial communication during aging. Cell 155(7):1624–1638

Grant CD, Jafari N, Hou L, Li Y, Stewart JD, Zhang G, Lamichhane A, Manson JE, Baccarelli AA, Whitsel EA, Conneely KN (2017) A longitudinal study of DNA methylation as a potential mediator of age-related diabetes risk. Geroscience 39(5–6):475–489

Habermehl TL, Parkinson KC, Hubbard GB, Ikeno Y, Engelmeyer JI, Schumacher B, Mason JB (2018) Extension of longevity and reduction of inflammation is ovarian-dependent, but germ cell-independent in post-reproductive female mice. Geroscience 41(1):25–38. https://doi.org/10.1007/s11357-018-0049-4

Hagstadius S, Risberg J (1989) Regional cerebral blood flow characteristics and variations with age in resting normal subjects. Brain Cogn 10(1):28–43

Imai SI, Guarente L (2016) It takes two to tango: NAD(+) and sirtuins in aging/longevity control. NPJ Aging Mech Dis 2:16017

Ingraham JP, Forbes ME, Riddle DR, Sonntag WE (2008) Aging reduces hypoxia-induced microvascular growth in the rodent hippocampus. J Gerontol A Biol Sci Med Sci 63(1):12–20

Johnson S, Wozniak DF, Imai S (2018) CA1 Nampt knockdown recapitulates hippocampal cognitive phenotypes in old mice which nicotinamide mononucleotide improves. NPJ Aging Mech Dis 4:10

Kawamura J, Terayama Y, Takashima S, Obara K, Pavol MA, Meyer JS, Mortel KF, Weathers S (1993) Leuko-araiosis and cerebral perfusion in normal aging. Exp Aging Res 19(3):225–240

Khan AS, Lynch CD, Sane DC, Willingham MC, Sonntag WE (2001) Growth hormone increases regional coronary blood flow and capillary density in aged rats. J Gerontol A Biol Sci Med Sci 56(8):B364–B371

Kim S, Wyckoff J, Morris AT, Succop A, Avery A, Duncan GE, Jazwinski SM (2018) DNA methylation associated with healthy aging of elderly twins. Geroscience 40(5–6):469–484

Koike T, Vernon RB, Gooden MD, Sadoun E, Reed MJ (2003) Inhibited angiogenesis in aging: a role for TIMP-2. J Gerontol A Biol Sci Med Sci 58(9):B798–B805

Konopka AR, Laurin JL, Musci RV, Wolff CA, Reid JJ, Biela LM, Zhang Q, Peelor FF 3rd, Melby CL, Hamilton KL, Miller BF (2017) Influence of Nrf2 activators on subcellular skeletal muscle protein and DNA synthesis rates after 6 weeks of milk protein feeding in older adults. Geroscience 39(2):175–186

Krejza J, Mariak Z, Walecki J, Szydlik P, Lewko J, Ustymowicz A (1999) Transcranial color Doppler sonography of basal cerebral arteries in 182 healthy subjects: age and sex variability and normal reference values for blood flow parameters. AJR Am J Roentgenol 172(1):213–218

Lahteenvuo J, Rosenzweig A (2012) Effects of aging on angiogenesis. Circ Res 110(9):1252–1264

Lee HJ, Feliers D, Barnes JL, Oh S, Choudhury GG, Diaz V, Galvan V, Strong R, Nelson J, Salmon A, Kevil CG, Kasinath BS (2018) Hydrogen sulfide ameliorates aging-associated changes in the kidney. Geroscience 40(2):163–176

Lewis KN, Rubinstein ND, Buffenstein R (2018) A window into extreme longevity; the circulating metabolomic signature of the naked mole-rat, a mammal that shows negligible senescence. Geroscience 40(2):105–121

Lynch CD, Cooney PT, Bennett SA, Thornton PL, Khan AS, Ingram RL, Sonntag WE (1999) Effects of moderate caloric restriction on cortical microvascular density and local cerebral blood flow in aged rats. Neurobiol Aging 20(2):191–200

Martin AJ, Friston KJ, Colebatch JG, Frackowiak RS (1991) Decreases in regional cerebral blood flow with normal aging. J Cereb Blood Flow Metab 11(4):684–689

Masser DR, Hadad N, Porter H, Stout MB, Unnikrishnan A, Stanford DR, Freeman WM (2018) Analysis of DNA modifications in aging research. Geroscience 40(1):11–29

Massudi H, Grant R, Braidy N, Guest J, Farnsworth B, Guillemin GJ (2012) Age-associated changes in oxidative stress and NAD+ metabolism in human tissue. PLoS One 7(7):e42357

Mills KF, Yoshida S, Stein LR, Grozio A, Kubota S, Sasaki Y, Redpath P, Migaud ME, Apte RS, Uchida K, Yoshino J, Imai SI (2016) Long-term administration of nicotinamide mononucleotide mitigates age-associated physiological decline in mice. Cell Metab 24(6):795–806

Mitschelen M, Garteiser P, Carnes BA, Farley JA, Doblas S, Demoe JH, Warrington JP, Yan H, Nicolle MM, Towner R, Sonntag WE (2009) Basal and hypercapnia-altered cerebrovascular perfusion predict mild cognitive impairment in aging rodents. Neuroscience 164(3):918–928

Miura S, Saitoh SI, Kokubun T, Owada T, Yamauchi H, Machii H, Takeishi Y (2017) Mitochondrial-targeted antioxidant maintains blood flow, mitochondrial function, and redox balance in old mice following prolonged limb ischemia. Int J Mol Sci 18(9). https://doi.org/10.3390/ijms18091897

Moeller JR, Ishikawa T, Dhawan V, Spetsieris P, Mandel F, Alexander GE, Grady C, Pietrini P, Eidelberg D (1996) The metabolic topography of normal aging. J Cereb Blood Flow Metab 16(3):385–398

Murugesan N, Demarest TG, Madri JA, Pachter JS (2012) Brain regional angiogenic potential at the neurovascular unit during normal aging. Neurobiol Aging 33(5):1004 e1001–1004 e1016

Nacarelli T, Azar A, Altinok O, Orynbayeva Z, Sell C (2018) Rapamycin increases oxidative metabolism and enhances metabolic flexibility in human cardiac fibroblasts. Geroscience 40:243–256

Olecka M, Huse K, Platzer M (2018) The high degree of cystathionine beta-synthase (CBS) activation by S-adenosylmethionine (SAM) may explain naked mole-rat's distinct methionine metabolite profile compared to mouse. Geroscience 40(4):359–360

Oomen CA, Farkas E, Roman V, van der Beek EM, Luiten PG, Meerlo P (2009) Resveratrol preserves cerebrovascular density and cognitive function in aging mice. Front Aging Neurosci 1:4

Pagani M, Salmaso D, Jonsson C, Hatherly R, Jacobsson H, Larsson SA, Wagner A (2002) Regional cerebral blood flow as assessed by principal component analysis and (99m)Tc-HMPAO SPET in healthy subjects at rest: normal distribution and effect of age and gender. Eur J Nucl Med Mol Imaging 29(1):67–75

Podlutsky A, Valcarcel-Ares MN, Yancey K, Podlutskaya V, Nagykaldi E, Gautam T, Miller RA, Sonntag WE, Csiszar A, Ungvari Z (2017) The GH/IGF-1 axis in a critical period early in life determines cellular DNA repair capacity by altering transcriptional regulation of DNA repair-related genes: implications for the developmental origins of cancer. Geroscience 39(2):147–160

Reed MJ, Bradshaw AD, Shaw M, Sadoun E, Han N, Ferara N, Funk S, Puolakkainen P, Sage EH (2005) Enhanced angiogenesis characteristic of SPARC-null mice disappears with age. J Cell Physiol 204(3):800–807

Reglodi D, Atlasz T, Szabo E, Jungling A, Tamas A, Juhasz T, Fulop BD, Bardosi A (2018) PACAP deficiency as a model of aging. Geroscience 40(5–6):437–452

Riddle DR, Sonntag WE, Lichtenwalner RJ (2003) Microvascular plasticity in aging. Ageing Res Rev 2(2):149–168

Sadoun E, Reed MJ (2003) Impaired angiogenesis in aging is associated with alterations in vessel density, matrix composition, inflammatory response, and growth factor expression. J Histochem Cytochem 51(9):1119–1130

Schultz MB, Sinclair DA (2016) Why NAD(+) declines during aging: it's destroyed. Cell Metab 23(6):965–966

Schultz SK, O'Leary DS, Boles Ponto LL, Watkins GL, Hichwa RD, Andreasen NC (1999) Age-related changes in regional cerebral blood flow among young to mid-life adults. Neuroreport 10(12):2493–2496

Sonntag WE, Csiszar A, Decabo R, Ferrucci L, Ungvari Z (2012) Diverse roles of growth hormone and insulin-like growth factor-1 in mammalian aging: progress and controversies. J Gerontol A Biol Sci Med Sci 67A:587–598

Sonntag WE, Lynch C, Thornton P, Khan A, Bennett S, Ingram R (2000) The effects of growth hormone and IGF-1 deficiency on cerebrovascular and brain ageing. J Anat 197(Pt 4):575–585

Sonntag WE, Lynch CD, Cooney PT, Hutchins PM (1997) Decreases in cerebral microvasculature with age are associated with the decline in growth hormone and insulin-like growth factor 1. Endocrinology 138(8):3515–3520

Sure VN, Sakamuri S, Sperling JA, Evans WR, Merdzo I, Mostany R, Murfee WL, Busija DW, Katakam PVG (2018) A novel high-throughput assay for respiration in isolated brain microvessels reveals impaired mitochondrial function in the aged mice. Geroscience 40(4):365–375

Tarantini S, Fulop GA, Kiss T, Farkas E, Zolei-Szenasi D, Galvan V, Toth P, Csiszar A, Ungvari Z, Yabluchanskiy A (2017a)

Demonstration of impaired neurovascular coupling responses in TG2576 mouse model of Alzheimer's disease using functional laser speckle contrast imaging. Geroscience 39(4): 465–473

Tarantini S, Tucsek Z, Valcarcel-Ares MN, Toth P, Gautam T, Giles CB, Ballabh P, Wei JY, Wren JD, Ashpole NM, Sonntag WE, Ungvari Z, Csiszar A (2016) Circulating IGF-1 deficiency exacerbates hypertension-induced microvascular rarefaction in the mouse hippocampus and retrosplenial cortex: implications for cerebromicrovascular and brain aging. Age (Dordr) 38(4):273–289

Tarantini S, Valcarcel-Ares MN, Toth P, Yabluchanskiy A, Tucsek Z, Kiss T, Hertelendy P, Kinter M, Ballabh P, Sule Z, Farkas E, Baur JA, Sinclair DA, Csiszar A, Ungvari Z (2019) Nicotinamide mononucleotide (NMN) supplementation rescues cerebromicrovascular endothelial function and neurovascular coupling responses and improves cognitive function in aged mice. Redox Biol 24:101192

Tarantini S, Valcarcel-Ares NM, Yabluchanskiy A, Fulop GA, Hertelendy P, Gautam T, Farkas E, Perz A, Rabinovitch PS, Sonntag WE, Csiszar A, Ungvari Z (2018) Treatment with the mitochondrial-targeted antioxidant peptide SS-31 rescues neurovascular coupling responses and cerebrovascular endothelial function and improves cognition in aged mice. Aging Cell 17(2):e12731

Tarantini S, Yabluchanksiy A, Fulop GA, Hertelendy P, Valcarcel-Ares MN, Kiss T, Bagwell JM, O'Connor D, Farkas E, Sorond F, Csiszar A, Ungvari Z (2017b) Pharmacologically induced impairment of neurovascular coupling responses alters gait coordination in mice. Geroscience 39(5–6):601–614

Toth P, Tarantini S, Csiszar A, Ungvari Z (2017) Functional vascular contributions to cognitive impairment and dementia: mechanisms and consequences of cerebral autoregulatory dysfunction, endothelial impairment, and neurovascular uncoupling in aging. Am J Physiol Heart Circ Physiol 312(1):H1–H20

Toth P, Tarantini S, Tucsek Z, Ashpole NM, Sosnowska D, Gautam T, Ballabh P, Koller A, Sonntag WE, Csiszar A, Ungvari ZI (2014) Resveratrol treatment rescues neurovascular coupling in aged mice: role of improved cerebromicrovascular endothelial function and down-regulation of NADPH oxidase. Am J Physiol Heart Circ Physiol 306(3):H299–H308

Toth P, Tucsek Z, Sosnowska D, Gautam T, Mitschelen M, Tarantini S, Deak F, Koller A, Sonntag WE, Csiszar A, Ungvari Z (2013) Age-related autoregulatory dysfunction and cerebromicrovascular injury in mice with angiotensin II-induced hypertension. J Cereb Blood Flow Metab 33(11):1732–1742

Tucsek Z, Noa Valcarcel-Ares M, Tarantini S, Yabluchanskiy A, Fulop G, Gautam T, Orock A, Csiszar A, Deak F, Ungvari Z (2017) Hypertension-induced synapse loss and impairment in synaptic plasticity in the mouse hippocampus mimics the aging phenotype: implications for the pathogenesis of vascular cognitive impairment. Geroscience 39:385–406

Tucsek Z, Toth P, Sosnowsk D, Gautam T, Mitschelen M, Koller A, Szalai G, Sonntag WE, Ungvari Z, Csiszar A (2014a) Obesity in aging exacerbates blood brain barrier disruption, neuroinflammation and oxidative stress in the mouse hippocampus: effects on expression of genes involved in beta-amyloid generation and Alzheimer's disease. J Gerontol A Biol Sci Med Sci 69(10):1212–1226

Tucsek Z, Toth P, Tarantini S, Sosnowska D, Gautam T, Warrington JP, Giles CB, Wren JD, Koller A, Ballabh P, Sonntag WE, Ungvari Z, Csiszar A (2014b) Aging exacerbates obesity-induced cerebromicrovascular rarefaction, neurovascular uncoupling, and cognitive decline in mice. J Gerontol A Biol Sci Med Sci 69(11):1339–1352

Ungvari Z, Csiszar A (2012) The emerging role of IGF-1 deficiency in cardiovascular aging: recent advances. J Gerontol A Biol Sci Med Sci 67A:599–610

Ungvari Z, Labinskyy N, Mukhopadhyay P, Pinto JT, Bagi Z, Ballabh P, Zhang C, Pacher P, Csiszar A (2009) Resveratrol attenuates mitochondrial oxidative stress in coronary arterial endothelial cells. Am J Physiol Heart Circ Physiol 297(5):H1876–H1881

Ungvari Z, Tarantini S, Donato AJ, Galvan V, Csiszar A (2018a) Mechanisms of vascular aging. Circ Res 123(7):849–867

Ungvari Z, Tarantini S, Hertelendy P, Valcarcel-Ares MN, Fulop GA, Logan S, Kiss T, Farkas E, Csiszar A, Yabluchanskiy A (2017a) Cerebromicrovascular dysfunction predicts cognitive decline and gait abnormalities in a mouse model of whole brain irradiation-induced accelerated brain senescence. Geroscience 39(1):33–42

Ungvari Z, Tarantini S, Kiss T, Wren JD, Giles CB, Griffin CT, Murfee WL, Pacher P, Csiszar A (2018b) Endothelial dysfunction and angiogenesis impairment in the ageing vasculature. Nat Rev Cardiol 15(9):555–565

Ungvari Z, Tucsek Z, Sosnowska D, Toth P, Gautam T, Podlutsky A, Csiszar A, Losonczy G, Valcarcel-Ares MN, Sonntag WE (2013) Aging-induced dysregulation of Dicer1-dependent MicroRNA expression impairs angiogenic capacity of rat cerebromicrovascular endothelial cells. J Gerontol A Biol Sci Med Sci 68(8):877–891

Ungvari Z, Valcarcel-Ares MN, Tarantini S, Yabluchanskiy A, Fulop GA, Kiss T, Csiszar A (2017b) Connective tissue growth factor (CTGF) in age-related vascular pathologies. Geroscience 39(5–6):491–498

Ungvari Z, Yabluchanskiy A, Tarantini S, Toth P, Kirkpatrick AC, Csiszar A, Prodan CI (2018c) Repeated Valsalva maneuvers promote symptomatic manifestations of cerebral microhemorrhages: implications for the pathogenesis of vascular cognitive impairment in older adults. Geroscience 40(5–6):485–496

Valcarcel-Ares MN, Gautam T, Warrington JP, Bailey-Downs L, Sosnowska D, de Cabo R, Losonczy G, Sonntag WE, Ungvari Z, Csiszar A (2012a) Disruption of Nrf2 signaling impairs angiogenic capacity of endothelial cells: implications for microvascular aging. J Gerontol A Biol Sci Med Sci 67(8):821–829

Valcarcel-Ares MN, Gautam T, Warrington JP, Bailey-Downs L, Sosnowska D, de Cabo R, Losonczy G, Sonntag WE, Ungvari Z, Csiszar A (2012b) Disruption of Nrf2 signaling impairs angiogenic capacity of endothelial cells: implications for microvascular aging. J Gerontol A Biol Sci Med Sci 67(8):821–829

Warrington JP, Csiszar A, Johnson DA, Herman TS, Ahmad S, Lee YW, Sonntag WE (2011) Cerebral microvascular rarefaction induced by whole brain radiation is reversible by

systemic hypoxia in mice. Am J Physiol Heart Circ Physiol 300(3):H736–H744

Warrington JP, Csiszar A, Mitschelen M, Lee YW, Sonntag WE (2012) Whole brain radiation-induced impairments in learning and memory are time-sensitive and reversible by systemic hypoxia. PLoS One 7(1):e30444

Yang H, Yang T, Baur JA, Perez E, Matsui T, Carmona JJ, Lamming DW, Souza-Pinto NC, Bohr VA, Rosenzweig A, de Cabo R, Sauve AA, Sinclair DA (2007) Nutrient-sensitive mitochondrial NAD+ levels dictate cell survival. Cell 130(6): 1095–1107

Yoshino J, Baur JA, Imai SI (2018) NAD(+) intermediates: the biology and therapeutic potential of NMN and NR. Cell Metab 27(3):513–528

Zhang H, Ryu D, Wu Y, Gariani K, Wang X, Luan P, D'Amico D, Ropelle ER, Lutolf MP, Aebersold R, Schoonjans K, Menzies KJ, Auwerx J (2016) NAD(+) repletion improves mitochondrial and stem cell function and enhances life span in mice. Science 352(6292):1436–1443

Zlokovic BV (2011) Neurovascular pathways to neurodegeneration in Alzheimer's disease and other disorders. Nat Rev Neurosci 12(12):723–738

Redox Biology 24 (2019) 101192

Contents lists available at ScienceDirect

Redox Biology

journal homepage: www.elsevier.com/locate/redox

Nicotinamide mononucleotide (NMN) supplementation rescues cerebromicrovascular endothelial function and neurovascular coupling responses and improves cognitive function in aged mice

Stefano Tarantini[a], Marta Noa Valcarcel-Ares[a], Peter Toth[a,b], Andriy Yabluchanskiy[a], Zsuzsanna Tucsek[a], Tamas Kiss[a], Peter Hertelendy[a], Michael Kinter[a,c], Praveen Ballabh[d], Zoltán Süle[e], Eszter Farkas[f], Joseph A. Baur[g], David A. Sinclair[h], Anna Csiszar[a,f], Zoltan Ungvari[a,f,i,j,*]

[a] Vascular Cognitive Impairment and Neurodegeneration Program, Reynolds Oklahoma Center on Aging/Department of Geriatric Medicine, University of Oklahoma Health Sciences Center, Oklahoma City, OK, USA
[b] Department of Neurosurgery, Medical School, University of Pecs, Hungary
[c] Aging and Metabolism Research Program, Oklahoma Medical Research Foundation, Oklahoma City, OK, 73104, USA
[d] Division of Neonatology, Department of Pediatrics, Albert Einstein College of Medicine, USA
[e] Department of Anatomy, University of Szeged, Szeged, Hungary
[f] Department of Medical Physics and Informatics, University of Szeged, Szeged, Hungary
[g] Department of Physiology and Institute for Diabetes, Obesity, and Metabolism, Perelman School of Medicine, University of Pennsylvania, Philadelphia, PA 19104, USA
[h] Department of Genetics, Harvard Medical School, Boston, USA
[i] Department of Public Health, Semmelweis University, Budapest, Hungary
[j] Department of Health Promotion Sciences, College of Public Health, University of Oklahoma Health Sciences Center, Oklahoma City, OK, USA

ARTICLE INFO

Keywords:
Oxidative stress
ROS
Endothelial dysfunction
Functional hyperemia
Microcirculation

ABSTRACT

Adjustment of cerebral blood flow (CBF) to neuronal activity via neurovascular coupling (NVC) has an essential role in maintenance of healthy cognitive function. In aging increased oxidative stress and cerebromicrovascular endothelial dysfunction impair NVC, contributing to cognitive decline. There is increasing evidence showing that a decrease in NAD^+ availability with age plays a critical role in a range of age-related cellular impairments but its role in impaired NVC responses remains unexplored. The present study was designed to test the hypothesis that restoring NAD^+ concentration may exert beneficial effects on NVC responses in aging. To test this hypothesis 24-month-old C57BL/6 mice were treated with nicotinamide mononucleotide (NMN), a key NAD^+ intermediate, for 2 weeks. NVC was assessed by measuring CBF responses (laser Doppler flowmetry) evoked by contralateral whisker stimulation. We found that NVC responses were significantly impaired in aged mice. NMN supplementation rescued NVC responses by increasing endothelial NO-mediated vasodilation, which was associated with significantly improved spatial working memory and gait coordination. These findings are paralleled by the sirtuin-dependent protective effects of NMN on mitochondrial production of reactive oxygen species and mitochondrial bioenergetics in cultured cerebromicrovascular endothelial cells derived from aged animals. Thus, a decrease in NAD^+ availability contributes to age-related cerebromicrovascular dysfunction, exacerbating cognitive decline. The cerebromicrovascular protective effects of NMN highlight the preventive and therapeutic potential of NAD^+ intermediates as effective interventions in patients at risk for vascular cognitive impairment (VCI).

1. Introduction

Maintenance of cerebral homeostasis requires a tightly-controlled supply of oxygen and nutrients as well as washout of harmful metabolites through uninterrupted cerebral blood flow (CBF), which represents 15% of cardiac output [1]. The human brain comprises only 2% of the body's mass, yet it accounts for 20% of the resting total body O_2 consumption. The brain has limited energy reserves and cerebral

* Corresponding author. Reynolds Oklahoma Center on Aging, Department of Geriatric Medicine University of Oklahoma Health Sciences Center 975 NE 10th Street, BRC 1311 Oklahoma City, OK 73104, USA.
E-mail address: zoltan-ungvari@ouhsc.edu (Z. Ungvari).

https://doi.org/10.1016/j.redox.2019.101192
Received 22 February 2019; Received in revised form 2 April 2019; Accepted 7 April 2019
Available online 10 April 2019

oxygen content can sustain unimpeded neuronal function for only a short time if CBF decreases [2]. Thus, during periods of intense neuronal activity there is a requirement for rapid adjustment of regional oxygen and glucose delivery to metabolic demand through spatially localized adaptive increases in CBF. This is ensured by an evolutionarily conserved physiological mechanism known as neurovascular coupling (NVC) or functional hyperemia [1]. The cellular mechanisms of NVC include release of vasodilator NO from the microvascular endothelium, in response to increased neuronal and astrocytic activation [3,4].

It is now increasingly recognized that (micro)vascular contributions to cognitive impairment and dementia (VCID) play a critical role in elderly patients [1]. There is growing evidence that NVC responses are compromised both in elderly subjects [5–8] and aged laboratory animals [4,9], which may importantly contribute to the age-related decline in higher cortical function, including cognition [10] and gait performance [11]. This concept is supported by recent findings that pharmacologically induced neurovascular dysfunction in mice mimics important aspects of age-related cognitive impairment [12]. Further, our recent studies demonstrate that rescue of NVC responses by treatment with the mitochondria-targeted antioxidative peptide SS-31 [13] or pharmacological SIRT1 activators [4,14] mitigates cognitive impairment in aged mice. These successful preclinical studies provide proof-of-concept that development of translationally relevant therapeutic interventions that target molecular/cellular mechanisms contributing to age-related neurovascular dysfunction is feasible for prevention/treatment of cognitive impairment in elderly patients [4].

NAD^+ is a rate-limiting co-substrate for sirtuin enzymes, which are key regulators of pro-survival pathways and mitochondrial function in the endothelial cells [15–18]. There is increasing evidence that with age cellular NAD^+ availability decreases [19,20], which is a critical driving force in aging processes. In support of this theory it was demonstrated that enhancing NAD^+ biosynthesis extends lifespan in lower organisms [21] and improves health-span in mouse models of aging [22]. There is particularly strong evidence that in aged mice enhancing NAD^+ biosynthesis by treatment with nicotinamide mononucleotide (NMN; a key NAD^+ intermediate) [23] reverses age-related dysfunction in multiple organs, including the eye [24], skeletal muscle [19] and peripheral arteries [15,25]. A key mechanism underlying the anti-aging action of NMN treatment is reversing age-related decline in mitochondrial function [24]. Although there is strong evidence that mitochondrial dysfunction and increased mitochondrial oxidative stress contribute to cardiovascular dysfunction [26–28] and neurovascular impairment in aging [13], the potential protective effects of NMN on the aged cerebral microvasculature and NVC responses have not been investigated.

The present study was designed to test the hypothesis that NMN supplementation can rescue neurovascular coupling responses in aged mice by attenuating mitochondrial oxidative stress in cerebromicrovascular endothelial cells. To achieve this goal, aged mice were treated with NMN for two weeks. Mice were behaviorally evaluated on a battery of tests for characterization of cognitive function and motor coordination, which are sensitive to alterations in NVC responses. Then, functional tests for NVC responses and cerebromicrovascular endothelial function were performed. Markers of oxidative stress and expression of genes regulating neurovascular coupling responses, antioxidant defenses and mitochondrial function were assessed. To substantiate the *in vivo* findings the effects of NMN on mitochondrial ROS production and mitochondrial bioenergetics in cerebromicrovascular endothelial cells derived from aged animals were obtained *in vitro*.

2. Material and methods

2.1. Animals, NMN supplementation

Young (3 month, n = 30) and aged (24 month, n = 40) male C57BL/6 mice were purchased from the aging colony maintained by the National Institute on Aging at Charles River Laboratories (Wilmington, MA). Animals were housed under specific pathogen-free barrier conditions in the Rodent Barrier Facility at University of Oklahoma Health Sciences Center under a controlled photoperiod (12 h light; 12 h dark) with unlimited access to water and were fed a standard AIN-93G diet (ad libitum). Mice in the aged cohort were assigned to two groups (n = 20 each group). One group of the aged mice was injected daily with NMN (i.p. injections of 500 mg NMN/kg body weight per day) or the equivalent volume of PBS for 14 consecutive days at 6 p.m. and 8 a.m. on day 14 and were sacrificed 4 h after last injection. Similar dosages of NMN has been shown to exert potent anti-aging effects on mouse health span [25]. All procedures were approved by the Institutional Animal Use and Care Committees of the University of Oklahoma Health Sciences Center. All animal experiments complied with the ARRIVE guidelines and were carried out in accordance with the National Institutes of Health guide for the care and use of Laboratory animals (NIH Publications No. 8023, revised 1978).

2.2. Behavioral studies

Previous studies suggest that alterations of neurovascular coupling responses associate with changes in cognition as well as sensory-motor function [12,29]. Thus, after the treatment period behavioral tasks were performed to characterize the effect of NMN supplementation on learning and memory, sensory-motor function, gait and locomotion (n = 20 in each group).

2.2.1. Radial arms water maze testing

Spatial memory and long term memory in each group of mice was tested by observing and recording escape latency, distance moved, and velocity during the time spend in the radial arms water maze as described [13,29]. The maze consisted of eight arms 9 cm wide that radiated out from an open central area, with a submerged escape platform located at the end of one of the arms. Paint was added into the water to make it opaque. The maze was surrounded by privacy blinds with extramaze visual cues. Intramaze visual cues were placed at the end of the arms. The mice were monitored by a video tracking system directly above the maze as they waded and parameters were measured using Ethovision software Noldus Information Technology Inc., Leesburg, VA, USA. Experimenters were unaware of the experimental conditions of the mice at the time of testing. During the learning period each day, mice were given the opportunity to learn the location of the submerged platform during two sessions each consisting of four consecutive acquisition trials. On each trial, the mouse was started in one arm not containing the platform and allowed to wade for up to one minute to find the escape platform. All mice spent 30 s on the platform following each trial before beginning the next trial. The platform was located in the same arm on each trial. Over the three days of training, mice in the young control group gradually improved performance as they learned the procedural aspects of the task. Upon entering an incorrect arm (all four paws within the distal half of the arm) or failing to select an arm after 15 s the mouse was charged an error. Learning capability was assessed by comparing performance on days 2 and 3 of the learning period.

2.2.2. Elevated plus maze learning protocol

Mice were also assessed for learning capacity using an elevated plus maze-based learning protocol as previously described [30]. A gray elevated plus maze apparatus was used. Two open arms (25 × 5 cm) and two (25 × 5 cm) closed arms were attached at right angles to a central platform (5 × 5 cm). The apparatus was 40 cm above the floor. Mice were placed individually at the end of an open arm with their back to the central platform. The time for mice to cross a line halfway along one of the closed arms was measured (transfer latency) on day 1 and day 2. Mice had to have their body and each paw on the other side of the line. If a mouse had not crossed the line after 120 s, it was placed

beyond it. After crossing the line, mice had 30 s for exploring the apparatus. Learning was defined as reduced transfer latency on day 2 compared to day 1. Higher relative difference in transfer latency on day 1 and day 2 indicates superior hippocampal function.

2.2.3. Novel object recognition test

The novel object recognition task was also performed to characterize the effect of NMN on learning and memory [12,31]. The results of the test are influenced by both hippocampal and cortical microvascular impairment. The test consists of a habituation phase, acquisition (familiarization) phase, and trial phase. During the habituation phase the animals explored the empty open-field arena for 5 min. Then, in the acquisition phase the mice explore two identical objects for 2 min. After a 4 h delay, a trial phase occurred. During this period animals explored the familiar object and a novel object for 2 min. Exploration of the objects was defined as directing the nose at a distance $\leq$2 cm to the object and/or touching it with the nose. For data collection and analysis Ethovision software (Noldus Information Technology Inc., Leesburg, VA, USA) was used. Sitting or climbing on it was not considered as an exploration. All objects used in this study were made of washable odorless plastic and were different in shapes and colors but identical in size. A percent of time spent exploring the novel object relative to the total time spent exploring both objects was used as a measure of novel object recognition. The Recognition Index (RI, representing the time spent investigating the novel object [T_{novel}] relative to the total object investigation) was used as the main index of retention, which was calculated according to the following formula: [$RI = T_{novel}/(T_{novel} + T_{familiar})$]. The arena and the objects were cleaned with 70% ethanol between the trials to prevent the existence of olfactory cues.

2.2.4. Rotarod performance

Motor coordination was assessed in each group of mice by using an automated four-lane rotarod (Columbus Instruments, Columbus, OH) as described [12]. In brief, mice were pre-trained by placing them on the moving rotarod at 10 r.p.m. until they performed at this speed for 120 s. On the day of testing, mice were habituated in their home cages and acclimate to the testing room for at least 15 min. The test phase consisted of 3 trials (separated by 15 min inter-trial intervals). The testing apparatus was set to accelerate from 4 to 40 r.p.m. in 300 s. One mouse was then placed on each lane and the rotarod was started with an initial rotation of 4 r.p.m. The rotational velocity was set to increase every 10 s and the latency to fall was recorded. Latency to fall was recorded in seconds by an infra-red beam across the fall path along with the max r.p.m. sustained by each mouse [32].

2.2.5. Grip strength test

A grip strength test was used to measure the maximal muscle strength of forelimbs of the mice [12]. Forelimb grip strength was assessed using a grip strength meter (Chatillon Ametek Force Measurement, Brooklyn, New York). The strength measurements of each group of mice were measured three times by the same investigator. The maximum grip strength values were used for subsequent analysis.

2.2.6. Analysis of gait function

To determine how aging and NMN treatment affect gait coordination, we tested the animals using an automated computer assisted method (CatWalk; Noldus Information Technology Inc. Leesburg, VA) as described [13,29,33]. Using the CatWalk system the detection of paw print size, pressure and pattern during volunteer running on an illuminated glass walkway by a camera placed under the glass surface provides an automated analysis of gait function and the spatial and temporal aspects of interlimb coordination [12,34]. Briefly, animals were trained to cross the walkway and then, in a dark and silent room (< 20 lux of illumination), animals were tested in three consecutive runs. Data were averaged across ten runs in which the animal maintained a constant speed across the walkway. After manual identification and labeling of each footprint, spatial and temporal indices of gait were calculated (including swing speed, cadence, regularity index, brake and propulsion phase duration, stand index, duty cycle; size-adjusted base of support, stride length and distance between ipsilateral prints; stride length and stride time coefficient of variance, interlimb couplings).

2.3. Measurement of neurovascular coupling responses and cerebral blood flow

After behavioral testing, mice in each group were anesthetized with isoflurane (4% induction and 1% maintenance), endotracheally intubated and ventilated (MousVent G500; Kent Scientific Co, Torrington, CT). A thermostatic heating pad (Kent Scientific Co, Torrington, CT) was used to maintain rectal temperature at 37 °C [4]. End-tidal CO_2 was controlled between 3.2% and 3.7% to keep blood gas values within the physiological range, as described [12,35]. The right femoral artery was canulated for arterial blood pressure measurement (Living Systems Instrumentations, Burlington, VT) [4]. The blood pressure was within the physiological range throughout the experiments (90–110 mmHg). Mice were immobilized and placed on a stereotaxic frame (Leica Microsystems, Buffalo Grove, IL) and the scalp and periosteum were pulled aside. Mice were equipped with an open cranial window and changes in CBF were assessed above the left barrel cortex using a laser Doppler probe (Transonic Systems Inc., Ithaca, NY), as described [4,12,35]. The cranial window was superfused with artificial cerebrospinal fluid (ACSF, composition: NaCl 119 mM, $NaHCO_3$ 26.2 mM, KCl 2.5 mM, NaH_2PO_4 1 mM, $MgCl_2$ 1.3 mM, glucose 10 mM, $CaCl_2$ 2.5 mM, pH = 7.3, 37 °C). The right whisker pad was stimulated by a bipolar stimulating electrode placed to the ramus infraorbitalis of the trigeminal nerve and into the masticatory muscles. The stimulation protocol used to investigate neurovascular coupling consisted of 10 stimulation presentation trials with an intertrial interval of 70 s, each delivering a 30-s train of electrical pulses (2 Hz, 0.2 mA, intensity, and 0.3 ms pulse width) to the mystacial pad after a 10-s prestimulation baseline period. Changes in CBF were averaged and expressed as percent (%) increase from the baseline value [36]. Experiments lasted ~20–30 min/mouse, which permitted stable physiological parameters to be obtained. To assess the role of NO mediation, CBF responses to whisker stimulation were repeated in the presence of the nitric oxide synthase inhibitor N^{ω}-Nitro-L-arginine methyl ester (L-NAME; 3×10^{-4} moL/L, 20 min). In separate experiments CBF responses to whisker stimulation were obtained before and after topical administration of the mitochondrial antioxidant mitoTEMPO (10^{-5} moL/L). To assess microvascular endothelial function, CBF responses to topical administration of acetylcholine (ACh; 10^{-5} moL/L) were obtained before and after topical administration of the mitochondrial antioxidant mitoTEMPO (10^{-5} moL/L).

Basal CBF was assessed in a separate cohort of control and experimental mice (n = 5 in each group) anesthetized with isoflurane using arterial spin labeling magnetic resonance imaging following published protocols [33].

In each study the experimenter was blinded to the treatment of the animals. At the end of the experiments the animals were transcardially perfused and decapitated. The brains were immediately removed and pieces of the somatosensory and motor cortex were isolated and frozen for subsequent analysis. All reagents used in this study were purchased from Sigma-Aldrich (St Louis, MO) unless otherwise indicated.

2.4. Assessment of the effect of NMN supplementation on markers of oxidative stress

To characterize the effect of NMN treatment on cellular redox homeostasis in aging, 3-nitrotyrosine (3-NT, a marker for peroxynitrite action) was assessed in homogenates of cortical samples using OxiSelect

Protein Nitrotyrosine ELISA Kits (Cell Biolabs), according to the manufacturer's guidelines, as previously described [4]. In the microcirculation of aged rodents endothelium-derived NO was shown to react with $O_2^{\cdot-}$ forming $ONOO^-$ thus decreasing the bioavailability of NO [37,38]. Previously we showed that aged mouse brains exhibit an increased 3-nitrotyrosine content [4], a biomarker of increased $ONOO^-$ formation, suggesting that impaired endothelial mediation of cerebromicrovascular dilation in aging is due to increased scavenging of vasodilator NO [9].

As an additional marker of oxidative stress, 8-isoprostane content in the cortical tissue was measured using the 8-isoprostane EIA kit (Cayman Chemical Company, Ann Arbor, MI) according to the manufacturer's guidelines as previously reported [4].

2.5. Assessment of endothelial function in the aorta

To assess the specific effect of NMN treatment on endothelial function, endothelium-dependent vasorelaxation was assessed in isolated aorta ring preparations as described previously [39]. In brief, aortas were cut into ring segments 1.5 mm in length and mounted in myographs chambers (Danish Myo Technology A/S, Inc., Denmark) for measurement of isometric tension. The vessels were superfused with Krebs buffer solution (118 mM NaCl, 4.7 mM KCl, 1.5 mM $CaCl_2$, 25 mM $NaHCO_3$, 1.1 mM $MgSO_4$, 1.2 mM KH_2PO_4, and 5.6 mM glucose; at 37 °C; gassed with 95% air and 5% CO_2). After an equilibration period of 1 h during which an optimal passive tension was applied to the rings (as determined from the vascular length-tension relationship), they were pre-contracted with 10^{-6} M phenylephrine and relaxation in response to acetylcholine was measured.

2.6. Assessment of vascular oxidative stress

To characterize vascular ROS production isolated segments of the aorta were loaded with the redox sensitive dye dihydroethidium (DHE, Invitrogen, Carlsbad CA; 3×10^{-6} moL/L; for 30 min) in oxygenated Krebs' solution (at 37 °C) as previously reported [34,39–42]. After loading the dye was washed out five times with warm Krebs buffer, and the vessels were allowed to equilibrate for another 20 min. Then, the vessels were embedded in OCT medium and cryosectioned. Confocal images were captured using a Leica SP2 confocal laser scanning microscope (Leica Microsystems GmbH, Wetzlar, Germany). Average nuclear DHE fluorescence intensities were assessed using the Metamorph software (Molecular Devices LLC, Sunnyvale, CA) and values for each animal in each group were averaged.

2.7. Measurement of vascular and endothelial NAD^+ levels

To confirm efficiency of NMN treatment, NAD^+ levels were measured in snap frozen aortas from young and aged mice using a bioluminescent assay (NAD/NADH-Glo Assay; Promega, Madison, WI), according to the manufacturer's instructions. Briefly, tissue was homogenized in PBS and lysed in a base solution with 1% DTAB. To measure the levels of the oxidized form, HCl was added to the solution and heated for 15 min at 60 °C. The luminescence signal was detected with a Tecan Infinite M200 plate reader. A similar protocol was followed for cultured endothelial cells (see below). Protein quantification was used for normalization purposes.

2.8. Establishment and characterization of primary CMVEC cultures

To evaluate the anti-aging action of NMN *in vitro*, we assessed the effects of NMN on cellular mtROS production and mitochondrial phenotype in cultured primary cerebromicrovascular endothelial cells (CMVECs). The establishment and characterization of the CMVEC strains used has been recently reported [4]. In brief, to establish primary cultures of CMVECs, the brains of male 3 and 24 month old F344xBN rats (obtained from the National Institute on Aging) were removed aseptically, rinsed in ice cold PBS and minced into ≈1 mm squares. The tissue was washed twice in ice cold 1X PBS by low-speed centrifugation (50 g, 2–3 min). The diced tissue was digested in a solution of collagenase (800U/g tissue), hyaluronidase (2.5U/g tissue) and elastase (3U/g tissue) in 1 ml PBS/100 mg tissue for 45 min at 37 °C in a rotating humid incubator. The digested tissue was passed through a 100 μm cell strainer. The single cell lysate was centrifuged for 2 min at 70 g. After removing the supernatant the pellet was washed twice in cold PBS supplemented with 2.5% fetal calf serum (FCS) and the suspension centrifuged at 300 g for 5 min at 4C. To create an endothelial cell enriched fraction the cell suspension was centrifuged using an OptiPrep gradient solution (Axi-Shield, PoC, Norway). Briefly, the cell pellet was resuspended in Hanks' balanced salt solution (HBSS) and mixed with 40% iodixanol thoroughly (final concentration: 17% (w/v) iodixanol solution; ρ = 1.096 g/ml). 2 ml of HBSS was layered on top and centrifuged at 400 *g* for 15 min at 20 °C. Endothelial cells, which banded at the interface between HBSS and the 17% iodixanol layer, were collected. The endothelial cell enriched fraction was incubated for 30 min at 4 °C in the dark with anti-CD31/PE (BD BD Biosciences, San Jose, CA, USA), anti-MCAM/FITC (BD Biosciences, San Jose, CA, USA). After washing the cells twice with MACS Buffer (Milltenyi Biotech, Cambridge, MA, USA) anti-FITC and anti-PE magnetic bead labeled secondary antibodies were used for 15 min at room temperature. Endothelial cells were collected by magnetic separation using the MACS LD magnetic separation columns according to the manufacturer's guidelines (Milltenyi Biotech, Cambridge, MA, USA). The endothelial fraction was cultured on fibronectin coated plates in Endothelial Growth Medium (Cell Application, San Diego, CA, USA) for 10 days. Endothelial cells were phenotypically characterized by flow cytometry (GUAVA 8HT, Merck Millipore, Billerica, MA, USA). Briefly, antibodies against five different endothelial specific markers were used (anti-CD31-PE, anti-erythropoietin receptor-APC, anti-VEGF R2-PerCP, anti-ICAM-fluorescein, anti-CD146-PE) and isotype specific antibody labeled fractions served as negative controls. Flow cytometric analysis showed that after the third cycle of immunomagnetic selection there were virtually no $CD31^-$, CD146-, EpoR- and VEGFR2-cells in the resultant cell populations. All antibodies were purchased from R&D Systems (R&D Systems, Minneapolis, MN, USA).

Primary CMVECs were cultured in custom-made Rat Brain Endothelial Cell Growth Medium (Cell Applications, Inc.) with reduced nicotinamide concentration (11.04 μM). Since the results of assays investigating mtROS, mitochondrial function and ATP concentration are affected by the number of viable cells, cell viability of each population was determined as described [43]. To assess the direct effects of NMN on endothelial mitochondrial function primary CMVECs derived from young and aged rats were treated with NMN (Santa Cruz, Dallas, TX) *in vitro* (5×10^{-4} moL/L; for 1–5 days).

2.9. SIRT1 and SIRT2 shRNA transfection

To determine the role of sirtuin signaling in the anti-aging endothelial effects of NMN treatment, the downregulation of SIRT1 and SIRT2, key anti-aging proteins whose activity is regulated by NAD levels, in CMVECs was achieved by RNA interference using proprietary, tested SIRT1 and SIRT2 short hairpin RNA (shRNA) sequences (GeneCopoeia, Rockville, MD). CMVECs were transfected using the electroporation-based Amaxa Nucleofector technology (Amaxa, Gaithersburg, MD), as we have previously reported [16,18]. Experiments were performed on day 2 after the transfection when gene silencing was optimal.

2.10. Measurement of mitochondrial ROS production and endothelial H_2O_2 and NO release

The assess the effect of NMN treatment on age-related

mitochondrial oxidative stress, mitochondrial production of ROS (mtROS) in CMVECs was measured using MitoSOX Red (Invitrogen/Thermo Fisher Scientific), a mitochondrion-specific hydroethidine-derivative fluorescent dye [27,28,44–48]. In brief, cells were incubated with MitoSox (5×10^{-6} moL/L; for 30 min, at 37 °C, in the dark). The cells were then washed with PBS and MitoSox fluorescence was measured by flow cytometry (GUAVA 8HT, Merck Millipore, Billerica, MA, USA).

In separate experiments, the effect of NMN treatment on age-related increases in cellular H_2O_2 production was measured fluorometrically in CMVECs using the Amplex red/horseish peroxidase assay as described [45]. The H_2O_2 generation rate was compared by measuring the time course of the buildup of resorufin fluorescence for 60 min by a Tecan Infinite M200 plate reader.

To assess the effect of NMN treatment on age-related decline in NO release, the production of NO in CMVECs was measured using the fluorescent indicator DAF-FM (4-amino-5-methylamino- 2′,7′-difluorescein; 5 μmoL/L for 30 min at 37 °C; Invitrogen/Thermo Fisher Scientific).

2.11. Measurement of mitochondrial membrane potential

To further elucidate the effects of NMN on mitochondrial function, we determined how it impacts mitochondrial membrane potential in CMVECs using the mitochondrial membrane potrential indicator fluorescent dye JC-1 (Guava Technologies, Hayward, CA). JC-1 is a cationic carbocyanine dye that accumulates in energized mitochondria. When it is present in its monomer form in the mitochondria at low concentrations (due to low mitochondrial potential), the dye exhibits green fluorescence. When it accumulates in the energized mitochondria and forms J-aggregates at higher concentrations (due to high mitochondrial potential), it exhibits red fluorescence. These characteristics render JC-1 a sensitive marker for mitochondrial membrane potential: a decrease in the aggregate red fluorescence and an increase in monomer green fluorescence is indicative of depolarization whereas an increase in the aggregate red fluorescence and a decrease in monomer green fluorescence is indicative of hyperpolarization. Cells were labeled with JC-1 for 30 min at 37 °C and fluorescence was analyzed with glow cytometry. The red/green fluorescence ratio was calculated as an indicator of mitochondrial membrane potential.

2.12. Mitochondrial bioenergetics assay

To substantiate the endothelium-protective effect of NMN, we performed real-time measurements of the oxygen consumption rate (OCR; a marker of oxidative phosphorylation) in young and aged CMVECs after treatment with NMN (5×10^{-4} mM NMN, for 5 days) using a Seahorse XF96 extracellular flux analyzer.

In brief, CMVECs were seeded into XF96 cell culture microplates in Seahorse XF-Assay media (Agilent Technologies) supplemented with 25 mM glucose and 1 mM sodium pyruvate (pH 7.4) the day before the assay. Plates were maintained for 45 min at 37 °C in 0% CO_2 prior to the measurement. Basal respiration, coupling efficiency, and spare respiratory capacity were compared using the Mito Stress Test Kit following the manufacturer's protocol. OCR was monitored before and after the addition of the electron transport inhibitors oligomycin (1.0 μM) and FCCP (1.0 μM), an ionophore that is a mobile ion carrier, and a mixture of antimycin-A (1.0 μM) (which is a complex III inhibitor) and rotenone (1.0 μM), a mitochondrial inhibitor that prevents the transfer of electrons from the Fe–S center in complex I to ubiquinone. Basal respiration (baseline respiration minus antimycin-A post injection respiration), ATP synthesis coupled respiration (baseline respiration minus oligomycin post injection respiration), maximal respiratory capacity (FCCP stimulated respiration minus antimycin-A post injection respiration) and reserve respiratory capacity (FCCP stimulated respiration minus baseline respiration) were calculated. Sample protein content was used for normalization purposes.

2.13. Quantification of ATP levels

To correlate these observed changes in OCR directly to ATP production, we also measured cellular ATP concentration in CMVECs. ATP levels in endothelial cells were assessed using the ENLITEN ATP bioluminescent assay (Promega) according to the manufacturer's instructions. Briefly, CMVEC were seeded in 96-well plates (for 24 h at 37 °C under 5% CO_2). For ATP determination the cells were homogenized in Passive Lysis Buffer (Promega). The samples were diluted 1:10 and mixed with an equal volume of the luciferase reagent. The plates were incubated at room temperature for 10 min and then the luminescence signal was detected with a Tecan Infinite M200 plate reader. ATP quantification was carried out from a standard curve using ATP disodium salt hydrate. BCA protein determination was performed for normalization purposes. Cell viability of each population was determined by flow cytometry (Guava easyCyte 8HT) to ensure similar viability of CMVECs in each group in a parallel experiment using the ViaCount Assay (Millipore).

2.14. Electron microscopy

Brains (n = 5 animals in each group) were perfusion fixed under 100 mmHg pressure using Karnowsky's method [49]. Thin sections were obtained with an ultramicrotome, stained with osmium tetroxide, and examined with a transmission electron microscope as previously described [50]. Mitochondrial volume densities were obtained in a blinded fashion using the principles of Weibel [51]. Data were expressed as relative changes in volume density (volume of mitochondria per cytoplasmic volume).

2.15. Measurement of mitochondrial DNA content in CMVECs

Total DNA was isolated from CMVECs using the QIAamp DNA Mini QIAcube Kit (QIAGEN). Mitochondrial DNA (mtDNA) copy number was determined by qPCR as described [17], using cytochrome oxidase III and β-actin as markers for the copy numbers of mtDNA and genomic DNA, respectively.

2.16. Quantitative real-time RT-PCR

A quantitative real time RT-PCR technique was used to analyze mRNA expression of genes relevant for neurovascular impairment and age-related mitochondrial dysfunction in cortical, cerebrovascular, aortic and endothelial samples using validated TaqMan probes (Applied Biosystems) and a Strategen MX3000 platform, as previously reported [4,35,52]. Targets included the nitric oxide synthases eNOS and nNOS (*Nos3* and *Nos1*, respectively), arginases (*Arg1, Arg2*; which regulate NO synthase activity and were proposed to contribute to endothelial dysfunction in aging [53]), antioxidant enzymes, enzymes involved in NAD metabolism and nuclear- and mitochondrion-encoded subunits of the electron transport chain. In brief, total RNA was isolated with a Mini RNA Isolation Kit (Zymo Research, Orange, CA) and was reverse transcribed using Superscript III RT (Invitrogen) as described previously [35]. Quantification was performed using the efficiency-corrected ΔΔCq method. The relative quantities of the reference genes *Hprt, Ywhaz, B2m*, *Actb* and S18 were determined and a normalization factor was calculated based on the geometric mean for internal normalization. Fidelity of the PCR reaction was determined by melting temperature analysis and visualization of the product on a 2% agarose gel.

2.17. Quantitative mass spectrometry analysis

Selective reaction monitoring (SRM) mass spectrometry was used to quantify vascular anti-oxidant protein expression, as previously

described [54]. For these assays, 60-μg amounts of aorta lysates were mixed with 8 pmol of bovine serum albumin (BSA) as an internal standard and 50 μl of 10% SDS. The samples were heated at 80 °C for 15 min before precipitating the proteins in 80% acetone overnight at −20 °C. The protein pellet was dissolved in 60 μl of sample buffer and a 20-μl aliquot containing 20 μg of protein run 1.5 cm into a 12.5% SDS-polyacrylamide gel. The gel was fixed and stained with GelCode Blue (Pierce). For each sample, the entire 1.5-cm lane was cut out of the gel and divided coarsely. The gel pieces were washed to remove the stain, reduced with DTT, alkylated with iodoacetamide, and digested with 1 μg of trypsin overnight at room temperature. The peptides produced in the digest were extracted with 50% methanol, 10% formic acid in water. The extract was evaporated to dryness and reconstituted in 150 μl of 1% acetic acid in water for analysis. The samples were analyzed using SRM with a triple quadrupole mass spectrometer (ThermoScientific TSQ Vantage) configured with a splitless capillary column HPLC system (Eksigent, Dublin, CA, USA). Samples (10 μl) were injected onto a 10 cm × 75 μm C18 capillary column (Phenomenex, Jupiter C18). The column was eluted at 160 nL/min with a 30-min linear gradient of acetonitrile in 0.1% formic acid. Data were processed by using Pinpoint to find and integrate the correct peptide chromatographic peaks. The response for each protein was taken as the total response for all peptides monitored. To quantify protein expression, the relative abundance of each protein was first normalized to the BSA internal standard and then normalized to the geometric mean of cellular reference proteins [54].

2.18. Statistical analysis

Statistical analysis was carried out by one-way ANOVA followed by Tukey's post hoc test or unpaired *t*-test, as appropriate. Dose-response curves for vascular relaxations were analyzed by two-way ANOVA for repeated measures followed by Bonferroni multiple comparison test. A p value less than 0.05 was considered statistically significant. Data are expressed as mean ± S.E.M.

3. Results

3.1. NMN supplementation rescues NVC responses in aged mice by restoring endothelial NO mediation

CBF responses in the whisker barrel cortex elicited by contralateral whisker stimulation were significantly decreased in aged mice compared to young animals indicating impaired NVC in aging (representative CBF tracings are shown in Fig. 1A, summary data are shown in Fig. 1B) [9]. We found that a 14-day treatment with NMN significantly increased CBF responses induced by contralateral whisker stimulation in aged mice, restoring NVC to levels observed in young mice (Fig. 1A–B). Further, perfusion mapping of cerebral coronal slices in each group of animals was performed by MRI. We found that basal CBF was decreased in aged mice as compared to young animals. NMN treatment significantly increased CBF in aged mice (Supplemental Fig. S1).

There is strong experimental evidence, obtained using both pharmacological inhibitors and genetically modified animals, that NO production by the microvascular endothelium plays a critical role in NVC responses and that cerebromicrovascular endothelial dysfunction significantly contributes to age-related neurovascular uncoupling [3,4]. Accordingly, in untreated aged animals administration of the NO synthase inhibitor L-NAME was without effect, whereas in young mice it significantly decreased NVC responses, eliminating the differences between the age groups (Fig. 1B). In NMN treated aged mice L-NAME significantly decreased CBF responses elicited by whisker stimulation (Fig. 1B), suggesting that NMN treatment restored the NO mediation of NVC in aged animals. To further ascertain the endothelial protective effects of NMN supplementation, endothelium-dependent vasodilator responses to acetylcholine were tested. In young mice topical administration of acetylcholine resulted in significant CBF increases, whereas these responses were significantly attenuated in aging mice. Treatment of aged mice with NMN significantly improved acetylcholine-induced vasodilation (Fig. 1C).

Previously we found that treatment with the mitochondria-targeted antioxidative peptide SS-31 can improve both NVC responses and acetylcholine-induced vasodilation in the brains of aged mice [13]. Our results showing that treatment with MitoTEMPO also restores NVC responses and acetylcholine-induced responses in aged mice extend these findings (Supplemental Fig. S2). Similar findings were obtained in isolated aorta ring preparations from aged mice supplemented with NMN (Fig. 1E). To assess the role of endothelium-derived NO, L-NAME was applied. L-NAME significantly inhibited acetylcholine-induced vasorelaxation, eliminating the differences between the three groups. These finding suggests that NMN significantly improves endothelial function by restoring endothelial NO mediation in aged vessels, extending recent findings [25]. Efficiency of NMN treatment was confirmed by demonstration of increased vascular NAD^+ levels (Fig. 1F). NMN treatment attenuated age-related increases in oxidative/nitrosative stress, as indicated by the reduced tissue 3-nitrotyrosine (Fig. 1D) and isoprostane (Supplemental Fig. S3, panel A) levels and vascular DHE staining (Supplemental Fig. S3, panel B), whereas it did not affect mRNA and protein expression of NO synthases or antioxidant enzymes (Supplemental Figs. S4 and S5, respectively). The effects of aging on expression of *Nmnat1, Nmnat3* and *Nampt* in cerebral vessels and aortas are shown in Supplemental Fig. S6 panels A and B.

3.2. NMN attenuates mitochondrial oxidative stress and improves mitochondrial bioenergetics in aged cerebromicrovascular endothelial cells

To substantiate the endothelial protective effects of NMN *in vitro*, we assessed the effects of NMN on cellular mtROS production in cultured primary cerebromicrovascular endothelial cells (CMVECs) derived from aged animals using the MitoSox fluorescence method. First we demonstrated that in aged CMVECs NAD^+ content was significantly decreased, whereas it was normalized by treatment with NMN (Fig. 2A). We found that in aged CMVECs mtROS production was significantly increased as compared to that in CMVECs derived from young animals (Fig. 2B and C), which associated with a decreased production of NO (DAF fluorescence; Fig. 2D) as well as impaired mitochondrial membrane potential (Fig. 2E), and decreased ATP levels (Fig. 2F). NMN treatment attenuated mtROS generation (Fig. 2B and C), increased NO production (Fig. 2D), rescued mitochondrial membrane potential (Fig. 2E) and restored cellular ATP content (Fig. 2E) in aged CMVECs, eliminating the difference between the two age groups. NMN treatment also attenuated increased H_2O_2 release from aged CMVECs as measured by the Amplex Red assay (Supplemental Fig. S7). Attenuation of mtROS production in NMN-treated aged CMVECs was associated with significant improvement of both basal and maximal mitochondrial respiration (Fig. 2G–H). Combined shRNA knockdown of SIRT1/SIRT2 prevented the beneficial effects of NMN on mtROS (Fig. 2C), NO production (Fig. 2D), mitochondrial membrane potential (Fig. 2E) and mitochondrial respiration (Fig. 2H) in aged CMVECs. The effects of aging on expression of *Nmnat1, Nmnat3* and *Nampt* in CMVECs are shown in Supplemental Fig. S6 panel C.

3.3. NMN reverses age-related decline in mitochondrially encoded genes without promoting mitochondrial biogenesis

We could exclude that mitochondrial protective effects of NMN are linked to promotion of mitochondrial biogenesis. Using electron microscopy and unbiased morphometric methods we found that mitochondrial volume density in endothelial cells in the cerebral microcirculation was unaffected by NMN treatment (Fig. 3A–D). NMN treatment of aged mice also does not affect mtDNA content in cerebral

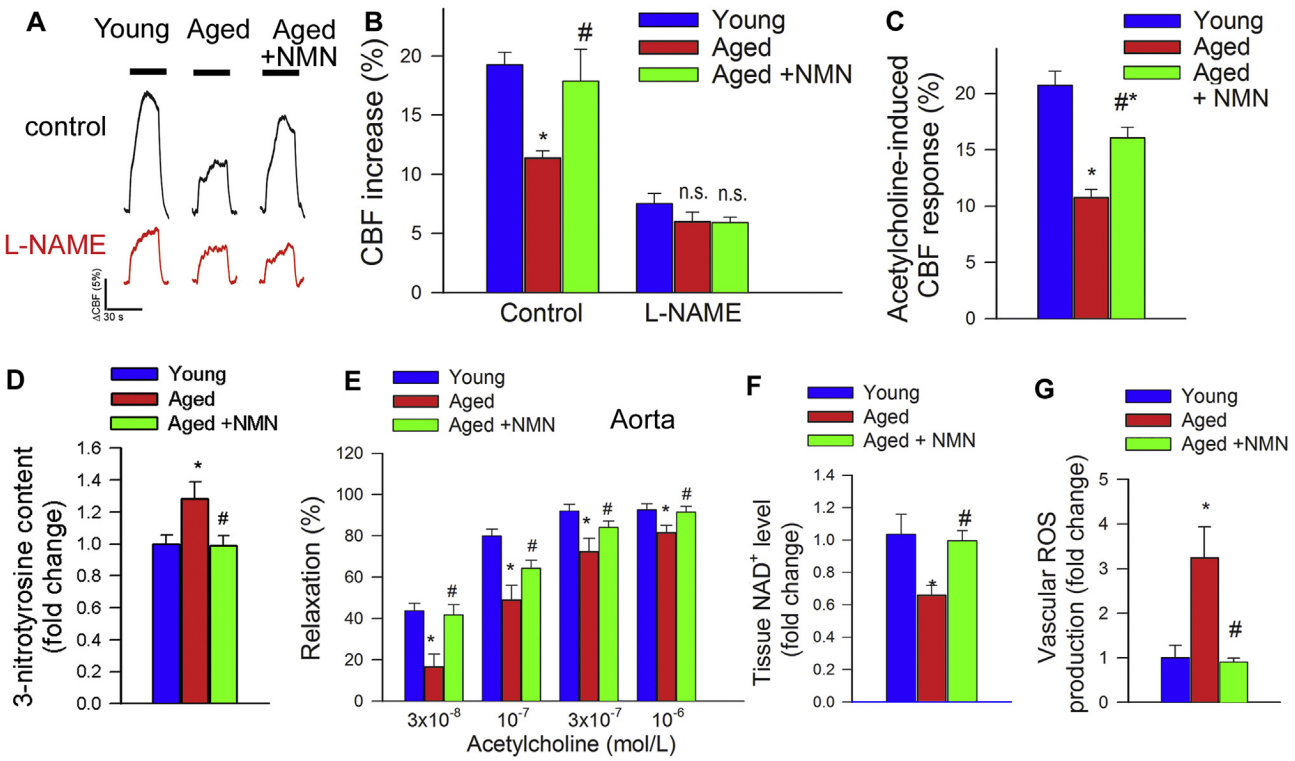

Fig. 1. NMN supplementation improves microvascular endothelial function and rescues NO mediation of neurovascular coupling responses in aged mice. A) Representative traces of cerebral blood flow (CBF; measured with a laser Doppler probe above the whisker barrel cortex) during contralateral whisker stimulation (30 s, 5 Hz) in the absence and presence of the NO synthase inhibitor L-NAME in young (3 month old), aged (24 month old) and NMN treated aged mice. B) Summary data showing that in aged mice NMN supplementation restores NO mediated component of NVC responses. C) In aged mice NMN supplementation improves endothelium-mediated CBF responses elicited by topical perfusion of acetylcholine. D) NMN supplementation decreases protein 3-nitrotyrosine content in the aged cortex, indicating decreased peroxynitrite formation. E-G) In aged mouse aortas NMN supplementation rescues acetylcholine-induced endothelium-mediated relaxation (E), increases tissue NAD^+ levels (F) and attenuates oxidative stress (G; see Methods). Data are mean ± S.E.M. (n = 5–8 for each data point).*P < 0.05 vs. Young; #P < 0.05 vs. Aged. (one-way ANOVA with post-hoc Tukey's test). n.s.: not significant.

arteries (Fig. 3E). Findings obtained in cultured CMVECs showing unaltered mtDNA content after NMN treatment extend the *in vivo* data (Fig. 3F).

Previous studies suggest that age-related decline in oxidative phosphorylation may be due to the specific loss of mitochondrially encoded transcripts [19]. Accordingly, we found that in aged cerebral arteries (Fig. 3G) and aged CMVECs (Supplemental Fig. S8) mRNA expression of mitochondrially encoded components of the electron transport chain was significantly decreased as compared to young ones, whereas those encoded by the nuclear genome remained unchanged with age (Supplemental Fig. S9). Importantly, NMN supplementation partially rescues age-related decreases in mRNA expression of mitochondrially encoded subunits of the electron transport chain both in cerebral arteries (Fig. 3G) and CMVECs (Supplemental Fig. S8).

3.4. Restoration of cerebromicrovascular function is associated with improved cognitive function in aged mice treated with NMN

Recently we demonstrated that specific, pharmacologically-induced neurovascular un-coupling results in detectable cognitive impairment [12]. To determine how rescue of cerebromicrovascular function by NMN supplementation impacts cognitive performance in aged mice, animals were tested in the radial arms water maze (Fig. 4A). We compared the learning performance of mice in each experimental group by analyzing the day-to-day changes in the combined error rate, working memory errors, successful escape rate, path length and time latency. During acquisition, mice from all groups showed a decrease in the combined error rate (Fig. 4B) across days, indicating learning of the task. After the first day of learning young mice consistently had lower combined error rate than aged mice (Fig. 4B). Decreases in the combined error rate induced by NMN supplementation in aged mice reached statistical significance by trial block 6.

To analyze working memory function (short-term memory that is involved in immediate conscious perception) we examined re-entries into incorrect arms (without hidden platform) that were previously attempted for escape. We found that working memory function was impaired in aged mice as compared to young controls (Fig. 4C). Aged mice with NMN supplementation showed significant restoration of working memory to levels comparable to young animals (Fig. 4C). NMN treatment thus resulted in complete behavioral rescue of working memory.

Successful escape rate from the maze was assessed by measuring the percent of animals that could find the hidden platform within the 60 s allowed for each trial. During acquisition, mice from all groups showed an increase in successful escape rate consistent with the learning of the task. Young mice exhibited significantly better escape success than untreated aged mice (Fig. 4D). Although in aged mice NMN treatment tended to increase the successful escape rate, the differences did not reach statistical significance (Fig. 4D).

We also compared path length (i.e. the distance that the mouse swam between maze entry and successful escape through the hidden platform) and escape latency (i.e. the time elapsed between entry and successful escape). During acquisition, mice from all groups displayed shorter path length (Fig. 4E) and lower escape latencies (Fig. 4F), indicating spatial learning. Young mice exhibited shorter path length (Fig. 4E) and lower escape latency (Fig. 4F) than untreated aged mice, which differences became pronounced by day 3. In aged mice NMN supplementation did not affect significantly either path length and

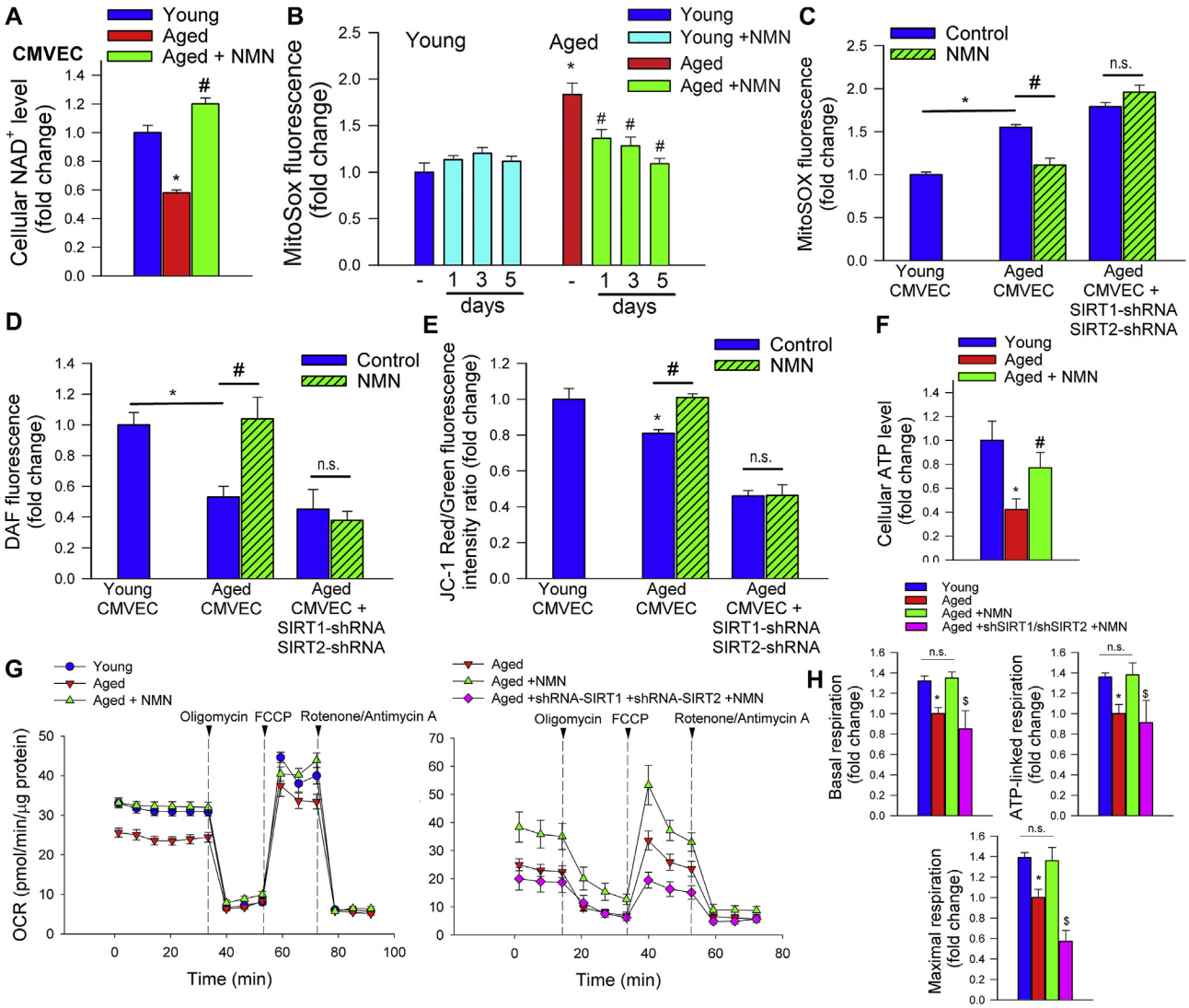

Fig. 2. Treatment with NMN improves mitochondrial energetics and attenuates mitochondrial ROS production in aged cerebromicrovascular endothelial cells (CMVECs). A) Treatment with NMN (5×10^{-4} moL/L; for 5 days) restores NAD^+ levels in primary CMVECs derived from aged rats. B) Treatment with NMN (5×10^{-4} moL/L; for 1–5 days) attenuates age-related increases in mtROS production in CMVECs (MitoSox fluorescence, assessed by flow cytometry). C) shRNA knockdown of SIRT1/SIRT2 prevents NMN-induced attenuation of mtROS in aged CMVECs. D-E) Treatment of aged CMVECs with NMN rescues cellular NO production (D; DAF fluorescence, assessed by flow cytometry) and increases mitochondrial membrane potential (E; JC-1 mitochondrial membrane potential probe) to levels observed in young cells. shRNA knockdown of SIRT1/SIRT2 prevents the NMN effect. F) Treatment of aged CMVECs with NMN restores cellular ATP levels. Data are mean ± S.E.M (n = 5–10 for each data point in A-F). *P < 0.05 vs. Young; #P < 0.05 vs. Aged. G) Attenuation of mtROS production and improved mitochondrial membrane potential in NMN treated aged CMVECs were associated with significant improvement of cellular oxygen consumption rate (OCR; a marker of oxidative phosphorylation; measured using the Seahorse XFe96 analyzer). Vertical dashed lines indicate assay drug injections. OCR in untreated young and aged CMVECs is shown for reference. Note the marked NMN-induced increase in both basal and maximal respiration in aged CMVECs. Right panel shows the effects of shRNA knockdown of SIRT1/SIRT2 on NMN-induced changes in OCR in aged CMVECs. OCR in aged CMVECs transfected with scrambled shRNA is shown for reference. H) Summary data showing the effects of aging and NMN on basal respiration, ATP-linked respiration and maximal respiration. Data are mean ± S.E.M., n = 9 for each data point.*P < 0.05 vs. Young; #P < 0.05 vs. Aged. $ P < 0.05 vs. Aged + NMN (one-way ANOVA with post-hoc Tukey's test). n.s.: not significant.

escape latencies. The analyses of noncognitive parameters revealed a slight age-related decline in swimming speed and an age-dependent increase in non-exploratory behavior (the cumulative time the mice spent not actively looking for the platform, e.g. floating), which were partially normalized toward young control levels by NMN treatment (Fig. 4G and H).

We also evaluated hippocampal-dependent learning and memory employing the elevated plus-maze. For young mice, transfer latency on day 2 was significantly decreased (by ~49%) compared to day 1 (Fig. 5A), indicating an intact learning effect. In contrast, for aged mice the transfer latency on day 1 and day 2 were similar, indicating impaired learning capability. NMN supplementation in aged mice restored learning performance to youthful levels (Fig. 5A).

Subsequently we also tested the performance of the mice in the novel object recognition test. We found no significant difference in the time that mice from each group spent exploring the two identical objects placed at the opposite ends of the arena during the acquisition phase, confirming that the location of the objects did not affect the exploration behavior of mice. In the trial phase with two different objects (one novel, the other familiar), young mice explored the novel object for a significantly longer time period, indicating their memory for the familiar object (Fig. 5B). In contrast, aged mice had a significantly lower calculated Recognition Index (RI). NMN supplementation in aged mice significantly improved their performance,

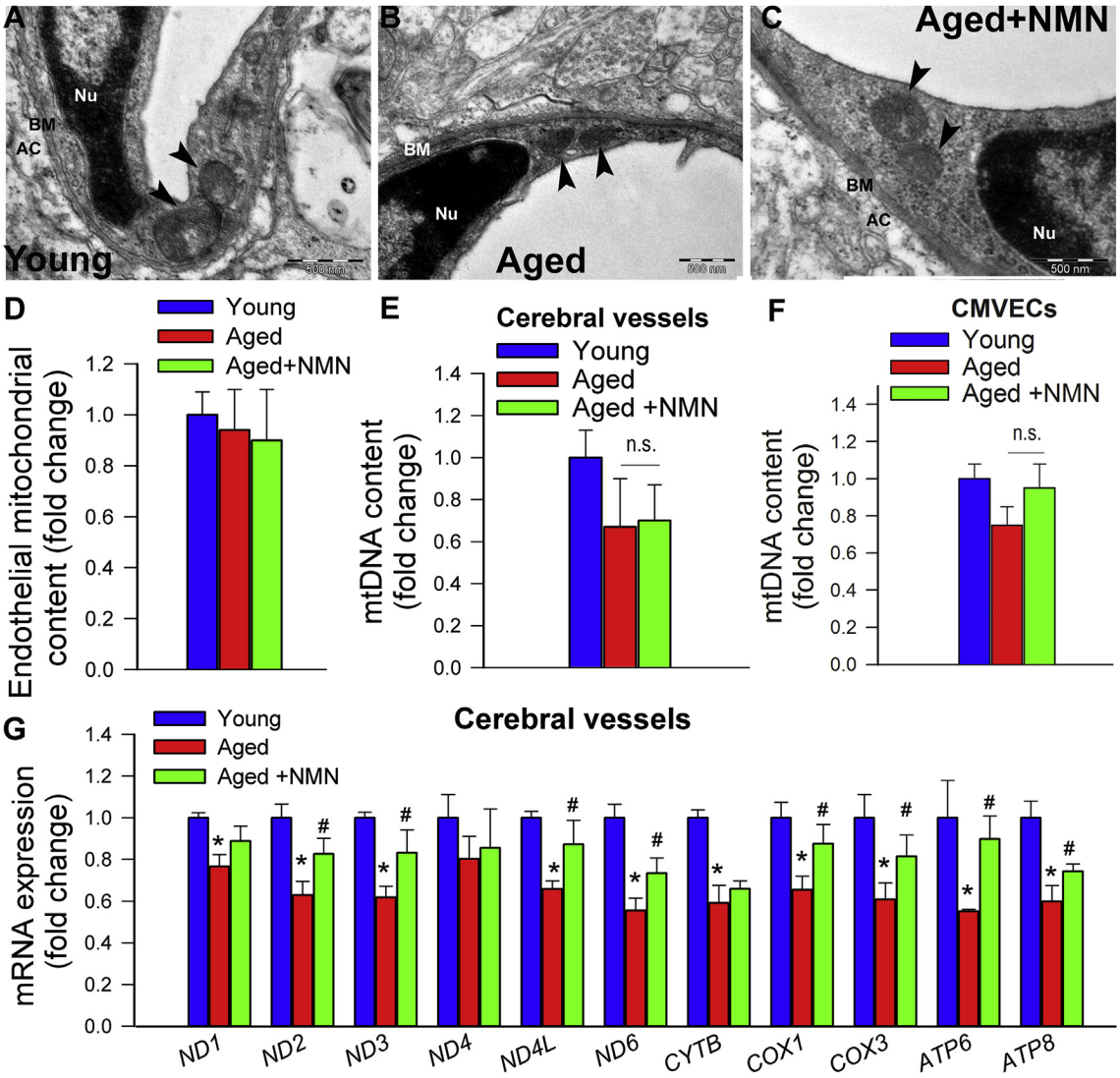

Fig. 3. Treatment with NMN rescues age-related downregulation of mitochondrially encoded subunits of the electron transport chain without promoting mitochondrial biogenesis. A-C) Representative electronmicrographs showing mitochondria in cerebromicrovascular endothelial cells in young (A), aged (B) and NMN treated aged mice (C); (arrowheads, mitochondria; nu, nucleus; bm, basal lamina; AC, astrocyte; scale bar: 500 nm). D) Summary data showing that NMN treatment does not affect mitochondrial volume density in aged cerebromicrovascular endothelial cells. E) NMN treatment of aged mice does affect mtDNA content in cerebral arteries. F) NMN treatment (5×10^{-4} moL/L; for 5 days) of aged CMVECs does not affect mtDNA content. G) NMN supplementation rescues age-related decreases in mRNA expression of mitochondrially encoded subunits of the electron transport chain in cerebral arteries. Data are mean ± SEM (n = 5–6 for each data point in D-G). *P < 0.05 vs. Young; #P < 0.05 vs. Aged. (one-way ANOVA with post-hoc Tukey's test). n.s.: not significant.

which is consistent with an improved hippocampal- and cortical-dependent recognition memory (Fig. 5B).

3.5. NMN supplementation improves gait performance in aged mice

To investigate the effects of age and NMN treatment on the motor performance of mice we measured performance of the accelerating rotarod and grip strength which evaluate muscle strength, balance, and endurance. NMN supplementation did not affect significantly age-related decreases in latency to fall from the rotarod (Fig. 5C) and did not reverse age-related decline in grip strength (Supplemental Fig. S10).

Age-related deficiencies in NVC responses in human patients [11] and animal models of aging [29] have been linked to gait abnormalities. Recent studies also demonstrate that pharmacologically-induced neurovascular uncoupling associates with subclinical gait alterations in mice [33]. To identify age- and treatment-related systematic differences between mouse gait patterns, principal component analysis (PCA) was carried out on the correlation matrix of spatial and temporal indices of gait. This analysis identified three principal components that accounted for ~63% of the variance in the data. We plotted the position of each mouse against the PC1, PC2, and PC3 axis in three-dimensional space (Fig. 5D). The most conspicuous trend was that aged and young mice were well separated along the PC1 axis, whereas NMN treated aged mice were clustered together with young mice. Collectively, the aforementioned results support the view that rescue of NVC by NMN treatment is associated with improved gait performance in aged mice. Selected individual gait parameters are shown in Supplemental Fig. S11.

4. Discussion

The key finding of this study is that short-term treatment with the NAD^+ precursor NMN rescues NVC responses and improves higher brain functions in a mouse model of aging that recapitulates key aspects of cerebromicrovascular dysfunction and cognitive deficit manifested in elderly patients.

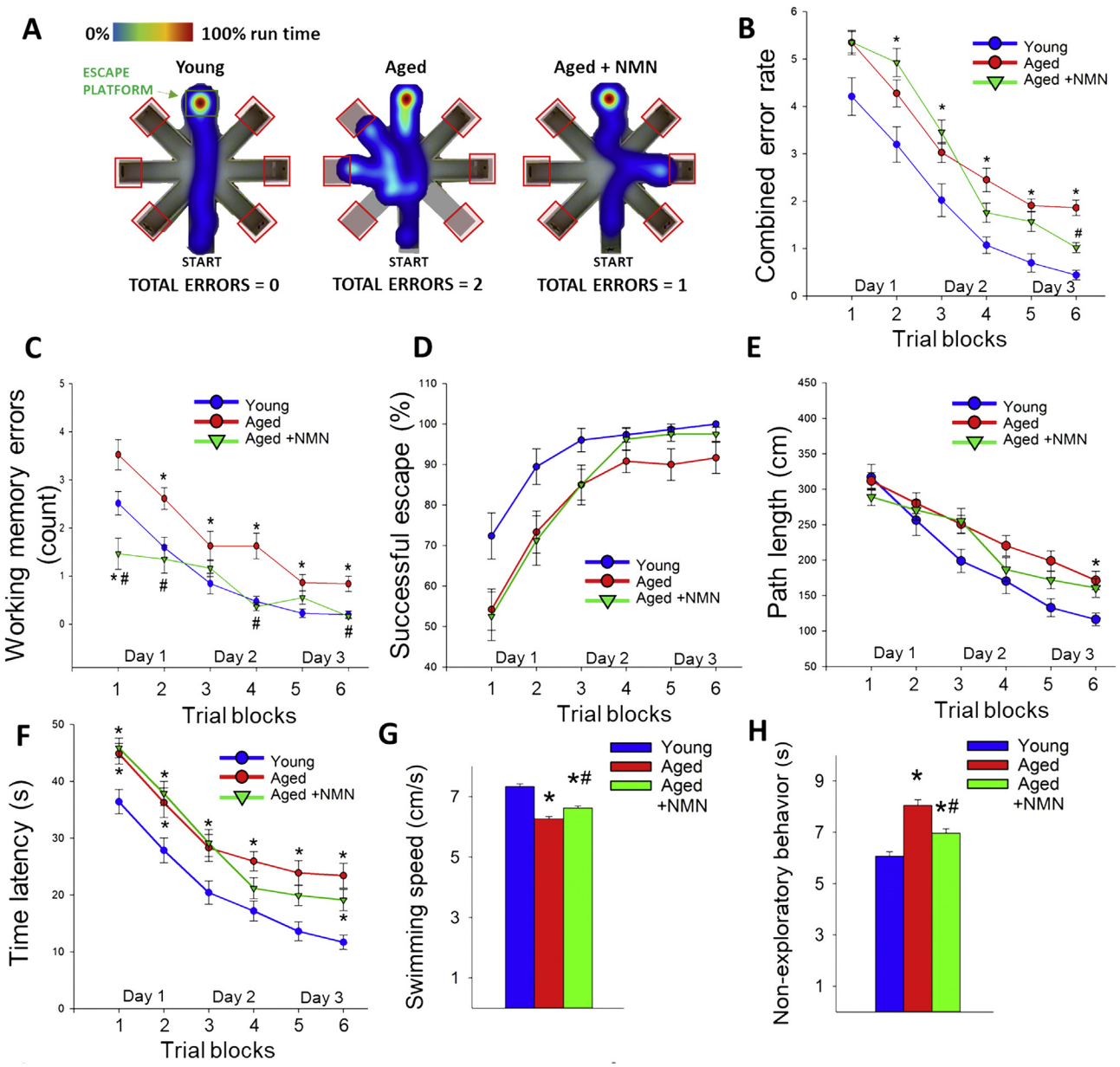

Fig. 4. In NMN treated aged mice rescue of neurovascular coupling responses associates with improved performance in the radial-arm water maze (RAWM). Young (3 month old), aged (24 month old) and NMN treated aged mice were tested in the RAWM. A) Heatmap representing the percentage of time spent in different locations in the maze for a randomly selected animal from each group during experimental day 3. Note that the untreated aged mouse required a greater amount of time and a longer path length in order to find the hidden escape platform. Older mice also re-enter a previously visited arm multiple time, accruing working memory errors. B) Older animals have higher combined error rates throughout day 2 and 3 of the learning phase. Combined error rate is calculated by adding 1 error for each incorrect arm entry as well as for every 15 s spent not exploring the arms. C) Older animals make significantly more working memory errors (repetitive incorrect arm entries) as compared to young mice. In contrast, aged mice treated with NMN perform this task significantly better than untreated aged mice. D) The ratio of successful escapes, averaged across trial blocks, is shown for each group. Note day-to-day improvement in the performance of young mice, which was significantly delayed in aged mice. Although aged mice treated with NMN tended to be more successful at finding the hidden escape platform in comparison to untreated age-matched controls, the difference did not reach statistical significance. Average path length (Panel E) and escape latencies (Panel F) required to reach the hidden platform in the RAWM for trial blocks 1–6. Young mice find the hidden platform sooner while swimming significantly less than aged animals. In aged mice treated with NMN the escape latencies and the average path length required to reach the hidden platform did not differ from that in aged mice. G) NMN had only marginal effect on the swimming speed. H) Aged control mice exhibited longer non-exploratory behavior compared to young mice. Treatment with NMN partially reduces the non-exploratory time to young levels. All data are shown as mean ± SEM. (n = 20 for each data point).

Elucidating the mechanisms by which aging impairs NVC responses is critical for the development of new targets and effective therapies for VCI. Here we show for the first time that NMN supplementation rescues NO mediation of NVC in aged mice supporting the concept that its potent cerebromicrovascular endothelial protective effects contribute significantly to its anti-aging, neuroprotective action. Additional evidence in support of this concept comes from the observations that NMN treatment restores NO release in aged CMVECs *in vitro* and that NMN supplementation also rescues endothelial NO-mediated vasodilation in the aortas of aged mice. Importantly, endothelium-derived NO plays versatile biological roles in addition to its role in vasoregulation. It is a paracrine regulator of cellular metabolism and mitochondrial function, it modulates the function of dozens of proteins by promoting nitrosylation on their cystine residues, it inhibits platelet aggregation,

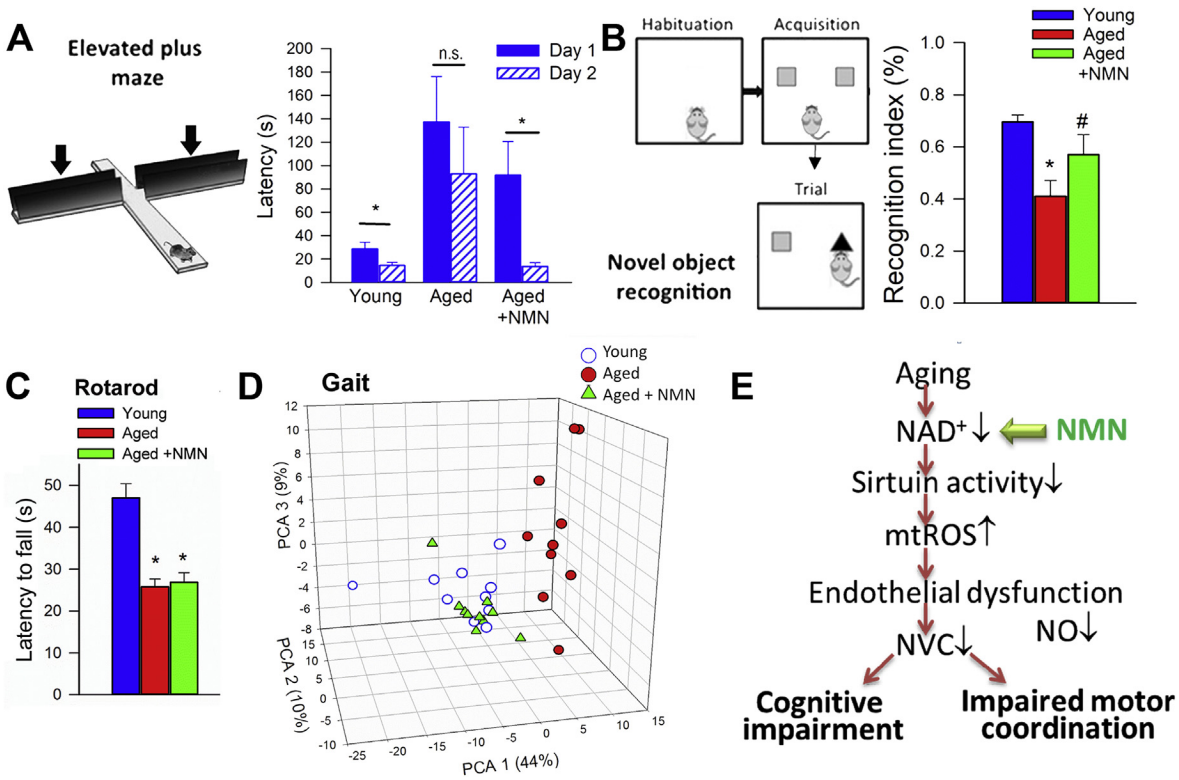

Fig. 5. In NMN treated aged mice rescue of neurovascular coupling responses associates with improved cognitive performance. A) NMN treatment improved learning ability in aged mice, as assessed using the elevated plus maze-based learning protocol (see Methods section). For young mice, transfer latency on day 2 was significantly decreased compared to day 1, indicating an intact learning effect. For aged mice the transfer latency on day 1 and day 2 were similar, indicating impaired learning capability. NMN supplementation in aged mice restored learning performance to youthful levels. B) NMN treatment restored recognition memory in aged mice as measured by the novel object recognition test (see Methods). Recognition memory is expressed as a recognition index which is defined as the ratio of time spent exploring the novel object over the total time spent exploring both familiar and novel objects. C) NMN supplementation in aged mice does not affect mean latencies to fall from the rotarod. All data are shown as mean ± SEM. (n = 20 for each data point). Statistical significance was calculated using one-way ANOVA with Tukey's post hoc test to determine differences among groups. *P < 0.05 vs. Young; #P < 0.05 vs. Aged control. D) NMN supplementation improves gait performance in aged mice. Shown is the 3D triplot of first three principal components (PC) identified by PCA on the correlation matrix of spatial and temporal indices of gait. Each point represents an individual mouse. Note, that mice in the same age groups clustered together. Differences between young and aged mouse gait were evident. NMN supplementation partially reverses age-related changes in mouse gait (MANOVA; P < 0.01 Aged vs. Aged treated; P < 0.01 Young vs. Aged). E) Scheme showing proposed role for increased NAD^+ deficiency and mitochondrial oxidative stress in cerebromicrovascular endothelial impairment and neurovascular dysfunction in aging and their pathophysiological consequences.

smooth muscle cell proliferation and leukocyte adhesion, promotes stability of atherosclerotic plaques and exerts potent anti-inflammatory, anti-apoptotic and pro-angiogenic effects. In that regard it is significant that NMN treatment was also shown to increase capillary density in the skeletal muscle [15]. Thus, rescue of cerebromicrovascular NO bioavailability by treatment with NAD precursors likely has clinical significance beyond restoration of NVC responses, potentially exerting diverse protective effects both on the cerebral vasculature and physiological function of other cell types, including neurons, astrocytes and microglia. The mechanisms underlying age-related decline in NAD^+ in endothelial cells are likely multifaceted and may include down-regulation of NAMPT (which catalyzes the rate limiting step in the biosynthesis of NAD^+) and increased utilization of NAD^+ by activated PARP-1 [55]. Thus, it is possible that combination treatments that simultaneously increase NAD production and inhibit its degradation (e.g. NMN plus a PARP-1 inhibitor) may offer additional benefits for neurovascular protection.

Our studies are the first to demonstrate that NMN treatment effectively attenuates age-related mitochondrial oxidative stress in cerebromicrovascular endothelial cells, suggesting a key role for this mechanism in NAD^+-mediated endothelial protection. In support of this concept using structurally different inhibitors/scavengers of mtROS production, including SS-31[13], resveratrol [4,45] and mitoTEMPO, we have demonstrated that age-related mitochondrial oxidative stress plays a central role in impaired NO mediation of NVC responses in aging. Recovery of endothelial function in aged peripheral arteries has also been reported using the SS-31[13], resveratrol [39] and MitoQ [56]. The mechanisms contributing to mitochondrial oxidative stress in the aged endothelium, which are affected by NMN treatment, are likely multifaceted and involve a dysfunctional electron transport chain. Reduced electron flow through the electron transport chain, in particular due to age-related dysfunction of complex I and complex III [57], likely increases electron leak and favors mtROS production. It is believed that dysregulation of mtDNA-encoded subunits of these complexes contribute to their age-related dysfunction. Increases in NAD^+ levels induced by NMN treatment were shown to activate SIRT1 [19], which regulates the expression of mtDNA-encoded subunits of the ETC [19]. Importantly, our results suggest that disruption of sirtuin signaling prevents NMN-induced mitochondrial protection and attenuation of mtROS production in aged CMVECs. Importantly, pharmacological sirtuin activators were also shown to attenuate mtROS and improve endothelial function in aged animals [58]. On the basis of the aforementioned findings and the data available in the literature [15,19] we speculate that increased sirtuin activation elicited by increased NAD^+ levels restores expression of mtDNA-encoded subunits, improving efficiency of the ETC, restoring bioenergetics and attenuating mtROS production. In addition, increased NAD^+:NADH ratio itself may also contribute to the reduction of mitochondrial oxidative stress [59],

whereas alterations in cellular and mitochondrial expression of antioxidant enzymes appear less important. Other mitochondrial factors affecting mtROS levels that may be potentially affected by sirtuin-regulated pathways include the mitochondrial Nox4-containing NADPH-oxidase, p66shc, as well as the ratios of reduced/oxidized cofactors (NAD(P)H, GSH) and thiol groups of proteins, that act as a mitochondrial redox buffer [26,59]. These factors should be investigated in future studies.

We find that restoration of NAD^+ levels by NMN treatment, in addition to reducing ROS generation, increases mitochondrial membrane potential and improves mitochondrial respiration in CMVECs in a sirtuin-dependent manner. We posit that sirtuin-mediated increases in mitochondrial membrane potential drives increased ATP production in NMN treated CMVECs. Such a mechanism is likely also operational in the cerebral microcirculation of NMN treated aged mice. In addition to sirtuin-mediated effects, because mitochondrial ATP production and membrane potential require NAD as an essential coenzyme, restoring an optimal NAD/NADH ratio itself should also promote efficient mitochondrial metabolism.

Normalization of mitochondrial membrane potential and increased efficiency of ATP generation likely also improve cellular functions independent of decreasing mtROS. For example, the microvascular endothelium in the brain, which maintains the blood-brain-barrier and exhibits controlled transcellular transport systems, has high energy demands. Future studies should determine how restoration of cellular energetics by NMN supplementation impacts barrier and transport function in capillaries in the aged brain. Interestingly, both NMN and the related NAD precursor nicotinamide riboside have recently been shown to improve neuronal mitochondrial function and behavioral phenotypes in models of neurodegenerative disease [60,61,62], suggesting that the net benefit *in vivo* could reflect effects on multiple distinct cell types within the brain. Astrocytic end feet also contain significant amounts of mitochondria. We predict that NMN treatment of aged mice may also exert beneficial effects on astrocytic functions that are affected by impaired mitochondrial energy metabolism and/or increased mtROS, including astrocytic contributions to NVC responses (e.g. release of ATP upon neuronal stimulation). This possibility should be tested in future studies.

There is a growing evidence from clinical [10,11] and experimental [12] studies that impairment of NVC responses contributes to the age-related decline in higher cortical functions. Restoration of this key homeostatic mechanism matching energy supply with the needs of active neuronal tissue is expected to exert beneficial effects on brain function in aging. The present study is the first to demonstrate that rescue of NVC by NMN supplementation in aging is associated with improvement of multiple domains of brain function, including hippocampal encoded memory functions. These results extend the findings of our previous studies demonstrating that rescue of NVC responses in aged mice by treatment with the mtROS inhibitors resveratrol [4] and SS-31 [13] is also associated with significant cognitive benefit [14]. In previous studies NMN supplementation was shown to improve health of obese aged mice [63]. Because there is strong evidence that aging and obesity exerts synergistic deleterious effects on NVC responses and mouse cognition [64], further studies are warranted to evaluate the potential benefits of NMN treatment on these endpoints in mouse models of geriatric obesity as well.

Neurovascular dysfunction in older adults [11] as well as in animal models of aging [29] has been linked to gait alterations. Recent experimental studies in mouse models of pharmacologically-induced neurovascular uncoupling established a mechanistic link between impaired NVC responses and gait abnormalities [12]. The present study extends these findings showing that rescue of NVC responses by NMN supplementation reverses age-related alterations in gait performance in mice. Gait dysfunction in geriatric patients is a major cause of functional impairment, contributes to falls and predicts increased risk of institutionalization and mortality. Identification of interventions targeting the cerebral microvasculature that can improve gait function in aging has great relevance for maintaining functional independence in late life and preventing falls.

4.1. Limitations of the study

A number of important limitations of the present study need to be considered. First, DHE is not specific to superoxide and is more considered a semi-quantitative assay. Also, the DAF assay is not specific to NO as it can also react with oxidation products of NO. Recent reports suggest that hydrogen sulfide can reverse aging-induced vascular alterations and promote NO synthesis, at least in part, by augmenting the effects NAD precursors [15,65,66]. Further studies are warranted to elucidate the interaction of hydrogen sulfide and NAD-dependent pathways as well as the role of reactive sulfur species in the aged cerebral microcirculation. We acknowledge as a limitation of the study that we could measure NAD + levels and ROS production only in the aorta.

5. Conclusions

In conclusion, our findings show that NMN supplementation exerts significant cerebromicrovascular protective effects in aged mice. NMN treatment attenuates endothelial oxidative stress, improves endothelial function and rescues NVC responses in the aged cortex, which likely contributes to improvement of higher cortical function (Fig. 5E). Our findings, taken together with the results of earlier studies [15,19,23,24], point to benefits at several levels of cerebrovascular and systemic pathology of aging and to the potential use of NMN as therapy for prevention of aging-induced vascular cognitive impairment. Importantly, NVC is compromised both in patients with Alzheimer's disease (AD) and in mouse models of AD, which is believed to accelerate clinical deterioration [1]. Thus, our findings are likely relevant to the treatment of AD in elderly patients as well. In laboratory animals long-term intake of NMN is well-tolerated without side effects [24] and clinical trials have been already started to assess the tolerability of NMN in humans [67] to develop it as an anti-aging nutraceutical. Thus, future clinical trials with NMN supplementation in elderly subjects are feasible, which would allow the potential of NMN in improving cerebromicrovascular and cognitive outcomes to be evaluated.

Declaration of interest

D.A.S. was supported by the Glenn Foundation for Medical Research and grants from the NIH (R37 AG028730, R01 AG019719, R21 DE027490 and R01 DK100263).

D.A.S. is a founder, equity owner, board member, advisor to, director of, consultant to, investor in and/or inventor on patents licensed to Vium, Jupiter Orphan Therapeutics, Cohbar, Galilei Biosciences, GlaxoSmithKline, OvaScience, EMD Millipore, Wellomics, Inside Tracker, Caudalie, Bayer Crop Science, Longwood Fund, Zymo Research, EdenRoc Sciences (and affiliates Arc-Bio, Dovetail Genomics, Claret Bioscience, Revere Biosensors, UpRNA and MetroBiotech (an NAD booster company), Liberty Biosecurity), Life Biosciences (and affiliates Selphagy, Senolytic Therapeutics, Spotlight Biosciences, Animal Biosciences, Iduna, Immetas, Prana, Continuum Biosciences, Jumpstart Fertility (an NAD booster company), and Lua Communications). D.A.S. sits on the board of directors of both companies. D.A.S. is an inventor on a patent application filed by Mayo Clinic and Harvard Medical School that has been licensed to Elysium Health; his personal royalty share is directed to the Sinclair lab. For more information see https://genetics.med.harvard.edu/sinclair-test/people/sinclair-other.php.

Author contribution

The experiments were conducted in the Reynolds Oklahoma Center

on Aging, University of Oklahoma, Oklahoma City, OK USA. ST, PT, MNVA, AY, AC, and ZU designed the experiments; PT, ST, AC, MNVA, AY, ZT, GAF, TK, PH, TG, MK, PB, FD, ZS and EF performed and analyzed the experiments; ST, PT, MNVA, JAB, DS, AC, and ZU interpreted the data, ST, AC and ZU wrote the manuscript and DS, JAB, EF, PB, TK and MNVA revised the manuscript. All authors approved the final version of the manuscript.

Acknowledgement

This work was supported by grants from the American Heart Association (ST, MNVA, ZT, ZU and AC), the Oklahoma Center for the Advancement of Science and Technology (to AC, AY, ZU), the National Institute on Aging (R01-AG047879; R01-AG038747; R01-AG055395; R01-AG043483), the National Institute of Neurological Disorders and Stroke (NINDS; R01-NS056218 to AC, R01-NS100782 to ZU), the National Heart, Lung, and Blood Institute (R01-HL132553), the National Institute of Diabetes and Digestive and Kidney Diseases (R01-DK098656)the NIA-supported Oklahoma Nathan Shock Center (to ZU and AC; 3P30AG050911-02S1), the Oklahoma Shared Clinical and Translational Resources (OSCTR) program funded by the National Institute of General Medical Sciences (GM104938, to AY), the Presbyterian Health Foundation (to ZU, AC, AY, FD). We thank Rheal A. Towner, Ph.D., the Director of the Advanced Magnetic Resonance Center at Oklahoma Medical Research Foundation for assistance with the performance of the small-animal MRI scans that greatly improved the manuscript. The authors acknowledge the support from the NIA-funded Geroscience Training Program in Oklahoma (T32AG052363). The funding sources had no role in the study design; in the collection, analysis and interpretation of data; in the writing of the report; and in the decision to submit the article for publication.

Appendix A. Supplementary data

Supplementary data to this article can be found online at https://doi.org/10.1016/j.redox.2019.101192.

References

[1] S. Tarantini, C.H. Tran, G.R. Gordon, Z. Ungvari, A. Csiszar, Impaired neurovascular coupling in aging and Alzheimer's disease: contribution of astrocyte dysfunction and endothelial impairment to cognitive decline, Exp. Gerontol. 94 (2016), https://doi.org/10.1016/j.exger.2016.11.004.

[2] P. Toth, S. Tarantini, A. Csiszar, Z. Ungvari, Functional vascular contributions to cognitive impairment and dementia: mechanisms and consequences of cerebral autoregulatory dysfunction, endothelial impairment, and neurovascular uncoupling in aging, Am. J. Physiol. Heart Circ. Physiol. 312 (2017) H1–H20.

[3] P. Toth, S. Tarantini, A. Davila, M.N. Valcarcel-Ares, Z. Tucsek, B. Varamini, P. Ballabh, W.E. Sonntag, J.A. Baur, A. Csiszar, Z. Ungvari, Purinergic glio-endothelial coupling during neuronal activity: role of P2Y1 receptors and eNOS in functional hyperemia in the mouse somatosensory cortex, Am. J. Physiol. Heart Circ. Physiol. 309 (2015) H1837–H1845.

[4] P. Toth, S. Tarantini, Z. Tucsek, N.M. Ashpole, D. Sosnowska, T. Gautam, P. Ballabh, A. Koller, W.E. Sonntag, A. Csiszar, Z.I. Ungvari, Resveratrol treatment rescues neurovascular coupling in aged mice:role of improved cerebromicrovascular endothelial function and down-regulation of NADPH oxidas, Am. J. Physiol. Heart Circ. Physiol. 306 (2014) H299–H308.

[5] M. Zaletel, M. Strucl, J. Pretnar-Oblak, B. Zvan, Age-related changes in the relationship between visual evoked potentials and visually evoked cerebral blood flow velocity response, Funct. Neurol. 20 (2005) 115–120.

[6] M.A. Topcuoglu, H. Aydin, E. Saka, Occipital cortex activation studied with simultaneous recordings of functional transcranial Doppler ultrasound (fTCD) and visual evoked potential (VEP) in cognitively normal human subjects: effect of healthy aging, Neurosci. Lett. 452 (2009) 17–22.

[7] I. Stefanova, T. Stephan, S. Becker-Bense, T. Dera, T. Brandt, M. Dieterich, Age-related changes of blood-oxygen-level-dependent signal dynamics during optokinetic stimulation, Neurobiol. Aging 34 (2013) 2277–2286.

[8] M. Fabiani, B.A. Gordon, E.L. Maclin, M.A. Pearson, C.R. Brumback-Peltz, K.A. Low, E. McAuley, B.P. Sutton, A.F. Kramer, G. Gratton, Neurovascular coupling in normal aging: a combined optical, ERP and fMRI study, Neuroimage 85 (Pt 1) (2014 Jan 15) 592–607, https://doi.org/10.1016/j.neuroimage.2013.04.113 Epub 2013 May 9.

[9] L. Park, J. Anrather, H. Girouard, P. Zhou, C. Iadecola, Nox2-derived reactive oxygen species mediate neurovascular dysregulation in the aging mouse brain, J. Cereb. Blood Flow Metab. 27 (2007) 1908–1918.

[10] F.A. Sorond, S. Hurwitz, D.H. Salat, D.N. Greve, N.D. Fisher, Neurovascular coupling, cerebral white matter integrity, and response to cocoa in older people, Neurology 81 (10) (Sep 3 2013) 904–909, https://doi.org/10.1212/WNL.0b013e3182a351aa Epub 2013 Aug 7.

[11] F.A. Sorond, D.K. Kiely, A. Galica, N. Moscufo, J.M. Serrador, I. Iloputaife, S. Egorova, E. Dell'Oglio, D.S. Meier, E. Newton, W.P. Milberg, C.R. Guttmann, L.A. Lipsitz, Neurovascular coupling is impaired in slow walkers: the MOBILIZE boston study, Ann. Neurol. 70 (2011) 213–220.

[12] S. Tarantini, P. Hertelendy, Z. Tucsek, M.N. Valcarcel-Ares, N. Smith, A. Menyhart, E. Farkas, E. Hodges, R. Towner, F. Deak, W.E. Sonntag, A. Csiszar, Z. Ungvari, P. Toth, Pharmacologically-induced neurovascular uncoupling is associated with cognitive impairment in mice, J. Cereb. Blood Flow Metab. 35 (2015) 1871–1881.

[13] S. Tarantini, N.M. Valcarcel-Ares, A. Yabluchanskiy, G.A. Fulop, P. Hertelendy, T. Gautam, E. Farkas, A. Perz, P.S. Rabinovitch, W.E. Sonntag, A. Csiszar, Z. Ungvari, Treatment with the mitochondrial-targeted antioxidant peptide SS-31 rescues neurovascular coupling responses and cerebrovascular endothelial function and improves cognition in aged mice, Aging Cell 17 (2018).

[14] C.A. Oomen, E. Farkas, V. Roman, E.M. van der Beek, P.G. Luiten, P. Meerlo, Resveratrol preserves cerebrovascular density and cognitive function in aging mice, Front. Aging Neurosci. 1 (2009) 4.

[15] A. Das, G.X. Huang, M.S. Bonkowski, A. Longchamp, C. Li, M.B. Schultz, L.J. Kim, B. Osborne, S. Joshi, Y. Lu, J.H. Trevino-Villarreal, M.J. Kang, T.T. Hung, B. Lee, E.O. Williams, M. Igarashi, J.R. Mitchell, L.E. Wu, N. Turner, Z. Arany, L. Guarente, D.A. Sinclair, Impairment of an endothelial NAD(+)-H2S signaling network is a reversible cause of vascular aging, Cell 173 (2018) 74–89 e20.

[16] A. Csiszar, N. Labinskyy, R. Jimenez, J.T. Pinto, P. Ballabh, G. Losonczy, K.J. Pearson, R. de Cabo, Z. Ungvari, Anti-oxidative and anti-inflammatory vasoprotective effects of caloric restriction in aging: role of circulating factors and SIRT1, Mech. Ageing Dev. 130 (2009) 518–527.

[17] A. Csiszar, N. Labinskyy, J.T. Pinto, P. Ballabh, H. Zhang, G. Losonczy, K.J. Pearson, R. de Cabo, P. Pacher, C. Zhang, Z.I. Ungvari, Resveratrol induces mitochondrial biogenesis in endothelial cells, Am. J. Physiol. Heart Circ. Physiol. 297 (1) (2009 Jul) H13–H20, https://doi.org/10.1152/ajpheart.00368.2009 Epub 2009 May 8.

[18] A. Csiszar, N. Labinskyy, A. Podlutsky, P.M. Kaminski, M.S. Wolin, C. Zhang, P. Mukhopadhyay, P. Pacher, F. Hu, R. de Cabo, P. Ballabh, Z. Ungvari, Vasoprotective effects of resveratrol and SIRT1: attenuation of cigarette smoke-induced oxidative stress and proinflammatory phenotypic alterations, Am. J. Physiol. Heart Circ. Physiol. 294 (2008) H2721–H2735.

[19] A.P. Gomes, N.L. Price, A.J. Ling, J.J. Moslehi, M.K. Montgomery, L. Rajman, J.P. White, J.S. Teodoro, C.D. Wrann, B.P. Hubbard, E.M. Mercken, C.M. Palmeira, R. de Cabo, A.P. Rolo, N. Turner, E.L. Bell, D.A. Sinclair, Declining NAD(+) induces a pseudohypoxic state disrupting nuclear-mitochondrial communication during aging, Cell 155 (2013) 1624–1638.

[20] H. Massudi, R. Grant, N. Braidy, J. Guest, B. Farnsworth, G.J. Guillemin, Age-associated changes in oxidative stress and NAD+ metabolism in human tissue, PLoS One 7 (2012) e42357.

[21] R.M. Anderson, K.J. Bitterman, J.G. Wood, O. Medvedik, H. Cohen, S.S. Lin, J.K. Manchester, J.I. Gordon, D.A. Sinclair, Manipulation of a nuclear NAD+ salvage pathway delays aging without altering steady-state NAD+ levels, J. Biol. Chem. 277 (2002) 18881–18890.

[22] S.J. Mitchell, M. Bernier, M.A. Aon, S. Cortassa, E.Y. Kim, E.F. Fang, H.H. Palacios, A. Ali, I. Navas-Enamorado, A. Di Francesco, T.A. Kaiser, T.B. Waltz, N. Zhang, J.L. Ellis, P.J. Elliott, D.W. Frederick, V.A. Bohr, M.S. Schmidt, C. Brenner, D.A. Sinclair, A.A. Sauve, J.A. Baur, R. de Cabo, Nicotinamide improves aspects of healthspan, but not lifespan, in mice, Cell Metabol. 27 (2018) 667–676 e4.

[23] J. Yoshino, J.A. Baur, S.I. Imai, NAD(+) intermediates: the biology and therapeutic potential of NMN and NR, Cell Metabol. 27 (2018) 513–528.

[24] K.F. Mills, S. Yoshida, L.R. Stein, A. Grozio, S. Kubota, Y. Sasaki, P. Redpath, M.E. Migaud, R.S. Apte, K. Uchida, J. Yoshino, S.I. Imai, Long-term administration of nicotinamide mononucleotide mitigates age-associated physiological decline in mice, Cell Metabol. 24 (2016) 795–806.

[25] N.E. de Picciotto, L.B. Gano, L.C. Johnson, C.R. Martens, A.L. Sindler, K.F. Mills, S. Imai, D.R. Seals, Nicotinamide mononucleotide supplementation reverses vascular dysfunction and oxidative stress with aging in mice, Aging Cell 15 (2016) 522–530.

[26] D.F. Dai, P.S. Rabinovitch, Z. Ungvari, Mitochondria and cardiovascular aging, Circ. Res. 110 (2012) 1109–1124.

[27] Z. Springo, S. Tarantini, P. Toth, Z. Tucsek, A. Koller, W.E. Sonntag, A. Csiszar, Z. Ungvari, Aging exacerbates pressure-induced mitochondrial oxidative stress in mouse cerebral arteries, J. Gerontol. A Biol. Sci. Med. Sci. 70 (2015) 1355–1359.

[28] Z. Ungvari, Z. Orosz, N. Labinskyy, A. Rivera, Z. Xiangmin, K. Smith, A. Csiszar, Increased mitochondrial H2O2 production promotes endothelial NF-kappaB activation in aged rat arteries, Am. J. Physiol. Heart Circ. Physiol. 293 (2007) H37–H47.

[29] Z. Ungvari, S. Tarantini, P. Hertelendy, M.N. Valcarcel-Ares, G.A. Fulop, S. Logan, T. Kiss, E. Farkas, A. Csiszar, A. Yabluchanskiy, Cerebromicrovascular dysfunction predicts cognitive decline and gait abnormalities in a mouse model of whole brain irradiation-induced accelerated brain senescence, Geroscience 39 (2017) 33–42.

[30] P. Toth, Z. Tucsek, D. Sosnowska, T. Gautam, M. Mitschelen, S. Tarantini, F. Deak, A. Koller, W.E. Sonntag, A. Csiszar, Z. Ungvari, Age-related autoregulatory dysfunction and cerebromicrovascular injury in mice with angiotensin II-induced hypertension, J. Cereb. Blood Flow Metab. 33 (2013) 1732–1742.

[31] A. Csiszar, Z. Tucsek, P. Toth, D. Sosnowska, T. Gautam, A. Koller, F. Deak, W.E. Sonntag, Z. Ungvari, Synergistic effects of hypertension and aging on cognitive function and hippocampal expression of genes involved in beta-amyloid generation

and Alzheimer's disease, Am. J. Physiol. Heart Circ. Physiol. 305 (2013) H1120–H1130.
[32] D.A. MacLaren, J.A. Santini, A.L. Russell, T. Markovic, S.D. Clark, Deficits in motor performance after pedunculopontine lesions in rats - impairment depends on demands of task, Eur. J. Neurosci. 40 (8) (2014 Oct) 3224–3236, https://doi.org/10.1111/ejn.12666 Epub 2014 Jul 4.
[33] S. Tarantini, A. Yabluchanksiy, G.A. Fulop, P. Hertelendy, M.N. Valcarcel-Ares, T. Kiss, J.M. Bagwell, D. O'Connor, E. Farkas, F. Sorond, A. Csiszar, Z. Ungvari, Pharmacologically induced impairment of neurovascular coupling responses alters gait coordination in mice, Geroscience 39 (2017) 601–614.
[34] P. Toth, S. Tarantini, Z. Springo, Z. Tucsek, T. Gautam, C.B. Giles, J.D. Wren, A. Koller, W.E. Sonntag, A. Csiszar, Z. Ungvari, Aging exacerbates hypertension-induced cerebral microhemorrhages in mice: role of resveratrol treatment in vasoprotection, Aging Cell 14 (2015) 400–408.
[35] P. Toth, S. Tarantini, N.M. Ashpole, Z. Tucsek, G.L. Milne, N.M. Valcarcel-Ares, A. Menyhart, E. Farkas, W.E. Sonntag, A. Csiszar, Z. Ungvari, IGF-1 deficiency impairs neurovascular coupling in mice: implications for cerebromicrovascular aging, Aging Cell 14 (2015) 1034–1044.
[36] K. Kazama, J. Anrather, P. Zhou, H. Girouard, K. Frys, T.A. Milner, C. Iadecola, Angiotensin II impairs neurovascular coupling in neocortex through NADPH oxidase-derived radicals, Circ. Res. 95 (2004) 1019–1026.
[37] A. Csiszar, Z. Ungvari, J.G. Edwards, P.M. Kaminski, M.S. Wolin, A. Koller, G. Kaley, Aging-induced phenotypic changes and oxidative stress impair coronary arteriolar function, Circ. Res. 90 (2002) 1159–1166.
[38] P. Pacher, J.S. Beckman, L. Liaudet, Nitric oxide and peroxynitrite in health and disease, Physiol. Rev. 87 (2007) 315–424.
[39] K.J. Pearson, J.A. Baur, K.N. Lewis, L. Peshkin, N.L. Price, N. Labinskyy, W.R. Swindell, D. Kamara, R.K. Minor, E. Perez, H.A. Jamieson, Y. Zhang, S.R. Dunn, K. Sharma, N. Pleshko, L.A. Woollett, A. Csiszar, Y. Ikeno, D. Le Couteur, P.J. Elliott, K.G. Becker, P. Navas, D.K. Ingram, N.S. Wolf, Z. Ungvari, D.A. Sinclair, R. de Cabo, Resveratrol delays age-related deterioration and mimics transcriptional aspects of dietary restriction without extending life span, Cell Metabol. 8 (2008) 157–168.
[40] Z. Ungvari, A. Csiszar, A. Huang, P.M. Kaminski, M.S. Wolin, A. Koller, High pressure induces superoxide production in isolated arteries via protein kinase C-dependent activation of NAD(P)H oxidase, Circulation 108 (2003) 1253–1258.
[41] N. Labinskyy, P. Mukhopadhyay, J. Toth, G. Szalai, M. Veres, G. Losonczy, J.T. Pinto, P. Pacher, P. Ballabh, A. Podlutsky, S.N. Austad, A. Csiszar, Z. Ungvari, Longevity is associated with increased vascular resistance to high glucose-induced oxidative stress and inflammatory gene expression in Peromyscus leucopus, Am. J. Physiol. Heart Circ. Physiol. 296 (2009) H946–H956.
[42] A. Csiszar, N. Labinskyy, Z. Orosz, Z. Xiangmin, R. Buffenstein, Z. Ungvari, Vascular aging in the longest-living rodent, the naked mole rat, Am. J. Physiol. 293 (2007) H919–H927.
[43] Z. Ungvari, A. Podlutsky, D. Sosnowska, Z. Tucsek, P. Toth, F. Deak, T. Gautam, A. Csiszar, W.E. Sonntag, Ionizing radiation promotes the acquisition of a senescence-associated secretory phenotype and impairs angiogenic capacity in cerebromicrovascular endothelial cells: role of increased DNA damage and decreased DNA repair capacity in microvascular radiosensitivity, J. Gerontol. A Biol. Sci. Med. Sci. 68 (2013) 1443–1457.
[44] K.M. Robinson, M.S. Janes, J.S. Beckman, The selective detection of mitochondrial superoxide by live cell imaging, Nat. Protoc. 3 (2008) 941–947.
[45] Z. Ungvari, N. Labinskyy, P. Mukhopadhyay, J.T. Pinto, Z. Bagi, P. Ballabh, C. Zhang, P. Pacher, A. Csiszar, Resveratrol attenuates mitochondrial oxidative stress in coronary arterial endothelial cells, Am. J. Physiol. Heart Circ. Physiol. 297 (2009) H1876–H1881.
[46] A. Csiszar, A. Podlutsky, N. Podlutskaya, W.E. Sonntag, S.Z. Merlin, E.E.R. Philipp, K. Doyle, A. Davila, F.A. Recchia, P. Ballabh, J.T. Pinto, Z. Ungvari, Testing the oxidative stress hypothesis of aging in primate fibroblasts: is there a correlation between species longevity and cellular ROS production? J. Gerontol. A Biol. Sci. Med. Sci. 67 (2012) 841–852.
[47] A. Csiszar, D. Sosnowska, M. Wang, E.G. Lakatta, W.E. Sonntag, Z. Ungvari, Age-associated proinflammatory secretory phenotype in vascular smooth muscle cells from the non-human primate Macaca mulatta: reversal by resveratrol treatment, J. Gerontol. A Biol. Sci. Med. Sci. 67 (2012) 811–820.
[48] P. Mukhopadhyay, M. Rajesh, G. Hasko, B.J. Hawkins, M. Madesh, P. Pacher, Simultaneous detection of apoptosis and mitochondrial superoxide production in live cells by flow cytometry and confocal microscopy, Nat. Protoc. 2 (2007) 2295–2301.
[49] M.J. Karnowsky, A formaldehyde-glutaraldehyde fixative of high osmolarity for use in electron microscopy, J. Cell Biol. 27 (1965) 137–138.
[50] Z.I. Ungvari, N. Labinskyy, S.A. Gupte, P.N. Chander, J.G. Edwards, A. Csiszar, Dysregulation of mitochondrial biogenesis in vascular endothelial and smooth muscle cells of aged rats, Am. J. Physiol. Heart Circ. Physiol. 294 (2008) H2121–H2128.
[51] E.R. Weibel, Stereological principles for morphometry in electron microscopic cytology, Int. Rev. Cytol. 26 (1969) 235–302.
[52] Z. Tucsek, M. Noa Valcarcel-Ares, S. Tarantini, A. Yabluchanskiy, G. Fulop, T. Gautam, A. Orock, A. Csiszar, F. Deak, Z. Ungvari, Hypertension-induced synapse loss and impairment in synaptic plasticity in the mouse hippocampus mimics the aging phenotype: implications for the pathogenesis of vascular cognitive impairment, Geroscience 39 (4) (2017 Aug) 385–406, https://doi.org/10.1007/s11357-017-9981-y Epub 2017 Jun 29.
[53] Z. Ungvari, G. Kaley, R. de Cabo, W.E. Sonntag, A. Csiszar, Mechanisms of vascular aging: new perspectives, J. Gerontol. A Biol. Sci. Med. Sci. 65 (2010) 1028–1041.
[54] C.S. Kinter, J.M. Lundie, H. Patel, P.M. Rindler, L.I. Szweda, M. Kinter, A quantitative proteomic profile of the Nrf2-mediated antioxidant response of macrophages to oxidized LDL determined by multiplexed selected reaction monitoring, PLoS One 7 (2012) e50016.
[55] P. Pacher, J.G. Mabley, F.G. Soriano, L. Liaudet, K. Komjati, C. Szabo, Endothelial dysfunction in aging animals: the role of poly(ADP-ribose) polymerase activation, Br. J. Pharmacol. 135 (2002) 1347–1350.
[56] R.A. Gioscia-Ryan, T.J. LaRocca, A.L. Sindler, M.C. Zigler, M.P. Murphy, D.R. Seals, Mitochondria-targeted antioxidant (MitoQ) ameliorates age-related arterial endothelial dysfunction in mice, J. Physiol. 592 (2014) 2549–2561.
[57] L.K. Kwong, R.S. Sohal, Age-related changes in activities of mitochondrial electron transport complexes in various tissues of the mouse, Arch. Biochem. Biophys. 373 (2000) 16–22.
[58] A. Csiszar, S. Tarantini, A. Yabluchanskiy, P. Balasubramanian, T. Kiss, E. Farkas, J.A. Baur, Z.I. Ungvari, Role of endothelial NAD+ deficiency in age-related vascular dysfunction, Am. J. Physiol. Heart Circ. Physiol. (2019 Mar 15), https://doi.org/10.1152/ajpheart.00039.2019 Epub ahead of print.
[59] D.B. Zorov, M. Juhaszova, S.J. Sollott, Mitochondrial reactive oxygen species (ROS) and ROS-induced ROS release, Physiol. Rev. 94 (2014) 909–950.
[60] B. Gong, Y. Pan, P. Vempati, W. Zhao, L. Knable, L. Ho, J. Wang, M. Sastre, K. Ono, A.A. Sauve, G.M. Pasinetti, Nicotinamide riboside restores cognition through an upregulation of proliferator-activated receptor-gamma coactivator 1alpha regulated beta-secretase 1 degradation and mitochondrial gene expression in Alzheimer's mouse models, Neurobiol. Aging 34 (2013) 1581–1588.
[61] E.F. Fang, H. Kassahun, D.L. Croteau, M. Scheibye-Knudsen, K. Marosi, H. Lu, R.A. Shamanna, S. Kalyanasundaram, R.C. Bollineni, M.A. Wilson, W.B. Iser, B.N. Wollman, M. Morevati, J. Li, J.S. Kerr, Q. Lu, T.B. Waltz, J. Tian, D.A. Sinclair, M.P. Mattson, H. Nilsen, V.A. Bohr, NAD(+) replenishment improves lifespan and healthspan in ataxia telangiectasia models via mitophagy and DNA repair, Cell Metabol. 24 (2016) 566–581.
[62] A.N. Long, K. Owens, A.E. Schlappal, T. Kristian, P.S. Fishman, R.A. Schuh, Effect of nicotinamide mononucleotide on brain mitochondrial respiratory deficits in an Alzheimer's disease-relevant murine model, BMC Neurol. 15 (2015) 19.
[63] J. Yoshino, K.F. Mills, M.J. Yoon, S. Imai, Nicotinamide mononucleotide, a key NAD(+) intermediate, treats the pathophysiology of diet- and age-induced diabetes in mice, Cell Metabol. 14 (2011) 528–536.
[64] Z. Tucsek, P. Toth, S. Tarantini, D. Sosnowska, T. Gautam, J.P. Warrington, C.B. Giles, J.D. Wren, A. Koller, P. Ballabh, W.E. Sonntag, Z. Ungvari, A. Csiszar, Aging exacerbates obesity-induced cerebromicrovascular rarefaction, neurovascular uncoupling, and cognitive decline in mice, J. Gerontol. A Biol. Sci. Med. Sci. 69 (2014) 1339–1352.
[65] H.J. Lee, D. Feliers, J.L. Barnes, S. Oh, G.G. Choudhury, V. Diaz, V. Galvan, R. Strong, J. Nelson, A. Salmon, C.G. Kevil, B.S. Kasinath, Hydrogen sulfide ameliorates aging-associated changes in the kidney, Geroscience 40 (2018) 163–176.
[66] N.L. Kanagy, C.G. Kevil, The pleiotropic effects of hydrogen sulfide, Am. J. Physiol. Heart Circ. Physiol. 314 (2018) H1–H2.
[67] Clinical Trial registration number UMIN000021309: assessment of the safety of nicotinamide mononucleotide (NMN) in healthy subjects; phase I study. The clinical trial to evaluate metabolic-syndrome-related parameters to develop NMN as Foods with Function Claims, Available at: https://upload.umin.ac.jp/cgi-open-bin/ctr/ctr.cgi?function=brows&action=brows&type=summary&language=J&recptno=R000024575 , Accessed date: 23 September 2017.

GeroScience
https://doi.org/10.1007/s11357-019-00095-x

ORIGINAL ARTICLE

Nicotinamide mononucleotide (NMN) supplementation promotes anti-aging miRNA expression profile in the aorta of aged mice, predicting epigenetic rejuvenation and anti-atherogenic effects

Tamas Kiss · Cory B. Giles · Stefano Tarantini · Andriy Yabluchanskiy · Priya Balasubramanian · Tripti Gautam · Tamas Csipo · Ádám Nyúl-Tóth · Agnes Lipecz · Csaba Szabo · Eszter Farkas · Jonathan D. Wren · Anna Csiszar · Zoltan Ungvari

Received: 8 July 2019 / Accepted: 21 August 2019

Abstract Understanding molecular mechanisms involved in vascular aging is essential to develop novel interventional strategies for treatment and prevention of age-related vascular pathologies. Recent studies provide critical evidence that vascular aging is characterized by NAD+ depletion. Importantly, in aged mice, restoration of

Tamas Kiss, Cory B. Giles and Stefano Tarantini contributed equally to this work.

T. Kiss · C. B. Giles · S. Tarantini · A. Yabluchanskiy · P. Balasubramanian · T. Gautam · T. Csipo · Á. Nyúl-Tóth · A. Lipecz · J. D. Wren · A. Csiszar · Z. Ungvari (✉)
Vascular Cognitive Impairment and Neurodegeneration Program, Reynolds Oklahoma Center on Aging/Department of Geriatric Medicine, University of Oklahoma Health Sciences Center, 975 NE 10th Street, BRC 1311, Oklahoma City, OK 73104, USA
e-mail: zoltan-ungvari@ouhsc.edu

T. Kiss · T. Csipo · A. Lipecz · E. Farkas · A. Csiszar · Z. Ungvari
Department of Medical Physics and Informatics / Theoretical Medicine Doctoral School, University of Szeged, Szeged, Hungary

C. B. Giles · J. D. Wren
Oklahoma Medical Research Foundation, Genes & Human Disease Research Program, Oklahoma City, OK and Department of Biochemistry and Molecular Biology, University of Oklahoma Health Science Center, Oklahoma City, OK, USA

S. Tarantini · A. Yabluchanskiy · A. Csiszar · Z. Ungvari
Translational Geroscience Laboratory, Department of Geriatric Medicine, University of Oklahoma Health Sciences Center, Oklahoma City, OK, USA

A. Yabluchanskiy · A. Csiszar · Z. Ungvari
The Peggy and Charles Stephenson Cancer Center, University of Oklahoma Health Sciences Center, Oklahoma City, OK 73104, USA

T. Csipo · A. Lipecz · Z. Ungvari
Department of Public Health / Doctoral School of Basic and Translational Medicine, Semmelweis University, Budapest, Hungary

Á. Nyúl-Tóth
Institute of Biophysics, Biological Research Centre / Theoretical Medicine Doctoral School, Hungarian Academy of Sciences, Szeged, Hungary

C. Szabo
Chair of Pharmacology, Department of Medicine, University of Fribourg, Fribourg, Switzerland

A. Csiszar
Institute of Human Physiology and Clinical Experimental Research, Semmelweis University, Budapest, Hungary

Z. Ungvari
Department of Health Promotion Sciences, College of Public Health, University of Oklahoma Health Sciences Center, Oklahoma City, OK, USA

Published online: 28 August 2019

cellular NAD+ levels by treatment with the NAD+ booster nicotinamide mononucleotide (NMN) exerts significant vasoprotective effects, improving endothelium-dependent vasodilation, attenuating oxidative stress, and rescuing age-related changes in gene expression. Strong experimental evidence shows that dysregulation of microRNAs (miRNAs) has a role in vascular aging. The present study was designed to test the hypothesis that age-related NAD+ depletion is causally linked to dysregulation of vascular miRNA expression. A corollary hypothesis is that functional vascular rejuvenation in NMN-treated aged mice is also associated with restoration of a youthful vascular miRNA expression profile. To test these hypotheses, aged (24-month-old) mice were treated with NMN for 2 weeks and miRNA signatures in the aortas were compared to those in aortas obtained from untreated young and aged control mice. We found that protective effects of NMN treatment on vascular function are associated with anti-aging changes in the miRNA expression profile in the aged mouse aorta. The predicted regulatory effects of NMN-induced differentially expressed miRNAs in aged vessels include anti-atherogenic effects and epigenetic rejuvenation. Future studies will uncover the mechanistic role of miRNA gene expression regulatory networks in the anti-aging effects of NAD+ booster treatments and determine the links between miRNAs regulated by NMN and sirtuin activators and miRNAs known to act in the conserved pathways of aging and major aging-related vascular diseases.

Keywords Senescence · Atherosclerosis · Vascular cognitive impairment · Epigenetics · Vascular aging · Endothelial dysfunction · Oxidative stress

Introduction

Age-related diseases of the cardiovascular system are a leading cause of morbidity and mortality in the elderly (Abdellatif et al. 2018; Minamino and Komuro 2007; Wang and Bennett 2012; Alfaras et al. 2016; Ungvari et al. 2018). Vascular aging is associated with stiffening of the large arteries, endothelial dysfunction, oxidative stress, and inflammation, promoting the development of atherosclerotic vascular diseases (ischemic heart diseases, stroke, peripheral artery disease) and aorta aneurysm (Wang and Bennett 2012; Ungvari et al. 2018). Microvascular aging is also a major contributing factor to the pathogenesis of vascular cognitive impairment (VCI), Alzheimer's disease, cerebral microhemorrhages, sarcopenia, heart failure, chronic kidney disease and (Ungvari et al. 2018; Mullins et al. 2014; Ungvari et al. 2017a; Toth et al. 2017; Tarantini et al. 2017a; Tarantini et al. 2016a; Sagare et al. 2013; Sweeney et al. 2018; Montagne et al. 2017; Kisler et al. 2017; Payne 2006; Hoenig et al. 2008; Long et al. 2012). Understanding molecular mechanisms involved in vascular aging is essential to develop novel interventional strategies for treatment and prevention of age-related vascular pathologies.

MicroRNAs (miRNA) are short, endogenous, non-coding transcripts that repress gene expression at the post-transcriptional level in both physiological and pathological conditions. Strong experimental evidence suggest that miRNAs have a role in regulation of lifespan in model organisms (Boehm and Slack 2005; Grillari and Grillari-Voglauer n.d.; Ibanez-Ventoso et al. 2006) and that alterations in cellular miRNA expression profile also play a role in mammalian aging (Bates et al. n.d.; Maes et al. 2008; Inukai et al. 2012; Inukai and Slack 2013; Ito et al. 2010; Mercken et al. 2013; Smith-Vikos and Slack 2012; Ungvari et al. 2013a; Zhang et al. 2012; Zovoilis et al. 2011; Smith-Vikos et al. 2016; ElSharawy et al. 2012). Importantly, miRNAs were also reported to regulate several important aspects of endothelial biology and vascular function (Bonauer et al. 2009; Doebele et al. n.d.; Kuehbacher et al. 2007; Chen et al. 2015a; Hergenreider et al. 2012; Kim et al. 2014; Leung et al. 2013; Lovren et al. 2012; O'Rourke and Olson 2011; Rotllan et al. 2013; Stellos and Dimmeler 2014; Weber et al. 2014; Zampetaki et al. 2014). Several studies have demonstrated that age-related miRNA dysregulation importantly contributes to the development of vascular aging phenotypes (Ito et al. 2010; Ungvari et al. 2013a,b; Menghini et al. 2014; Badi et al. 2018; Guo et al. 2017; Hazra et al. 2016; Regina et al. 2016; Boon et al. 2013; Csiszar et al. 2014) and promotes the pathogenesis of atherosclerotic diseases (Ono et al. 2011) encompassing every step from sterile vascular inflammation, plaque formation to plaque destabilization and rupture (Hartmann et al. 2016; Lu et al. 2018; Zhang et al. 2018). Dysregulation of miRNA expression has also been linked to microvascular aging phenotypes, including impaired angiogenesis (Ungvari et al. 2013b; Csiszar et al. 2014; Che et al. 2014; Jansen et al. 2015). Experimental interventions that both extend lifespan and prevent/delay age-related vascular dysfunction in rodents, including caloric restriction (Csiszar et al. 2014) and induction of early-life IGF-1 deficiency (Tarantini et al. 2016b), were shown to reverse aging-induced alterations in vascular miRNA

expression. Despite these advances, fundamental cellular and molecular processes of aging that are responsible for dysregulation of vascular miRNA expression have not been elucidated.

NAD^+ is a rate-limiting co-substrate for sirtuin enzymes, which are key regulators of pro-survival pathways in the vasculature (Das et al. 2018; Csiszar et al. 2009a; Csiszar et al. 2009b; Csiszar et al. 2008). Aging is associated with cellular NAD^+ depletion (Gomes et al. 2013; Massudi et al. 2012), which has been proposed to be a critical driving force of aging processes. In support of this theory, it was demonstrated that enhancing NAD^+ biosynthesis extends lifespan in lower organisms (Anderson et al. 2002) and improves health-span in mouse models of aging (Mitchell et al. 2018). Recent studies provide critical evidence that vascular aging is also characterized by NAD+ depletion (Tarantini et al. 2019; Csiszar et al. 2019; Kiss et al. 2019). Importantly, we 69 and other laboratories demonstrated (Das et al. 2018; de Picciotto et al. 2016) that in aged mice restoration of cellular NAD^+ levels by treatment with the NAD+ precursor nicotinamide mononucleotide (NMN) (Yoshino et al. 2018) confers potent anti-aging vascular effects, reversing endothelial dysfunction, improving mitochondrial function, and attenuating oxidative stress.

The present study was designed to test the hypothesis that age-related NAD+ depletion is causally linked to dysregulation of vascular miRNA expression. A corollary hypothesis is that functional vascular rejuvenation in NMN-treated aged mice is also associated with restoration of a youthful vascular miRNA expression profile. To test these hypotheses, aged mice were treated with NMN for 2 weeks and miRNA signatures in the aortas were compared to those in aortas obtained from untreated young and aged control mice.

Methods

Animals, NMN supplementation

Young (3-month-old) and aged (24-month-old) male C57BL/6 mice were purchased from the aging colony maintained by the National Institute on Aging at Charles River Laboratories (Wilmington, MA). The biological age of 24-month-old mice corresponds to that of ~ 60-year-old humans. Mice were housed under specific pathogen-free barrier conditions in the Rodent Barrier Facility at University of Oklahoma Health Sciences Center under a controlled photoperiod (12 h light; 12 h dark) with unlimited access to water and were fed a standard AIN-93G diet (ad libitum). Mice in the aged cohort were assigned to two groups. One group of the aged mice was injected daily with NMN (i.p. injections of 500 mg NMN/kg body weight per day) or the equivalent volume of PBS for 14 consecutive days at 6 PM and 8 AM on day 14 and were sacrificed 4 h after last injection. Similar dosages of NMN have been shown to exert potent anti-aging effects on mouse health span (de Picciotto et al. 2016). All procedures were approved by the Institutional Animal Use and Care Committees of the University of Oklahoma Health Sciences Center. All animal experiments complied with the ARRIVE guidelines and were carried out in accordance with the National Institutes of Health guide for the care and use of Laboratory animals (NIH Publications No. 8023, revised 1978). The effects of NMN treatment on cognitive function, cerebromicrovascular responses, and aorta endothelial function in the same cohort of mice have been recently reported (Tarantini et al. 2019).

Quantitative real-time RT-PCR and miRNA expression profiling

A quantitative real time RT-PCR technique was used to analyze miRNA expression profiles in the aorta of mice from each experimental group as reported (Ungvari et al. 2013b; Csiszar et al. 2014; Tarantini et al. 2016b). In brief, total RNA was isolated with a mirVana™ miRNA Isolation Kit (ThermoFisher Scientific) and was reverse transcribed using TaqMan® MicroRNA Reverse Transcription Kit as described previously (Ungvari et al. 2013b; Csiszar et al. 2014; Tarantini et al. 2016b). The expression profile of mouse miRNAs in aortas derived from young and aged control mice and aged NMN-treated mice was analyzed using the TaqMan Array Rodent MicroRNA A+B Cards Set v3.0 (ThermoFisher Scientific). The qPCR data were quantified using the $\Delta\Delta$Ct method (Livak and Schmittgen 2001). Predicted and experimentally validated microRNA targets were obtained from the TargetScan database (Agarwal et al. 2015), and Gene Ontology enrichment analysis was performed on differentially expressed microRNA targets using Fisher's exact test between TargetScan targets and annotations from the Gene Ontology database (Harris et al. 2004). To identify relationships between miRNA targets and terms in the biomedical literature, we utilized

the IRIDESCENT system (Wren and Garner 2004). IRIDESCENT uses a statistical model to determine whether each target gene co-occurs with a term of interest more frequently than would be expected by chance, and quantifies this in terms of the mutual information measure.

Results

Changes in vascular miRNA expression profile in mice associated with aging and with NMN treatment

We assessed changes in miRNA expression in the mouse aorta associated with aging and with NMN treatment. Hierarchical clustering (Fig. 1a) and principal component analysis (Fig. 1b) of miRNA expression showed a clear separation between the young and aged groups. Aged control mice and aged NMN-treated mice were also separated in the principal component analysis and hierarchical clustering. In contrast, miRNA expression in young mice and NMN-treated aged mice was similar and these groups did not separate well in the principal component analysis and hierarchical clustering. The Venn diagram in Fig. 1c shows that expression of several miRNAs, which are differentially expressed in the aortas of young and aged mice, was restored to youthful levels in aortas of NMN-treated aged mice. These data suggest that NAD^+ depletion has a critical role in age-related dysregulation of vascular miRNA expression. Figure 2 shows changes in expressions of individual miRNAs in the mouse aorta associated with age and NMN treatment.

Since the discovery of miRNA regulation of genes, several studies have been focused on predicting the biologically relevant target genes for miRNAs. We have used TargetScan database to predict putative biological targets of miRNAs differentially expressed with age whose expression is restored to youthful levels in aortas of aged mice by NMN supplementation (Table 1). GO terms enriched among miRNAs differentially expressed with age whose expression is restored to youthful levels in aortas of aged mice by NMN supplementation are shown in Table 2. Analysis of the differentially expressed miRNAs indicated that a statistically significant number of them had target sites within genes associated with pathways regulating the intracellular signaling, protein homeostasis, and inflammation (Table 2). The results are consistent with the predicted anti-aging effects of NMN treatment.

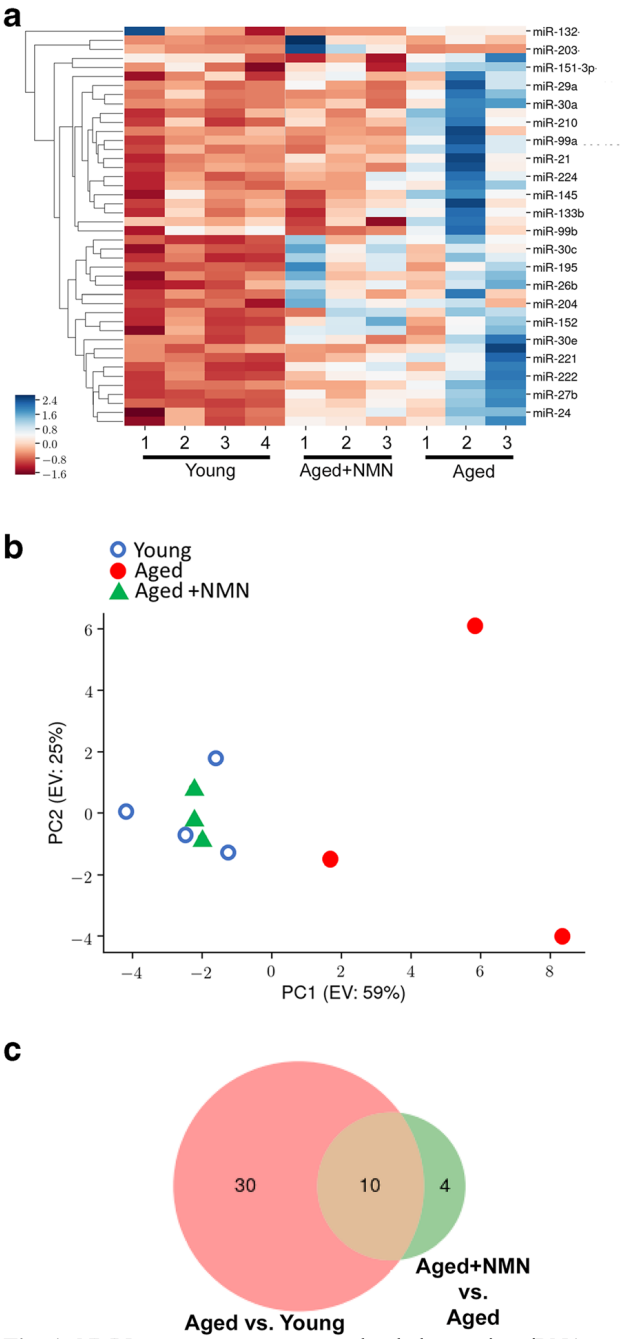

Fig. 1 NMN treatment reverses age-related changes in miRNA expression profile in the mouse aorta. **a** The heat map is a graphic representation of normalized miRNA expression values in aortas derived from young (3-month-old), aged (24-month-old), and NMN-treated aged mice. Hierarchical clustering analysis revealed the similarities on miRNA expression profiles of aortas from young and NMN-treated aged mice. **b** Principal component analysis (PCA) plot of miRNA expression profiles from aortas derived from young, aged control, and NMN-treated aged mice. The profiles from aged mice (red dots) cluster separately to clusters representative of young mice (blue circles) and NMN-treated aged mice (green triangles). PC1 and PC2: Principal components 1 and 2, respectively. **c** Venn diagrams showing the differentially expressed miRNAs in each group, which are significantly up- or down-regulated in aortas from aged mice compared to those from young mice or aged NMN-treated mice

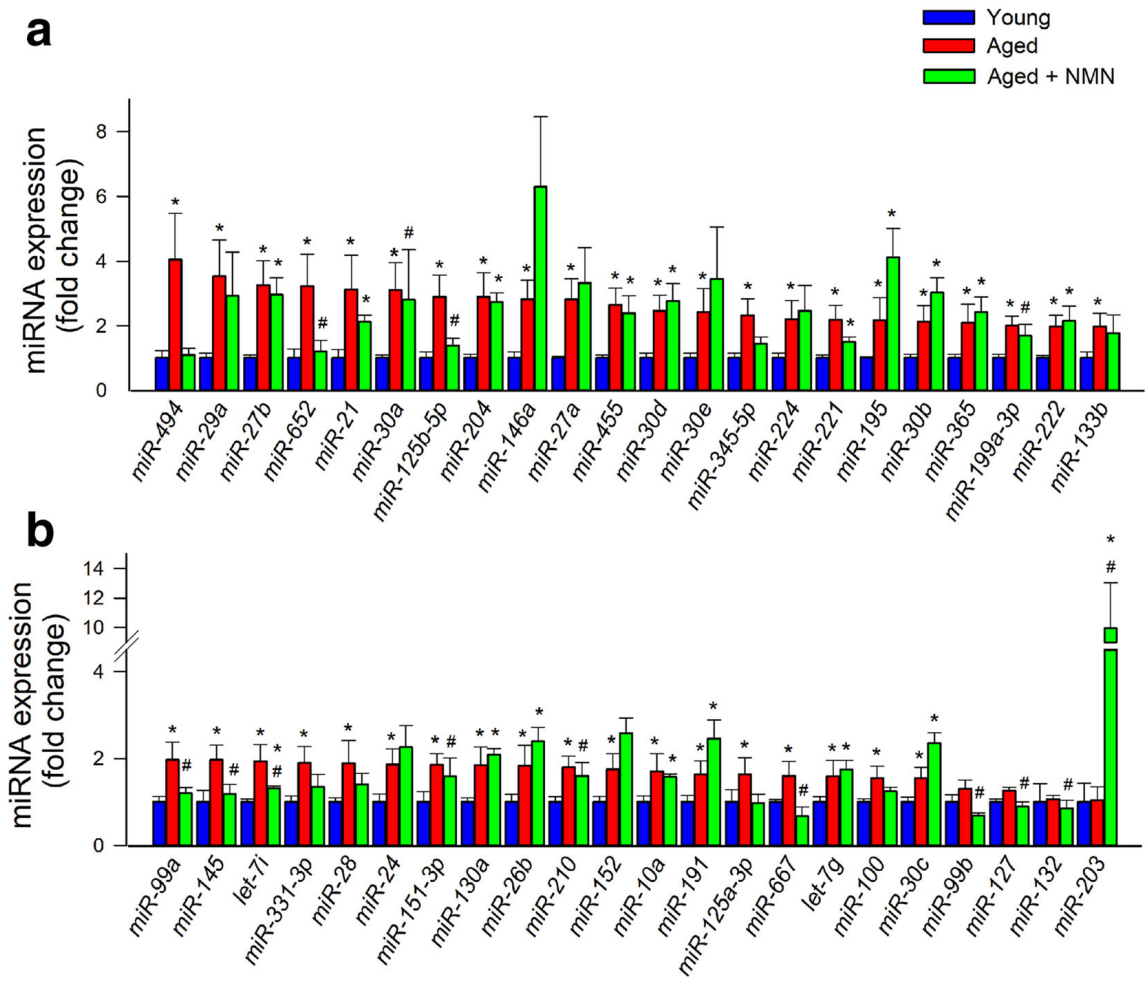

Fig. 2 Effects of aging and NMN treatment on miRNA expression in the mouse aorta. **a**, **b** qPCR data showing miRNA expression in aortas isolated from young (3-month-old), aged (24-month-old), and NMN-treated aged mice. Data are mean ± S.E.M. ($n = 3$–4 for each data point). *$P < 0.05$ vs. young; #$P < 0.05$ vs. aged

We also attempted to predict the biological effects of the differentially expressed miRNAs by identifying relationships between miRNA targets and terms in the biomedical literature utilizing the IRIDESCENT system (Wren and Garner 2004). The results of this analysis suggest that NMN supplementation likely promotes epigenetic rejuvenation and confers anti-atherogenic effects (Table 3).

Discussion

Our study demonstrates that protective effects of NMN treatment on vascular function is associated with anti-aging changes in the miRNA expression profile in the aorta in a mouse model of aging that recapitulates vascular alterations and deficits present in elderly humans at risk for cardiovascular and cerebrovascular diseases.

Age-related changes in vascular miRNA expression likely play important pathogenic roles targeting critical signaling pathways, inflammatory processes, and cellular mechanisms involved in protein homeostasis and thereby impairing the structural and functional integrity of the vasculature (Fig. 3). Among others, miR-29a (Huang et al. 2016), miR-27b (Signorelli et al. 2016), miR-652 (Pilbrow et al. 2014), miR-221 (Wei et al. 2013), miR-28 (Wang et al. 2017), miR-21 (Urbich et al. 2008), miR-125b-5p (Ohukainen et al. 2015) , miR-494 (Wezel et al. 2015), and miR-145 (Faccini et al. 2017), which are up-regulated in aging, have been implicated in vascular inflammation and atherogenesis.

Table 1 Selected genes, whose expression changes with age and are predicted to be targeted by NMN-dependent differentially expressed miRNAs. Shown are (1) the number of miRNAs targeting the gene, whose expression is significantly changed my NMN treatment; (2) relative age-dependent changes in gene expression, predicted by the AgeAtlas software; and (3) cellular function of the protein encoded by the gene and its putative role in vascular pathologies

Gene symbol	Gene full name	NMN-induced significant miRNAs	AgeAtlas change	Cellular function	Role in vascular pathology
Sec62	SEC62 homolog	4	− 0.0089	Component of the protein translocation apparatus	Single nucleotide polymorphism is associated with vulnerable plaque (de Boer et al. 2018)
Nbeal1	neurobeachin like 1	3	− 0.81	Plays a role in vesicle trafficking, membrane dynamics, receptor signaling, pre-mRNA processing, signal transduction and cyto-skeleton assembly	Single nucleotide polymorphism is associated with early atherogenesis (Hixson et al. 2017) and development of ischemic white matter hyperintensities in stroke patients (Traylor et al. 2016)
Fyn	Fyn proto-oncogene	2	− 0.31	Kinase	Genome-wide analysis of DNA methylation showed association with aortic atherosclerosis (Yamada et al. 2014); in vitro overexpressed in activated smooth muscle cells (Singh et al. 2017);
Mef2a	myocyte enhancer factor 2A	2	− 0.094	Transcription factor	In vitro increased expression in senescence endothelial cell; increased plasma level in coronary artery disease patients (Liu et al. 2019)
Tet2	tet methylcytosine dioxygenase 2	2	− 0.45	Epigenetic regulator	Contributes to the development of atherosclerosis by epigenetic modification (Aavik et al. 2019; Peng et al. 2016; Liu et al. 2013)
Ptch1	patched 1	2	− 0.0072	Hedgehog signaling pathway	Overexpressed in atherosclerotic plaque in mouse carotid artery (Ali et al. 2013)
Adra2b	adrenergic receptor, alpha 2b	2	− 0.061	Seven-pass transmembrane protein	role in hypertension (Kintsurashvili et al. 2009)
Abcg4	ATP-binding cassette, sub-family G (WHITE), member 4	2	− 0.0038	ABC-transporter	Cholesterol transporter, strongly linked to atherosclerosis and other cardiovascular disease (Schumacher and Benndorf 2017; Westerterp et al. 2014)
Epha6	Eph receptor A6	2	− 0.59	Ephrin receptor	GenSalt and MESA studies: SNP variant associated with hypertension (Li et al. 2016; Kim et al. 2017); in vitro activated in cells relevant for atherogenesis (Sakamoto et al. 2011)

Table 1 (continued)

Gene symbol	Gene full name	NMN-induced significant miRNAs	AgeAtlas change	Cellular function	Role in vascular pathology
Atf2	activating transcription factor 2	2	− 0.34	Transcription factor	In mouse models participates in foam cells activation signaling (Raghavan et al. 2018); vascular smooth cell activation (Wu et al. 2014)
Homer2	homer scaffolding protein 2	2	− 0.31	Glutamate signaling pathway	Biomarker of atherosclerosis (Zhu et al. 2016)
Kcnb1	potassium voltage gated channel, Shab-related subfamily, member 1	3	− 0.21	Potassium channel subunit	Changed expression in arteries in rat model of hypertension (Cox et al. 2008)
Rap1a	RAS-related protein-1a	2	− 0.52	Ras signaling pathway	Potential role in carotid atherosclerosis (Mao et al. 2018)
Fryl	FRY like transcription coactivator	2	− 0.71	Transcription factor; Notch signaling	Downregulated in hypertensive mouse aorta (Rippe et al. 2017)

To our knowledge, this is the first study to demonstrate that NMN treatment in aged mice reverses, at least in part, age-related, pro-inflammatory, and pro-atherogenic alterations in miRNA expression profile in the aorta. These findings raise the possibility that changes in post-transcriptional control of expression of genes that encode critical targets for vascular health contribute to the beneficial effects of treatment with NAD+ boosters on health span. Demonstration of NMN-induced changes in miRNA biology in the vasculature is particularly important as alterations in miRNA expression profile have been causally linked to the development of cardiovascular aging phenotypes (Ungvari et al. 2013a; Boon et al. 2013; Csiszar et al. 2014) and the pathogenesis of cardiovascular diseases (Ono et al. 2011). A single miRNA can target up to several hundred mRNAs, thus capable of significantly altering gene expression regulatory networks. Systematic prediction of target pathways supports the concept that chronic NMN treatment may exert significant anti-atherogenic effects via epigenetic rejuvenation of the vasculature. These miRNA-mediated vasoprotective effects of NMN treatment appear to be synergistic with its endothelial protective, anti-aging, and pro-angiogenic effects demonstrated by recent studies (Tarantini et al. 2019; Csiszar et al. 2019; Kiss et al. 2019).

The molecular mechanisms contributing to aging-induced decline in NAD^+ in the vasculature are likely multifaceted and may include down-regulation of nicotinamide phosphoribosyltransferase (NAMPT, also known as NMN synthase; which catalyzes the rate limiting step in the biosynthesis of NAD^+) (Tarantini et al. 2019) and increased utilization of NAD^+ by activated Poly [ADP-ribose] polymerase 1 (PARP-1) (Csiszar et al. 2019; Pacher et al. 2002). Additional studies are warranted to determine the efficacy of combination treatments that simultaneously increase NAD+ production and inhibit its degradation (e.g., NMN plus a PARP-1 inhibitor) for the prevention of age-related vascular pathologies.

Previous studies demonstrate that restoration of NAD^+ levels by NMN treatment exert protective effects on endothelial vasodilation in aged rodents by reducing ROS generation and restoring mitochondrial function in a sirtuin-dependent manner (Tarantini et al. 2019). The mechanisms by which

Table 2 Predicted regulatory effects of miRNAs whose expression is restored to youthful levels in aortas of aged mice by NMN supplementation. Shown are GO terms enriched among miRNAs differentially expressed with age in the aorta whose expression is significantly affected by NMN treatment. *N* = genes in each GO category, targeted by miRNAs that are differentially regulated in the aged mouse aorta. Significance was determined by Fisher's exact test; odds ratio: (observed to expected ratio); SLPV: signed log10 *P* value

GO term ID	Name of biological process/molecular function	N	Odds Ratio	SLPV
6886	Intracellular protein transport	20	3.17	3.26
7218	Neuropeptide signaling pathway	7	7.32	2.54
5198	Structural molecule activity	6	9.40	2.45
51082	Unfolded protein binding	7	5.49	2.20
45778	Positive regulation of ossification	6	6.27	2.07
50839	Cell adhesion molecule binding	10	3.49	1.92
15137	Citrate transmembrane transporter activity	3	inf	1.84
48227	Plasma membrane to endosome transport	3	inf	1.84
8188	Neuropeptide receptor activity	3	inf	1.84
7217	Tachykinin receptor signaling pathway	3	inf	1.84
42594	Response to starvation	3	inf	1.84
70536	Protein K63-linked deubiquitination	6	4.70	1.77
71108	Protein K48-linked deubiquitination	6	4.70	1.77
5102	Receptor binding	27	1.82	1.72
90630	Activation of GTPase activity	10	2.85	1.71
31338	Regulation of vesicle fusion	7	3.66	1.68
1664	G-protein coupled receptor binding	6	3.76	1.52
6631	Fatty acid metabolic process	6	3.76	1.52
45777	Positive regulation of blood pressure	4	6.25	1.47
32924	Activin receptor signaling pathway	4	6.25	1.47
70530	K63-linked polyubiquitin binding	4	6.25	1.47
10863	Positive regulation of phospholipase C activity	4	6.25	1.47
16579	Protein deubiquitination	8	3.13	1.47
18107	Peptidyl-threonine phosphorylation	9	2.57	1.42
48015	Phosphatidylinositol-mediated signaling	5	3.91	1.36
7200	Phospholipase C-activating G-protein coupled receptor signaling pathway	5	3.91	1.36
71837	HMG box domain binding	5	3.91	1.36
61578	Lys63-specific deubiquitinase activity	3	9.37	1.33
33674	Positive regulation of kinase activity	3	9.37	1.33
43122	Regulation of I-kappaB kinase/NF-kappaB signaling	3	9.37	1.33
50995	Negative regulation of lipid catabolic process	3	9.37	1.33

NAD+ boosters regulate miRNA expression are likely multifaceted and may include both transcriptional and post-transcriptional regulatory mechanisms (Fig. 3). NMN-induced transcriptional regulation may involve changes in the expression of miRNA genes due to altered transcription factor activity, changes in genome accessibility (e.g., histone modifications), and altered methylation status of the promoter of the miRNA genes. Post-transcriptional mechanisms affected by NMN treatment may include rescue of miRNA processing pathways (Ungvari et al. 2013b) and miRNA stability. Activation of sirtuins by NAD+ boosters, which has been linked to attenuation of age-related vascular oxidative stress (Tarantini et al. 2019; Kiss et al. 2019), may potentially contribute to both transcriptional and post-transcriptional regulation of miRNA expression in the vasculature. In particular, future

Table 3 Literature commonalities of the genes targeted by miRNAs whose expression is restored to youthful levels in aortas of aged mice by NMN supplementation. The IRIDESCENT literature-mining software was used to identify commonalities (e.g., genes, diseases, phenotypes, biological processes) of the genes predicted to be targeted by the miRNAs. A network of related objects was established by their co-occurrence within MEDLINE records, shared relationships were identified, and their statistical relevance was scored by comparing observed frequencies with what would be expected in a random network model. Number of shared relationships is the number of genes (out of the top 100 most significant) co-mentioned with the terms in the left-hand column. The observed to expected (obs/exp) ratio is the enrichment for the term. References and notes on how each one relates to vascular pathophysiology of aging are shown in the rightmost column

Literature associations	Remark/full name	# shared relationships	Obs/exp	Score	Biological process/function
CTNNB1	Catenin Beta 1	63	2.25	139.9	Adherent junctions; Wnt/beta-catenin signaling in VSMCs contribute to Intimal thickening (Tsaousi et al. 2011)
Wnt		56	2.02	110.8	Wnt signaling regulates atherogenesis (Zhao et al. 2018; Bhatt et al. 2012)
PTEN	Phosphatase and tensin homolog	43	2.2	93	Regulates VSMC phenotype (Moulton et al. 2018)
epithelial-mesenchymal transition		41	2.07	83.3	Endothelial to menesnchymal transition contributes to atherogenesis (Bostrom et al. 2016; Evrard et al. 2016; Moonen et al. 2015)
SMARCA4	SWI/SNF related, matrix associated, actin dependent regulator of chromatin, subfamily a, member 4	22	3.73	81	Chromatin remodeling; genome wide association study showed its potential role in atherosclerosis (Mao et al. 2017)
FGFR1	Fibroblast growth factor receptor 1	28	2.63	72.3	Receptor; FGF receptor signaling regulates atherogenesis (Che et al. 2011)
EP300	E1A binding protein p300	32	2.27	71.3	Transcriptional coactivator; VEGFA triggers changes in transcriptional activity of endothelial cells via epigenetic regulation with the help of EP300 (Zhang et al. 2013)
EZH2	Enhancer of zeste 2 polycomb repressive complex 2 subunit	25	2.78	68.6	Histone methyltransferase; epigenetic suppression of gene expression
sumoylation		24	2.56	60.6	Sumolylation reactions play a role in atherogenesis (Heo et al. 2013; Heo et al. 2015; Stein et al. 2014)
RNA polymerase II		29	2.08	58.9	mRNA transcription
SOX2	Sex determining region Y-box 2	27	2.15	57.7	Transcription factor, stem cell function; upregulated in aortic endothelial cells

Table 3 (continued)

Literature associations	Remark/full name	# shared relationships	Obs/exp	Score	Biological process/function
					in atherosclerotic mice (Bostrom et al. 2016). Limiting Sox2 decreases calcification in aortas of ApoE(-/-) mice (Bostrom et al. 2016).
chromatin remodeling		29	2.03	57.3	(Khyzha et al. 2017)
CDH2	N-cadherin	27	2.11	55.5	Adherent junctions; neointima formation (Jones et al. 2002)
CDKN1A	Cyclin-dependent kinase inhibitor 1; p21	27	2.02	53.3	Senescence; regulates atherogenesis and neointima fromation (Yang et al. 1996)
KMT2D	Histone-lysine N-methyltransferase 2D	15	3.6	53	Histone methyltransferase; epigenetic regulation of gene expression
SMAD4	Mothers against decapentaplegic homolog 4	23	2.26	51	Transcription factor, mediates TGFβ signaling, regulates pathways involved in atherogenesis (Kintscher et al. 2002)
KDM1A	Lysine-specific histone demethylase 1A	16	3.02	47.2	Histone methyltransferase; epigenetic regulation of gene expression (Pojoga et al. 2011)
FGFR2	Fibroblast growth factor receptor 2	23	2.08	47	FGF receptor signaling regulates atherogenesis (Che et al. 2011)
BCOR	BCL-6 corepressor	12	3.96	46.4	transcription repressor
PAX6	Paired box 6	20	2.34	46.1	Transcription factor;
DNMT1	DNA methyltransferase (cytosine-5) 1	22	2.05	44.5	Chromatin remodeling; mediate macrophage activation and participate inflammation in atherosclerotic lesions (Yu et al. 2016)
polycomb		19	2.31	42.7	Chromatin remodeling, regulate ABCA1 expression in the macrophages and consequently has an important role in the development of the inflammation in the atherosclerotic lesion (Lv et al. 2016)
MECP2	Methyl CpG binding protein 2	18	2.25	39.5	Key epigenetic factor regulating global gene transcription by gathering the histone deacetylase complex to the

Table 3 (continued)

Literature associations	Remark/full name	# shared relationships	Obs/exp	Score	Biological process/function
					promoter regions of the genes; with polycomb, it regulates ABCA1 expression in the macrophages (Lv et al. 2016)
TSC1	TSC complex subunit 1	16	2.48	38.9	Tumor suppressor gene; regulates mammalian target of rapamycin complex 1 (mTORC1) signaling, thought the mTHOR pathway it plays a critical role in the development of atherosclerotic lesions (Kurdi et al. 2016)
CREBBP	CREB binding protein	18	2.18	38.4	Involved in the transcriptional coactivation of many different transcription factors
ID2	Inhibitor of DNA binding 2	16	2.42	37.9	Transcriptional regulator, inhibit the functions of basic helix-loop-helix transcription factors; vascular smooth muscle phenotypic change in atherosclerosis (Zhu et al. 2015)
BAP1	BRCA1 associated protein 1	12	3.02	35.9	Ubiquitin C-terminal hydrolase, removes ubiquitin from proteins
TCF4 (alias of TCF7L2)	transcription factor 7 like 2	17	2.12	35.5	Transcription factor; epidemiological data shows SNP polymorphism associated with atherosclerosis (Estrada-Velasco et al. 2013; Muendlein et al. 2011)
PIK3CA	Phosphatidylinositol-4,5-bisphosphate 3-kinase catalytic subunit alpha	16	2.12	33.5	Kinase activity; somatic mutation causes venous (Limaye et al. 2015) and lymphatic malformation (Blesinger et al. 2018)
ARHGEF2	Rho/Rac guanine nucleotide exchange factor 2	16	2.05	32.2	Participates in the rho-dependent signaling pathway
PAX8	Paired box 8	13	2.56	32.2	Transcription factor
FGF8	Fibroblast growth factor 8	14	2.35	31.5	Mitogenic and cell survival activities; regulates the cardiovascular development (Brown et al. 2004)
BTG2	BTG anti-proliferation factor 2	11	2.87	30.8	Involved in the regulation of the G1/S transition of the cell cycle

Table 3 (continued)

Literature associations	Remark/full name	# shared relationships	Obs/exp	Score	Biological process/function
FBXW7	F-box and WD repeat domain containing 7	12	2.48	29.6	Phosphorylation-dependent protein ubiquitination; regulates angiogenesis (Izumi et al. 2012) and the barrier function of endothelial cells (Pronk et al. 2019)
FMR1	Fragile X mental retardation 1	14	2.09	28.9	Controls the proliferation and angiogenesis of endothelial cells via the miR-181a-mediated calmodulin (CaM)/CaMKII pathway (Zhao et al. 2018)
MSTN	Myostatin	14	2.11	28.8	Participates in TGF-beta signaling; increased expression in atherosclerotic lesions, especially in vascular smooth muscle cells (Verzola et al. 2017)
HDAC3	Histone deacetylase 3	14	2.07	28.5	Transcriptional regulator by epigenetic modification of DNA; regulats the atherosclerotic phenotype of macrophages (Hoeksema et al. 2014)
CCNE1	Cyclin E1	12	2.35	27.9	Regulator of cell cycle
SMARCB1	SWI/SNF related, matrix associated, actin dependent regulator of chromatin, subfamily b, member 1	11	2.54	27.5	Chromatin remodeling
AXIN2	Axin 2	12	2.31	27.3	Participates in G-protein signaling; participate in Wnt signaling which known to regulates atherosclerosis (Zhao et al. 2018; Bhatt et al. 2012; Tian et al. 2017)
RASSF1	Ras association domain family member 1	12	2.29	26.9	regulator of DNA methylation and DNA repair
FOXP1	Forkhead box P1	11	2.48	26.7	Transcription factor; in atherosclerosis downregulation of miR-206 causes the upregulation of FOXP1 contributing the development of the plaque (Xing et al. 2017)
TOP2A	DNA topoisomerase II alpha	12	2.21	26.1	Controls and alters the topologic states of DNA during transcription; Topo II inhibitor teniposide reduce

Table 3 (continued)

Literature associations	Remark/full name	# shared relationships	Obs/exp	Score	Biological process/function
					calcification of atherosclerotic lesions (Liu et al. 2018)
ASCL1	Achaete-scute family bHLH transcription factor 1	11	2.42	26	Transcription factor; presence of ASCL1 polymorphism correlate with the development of subclinical atherosclerosis (Lopez-Mejias et al. 2016)
FOXA1	Forkhead box A1	11	2.21	23.9	Transcription factor
AXIN1	Axin 1	11	2.15	23.2	Participate in G-protein signaling
SOX10	Sex determining region Y-box 10	11	2.08	22.4	Transcription factor
MAP2K4	Mitogen-activated protein kinase kinase 4	11	2	21.6	Protein kinase; participates in VEGF signaling (Sullivan et al. 2019)

studies should determine how NMN treatment and sirtuin activation affect activity/expression of the Dicer/TRBP complex (Ungvari et al. 2013b). Further, the anti-aging vascular effects of caloric restriction also have been causally linked to sirtuin activation (Csiszar et al. 2009a). Importantly, caloric restriction also promotes significant anti-inflammatory and anti-atherogenic changes in vascular miRNA expression (Csiszar et al. 2014). Various humoral factors (e.g., hormones, cytokines) can also affect vascular miRNA expression. Additional studies are needed to determine the indirect effects of NMN-induced changes in humoral factors (e.g., adipokines) on vascular miRNA expression profile. The available evidence also supports the concept that a bi-directional link exists between NAD+ levels and miRNA expression (Choi et al. 2013). Recent studies identify the miR-34a/NAMPT (nicotinamide phosphoribosyltransferase) regulatory axis, which regulates SIRT1 activity through altering NAD+ levels (Choi et al. 2013). Interestingly, miR-34a tends to be increased in the aged mouse aorta (~ 2.9-fold), which associates with a down-regulation of NAMPT (Tarantini et al. 2019).

Conclusions

In conclusion, rescue of vascular function and attenuation of oxidative stress in the vasculature of NMN-treated aged mice is accompanied by anti-aging changes in miRNA expression profile in the aorta. The predicted regulatory effects of NMN-induced differentially expressed miRNAs in aged vessels include anti-atherogenic affects and epigenetic rejuvenation (Fig. 3) and are consistent with the anti-aging functional effects of treatment with both NMN (Das et al. 2018; Tarantini et al. 2019; Kiss et al. 2019; de Picciotto et al. 2016) and sirtuin activators (Pearson et al. 2008; Csiszar et al. 2012; Mattison et al. 2014; Toth et al. 2015; Toth et al. 2014; Zhang et al. 2009; Oomen et al. 2009; Minor et al. 2011; Chen et al. 2015b; Gano et al. 2014) observed both *in vivo* and *ex vivo*. We hope that our findings will facilitate future endeavor of uncovering the mechanistic role of miRNA gene expression regulatory networks in the anti-aging effects of NAD+ booster treatments. Future studies should also investigate the links between miRNAs

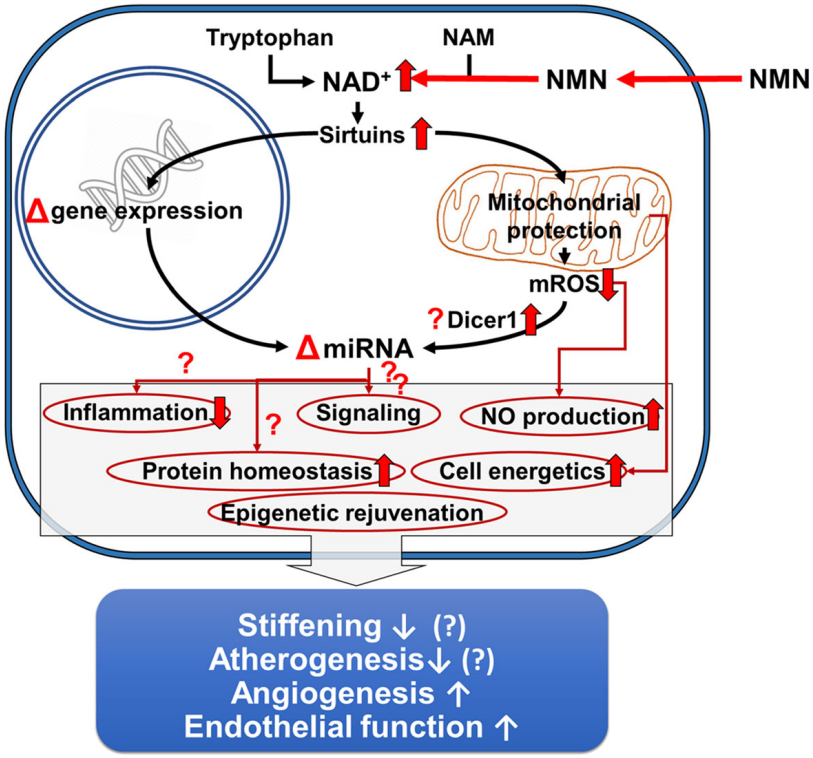

Fig. 3 Proposed scheme for the mechanisms by which restoration of NAD+ levels in the aged vasculature by NMN supplementation promotes anti-aging miRNA expression profile, rescues endothelial function, and prevents atherogenesis. The model, based on our present and previous findings and earlier data from the literature (Tarantini et al. 2019; Csiszar et al. 2019), predicts that increased NAD+ activates sirtuin-mediated pathways, restores cellular energetics and attenuates mitochondrial ROS (mtROS) production, which lead to epigenetic changes promoting youthful gene/miRNA expression, restore Dicer1-mediated miRNA processing, increase NO bioavailability, decrease inflammation, and improve protein homeostasis. All of these effects are predicted to act to decrease large artery stiffness, inhibit atherogenesis, improve vasodilation, and promote angiogenesis at the level of the microcirculation

regulated by NMN and sirtuin activators and miRNAs known to act in the conserved pathways of aging (Ungvari et al. 2018; Menghini et al. 2014; Tarantini et al. 2016b; Kennedy et al. 2014; An et al. 2017; Ashpole et al. 2017; Bennis et al. 2017; Deepa et al. 2017; Fang et al. 2017; Fulop et al. 2018; Lee et al. 2018; Reglodi et al. 2018; Menghini et al. 2009; Fan et al. 2018) and major aging-related diseases (Csiszar et al. 2017; Meschiari et al. 2017; Tarantini et al. 2017b; Tucsek et al. 2017; Ungvari et al. 2017b; Carlson et al. 2018; Csipo et al. 2018; Tana et al. 2017; Feinberg and Moore 2016). Potentially, miRNA-regulated anti-aging mechanisms of NAD+ booster treatments and sirtuin activators could be harnessed for development of new pharmacological approaches for the prevention and treatment of age-related vascular diseases.

Funding information This work was supported by grants from the American Heart Association (ST), the Oklahoma Center for the Advancement of Science and Technology (to AC, AY, ZU), the National Institute on Aging (R01-AG047879; R01-AG038747; R01-AG055395), the National Institute of Neurological Disorders and Stroke (NINDS; R01-NS056218 to AC, R01-NS100782 to ZU), the Oklahoma Shared Clinical and Translational Resources (OSCTR) program funded by the National Institute of General Medical Sciences (GM104938, to AY and JW), the Presbyterian Health Foundation (to ZU, AC, AY), the NIA-supported Geroscience Training Program in Oklahoma (T32AG052363), the Oklahoma Nathan Shock Center (P30AG050911), and the Cellular and Molecular GeroScience CoBRE (1P20GM125528, sub#5337). The funding sources had no role in the study design; in the collection, analysis, and interpretation of data; in the writing of the report; and in the decision to submit the article for publication.

References

Aavik E, Babu M, Yla-Herttuala S (2019) DNA methylation processes in atheosclerotic plaque. *Atherosclerosis*. 281: 168–179

Abdellatif M, Sedej S, Carmona-Gutierrez D, Madeo F, Kroemer G (2018) Autophagy in cardiovascular aging. Circ Res 123: 803–824

Agarwal V, Bell GW, Nam JW, Bartel DP (2015) Predicting effective microRNA target sites in mammalian mRNAs. *Elife*. 4

Alfaras I, Di Germanio C, Bernier M, Csiszar A, Ungvari Z, Lakatta EG, de Cabo R (2016) Pharmacological strategies to retard cardiovascular aging. Circ Res 118:1626–1642

Ali H, Emoto N, Yagi K, Vignon-Zellweger N, Nakayama K, Hatakeyama K, Asada Y, Rikitake Y, Hirata K (2013) Localization and characterization of a novel secreted protein, SCUBE2, in the development and progression of atherosclerosis. Kobe J Med Sci 59:E122–E131

An JY, Quarles EK, Mekvanich S, Kang A, Liu A, Santos D, Miller RA, Rabinovitch PS, Cox TC and Kaeberlein M. Rapamycin treatment attenuates age-associated periodontitis in mice. Geroscience. 2017;https://doi.org/10.1007/s11357-017-9994-6.

Anderson RM, Bitterman KJ, Wood JG, Medvedik O, Cohen H, Lin SS, Manchester JK, Gordon JI, Sinclair DA (2002) Manipulation of a nuclear NAD+ salvage pathway delays aging without altering steady-state NAD+ levels. J Biol Chem 277:18881–18890

Ashpole NM, Logan S, Yabluchanskiy A, Mitschelen MC, Yan H, Farley JA, Hodges EL, Ungvari Z, Csiszar A, Chen S, Georgescu C, Hubbard GB, Ikeno Y, Sonntag WE (2017) IGF-1 has sexually dimorphic, pleiotropic, and time-dependent effects on healthspan, pathology, and lifespan. Geroscience. 39:129–145

Badi I, Mancinelli L, Polizzotto A, Ferri D, Zeni F, Burba I, Milano G, Brambilla F, Saccu C, Bianchi ME, Pompilio G, Capogrossi MC, Raucci A (2018) miR-34a Promotes vascular smooth muscle cell calcification by downregulating SIRT1 (Sirtuin 1) and Axl (AXL receptor tyrosine kinase). Arterioscler Thromb Vasc Biol 38:2079–2090

Bates DJ, Li N, Liang R, Sarojini H, An J, Masternak MM, Bartke A, Wang E MicroRNA regulation in Ames dwarf mouse liver may contribute to delayed aging. Aging Cell 9:1–18

Bennis MT, Schneider A, Victoria B, Do A, Wiesenborn DS, Spinel L, Gesing A, Kopchick JJ, Siddiqi SA, Masternak MM (2017) The role of transplanted visceral fat from the long-lived growth hormone receptor knockout mice on insulin signaling. Geroscience. 39:51–59

Bhatt PM, Lewis CJ, House DL, Keller CM, Kohn LD, Silver MJ, McCall KD, Goetz DJ, Malgor R (2012) Increased Wnt5a mRNA expression in advanced atherosclerotic lesions, and oxidized LDL treated human monocyte-derived macrophages. Open Circ Vasc J 5:1–7

Blesinger H, Kaulfuss S, Aung T, Schwoch S, Prantl L, Rossler J, Wilting J, Becker J (2018) PIK3CA mutations are specifically localized to lymphatic endothelial cells of lymphatic malformations. PLoS One 13:e0200343

Boehm M, Slack F (2005) A developmental timing microRNA and its target regulate life span in C. elegans. Science. 310: 1954–1957

de Boer S, Baran Y, Garcia-Garcia HM, Eskin I, Lenzen MJ, Kleber ME, Regar E, de Jaegere PJ, Ligthart JM, van Geuns RJ, Lehtimaki T, Laaksonen R, Boersma E, Marz W, Halperin E, Serruys PW, Koenig W (2018) The European collaborative project on inflammation and vascular wall remodeling in atherosclerosis - intravascular ultrasound (ATHEROREMO-IVUS) study. EuroIntervention. 14:194–203

Bonauer A, Carmona G, Iwasaki M, Mione M, Koyanagi M, Fischer A, Burchfield J, Fox H, Doebele C, Ohtani K, Chavakis E, Potente M, Tjwa M, Urbich C, Zeiher AM, Dimmeler S (2009) MicroRNA-92a controls angiogenesis and functional recovery of ischemic tissues in mice. Science. 324:1710–1713

Boon RA, Iekushi K, Lechner S, Seeger T, Fischer A, Heydt S, Kaluza D, Treguer K, Carmona G, Bonauer A, Horrevoets AJ, Didier N, Girmatsion Z, Biliczki P, Ehrlich JR, Katus HA, Muller OJ, Potente M, Zeiher AM, Hermeking H, Dimmeler S (2013) MicroRNA-34a regulates cardiac ageing and function. Nature. 495:107–110

Bostrom KI, Yao J, Guihard PJ, Blazquez-Medela AM, Yao Y (2016) Endothelial-mesenchymal transition in atherosclerotic lesion calcification. Atherosclerosis. 253:124–127

Brown CB, Wenning JM, Lu MM, Epstein DJ, Meyers EN, Epstein JA (2004) Cre-mediated excision of Fgf8 in the Tbx1 expression domain reveals a critical role for Fgf8 in cardiovascular development in the mouse. Dev Biol 267: 190–202

Carlson BW, Craft MA, Carlson JR, Razaq W, Deardeuff KK, Benbrook DM (2018) Accelerated vascular aging and persistent cognitive impairment in older female breast cancer survivors. Geroscience. 40:325–336

Che J, Okigaki M, Takahashi T, Katsume A, Adachi Y, Yamaguchi S, Matsunaga S, Takeda M, Matsui A, Kishita E, Ikeda K, Yamada H, Matsubara H (2011) Endothelial FGF receptor signaling accelerates atherosclerosis. Am J Physiol Heart Circ Physiol 300:H154–H161

Che P, Liu J, Shan Z, Wu R, Yao C, Cui J, Zhu X, Wang J, Burnett MS, Wang S, Wang J (2014) miR-125a-5p impairs endothelial cell angiogenesis in aging mice via RTEF-1 downregulation. Aging Cell 13:926–934

Chen LJ, Chuang L, Huang YH, Zhou J, Lim SH, Lee CI, Lin WW, Lin TE, Wang WL, Chen L, Chien S, Chiu JJ (2015a) MicroRNA mediation of endothelial inflammatory response to smooth muscle cells and its inhibition by atheroprotective shear stress. Circ Res 116:1157–1169

Chen YX, Zhang M, Cai Y, Zhao Q, Dai W (2015b) The Sirt1 activator SRT1720 attenuates angiotensin II-induced atherosclerosis in apoE(-)/(-) mice through inhibiting vascular inflammatory response. Biochem Biophys Res Commun 465: 732–738

Choi SE, Fu T, Seok S, Kim DH, Yu E, Lee KW, Kang Y, Li X, Kemper B, Kemper JK (2013) Elevated microRNA-34a in obesity reduces NAD+ levels and SIRT1 activity by directly targeting NAMPT. Aging Cell 12:1062–1072

Cox RH, Fromme SJ, Folander KL, Swanson RJ (2008) Voltage gated K+ channel expression in arteries of Wistar-Kyoto and spontaneously hypertensive rats. Am J Hypertens 21:213–218

Csipo T, Fulop GA, Lipecz A, Tarantini S, Kiss T, Balasubramanian P, Csiszar A (2018) Ungvari Z and Yabluchanskiy A. Short-term weight loss reverses obesity-induced microvascular endothelial dysfunction, Geroscience

Csiszar A, Labinskyy N, Podlutsky A, Kaminski PM, Wolin MS, Zhang C, Mukhopadhyay P, Pacher P, Hu F, de Cabo R, Ballabh P, Ungvari Z (2008) Vasoprotective effects of resveratrol and SIRT1: attenuation of cigarette smoke-induced oxidative stress and proinflammatory phenotypic alterations. Am J Physiol Heart Circ Physiol 294:H2721–H2735

Csiszar A, Labinskyy N, Jimenez R, Pinto JT, Ballabh P, Losonczy G, Pearson KJ, de Cabo R, Ungvari Z (2009a) Anti-oxidative and anti-inflammatory vasoprotective effects of caloric restriction in aging: role of circulating factors and SIRT1. Mech Ageing Dev 130:518–527

Csiszar A, Labinskyy N, Pinto JT, Ballabh P, Zhang H, Losonczy G, Pearson KJ, de Cabo R, Pacher P, Zhang C, Ungvari ZI (2009b) Resveratrol induces mitochondrial biogenesis in endothelial cells. Am J Physiol Heart Circ Physiol

Csiszar A, Sosnowska D, Wang M, Lakatta EG, Sonntag WE, Ungvari Z (2012) Age-associated proinflammatory secretory phenotype in vascular smooth muscle cells from the non-human primate Macaca mulatta: reversal by resveratrol treatment. J Gerontol A Biol Sci Med Sci 67:811–820

Csiszar A, Gautam T, Sosnowska D, Tarantini S, Banki E, Tucsek Z, Toth P, Losonczy G, Koller A, Reglodi D, Giles CB, Wren JD, Sonntag WE, Ungvari Z (2014) Caloric restriction confers persistent anti-oxidative, pro-angiogenic, and anti-inflammatory effects and promotes anti-aging miRNA expression profile in cerebromicrovascular endothelial cells of aged rats. Am J Physiol Heart Circ Physiol 307:H292–H306

Csiszar A, Tarantini S, Fulop GA, Kiss T, Valcarcel-Ares MN, Galvan V, Ungvari Z, Yabluchanskiy A (2017) Hypertension impairs neurovascular coupling and promotes microvascular injury: role in exacerbation of Alzheimer's disease. Geroscience.

Csiszar A, Tarantini S, Yabluchanskiy A, Balasubramanian P, Kiss T, Farkas E, Baur JA and Ungvari ZI (2019) Role of endothelial NAD+ deficiency in age-related vascular dysfunction. Am J Physiol Heart Circ Physiol:in press.

Das A, Huang GX, Bonkowski MS, Longchamp A, Li C, Schultz MB, Kim LJ, Osborne B, Joshi S, Lu Y, Trevino-Villarreal JH, Kang MJ, Hung TT, Lee B, Williams EO, Igarashi M, Mitchell JR, Wu LE, Turner N, Arany Z, Guarente L, Sinclair DA (2018) Impairment of an endothelial NAD(+)-H2S signaling network is a reversible cause of vascular aging. Cell. 173:74–89 e20

Deepa SS, Bhaskaran S, Espinoza S, Brooks SV, McArdle A, Jackson MJ, Van Remmen H, Richardson A (2017) A new mouse model of frailty: the Cu/Zn superoxide dismutase knockout mouse. Geroscience. 39:187–198

Doebele C, Bonauer A, Fischer A, Scholz A, Reiss Y, Urbich C, Hofmann WK, Zeiher AM, Dimmeler S Members of the microRNA-17-92 cluster exhibit a cell intrinsic anti-angiogenic function in endothelial cells. Blood.

ElSharawy A, Keller A, Flachsbart F, Wendschlag A, Jacobs G, Kefer N, Brefort T, Leidinger P, Backes C, Meese E, Schreiber S, Rosenstiel P, Franke A, Nebel A (2012) Genome-wide miRNA signatures of human longevity. Aging Cell 11:607–616

Estrada-Velasco BI, Cruz M, Madrid-Marina V, Martinez-Nava GA, Gomez-Zamudio J, Burguete-Garcia AI (2013) IRS1, TCF7L2, ADRB1, PPARG, and HHEX polymorphisms associated with atherogenic risk in Mexican population. Biomed Res Int 2013:394523

Evrard SM, Lecce L, Michelis KC, Nomura-Kitabayashi A, Pandey G, Purushothaman KR, d'Escamard V, Li JR, Hadri L, Fujitani K, Moreno PR, Benard L, Rimmele P, Cohain A, Mecham B, Randolph GJ, Nabel EG, Hajjar R, Fuster V, Boehm M, Kovacic JC (2016) Endothelial to mesenchymal transition is common in atherosclerotic lesions and is associated with plaque instability. Nat Commun 7:11853

Faccini J, Ruidavets JB, Cordelier P, Martins F, Maoret JJ, Bongard V, Ferrieres J, Roncalli J, Elbaz M, Vindis C (2017) Circulating miR-155, miR-145 and let-7c as diagnostic biomarkers of the coronary artery disease. Sci Rep 7: 42916

Fan B, Luk AOY, Chan JCN, Ma RCW (2018) MicroRNA and diabetic complications: a clinical perspective. Antioxid Redox Signal 29:1041–1063

Fang Y, McFadden S, Darcy J, Hill CM, Huber JA, Verhulst S, Kopchick JJ, Miller RA, Sun LY, Bartke A (2017) Differential effects of early-life nutrient restriction in long-lived GHR-KO and normal mice. Geroscience. 39:347–356

Feinberg MW, Moore KJ (2016) MicroRNA regulation of atherosclerosis. *Circ Res* 118:703–720

Fulop GA, Kiss T, Tarantini S, Balasubramanian P, Yabluchanskiy A, Farkas E, Bari F, Ungvari Z, Csiszar A (2018) Nrf2 deficiency in aged mice exacerbates cellular senescence promoting cerebrovascular inflammation. Geroscience. 40:513–521

Gano LB, Donato AJ, Pasha HM, Hearon CM Jr, Sindler AL, Seals DR (2014) The SIRT1 activator SRT1720 reverses vascular endothelial dysfunction, excessive superoxide production, and inflammation with aging in mice. Am J Physiol Heart Circ Physiol 307:H1754–H1763

Gomes AP, Price NL, Ling AJ, Moslehi JJ, Montgomery MK, Rajman L, White JP, Teodoro JS, Wrann CD, Hubbard BP, Mercken EM, Palmeira CM, de Cabo R, Rolo AP, Turner N, Bell EL, Sinclair DA (2013) Declining NAD(+) induces a pseudohypoxic state disrupting nuclear-mitochondrial communication during aging. Cell. 155:1624–1638

Grillari J, Grillari-Voglauer R Novel modulators of senescence, aging, and longevity: small non-coding RNAs enter the stage. Exp Gerontol 45:302–311

Guo Y, Li P, Gao L, Zhang J, Yang Z, Bledsoe G, Chang E, Chao L, Chao J (2017) Kallistatin reduces vascular senescence and aging by regulating microRNA-34a-SIRT1 pathway. Aging Cell 16:837–846

Harris MA, Clark J, Ireland A, Lomax J, Ashburner M, Foulger R, Eilbeck K, Lewis S, Marshall B, Mungall C, Richter J, Rubin GM, Blake JA, Bult C, Dolan M, Drabkin H, Eppig JT, Hill DP, Ni L, Ringwald M, Balakrishnan R, Cherry JM, Christie KR, Costanzo MC, Dwight SS, Engel S, Fisk DG, Hirschman JE, Hong EL, Nash RS, Sethuraman A, Theesfeld CL, Botstein D, Dolinski K, Feierbach B, Berardini T, Mundodi S, Rhee SY, Apweiler R, Barrell D, Camon E, Dimmer E, Lee V, Chisholm R, Gaudet P, Kibbe W, Kishore R, Schwarz EM, Sternberg P, Gwinn M, Hannick L, Wortman J, Berriman M, Wood V, de la Cruz N, Tonellato P, Jaiswal P, Seigfried T, White R, Gene Ontology C (2004) The gene ontology (GO) database and informatics resource. Nucleic Acids Res 32:D258–D261

Hartmann P, Zhou Z, Natarelli L, Wei Y, Nazari-Jahantigh M, Zhu M, Grommes J, Steffens S, Weber C, Schober A (2016) Endothelial Dicer promotes atherosclerosis and vascular inflammation by miRNA-103-mediated suppression of KLF4. Nat Commun 7:10521

Hazra S, Henson GD, Morgan RG, Breevoort SR, Ives SJ, Richardson RS, Donato AJ, Lesniewski LA (2016)

Experimental reduction of miR-92a mimics arterial aging. Exp Gerontol 83:165–170

Heo KS, Chang E, Le NT, Cushman H, Yeh ET, Fujiwara K, Abe J (2013) De-SUMOylation enzyme of sentrin/SUMO-specific protease 2 regulates disturbed flow-induced SUMOylation of ERK5 and p53 that leads to endothelial dysfunction and atherosclerosis. Circ Res 112:911–923

Heo KS, Le NT, Cushman HJ, Giancursio CJ, Chang E, Woo CH, Sullivan MA, Taunton J, Yeh ET, Fujiwara K, Abe J (2015) Disturbed flow-activated p90RSK kinase accelerates atherosclerosis by inhibiting SENP2 function. J Clin Invest 125: 1299–1310

Hergenreider E, Heydt S, Treguer K, Boettger T, Horrevoets AJ, Zeiher AM, Scheffer MP, Frangakis AS, Yin X, Mayr M, Braun T, Urbich C, Boon RA, Dimmeler S (2012) Atheroprotective communication between endothelial cells and smooth muscle cells through miRNAs. Nat Cell Biol 14: 249–256

Hixson JE, Jun G, Shimmin LC, Wang Y, Yu G, Mao C, Warren AS, Howard TD, Heide RSV, Van Eyk J, Wang Y, Herrington DM (2017) Whole exome sequencing to identify genetic variants associated with raised atherosclerotic lesions in young persons. Sci Rep 7:4091

Hoeksema MA, Gijbels MJ, Van den Bossche J, van der Velden S, Sijm A, Neele AE, Seijkens T, Stoger JL, Meiler S, Boshuizen MC, Dallinga-Thie GM, Levels JH, Boon L, Mullican SE, Spann NJ, Cleutjens JP, Glass CK, Lazar MA, de Vries CJ, Biessen EA, Daemen MJ, Lutgens E, de Winther MP (2014) Targeting macrophage Histone deacetylase 3 stabilizes atherosclerotic lesions. EMBO Mol Med 6:1124–1132

Hoenig MR, Bianchi C, Rosenzweig A, Sellke FW (2008) The cardiac microvasculature in hypertension, cardiac hypertrophy and diastolic heart failure. Curr Vasc Pharmacol 6:292–300

Huang YQ, Cai AP, Chen JY, Huang C, Li J, Feng YQ (2016) The relationship of plasma miR-29a and oxidized low density lipoprotein with atherosclerosis. Cell Physiol Biochem 40: 1521–1528

Ibanez-Ventoso C, Yang M, Guo S, Robins H, Padgett RW, Driscoll M (2006) Modulated microRNA expression during adult lifespan in Caenorhabditis elegans. *Aging Cell* 5:235–246

Inukai S, Slack F (2013) MicroRNAs and the genetic network in aging. J Mol Biol

Inukai S, de Lencastre A, Turner M, Slack F (2012) Novel microRNAs differentially expressed during aging in the mouse brain. PLoS One 7:e40028

Ito T, Yagi S, Yamakuchi M (2010) MicroRNA-34a regulation of endothelial senescence. Biochem Biophys Res Commun 398:735–740

Izumi N, Helker C, Ehling M, Behrens A, Herzog W, Adams RH (2012) Fbxw7 controls angiogenesis by regulating endothelial Notch activity. *PLoS One* 7:e41116

Jansen F, Yang X, Nickenig G, Werner N, Vasa-Nicotera M (2015) Role, function and therapeutic potential of microRNAs in vascular aging. Curr Vasc Pharmacol 13:324–330

Jones M, Sabatini PJ, Lee FS, Bendeck MP, Langille BL (2002) N-cadherin upregulation and function in response of smooth muscle cells to arterial injury. Arterioscler Thromb Vasc Biol 22:1972–1977

Kennedy BK, Berger SL, Brunet A, Campisi J, Cuervo AM, Epel ES, Franceschi C, Lithgow GJ, Morimoto RI, Pessin JE, Rando TA, Richardson A, Schadt EE, Wyss-Coray T, Sierra F (2014) Geroscience: linking aging to chronic disease. Cell. 159:709–713

Khyzha N, Alizada A, Wilson MD, Fish JE (2017) Epigenetics of atherosclerosis: emerging mechanisms and methods. Trends Mol Med 23:332–347

Kim CW, Kumar S, Son DJ, Jang IH, Griendling KK, Jo H (2014) Prevention of abdominal aortic aneurysm by anti-microRNA-712 or anti-microRNA-205 in angiotensin II-infused mice. Arterioscler Thromb Vasc Biol 34:1412–1421

Kim M, Yoo HJ, Kim M, Kim J, Baek SH, Song M, Lee JH (2017) EPHA6 rs4857055 C > T polymorphism associates with hypertension through triglyceride and LDL particle size in the Korean population. Lipids Health Dis 16:230

Kintscher U, Lyon C, Wakino S, Bruemmer D, Feng X, Goetze S, Graf K, Moustakas A, Staels B, Fleck E, Hsueh WA, Law RE (2002) PPARalpha inhibits TGF-beta-induced beta5 integrin transcription in vascular smooth muscle cells by interacting with Smad4. Circ Res 91:e35–e44

Kintsurashvili E, Shenouda S, Ona D, Ona L, Ahmad S, Ravid K, Gavras I, Gavras H (2009) Hypertension in transgenic mice with brain-selective overexpression of the alpha(2B)-adrenoceptor. Am J Hypertens 22:41–45

Kisler K, Nelson AR, Montagne A, Zlokovic BV (2017) Cerebral blood flow regulation and neurovascular dysfunction in Alzheimer disease. Nat Rev Neurosci 18:419–434

Kiss T, Balasubramanian P, Valcarcel-Ares MN, Tarantini S, Yabluchanskiy A, Csipo T, Lipecz A, Reglodi D, Zhang XA, Bari F, Farkas E, Csiszar A and Ungvari Z (2019) Nicotinamide mononucleotide (NMN) treatment attenuates oxidative stress and rescues angiogenic capacity in aged cerebromicrovascular endothelial cells: a potential mechanism for prevention of vascular cognitive impairment. GeroScience.:in press.

Kuehbacher A, Urbich C, Zeiher AM, Dimmeler S (2007) Role of Dicer and Drosha for endothelial microRNA expression and angiogenesis. Circ Res 101:59–68

Kurdi A, De Meyer GR, Martinet W (2016) Potential therapeutic effects of mTOR inhibition in atherosclerosis. Br J Clin Pharmacol 82:1267–1279

Lee HJ, Feliers D, Barnes JL, Oh S, Choudhury GG, Diaz V, Galvan V, Strong R, Nelson J, Salmon A, Kevil CG, Kasinath BS (2018) Hydrogen sulfide ameliorates aging-associated changes in the kidney. Geroscience. 40:163–176

Leung A, Trac C, Jin W, Lanting L, Akbany A, Saetrom P, Schones DE, Natarajan R (2013) Novel long noncoding RNAs are regulated by angiotensin II in vascular smooth muscle cells. Circ Res 113:266–278

Li C, He J, Chen J, Zhao J, Gu D, Hixson JE, Rao DC, Jaquish CE, Gu CC, Chen J, Huang J, Chen S, Kelly TN (2016) Genome-wide gene-sodium interaction analyses on blood pressure: the genetic epidemiology network of salt-sensitivity study. Hypertension. 68:348–355

Limaye N, Kangas J, Mendola A, Godfraind C, Schlogel MJ, Helaers R, Eklund L, Boon LM, Vikkula M (2015) Somatic activating PIK3CA mutations cause venous malformation. Am J Hum Genet 97:914–921

Liu R, Jin Y, Tang WH, Qin L, Zhang X, Tellides G, Hwa J, Yu J, Martin KA (2013) Ten-eleven translocation-2 (TET2) is a

master regulator of smooth muscle cell plasticity. Circulation. 128:2047–2057

Liu L, Zeng P, Yang X, Duan Y, Zhang W, Ma C, Zhang X, Yang S, Li X, Yang J, Liang Y, Han H, Zhu Y, Han J, Chen Y (2018) Inhibition of vascular calcification. Arterioscler Thromb Vasc Biol 38:2382–2395

Liu B, Wang L, Jiang W, Xiong Y, Pang L, Zhong Y, Zhang C, Ou W, Tian C, Chen X and Liu SM (2019) Myocyte enhancer factor 2A delays vascular endothelial cell senescence by activating the PI3K/p-Akt/SIRT1 pathway. *Aging (Albany NY)*..

Livak KJ, Schmittgen TD (2001) Analysis of relative gene expression data using real-time quantitative PCR and the 2(-Delta Delta C(T)) Method. Methods. 25:402–408

Long DA, Norman JT, Fine LG (2012) Restoring the renal microvasculature to treat chronic kidney disease. Nat Rev Nephrol 8:244–250

Lopez-Mejias R, Genre F, Remuzgo-Martinez S, Gonzalez-Juanatey C, Robustillo-Villarino M, Llorca J, Corrales A, Vicente E, Miranda-Filloy JA, Magro C, Tejera-Segura B, Ramirez Huaranga MA, Pina T, Blanco R, Alegre-Sancho JJ, Raya E, Mijares V, Ubilla B, Minguez Sanchez MD, Gomez-Vaquero C, Balsa A, Pascual-Salcedo D, Lopez-Longo FJ, Carreira P, Gonzalez-Alvaro I, Rodriguez-Rodriguez L, Fernandez-Gutierrez B, Ferraz-Amaro I, Castaneda S, Martin J, Gonzalez-Gay MA (2016) Influence of elevated-CRP level-related polymorphisms in non-rheumatic Caucasians on the risk of subclinical atherosclerosis and cardiovascular disease in rheumatoid arthritis. Sci Rep 6: 31979

Lovren F, Pan Y, Quan A, Singh KK, Shukla PC, Gupta N, Steer BM, Ingram AJ, Gupta M, Al-Omran M, Teoh H, Marsden PA, Verma S (2012) MicroRNA-145 targeted therapy reduces atherosclerosis. Circulation. 126:S81–S90

Lu Y, Thavarajah T, Gu W, Cai J, Xu Q (2018) Impact of miRNA in atherosclerosis. Arterioscler Thromb Vasc Biol 38:e159–e170

Lv YC, Tang YY, Zhang P, Wan W, Yao F, He PP, Xie W, Mo ZC, Shi JF, Wu JF, Peng J, Liu D, Cayabyab FS, Zheng XL, Tang XY, Ouyang XP, Tang CK (2016) Histone methyltransferase enhancer of zeste homolog 2-mediated ABCA1 promoter DNA methylation contributes to the progression of atherosclerosis. PLoS One 11:e0157265

Maes OC, An J, Sarojini H, Wang E (2008) Murine microRNAs implicated in liver functions and aging process. Mech Ageing Dev 129:534–541

Mao C, Howard TD, Sullivan D, Fu Z, Yu G, Parker SJ, Will R, Vander Heide RS, Wang Y, Hixson J, Van Eyk J, Herrington DM (2017) Bioinformatic analysis of coronary disease associated SNPs and genes to identify proteins potentially involved in the pathogenesis of atherosclerosis. J Proteom Genom Res 2:1–12

Mao Z, Wu F, Shan Y (2018) Identification of key genes and miRNAs associated with carotid atherosclerosis based on mRNA-seq data. Medicine (Baltimore) 97:e9832

Massudi H, Grant R, Braidy N, Guest J, Farnsworth B, Guillemin GJ (2012) Age-associated changes in oxidative stress and NAD+ metabolism in human tissue. PLoS One 7:e42357

Mattison JA, Wang M, Bernier M, Zhang J, Park SS, Maudsley S, An SS, Santhanam L, Martin B, Faulkner S, Morrell C, Baur JA, Peshkin L, Sosnowska D, Csiszar A, Herbert RL, Tilmont EM, Ungvari Z, Pearson KJ, Lakatta EG, de Cabo R (2014) Resveratrol prevents high fat/sucrose diet-induced central arterial wall inflammation and stiffening in nonhuman primates. Cell Metab 20:183–190

Menghini R, Casagrande V, Cardellini M, Martelli E, Terrinoni A, Amati F, Vasa-Nicotera M, Ippoliti A, Novelli G, Melino G, Lauro R, Federici M (2009) MicroRNA 217 modulates endothelial cell senescence via silent information regulator 1. Circulation. 120:1524–1532

Menghini R, Stohr R, Federici M (2014) MicroRNAs in vascular aging and atherosclerosis. Ageing Res Rev 17:68–78

Mercken EM, Majounie E, Ding J, Guo R, Kim J, Bernier M, Mattison J, Cookson MR, Gorospe M, de Cabo R, Abdelmohsen K (2013) Age-associated miRNA alterations in skeletal muscle from rhesus monkeys reversed by caloric restriction. Aging (Albany NY) 5:692–703

Meschiari CA, Ero OK, Pan H, Finkel T, Lindsey ML (2017) The impact of aging on cardiac extracellular matrix. Geroscience. 39:7–18

Minamino T, Komuro I (2007) Vascular cell senescence: contribution to atherosclerosis. Circ Res 100:15–26

Minor RK, Baur JA, Gomes AP, Ward TM, Csiszar A, Mercken EM, Abdelmohsen K, Shin YK, Canto C, Scheibye-Knudsen M, Krawczyk M, Irusta PM, Martin-Montalvo A, Hubbard BP, Zhang Y, Lehrmann E, White AA, Price NL, Swindell WR, Pearson KJ, Becker KG, Bohr VA, Gorospe M, Egan JM, Talan MI, Auwerx J, Westphal CH, Ellis JL, Ungvari Z, Vlasuk GP, Elliott PJ, Sinclair DA, de Cabo R (2011) SRT1720 improves survival and healthspan of obese mice. Sci Rep 1. https://doi.org/10.1038/srep00070

Mitchell SJ, Bernier M, Aon MA, Cortassa S, Kim EY, Fang EF, Palacios HH, Ali A, Navas-Enamorado I, Di Francesco A, Kaiser TA, Waltz TB, Zhang N, Ellis JL, Elliott PJ, Frederick DW, Bohr VA, Schmidt MS, Brenner C, Sinclair DA, Sauve AA, Baur JA, de Cabo R (2018) Nicotinamide improves aspects of healthspan, but not lifespan, in mice. Cell Metab 27:667–676 e4

Montagne A, Zhao Z, Zlokovic BV (2017) Alzheimer's disease: a matter of blood-brain barrier dysfunction? J Exp Med 214: 3151–3169

Moonen JR, Lee ES, Schmidt M, Maleszewska M, Koerts JA, Brouwer LA, van Kooten TG, van Luyn MJ, Zeebregts CJ, Krenning G, Harmsen MC (2015) Endothelial-to-mesenchymal transition contributes to fibro-proliferative vascular disease and is modulated by fluid shear stress. Cardiovasc Res 108:377–386

Moulton KS, Li M, Strand K, Burgett S, McClatchey P, Tucker R, Furgeson SB, Lu S, Kirkpatrick B, Cleveland JC, Nemenoff RA, Ambardekar AV, Weiser-Evans MC (2018) PTEN deficiency promotes pathological vascular remodeling of human coronary arteries. JCI Insight 3

Muendlein A, Saely CH, Geller-Rhomberg S, Sonderegger G, Rein P, Winder T, Beer S, Vonbank A, Drexel H (2011) Single nucleotide polymorphisms of TCF7L2 are linked to diabetic coronary atherosclerosis. PLoS One 6:e17978

Mullins RF, Khanna A, Schoo DP, Tucker BA, Sohn EH, Drack AV, Stone EM (2014) Is age-related macular degeneration a microvascular disease? Adv Exp Med Biol 801:283–289

O'Rourke JR, Olson EN (2011) Modulating the MicroRNArchitecture of an aging aorta. Circ Res 109: 1098–1099

Ohukainen P, Syvaranta S, Napankangas J, Rajamaki K, Taskinen P, Peltonen T, Helske-Suihko S, Kovanen PT, Ruskoaho H, Rysa J (2015) MicroRNA-125b and chemokine CCL4 expression are associated with calcific aortic valve disease. Ann Med 47:423–429

Ono K, Kuwabara Y, Han J (2011) MicroRNAs and cardiovascular diseases. FEBS J 278:1619–1633

Oomen CA, Farkas E, Roman V, van der Beek EM, Luiten PG, Meerlo P (2009) Resveratrol preserves cerebrovascular density and cognitive function in aging mice. Front Aging Neurosci 1:4

Pacher P, Mabley JG, Soriano FG, Liaudet L, Komjati K, Szabo C (2002) Endothelial dysfunction in aging animals: the role of poly(ADP-ribose) polymerase activation. Br J Pharmacol 135:1347–1350

Payne GW (2006) Effect of inflammation on the aging microcirculation: impact on skeletal muscle blood flow control. Microcirculation. 13:343–352

Pearson KJ, Baur JA, Lewis KN, Peshkin L, Price NL, Labinskyy N, Swindell WR, Kamara D, Minor RK, Perez E, Jamieson HA, Zhang Y, Dunn SR, Sharma K, Pleshko N, Woollett LA, Csiszar A, Ikeno Y, Le Couteur D, Elliott PJ, Becker KG, Navas P, Ingram DK, Wolf NS, Ungvari Z, Sinclair DA, de Cabo R (2008) Resveratrol delays age-related deterioration and mimics transcriptional aspects of dietary restriction without extending life span. Cell Metab 8:157–168

Peng J, Yang Q, Li AF, Li RQ, Wang Z, Liu LS, Ren Z, Zheng XL, Tang XQ, Li GH, Tang ZH, Jiang ZS, Wei DH (2016) Tet methylcytosine dioxygenase 2 inhibits atherosclerosis via upregulation of autophagy in ApoE-/- mice. Oncotarget. 7: 76423–76436

de Picciotto NE, Gano LB, Johnson LC, Martens CR, Sindler AL, Mills KF, Imai S, Seals DR (2016) Nicotinamide mononucleotide supplementation reverses vascular dysfunction and oxidative stress with aging in mice. Aging Cell 15:522–530

Pilbrow AP, Cordeddu L, Cameron VA, Frampton CM, Troughton RW, Doughty RN, Whalley GA, Ellis CJ, Yandle TG, Richards AM, Foo RS (2014) Circulating miR-323-3p and miR-652: candidate markers for the presence and progression of acute coronary syndromes. Int J Cardiol 176:375–385

Pojoga LH, Williams JS, Yao TM, Kumar A, Raffetto JD, do Nascimento GR, Reslan OM, Adler GK, Williams GH, Shi Y, Khalil RA (2011) Histone demethylase LSD1 deficiency during high-salt diet is associated with enhanced vascular contraction, altered NO-cGMP relaxation pathway, and hypertension. Am J Physiol Heart Circ Physiol 301:H1862–H1871

Pronk MCA, Majolee J, Loregger A, van Bezu JSM, Zelcer N, Hordijk PL, Kovacevic I (2019) FBXW7 regulates endothelial barrier function by suppression of the cholesterol synthesis pathway and prenylation of RhoB. Mol Biol Cell 30:607–621

Raghavan S, Singh NK, Gali S, Mani AM, Rao GN (2018) Protein kinase Ctheta via activating transcription factor 2-mediated CD36 expression and foam cell formation of Ly6C(hi) cells contributes to atherosclerosis. Circulation. 138:2395–2412

Regina C, Panatta E, Candi E, Melino G, Amelio I, Balistreri CR, Annicchiarico-Petruzzelli M, Di Daniele N, Ruvolo G (2016) Vascular ageing and endothelial cell senescence: Molecular mechanisms of physiology and diseases. Mech Ageing Dev 159:14–21

Reglodi D, Atlasz T, Szabo E, Jungling A, Tamas A, Juhasz T, Fulop BD, Bardosi A (2018) PACAP deficiency as a model of aging. Geroscience. 40:437–452

Rippe C, Zhu B, Krawczyk KK, Bavel EV, Albinsson S, Sjolund J, Bakker E, Sward K (2017) Hypertension reduces soluble guanylyl cyclase expression in the mouse aorta via the Notch signaling pathway. Sci Rep 7:1334

Rotllan N, Ramirez CM, Aryal B, Esau CC, Fernandez-Hernando C (2013) Therapeutic silencing of microRNA-33 inhibits the progression of atherosclerosis in Ldlr-/- mice–brief report. Arterioscler Thromb Vasc Biol 33:1973–1977

Sagare AP, Bell RD, Zlokovic BV (2013) Neurovascular defects and faulty amyloid-beta vascular clearance in Alzheimer's disease. J Alzheimers Dis 33(Suppl 1):S87–S100

Sakamoto A, Sugamoto Y, Tokunaga Y, Yoshimuta T, Hayashi K, Konno T, Kawashiri MA, Takeda Y, Yamagishi M (2011) Expression profiling of the ephrin (EFN) and Eph receptor (EPH) family of genes in atherosclerosis-related human cells. J Int Med Res 39:522–527

Schumacher T, Benndorf RA (2017) ABC transport proteins in cardiovascular disease-a brief summary. Molecules. 22

Signorelli SS, Volsi GL, Pitruzzella A, Fiore V, Mangiafico M, Vanella L, Parenti R, Rizzo M, Volti GL (2016) Circulating miR-130a, miR-27b, and miR-210 in patients with peripheral artery disease and their potential relationship with oxidative stress. Angiology. 67:945–950

Singh NK, Janjanam J, Rao GN (2017) p115 RhoGEF activates the Rac1 GTPase signaling cascade in MCP1 chemokine-induced vascular smooth muscle cell migration and proliferation. J Biol Chem 292:14080–14091

Smith-Vikos T, Slack FJ (2012) MicroRNAs and their roles in aging. J Cell Sci 125:7–17

Smith-Vikos T, Liu Z, Parsons C, Gorospe M, Ferrucci L, Gill TM, Slack FJ (2016) A serum miRNA profile of human longevity: findings from the Baltimore Longitudinal Study of Aging (BLSA). Aging (Albany NY) 8:2971–2987

Stein S, Oosterveer MH, Mataki C, Xu P, Lemos V, Havinga R, Dittner C, Ryu D, Menzies KJ, Wang X, Perino A, Houten SM, Melchior F, Schoonjans K (2014) SUMOylation-dependent LRH-1/PROX1 interaction promotes atherosclerosis by decreasing hepatic reverse cholesterol transport. Cell Metab 20:603–613

Stellos K, Dimmeler S (2014) Vascular microRNAs: from disease mechanisms to therapeutic targets. Circ Res 114:3–4

Sullivan I, Riera P, Andres M, Altes A, Majem M, Blanco R, Capdevila L, Barba A, Barnadas A and Salazar J (2019) Prognostic effect of VEGF gene variants in metastatic non-small-cell lung cancer patients. *Angiogenesis*.

Sweeney MD, Kisler K, Montagne A, Toga AW, Zlokovic BV (2018) The role of brain vasculature in neurodegenerative disorders. Nat Neurosci 21:1318–1331

Tana C, Giamberardino MA, Cipollone F (2017) microRNA profiling in atherosclerosis, diabetes, and migraine. Ann Med 49: 93–105

Tarantini S, Tran CH, Gordon GR, Ungvari Z, Csiszar A (2016a) Impaired neurovascular coupling in aging and Alzheimer's disease: contribution of astrocyte dysfunction and endothelial impairment to cognitive decline. Exp Gerontol 94. https://doi.org/10.1016/j.exger.2016.11.004

Tarantini S, Giles CB, Wren JD, Ashpole NM, Valcarcel-Ares MN, Wei JY, Sonntag WE, Ungvari Z, Csiszar A (2016b)

IGF-1 deficiency in a critical period early in life influences the vascular aging phenotype in mice by altering miRNA-mediated post-transcriptional gene regulation: implications for the developmental origins of health and disease hypothesis. Age (Dordr) 38:239–258

Tarantini S, Tran CHT, Gordon GR, Ungvari Z, Csiszar A (2017a) Impaired neurovascular coupling in aging and Alzheimer's disease: contribution of astrocyte dysfunction and endothelial impairment to cognitive decline. Exp Gerontol 94:52–58

Tarantini S, Fulop GA, Kiss T, Farkas E, Zolei-Szenasi D, Galvan V, Toth P, Csiszar A, Ungvari Z, Yabluchanskiy A (2017b) Demonstration of impaired neurovascular coupling responses in TG2576 mouse model of Alzheimer's disease using functional laser speckle contrast imaging. Geroscience.

Tarantini S, Valcarcel-Ares MN, Toth P, Yabluchanskiy A, Tucsek Z, Kiss T, Hertelendy P, Kinter M, Ballabh P, Sule Z, Farkas E, Baur JA, Sinclair DA, Csiszar A, Ungvari Z (2019) Nicotinamide mononucleotide (NMN) supplementation rescues cerebromicrovascular endothelial function and neurovascular coupling responses and improves cognitive function in aged mice. Redox Biol 24:101192

Tian L, Chen K, Cao J, Han Z, Wang Y, Gao L, Fan Y, Wang C (2017) Galectin3 induces the phenotype transformation of human vascular smooth muscle cells via the canonical Wnt signaling. Mol Med Rep 15:3840–3846

Toth P, Tarantini S, Tucsek Z, Ashpole NM, Sosnowska D, Gautam T, Ballabh P, Koller A, Sonntag WE, Csiszar A, Ungvari ZI (2014) Resveratrol treatment rescues neurovascular coupling in aged mice:role of improved cerebromicrovascular endothelial function and down-regulation of NADPH oxidas. Am J Physiol Heart Circ Physiol 306:H299–H308

Toth P, Tarantini S, Springo Z, Tucsek Z, Gautam T, Giles CB, Wren JD, Koller A, Sonntag WE, Csiszar A, Ungvari Z (2015) Aging exacerbates hypertension-induced cerebral microhemorrhages in mice: role of resveratrol treatment in vasoprotection. Aging Cell 14:400–408

Toth P, Tarantini S, Csiszar A, Ungvari Z (2017) Functional vascular contributions to cognitive impairment and dementia: mechanisms and consequences of cerebral autoregulatory dysfunction, endothelial impairment, and neurovascular uncoupling in aging. Am J Physiol Heart Circ Physiol 312: H1–H20

Traylor M, Zhang CR, Adib-Samii P, Devan WJ, Parsons OE, Lanfranconi S, Gregory S, Cloonan L, Falcone GJ, Radmanesh F, Fitzpatrick K, Kanakis A, Barrick TR, Moynihan B, Lewis CM, Boncoraglio GB, Lemmens R, Thijs V, Sudlow C, Wardlaw J, Rothwell PM, Meschia JF, Worrall BB, Levi C, Bevan S, Furie KL, Dichgans M, Rosand J, Markus HS, Rost N, International Stroke Genetics C (2016) Genome-wide meta-analysis of cerebral white matter hyperintensities in patients with stroke. Neurology 86:146–153

Tsaousi A, Williams H, Lyon CA, Taylor V, Swain A, Johnson JL, George SJ (2011) Wnt4/beta-catenin signaling induces VSMC proliferation and is associated with intimal thickening. Circ Res 108:427–436

Tucsek Z, Noa Valcarcel-Ares M, Tarantini S, Yabluchanskiy A, Fulop G, Gautam T, Orock A, Csiszar A, Deak F, Ungvari Z (2017) Hypertension-induced synapse loss and impairment in synaptic plasticity in the mouse hippocampus mimics the aging phenotype: implications for the pathogenesis of vascular cognitive impairment. Geroscience.

Ungvari Z, Tucsek Z, Sosnowska D, Toth P, Gautam T, Podlutsky A, Csiszar A, Losonczy G, Valcarcel-Ares MN, Sonntag WE, Csiszar A (2013a) Aging-induced dysregulation of dicer1-dependent microRNA expression impairs angiogenic capacity of rat cerebromicrovascular endothelial cells. J Gerontol A Biol Sci Med Sci 68:877–891

Ungvari Z, Tucsek Z, Sosnowska D, Toth P, Gautam T, Podlutsky A, Csiszar A, Losonczy G, Valcarcel-Ares MN, Sonntag WE (2013b) Aging-induced dysregulation of Dicer1-dependent microRNA expression impairs angiogenic capacity of rat cerebromicrovascular endothelial cells. J Gerontol A Biol Sci Med Sci 68:877–891

Ungvari Z, Tarantini S, Kirkpatrick AC, Csiszar A, Prodan CI (2017a) Cerebral microhemorrhages: mechanisms, consequences, and prevention. Am J Physiol Heart Circ Physiol 312:H1128–H1143

Ungvari Z, Tarantini S, Hertelendy P, Valcarcel-Ares MN, Fulop GA, Logan S, Kiss T, Farkas E, Csiszar A, Yabluchanskiy A (2017b) Cerebromicrovascular dysfunction predicts cognitive decline and gait abnormalities in a mouse model of whole brain irradiation-induced accelerated brain senescence. Geroscience. 39:33–42

Ungvari Z, Tarantini S, Donato AJ, Galvan V, Csiszar A (2018) Mechanisms of vascular aging. Circ Res 123:849–867

Urbich C, Kuehbacher A, Dimmeler S (2008) Role of microRNAs in vascular diseases, inflammation, and angiogenesis. Cardiovasc Res 79:581–588

Verzola D, Milanesi S, Bertolotto M, Garibaldi S, Villaggio B, Brunelli C, Balbi M, Ameri P, Montecucco F, Palombo D, Ghigliotti G, Garibotto G, Lindeman JH, Barisione C (2017) Myostatin mediates abdominal aortic atherosclerosis progression by inducing vascular smooth muscle cell dysfunction and monocyte recruitment. Sci Rep 7:46362

Wang JC, Bennett M (2012) Aging and atherosclerosis: mechanisms, functional consequences, and potential therapeutics for cellular senescence. Circ Res 111:245–259

Wang A, Kwee LC, Grass E, Neely ML, Gregory SG, Fox KAA, Armstrong PW, White HD, Ohman EM, Roe MT, Shah SH, Chan MY (2017) Whole blood sequencing reveals circulating microRNA associations with high-risk traits in non-ST-segment elevation acute coronary syndrome. Atherosclerosis. 261:19–25

Weber M, Kim S, Patterson N, Rooney K, Searles CD (2014) MiRNA-155 targets myosin light chain kinase and modulates actin cytoskeleton organization in endothelial cells. Am J Physiol Heart Circ Physiol 306:H1192–H1203

Wei Y, Schober A, Weber C (2013) Pathogenic arterial remodeling: the good and bad of microRNAs. Am J Physiol Heart Circ Physiol 304:H1050–H1059

Westerterp M, Bochem AE, Yvan-Charvet L, Murphy AJ, Wang N, Tall AR (2014) ATP-binding cassette transporters, atherosclerosis, and inflammation. Circ Res 114:157–170

Wezel A, Welten SM, Razawy W, Lagraauw HM, de Vries MR, Goossens EA, Boonstra MC, Hamming JF, Kandimalla ER, Kuiper J, Quax PH, Nossent AY, Bot I (2015) Inhibition of microRNA-494 reduces carotid artery atherosclerotic lesion development and increases plaque stability. Ann Surg 262: 841–847 discussion 847-8

Wren JD, Garner HR (2004) Shared relationship analysis: ranking set cohesion and commonalities within a literature-derived relationship network. Bioinformatics. 20:191–198

Wu ML, Chen CH, Lin YT, Jheng YJ, Ho YC, Yang LT, Chen L, Layne MD, Yet SF (2014) Divergent signaling pathways cooperatively regulate TGFbeta induction of cysteine-rich protein 2 in vascular smooth muscle cells. Cell Commun Signal 12:22

Xing T, Du L, Zhuang X, Zhang L, Hao J, Wang J (2017) Upregulation of microRNA-206 induces apoptosis of vascular smooth muscle cells and decreases risk of atherosclerosis through modulating FOXP1. Exp Ther Med 14:4097–4103

Yamada Y, Nishida T, Horibe H, Oguri M, Kato K, Sawabe M (2014) Identification of hypo- and hypermethylated genes related to atherosclerosis by a genome-wide analysis of DNA methylation. Int J Mol Med 33:1355–1363

Yang ZY, Simari RD, Perkins ND, San H, Gordon D, Nabel GJ, Nabel EG (1996) Role of the p21 cyclin-dependent kinase inhibitor in limiting intimal cell proliferation in response to arterial injury. Proc Natl Acad Sci U S A 93:7905–7910

Yoshino J, Baur JA, Imai SI (2018) NAD(+) intermediates: the biology and therapeutic potential of NMN and NR. Cell Metab 27:513–528

Yu J, Qiu Y, Yang J, Bian S, Chen G, Deng M, Kang H, Huang L (2016) DNMT1-PPARgamma pathway in macrophages regulates chronic inflammation and atherosclerosis development in mice. Sci Rep 6:30053

Zampetaki A, Attia R, Mayr U, Gomes RS, Phinikaridou A, Yin X, Langley SR, Willeit P, Lu R, Fanshawe B, Fava M, Barallobre-Barreiro J, Molenaar C, So PW, Abbas A, Jahangiri M, Waltham M, Botnar R, Smith A, Mayr M (2014) Role of miR-195 in aortic aneurysmal disease. Circ Res 115:857–866

Zhang H, Zhang J, Ungvari Z, Zhang C (2009) Resveratrol improves endothelial function: role of TNF {alpha} and vascular oxidative stress. Arterioscler Thromb Vasc Biol 29:1164–1171

Zhang X, Azhar G, Wei JY (2012) The expression of microRNA and microRNA clusters in the aging heart. PLoS One 7: e34688

Zhang B, Day DS, Ho JW, Song L, Cao J, Christodoulou D, Seidman JG, Crawford GE, Park PJ, Pu WT (2013) A dynamic H3K27ac signature identifies VEGFA-stimulated endothelial enhancers and requires EP300 activity. Genome Res 23:917–927

Zhang F, Zhang R, Zhang X, Wu Y, Li X, Zhang S, Hou W, Ding Y, Tian J, Sun L, Kong X (2018) Comprehensive analysis of circRNA expression pattern and circRNA-miRNA-mRNA network in the pathogenesis of atherosclerosis in rabbits. Aging (Albany NY) 10:2266–2283

Zhao X, Wang Y, Meng C, Fang N (2018) FMRP regulates endothelial cell proliferation and angiogenesis via the miR-181a-CaM-CaMKII pathway. Cell Biol Int 42:1432–1444

Zhu SB, Zhu J, Zhou ZZ, Xi EP, Wang RP, Zhang Y (2015) TGF-beta1 induces human aortic vascular smooth muscle cell phenotype switch through PI3K/AKT/ID2 signaling. Am J Transl Res 7:2764–2774

Zhu M, Zuo J, Shen J, Jing W, Luo P, Li N, Wen X, Wang C, Yu M, Liang C, Tu J (2016) Diagnostic potential of differentially expressed Homer1 and Homer2 in ischemic stroke. Cell Physiol Biochem 39:2353–2363

Zovoilis A, Agbemenyah HY, Agis-Balboa RC, Stilling RM, Edbauer D, Rao P, Farinelli L, Delalle I, Schmitt A, Falkai P, Bahari-Javan S, Burkhardt S, Sananbenesi F, Fischer A (2011) microRNA-34c is a novel target to treat dementias. EMBO J 30:4299–4308

GeroScience (2020) 42:527–546
https://doi.org/10.1007/s11357-020-00165-5

ORIGINAL ARTICLE

Nicotinamide mononucleotide (NMN) supplementation promotes neurovascular rejuvenation in aged mice: transcriptional footprint of SIRT1 activation, mitochondrial protection, anti-inflammatory, and anti-apoptotic effects

Tamas Kiss · Ádám Nyúl-Tóth · Priya Balasubramanian · Stefano Tarantini · Chetan Ahire · Andriy Yabluchanskiy · Tamas Csipo · Eszter Farkas · Jonathan D. Wren · Lori Garman · Anna Csiszar · Zoltan Ungvari

Received: 8 January 2020 / Accepted: 29 January 2020 / Published online: 13 February 2020

Abstract Aging-induced structural and functional alterations of the neurovascular unit lead to impairment of neurovascular coupling responses, dysregulation of cerebral blood flow, and increased neuroinflammation, all of which contribute importantly to the pathogenesis of age-related vascular cognitive impairment (VCI). There is increasing evidence showing that a decrease in NAD^+ availability with age plays a critical role in age-related neurovascular and cerebromicrovascular dysfunction. Our recent studies demonstrate that restoring cellular NAD^+ levels in aged mice rescues neurovascular function, increases cerebral blood flow,

Tamas Kiss, Ádám Nyúl-Tóth, Priya Balasubramanian and Stefano Tarantini contributed equally to this work.

T. Kiss · Á. Nyúl-Tóth · P. Balasubramanian · S. Tarantini · C. Ahire · A. Yabluchanskiy · T. Csipo · J. D. Wren · Z. Ungvari
Vascular Cognitive Impairment and Neurodegeneration Program, Reynolds Oklahoma Center on Aging/Center for Geroscience and Healthy Brain Aging, Department of Biochemistry and Molecular Biology, University of Oklahoma Health Sciences Center, 975 NE 10th Street, BRC 1311, Oklahoma City, OK 73104, USA

T. Kiss · E. Farkas · A. Csiszar · Z. Ungvari
International Training Program in Geroscience, Theoretical Medicine Doctoral School/Department of Medical Physics and Informatics, University of Szeged, Szeged, Hungary

Á. Nyúl-Tóth
Institute of Biophysics, Biological Research Centre, Szeged, Hungary

S. Tarantini · T. Csipo · A. Csiszar · Z. Ungvari
International Training Program in Geroscience, Doctoral School of Basic and Translational Medicine/Department of Public Health, Semmelweis University, Budapest, Hungary

T. Csipo
International Training Program in Geroscience, Department of Cardiology, Division of Clinical Physiology, Faculty of Medicine, University of Debrecen, Debrecen, Hungary

J. D. Wren · L. Garman
Genes & Human Disease Research Program, Oklahoma Medical Research Foundation, Oklahoma City, OK, USA

A. Csiszar · Z. Ungvari
The Peggy and Charles Stephenson Cancer Center, University of Oklahoma Health Sciences Center, Oklahoma City, OK 73104, USA

Z. Ungvari (✉)
Department of Health Promotion Sciences, College of Public Health, University of Oklahoma Health Sciences Center, Oklahoma City, OK, USA
e-mail: zoltan-ungvari@ouhsc.edu

and improves performance on cognitive tasks. To determine the effects of restoring cellular NAD^+ levels on neurovascular gene expression profiles, 24-month-old C57BL/6 mice were treated with nicotinamide mononucleotide (NMN), a key NAD^+ intermediate, for 2 weeks. Transcriptome analysis of preparations enriched for cells of the neurovascular unit was performed by RNA-seq. Neurovascular gene expression signatures in NMN-treated aged mice were compared with those in untreated young and aged control mice. We identified 590 genes differentially expressed in the aged neurovascular unit, 204 of which are restored toward youthful expression levels by NMN treatment. The transcriptional footprint of NMN treatment indicates that increased NAD^+ levels promote SIRT1 activation in the neurovascular unit, as demonstrated by analysis of upstream regulators of differentially expressed genes as well as analysis of the expression of known SIRT1-dependent genes. Pathway analysis predicts that neurovascular protective effects of NMN are mediated by the induction of genes involved in mitochondrial rejuvenation, anti-inflammatory, and anti-apoptotic pathways. In conclusion, the recently demonstrated protective effects of NMN treatment on neurovascular function can be attributed to multifaceted sirtuin-mediated anti-aging changes in the neurovascular transcriptome. Our present findings taken together with the results of recent studies using mitochondria-targeted interventions suggest that mitochondrial rejuvenation is a critical mechanism to restore neurovascular health and improve cerebral blood flow in aging.

Keywords Aging · Geroscience · Vascular cognitive impairment · Mitochondria dysfunction · Transcriptomics

Introduction

In recent years, there has been increasing appreciation that the health of the neurovascular unit (NVU) is critical for brain health (Kisler et al. 2017; Zlokovic 2010, 2011; Iadecola 2017; Stanimirovic and Friedman 2012). The extended NVU consists of cerebral microvessels that receive input from neurons via astrocytic endfeet, pericytes, and perivascular microglia (Iadecola 2017; Stanimirovic and Friedman 2012). The NVU is responsible for the tight coupling between neural activity and regional cerebral blood flow ("neurovascular coupling"), which ensures adequate oxygen and nutrient delivery to the brain (Tarantini et al. 2017a; Toth et al. 2017). Endothelial dysfunction and/or impaired astrocytic function results in neurovascular uncoupling contributing to cognitive impairment (Toth et al. 2017; Tarantini et al. 2015, 2018, 2017b). In addition, cells constituting the NVU form and maintain the blood-brain barrier (Zlokovic 2010, 2011; Montagne et al. 2017; Sweeney et al. 2018, 2019a; Zlokovic 2008), regulate transport processes and waste removal, deposit the extracellular matrix, control the structural remodeling of the cerebral microcirculation (including angiogenesis, vessel regression, adaptation to hypertension (Csiszar et al. 2017; Tarantini et al. 2016, 2017c; Tucsek et al. 2014; Warrington et al. 2013; Ungvari et al. 2013, 2018a, 2017; Toth et al. 2015)), form and operate the glymphatic system (Iliff et al. 2013; Jessen et al. 2015; Kress et al. 2014), maintain stem-cell niches (Solano Fonseca et al. 2016), synthesize the glycocalyx, and control the adhesion and extravasation of inflammatory circulating cells that participate in central nervous system immune surveillance (Stanimirovic and Friedman 2012). With age, the phenotype and function of the cells constituting the NVU are altered, which fundamentally affects all of the aforementioned physiological processes (Kisler et al. 2017; Zlokovic 2010, 2011; Tarantini et al. 2017a). Age-related neurovascular dysfunction is now considered as a critical contributing factor to the pathogenesis of both vascular cognitive impairment (VCI) and neurodegenerative diseases, including Alzheimer's disease (Sweeney et al. 2019b). In order to develop novel methods for prevention and treatment of these diseases and to preserve cognitive function in older adults, it is important to identify therapeutic interventions that can reverse age-related impairment of the NVU. Understanding the role of fundamental cellular and molecular mechanisms of aging in age-related neurovascular impairment is critical in that regard.

Nicotinamide adenine dinucleotide (NAD^+) is a coenzyme central to hundreds of redox reactions in eukaryotic cells. NAD^+ also has a critical role in the regulation of the activity of NAD^+-consuming enzymes, including SIRT1 and other sirtuins (Gomes et al. 2013; Michan et al. 2010; Mitchell et al. 2014; Yang et al. 2007). Sirtuin enzymes are implicated in regulation of cellular processes of aging, mitochondrial function, stress resilience, apoptosis, and inflammation (Das et al. 2018; Csiszar et al. 2009a, b, 2008a). Aging is associated with cellular NAD^+ depletion (Gomes et al. 2013; Massudi et al. 2012) (Yoshino, 2018 #10180),

which has been proposed to be a critical driving force of aging processes (Imai and Guarente 2014), impairing nuclear and mitochondrial functions and contributing to the genesis of many age-associated pathologies. Accordingly, restoration of cellular NAD^+ biosynthesis extends lifespan in model organisms (Anderson et al. 2002) and improves health span and extends lifespan in murine models of aging (Zhang, 2016 #10167) (Mitchell et al. 2018). There is emerging evidence that vascular aging is also characterized by cellular NAD^+ depletion (Tarantini et al. 2019a; Csiszar et al. 2019; Kiss et al. 2019a). Importantly, our recent studies showed (Tarantini et al. 2019a) that in murine models of aging restoration of cellular NAD^+ levels by chronic treatment with the NAD^+ precursor, nicotinamide mononucleotide (NMN) (Yoshino et al. 2018) confers potent anti-aging neurovascular effects, rescuing cerebromicrovascular endothelial dysfunction and neurovascular coupling responses, increasing cerebral blood flow, and improving cognitive performance. In cultured cerebromicrovascular endothelial cells derived from aged rats, 5 days of treatment with NMN restored NAD^+ levels and rescued mitochondrial function and attenuated mitochondrial oxidative stress in a sirtuin-dependent manner (Tarantini et al. 2019a).

The present study was designed to test the hypothesis that age-related NAD^+ depletion in the NVU is causally linked to dysregulated expression of genes important for normal neurovascular function. A corollary hypothesis is that functional neurovascular rejuvenation in NMN-treated aged mice is associated with SIRT1-mediated restoration of a youthful neurovascular mRNA expression profile. To test these hypotheses, aged mice were treated with NMN for 2 weeks and transcriptomic signatures in cells of the neurovascular unit were compared with those in cells obtained from untreated young and aged control mice. The transcriptomic footprint of SIRT1 activation was analyzed, and the predicted multifaceted protective effects of NMN supplementation on diverse aspects of cerebromicrovascular and neurovascular biology were tested.

Methods

Animals, NMN supplementation

Young (3 months old) and aged (24 months old) male C57BL/6 mice were purchased from the aging colony maintained by the National Institute on Aging at Charles River Laboratories (Wilmington, MA). The biological age of 24-month-old mice corresponds to that of ~ 60-year-old humans. Mice were housed under specific pathogen-free barrier conditions in the Rodent Barrier Facility at University of Oklahoma Health Sciences Center under a controlled photoperiod (12 h light; 12 h dark) with unlimited access to water and were fed a standard AIN-93G diet (ad libitum). Mice in the aged cohort were assigned to two groups. One group of the aged mice was injected daily with NMN (IP injections of 500 mg NMN/kg body weight per day) or the equivalent volume of PBS for 14 consecutive days at 6 PM and 8 AM on day 14 and were sacrificed 4 h after last injection. Similar dosages of NMN has been shown to exert potent anti-aging effects on mouse health span (Csiszar et al. 2019; de Picciotto et al. 2016), including rescue of neurovascular coupling responses, attenuation of vascular oxidative stress, and rescue of gene expression changes in the aorta (Tarantini et al. 2019a; Kiss et al. 2019b). All procedures were approved by the Institutional Animal Use and Care Committees of the University of Oklahoma Health Sciences Center. All animal experiments complied with the ARRIVE guidelines and were carried out in accordance with the National Institutes of Health guide for the care and use of Laboratory animals (NIH Publications No. 8023, revised 1978). The effects of NMN treatment on cognitive function, neurovascular coupling responses, and microvascular and aorta endothelial function in a similar cohort of mice have been recently reported (Tarantini et al. 2019a).

Isolation of cells of the neurovascular unit

Animals were killed and transcardially perfused with PBS as previously described (Tarantini et al. 2019a; Kiss et al. 2019b). The brains were quickly removed and rinsed in ice-cold PBS, and minced into ≈ 1 mm^2 pieces. The tissue was washed twice in ice-cold 1× PBS by low-speed centrifugation (50*g*, 3 min). The diced tissue was digested in a buffer solution containing collagenase (800 U/g tissue), hyaluronidase (2.5 U/g tissue), and elastase (3 U/g tissue) in 1 mL PBS/100 mg tissue for 45 min at 37 °C in a rotating humid incubator. The digested tissue was passed through a 100-μm cell strainer. The single-cell lysate was centrifuged for 2 min at 70*g*. After removing the supernatant, the pellet was washed twice in cold PBS supplemented with 2.5% fetal

calf serum (FCS), and the suspension was centrifuged at 300*g* for 5 min at 4 °C. To create fraction enriched for cells of the neurovascular unit, the cell suspension was centrifuged using an OptiPrep gradient solution (Axi-Shield, PoC, Norway). Briefly, the cell pellet was resuspended in Hanks' balanced salt solution (HBSS) and mixed with 40% iodixanol thoroughly (final concentration 17% (v/v) iodixanol solution; $\rho = 1.096$ g/mL). Two milliliters of HBSS was layered on top and centrifuged at 400*g* for 15 min at 20 °C. Endothelial cells with attached astrocytes and pericytes, which banded at the interface between HBSS and the 17% iodixanol layer, were collected. The neurovascular-enriched fraction was incubated for 30 min at 4 °C in the dark with anti-CD31/PE (BD Biosciences, San Jose, CA, USA) and anti-MCAM/FITC (BD Biosciences, San Jose, CA, USA). After washing the cells twice with MACS buffer (Milltenyi Biotech, Cambridge, MA, USA), anti-FITC and anti-PE magnetic bead–labeled secondary antibodies were used for 15 min at room temperature. The endothelial/neurovascular enriched fraction was collected by magnetic separation using the MACS LD magnetic separation columns according to the manufacturer's guidelines (Milltenyi Biotech, Cambridge, MA, USA). Our pilot studies indicated that this method using gentle cell dissociation protocols results in enrichment for cerebromicorvascular endothelial cells with astrocytes and pericytes.

RNA isolation, cDNA synthesis, library construction, and next generation sequencing

RNA was isolated from the samples using AllPrep DNA/RNA Mini Kit (Qiagen) as previously described (Imperio et al. 2016; Valcarcel-Ares et al. 2018). RNA quantity and quality (> 8 RNA integrity number) were measured using the RNA 6000 Nano Assay with an Agilent 2100 Bioanalyzer (Agilent, Palo Alto, CA). Using 1 μg RNA, cDNA was synthesized from purified RNA using ABI High-capacity cDNA Reverse Transcription Kit (Applied Biosystems, Foster City, CA) (Imperio et al. 2016; Valcarcel-Ares et al. 2018). Library construction was performed in a stranded manner to retain the directionality of the transcripts for as described (Valcarcel-Ares et al. 2018). In brief, prior to RNA-seq analysis, quality control measures were implemented. Concentration of RNA was ascertained via fluorometric analysis on a Thermo Fisher Qubit Fluorometer. Overall quality of RNA was verified using an Agilent Tapestation instrument. Following initial QC steps, sequencing libraries were generated using the Illumina Truseq Stranded mRNA with library prep kit according to the manufacturers protocol. Briefly, mature mRNA was enriched for via pull down with beads coated with oligo-dT homopolymers. The mRNA molecules were then chemically fragmented, and the first strand of cDNA was generated using random primers. Following RNase digestion, the second strand of cDNA was generated replacing dTTP in the reaction mix with dUTP. Double stranded cDNA then underwent adenylation of 3′ ends following ligation of Illumina-specific adapter sequences. Subsequent PCR enrichment of ligated products was further selected for those strands not incorporating dUTP, leading to strand-specific sequencing libraries. Final libraries for each sample were assayed on the Agilent Tapestation for appropriate size and quantity. These libraries were then pooled in equimolar amounts as ascertained via fluorometric analyses. Final pools were absolutely quantified using qPCR on a Roche LightCycler 480 instrument with Kapa Biosystems Illumina Library Quantification reagents. Sequencing was performed on an Illumina NovaSeq 6000 instrument with paired-end 50 bp reads.

RNA-seq data analysis and visualization

Raw sequencing reads were trimmed of their Illumina TruSeq adapter sequences using *Trimmomatic v0.*35 (Bolger et al. 2014), then aligned to the mouse genome version GRCm38 using *Kallisto v0.43.03* (Bray et al. 2016). Samples were checked for outliers and separation by principle components analysis (PCA) with the R function *prcomp*. Raw expression counts were summarized at the gene level to transcript-length adjusted, library-size scaled counts per million (CPM) with the R package *tximport* (Soneson et al. 2015). Differential expression analysis was performed using the empirical Bayes approach implemented in the R/Bioconductor package *DESeq2* (Love et al. 2014). Significantly differentially expressed (DE) genes had an absolute log2 fold-change ≥ 0.585 (corresponding to a change of 50% or more in expression) and the false discovery rate (FDR)-adjusted p value ≤ 0.05. Gene annotation was done using *biomaRt* (Durinck et al. 2009) in R/Bioconductor package. Hierarchical clustering was performed via the R package ComplexHeatmap.

Functional annotation

The *org.Mm.eg.db v3.8.2* R/Bioconductor package was used to collect Gene Ontology terms associated with our differentially expressed genes. The hypergeometric test implemented in *GOstats v2.51.0* R/Bioconductor package was used to calculate enrichment of the individual terms (Falcon and Gentleman 2007).

We used upstream regulator analysis (URA) algorithm (Kramer et al. 2014) implemented in the Ingenuity Pathway Analysis (QIAGEN) software find upstream regulators that potentially explains the observed gene expression changes in our samples. The IPA uses a manually curated database (Ingenuity Knowledge Base) to calculate "enrichment" score (Fisher's exact test (FET) p value), measures the overlap of observed and predicted regulated gene sets, and a z-score assessing the match of observed and predicted up/downregulation patterns.

Results

NMN treatment reverses age-related changes in neurovascular mRNA expression profile in mice

To isolate NVU-enriched mRNA, we employed an endothelial cell isolation-based strategy. Using RNA-seq to sequence the neurovascular transcriptome, we compared normalized mRNA expression values for each sample to that in individual cell types constituting the NVU (endothelial cells, astrocytes, and pericytes). To achieve that goal, we developed a list of cell-specific markers from published RNA-seq data of purified cortical cell types (GEO dataset GSE52564 (Zhang et al. 2014)). Comparison of mRNA levels in the NVU samples with the input shows a significant enrichment for endothelial cell, astrocyte, and pericyte genes (Fig. 1a).

We assessed transcriptomic changes in the NVU associated with aging and with NMN treatment (Fig. 1b). We performed unsupervised clustering of RNA-seq data from all samples using the topmost variably expressed genes across all samples. This showed that biological replicates from the same group cluster together, and that young samples segregate away from aged ones (Fig. 1b). PCA (Fig. 1c) of the transcriptomic data also showed a clear separation between the young and aged groups. Aged control mice and aged NMN-treated mice were also segregated in the PCA and hierarchical clustering. This finding indicated a clear difference between the transcriptome profiles of the two age groups. In contrast, mRNA expression in young mice and NMN-treated aged mice were similar, and these groups did not separate well in the PCA and hierarchical clustering.

We then determined the number of genes that are significantly upregulated or downregulated (DE, fold-change ≥ 1.5 or ≤ 0.67; $p < 0.05$ adjusted for multiple comparisons) in the NVU by aging or by NMN treatment. We then filtered for genes that are significantly altered (adjusted $p < 0.05$), expressed at an appreciable level (fragments per kilobase of transcript per million mapped reads > 1), and are expressed in cells of the NVU. We identified 590 differentially expressed genes in aged animals compared with young controls. We also identified 459 DE genes in the NMN-treated aged mice compared with the untreated aged controls. In Fig. 1d, a volcano plot shows statistical significance (p value) versus magnitude of age-related change in gene expression. Red symbols denote genes, whose expression levels differed in the aged phenotype, but have shifted back toward the young phenotype by NMN treatment (discordant DE genes). The Venn diagram in Fig. 1f shows that neurovascular expression of 204 genes, which are differentially expressed in aged mice, was shifted back toward youthful levels by NMN treatment of aged mice.

We realized that significance cutoffs to identify differentially expressed genes shared between the age-effect and NMN-effect datasets may be too stringent, and the analysis illustrated in Fig. 1d may miss discordant patterns (youthful shifts) of gene expression with important biological relevance for NMN-induced neurovascular rejuvenation. Thus, we also used an approach to detect discordant transcriptional patterns (youthful shifts) by comparing the age-effect and NMN-effect gene expression datasets using combination criteria that took into account the effect direction. Genes were ranked by their effect size direction, and ranked lists were compared to identify overlapping genes across a continuous significance gradient. Our analysis required that discordant genes with youthful shifts (1) are "differentially expressed" based on both p value and fold-change criteria either in aging or the NMN treatment group, (2) satisfy a fold-change criterion with a cutoff of ≥ 1.5 or ≤ 0.67 in the group in which expression did not satisfy the statistical significance $p < 0.05$, and (3) satisfy the criterion that the effect

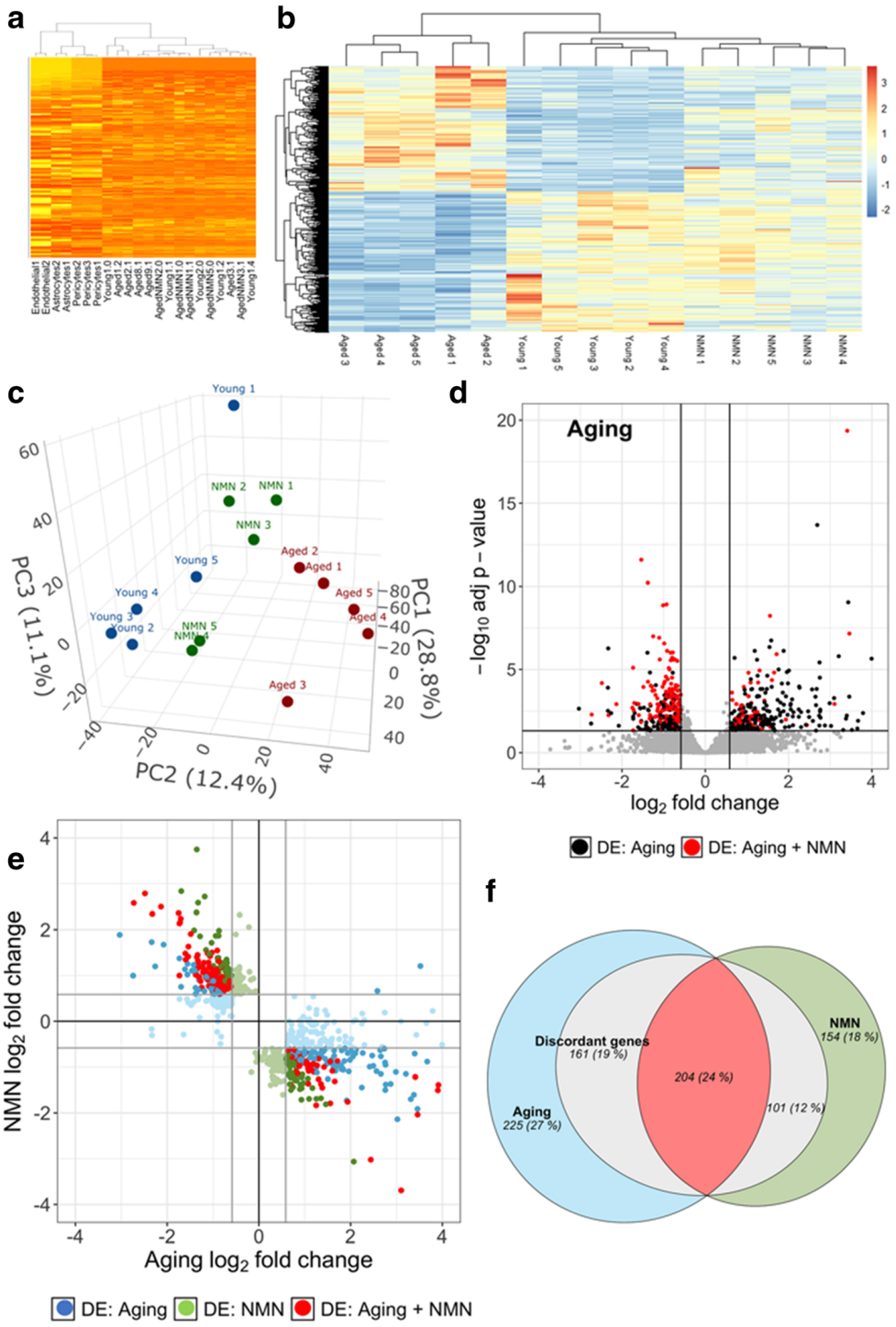

directions of the age-effect and NMN-effect are opposite. We found that these combination criteria found more biologically meaningful sets of genes than *p* values alone.

In Fig. 1e, the magnitude of age-related changes in gene expression is plotted against the magnitude of NMN-induced changes in gene expression. Red symbols denote discordant DE genes, whose expression levels shifted back toward the young phenotype by NMN treatment with statistical significance. Genes which are DE only in one group but otherwise satisfy the other criteria are denoted by blue (DE in aging) and

◀ **Fig. 1** NMN treatment reverses age-related changes in neurovascular mRNA expression profile. **a** Heatmap displaying normalized mRNA expression values for each sample as compared with that in cells of the neurovascular unit (endothelial cells, astrocytes, and pericytes) from the reference datasets by Zhang et al. (2014). Note that neurovascular genes are enriched in the samples. **b** The heat map is a graphic representation of normalized expression values of differentially expressed genes in neurovascular samples derived from young (3 months old), aged (24 months old), and NMN-treated aged mice. Hierarchical clustering analysis revealed the similarities on neurovascular mRNA expression profiles in young and NMN-treated aged mice. **c** Principal component analysis (PCA) plot of neurovascular mRNA expression profiles in young, aged control, and NMN-treated aged mice. The profiles from aged mice (red) cluster separately from clusters representing young mice (blue) and NMN-treated aged mice (green). PC1, PC2, and PC3 are principal components 1, 2, and 3, respectively. **d** Volcano plot depicting differentially expressed genes comparing neurovascular samples derived from young and aged mice. Stratified *p* values are plotted against expression fold-changes for results obtained in aged samples normalized to young samples. Colored points refer to genes whose expression is significantly altered by NMN treatment. **e** NMN-induced changes in gene expression plotted against age-related changes in the neurovascular transcriptome. Red symbols indicate discordant differentially expressed genes with youthful shifts, whose expression significantly changes with age and is restored by NMN treatment toward youthful levels. Blue and green symbols denote discordant genes with youthful shifts, whose expression changes in aging and is restored by NMN treatment toward youthful levels, but only the aging (blue) or the NMN effect (green) reaches the cutoff for statistical significance. **f** Venn diagrams sowing the numbers of differentially expressed mRNAs in each group. The blue circle represents neurovascular genes, which are significantly up or downregulated in aged mice as compared with young mice. The green circle represents neurovascular genes, which are significantly up or downregulated in aged mice by NMN treatment. The red area represents discordant differentially expressed genes. Gray areas represent discordant genes, whose expression is changed by NMN treatment toward youthful levels, but the effect does not reach the cutoff for statistical significance

green (DE in NMN-treated) symbols. Using this approach, we have identified 466 discordant genes with youthful shifts, which changed in opposite directions between the two datasets (Fig. 1f). These data suggest that NAD^+ depletion has a critical role in age-related dysregulation of neurovascular gene expression.

Transcriptional footprint of neurovascular SIRT1 activation in NMN-treated aged mice

Previous studies suggested that restoration of NAD^+ levels in aged cells by NMN treatment activates the NAD^+-dependent histone deacetylase enzyme SIRT1 (Gomes et al. 2013; Tarantini et al. 2019a). To provide additional evidence that SIRT1 activation contributes to the neurovascular protective effects of NMN, we examined the transcriptional footprint of neurovascular SIRT1 activation in NMN-treated aged mice using three approaches. First, we analyzed age-related and NMN-induced changes in expression of SIRT1-regulated genes identified by IPA. We found that aging is associated with changes in the expression of several known SIRT1-regulated genes and that majority of these transcriptional changes are reversed by NMN treatment (Fig. 2a).

Ingenuity upstream regulator analysis

We have also performed IPA upstream regulator analysis (Kramer et al. 2014) to identify upstream transcriptional regulators that may contribute to the observed transcriptomic changes in our dataset, which can help to identify the mechanism of action of NMN in the aged neurovascular unit. The upstream regulator analysis is based on information in the Ingenuity Knowledge Base (a curated relational database of the available biomedical literature) on the expected effects between transcriptional regulators and their target genes. Using the IPA upstream regulator analysis, it was examined how many known targets of each transcriptional regulator were differentially expressed in our samples, and the direction of these gene expression changes were compared with what is expected from the literature. On the basis of the observed direction of change, a prediction of the activation state of the predicted transcriptional regulators ("activated" or "inhibited") were made (not shown). For each potential transcriptional regulator, two statistical measures, an overlap *p* value and an activation z-score, were computed. The overlap *p* value calls likely upstream regulators based on significant overlap between the differentially expressed genes and known targets regulated by that particular transcriptional regulator. The activation z-score is used to infer the activation state of the predicted transcriptional regulators ("activated" or "inhibited") based on comparison with a model that assigns random regulation directions. The results of the IPA upstream regulator analysis are visualized in Fig. 2b. We also determined the link between the predicted upstream regulators activated by NMN and SIRT1 using IPA. As indicated in Fig. 2b, we found that ~ 38% of the predicted upstream regulators activated by

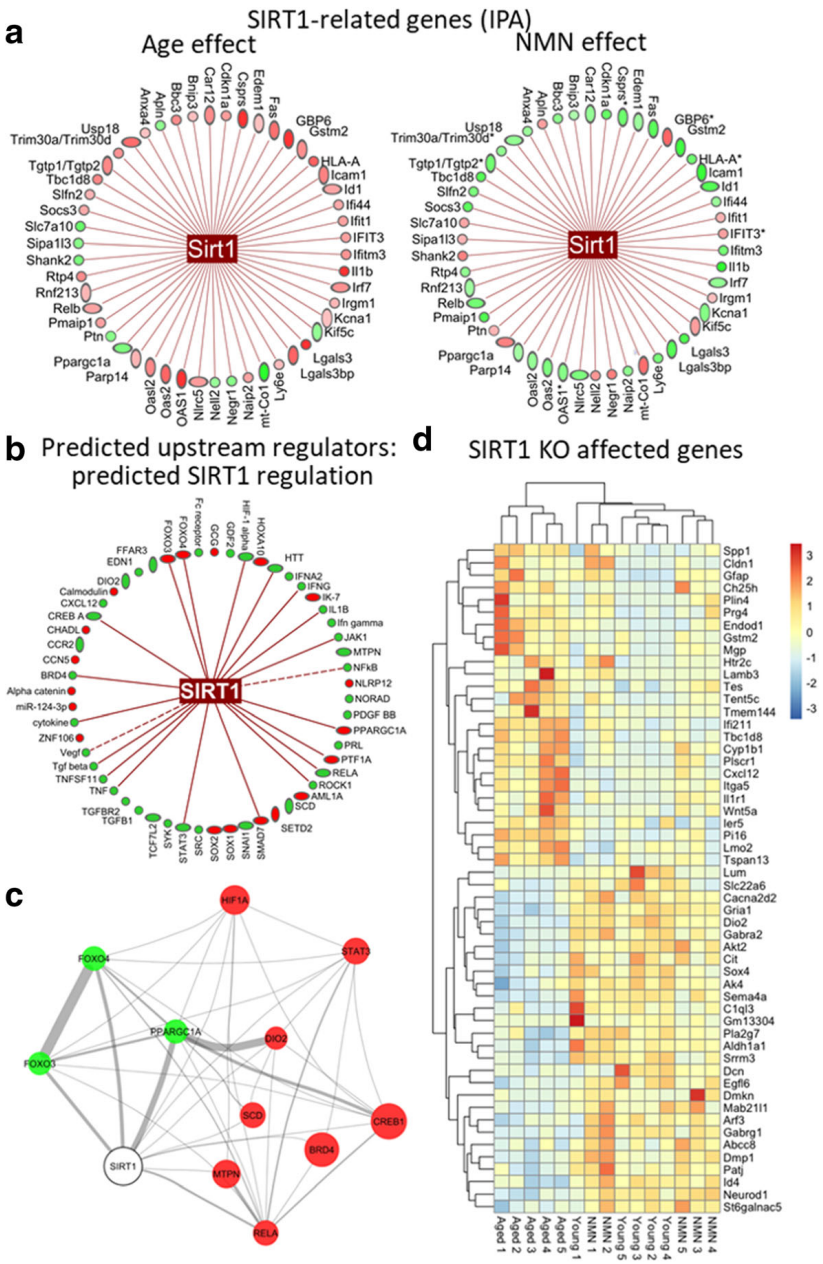

Fig. 2 NMN reverses age-related changes in neurovascular expression of SIRT1-regulated genes. **a** IPA results showing age-related (left) and NMN-induced (right) changes in the expression of SIRT1-regulated genes (classified as such by IPA). Green, downregulation; red, upregulation. **b** Results of the IPA upstream regulator analysis. Shown are predicted upstream transcriptional regulators that may contribute to the observed NMN-induced transcriptomic changes in our dataset. Known links between the predicted upstream regulators activated by NMN and SIRT1 activity are indicated. **c** Literature-based relationships with positive mutual information among the predicted upstream regulators. Node size correlates with the activation z-score from IPA (bigger = higher z-score), edge width correlates with the mutual information of the genes within the literature, green marks which are predicted activators and red marks predicted repressors. **d** The heat map is a graphic representation of normalized expression values of differentially expressed SIRT1-dependent genes in neurovascular samples derived from young (3 months old), aged (24 months old), and NMN-treated aged mice. Hierarchical clustering analysis revealed the similarities on neurovascular expression profiles of SIRT1-dependent genes in young and NMN-treated aged mice. SIRT1-dependent genes were identified based on their differential expression in the brain of SIRT1$^{-/-}$ mice (Libert et al. 2011)

NMN are known to be regulated by SIRT1-dependent pathways. In particular, the IPA upstream regulator analysis predicts that NMN-induced SIRT1 activation upregulates PGC-1α (PPARGC1A), FOXO3- and FOXO4-mediated pathways, whereas it inhibits HIF-1α-regulated pathways (Fig. 2b). We also attempted to

predict NMN-activated, SIRT1-dependent regulatory networks by identifying relationships between SIRT1 and the predicted upstream regulators utilizing the IRIDESCENT (Implicit Relationship IDEntification by in-Silico Construction of an Entity-based Network from Text) system (Wren and Garner 2004). IRIDESCENT processes all available MEDLINE abstracts and uses a statistical model to determine whether each upstream regulator co-occurs with a term of interest more frequently than would be expected by chance, and quantifies this in terms of the mutual information measure. The results of this analysis provide additional support to the view that the predicted NMN-induced SIRT1 activation results in inhibition of HIF-1α[29] and activation of PGC-1α- and FOXO3-dependent pathways (Hubbard et al. 2013). PGC-1α and FOXOs are known targets for SIRT1-mediated deacetylation (Fig. 2c).

In addition, we also intersected the list of differentially expressed genes in our dataset with the list of genes differentially expressed in the brains of SIRT1$^{-/-}$ mice (NCBI Gene Expression Omnibus: GSE28790) (Libert et al. 2011). The heat map showing the expression pattern of these SIRT1-sensitive genes is shown in Fig. 2d. Hierarchical clustering of the data showed a clear separation between the young and aged groups. Aged control mice and aged NMN-treated mice were also clearly separated. In contrast, expression of SIRT1-sensitive genes in young mice and NMN-treated aged mice were similar, and these groups did not separate well in the hierarchical clustering, consistent with the idea that aging is associated with dysregulation of SIRT1-sensitive genes, which is rescued by NMN treatment.

NMN-induced neurovascular transcriptomic changes in aged mice predict mitochondrial rejuvenation

We performed GO enrichment analysis to explore potential biological functions of the NMN-regulated discordant differentially expressed genes with youthful shifts. GO enrichment analysis of discordant differentially expressed genes with youthful shifts identified functions in mitochondrial regulation and oxidative stress, apoptosis, inflammation, endothelial activation, and transcriptional regulation (Fig. 3).

Our recent studies, demonstrate that aging is associated with mitochondrial dysfunction and oxidative stress in cerebromicrovascular endothelial cells, which play a critical role in dysregulation of cerebral blood flow and impaired neurovascular coupling responses in aged mice (Tarantini et al. 2018, 2019a). To find out whether mitochondria-related gene expression is altered in the aging NVU, we analyzed expression of both nuclear-encoded and mtDNA-encoded mitochondria-related genes. We have used existing databases to compile a list of genes with mitochondrial targeting sequences and known functions related to regulation of mitochondrial processes. We used Gene Set Enrichment Analysis (GSEA) for interpreting expression of mitochondria-related genes (Subramanian et al. 2005). GSEA of mtDNA-encoded genes encoding components of the mitochondrial electron transport chain (ETC) was performed using a pre-ranked gene list based on the magnitude of the fold-change (largest upregulation to most downregulated; Fig. 4a, b). Figure 4a, b depict a running-sum statistic (enrichment score) based on Fig. 4, increasing when a gene is a member of the mtDNA-encoded ETC gene set and decreasing when it is not. Note that in aged mice, GSEA scores increased predominantly on the right indicating downregulation of mtDNA-encoded ETC genes by aging. In contrast, in NMN-treated aged mice GSEA scores increased predominantly on the left indicating upregulation of mtDNA-encoded ETC genes by NMN treatment in aged mice. The heat maps showing the expression pattern of nuclear-encoded and mtDNA-encoded mitochondria-related genes are shown in Fig. 4 c and d, respectively. Hierarchical clustering of the data showed a clear separation between the young and aged groups. Aged control mice and aged NMN-treated mice were also separated. In contrast, expression of mitochondria-related genes in young mice and NMN-treated aged mice were similar, and these groups did not separate well in the hierarchical clustering, consistent with the idea that age-related dysregulation of mitochondria-related genes in the NVU is reversed, at least in part, by NMN treatment.

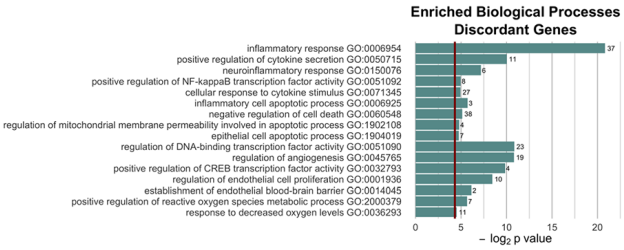

Fig. 3 Most significantly enriched Gene Ontology (GO) terms for discordant genes. Note that NMN treatment is associated with transcriptional changes indicating multifaceted anti-inflammatory, anti-apoptotic, mitochondrial protective, and anti-oxidative effects

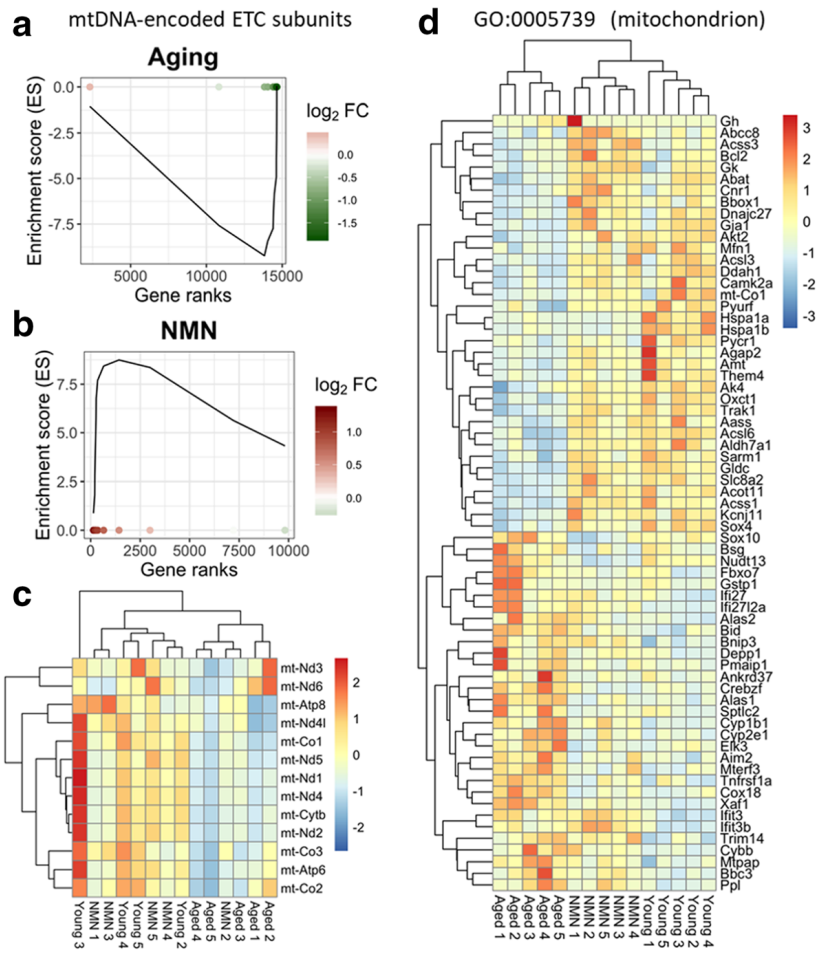

Fig. 4 NMN treatment reverses age-related changes in neurovascular expression of mitochondria-related genes. Gene Set Enrichment Analysis (GSEA) to test for enrichment of the set of mtDNA-endcoded subunits of the electron transport chain (ETC) by comparing NVU samples derived from aged (24 months old) mice with NVU samples derived from young (3 months old) mice (**a**) and NMN-treated aged NVU samples with untreated aged NVU samples (**b**). Aging-induced gene expression changes were ranked from most upregulated (left, red) to most downregulated (right, green). Dots represent identified mtDNA-encoded ETC genes. Panels **a**, **b** depict a running-sum statistic (enrichment score) based on panel **c**, increasing when a gene is a member of the mtDNA-encoded ETC gene set and decreasing when it is not. Note that in aged mice, GSEA scores increased predominantly on the right indicating downregulation of mtDNA encoded ETC genes by aging. In contrast, in NMN-treated aged mice GSEA scores increased predominantly on the left indicating upregulation of mtDNA-encoded ETC genes by NMN treatment in aged mice. The heat maps are graphic representations of normalized expression values of differentially expressed mtDNA-encoded ETC genes (**c**) and nuclear-encoded mitochondria-related genes (**d**). Hierarchical clustering analysis revealed the similarities on neurovascular expression profiles of mitochondria-related genes in young and NMN-treated aged mice. Mitochondria-related genes were identified on the basis of GO classifications (GO:0005739). Note that one young sample was a statistical outlier and was therefore excluded from the mtDNA-encoded gene expression analysis

NMN-induced neurovascular transcriptomic changes in aged mice predict anti-apoptotic effects

Previous studies suggest that endothelial cell apoptosis plays a critical role in age-related structural remodeling of cerebromicrovascular network by contributing to microvascular rarefaction (Ungvari et al. 2018a, b). To determine how NMN treatment alters apoptosis-related gene expression in the aging NVU, we analyzed expression of genes known to be involved in regulation of programmed cell death. Apoptosis-related genes were identified based on GO classification. GSEA analysis suggested that aging is associated with upregulation of pro-apoptotic genes, which tends to be reversed by NMN treatment (Fig. 5a, b). KEGG pathway map depicting age- and NMN treatment-related changes in the expression of genes in the apoptosis pathways is shown in Fig. 5c.

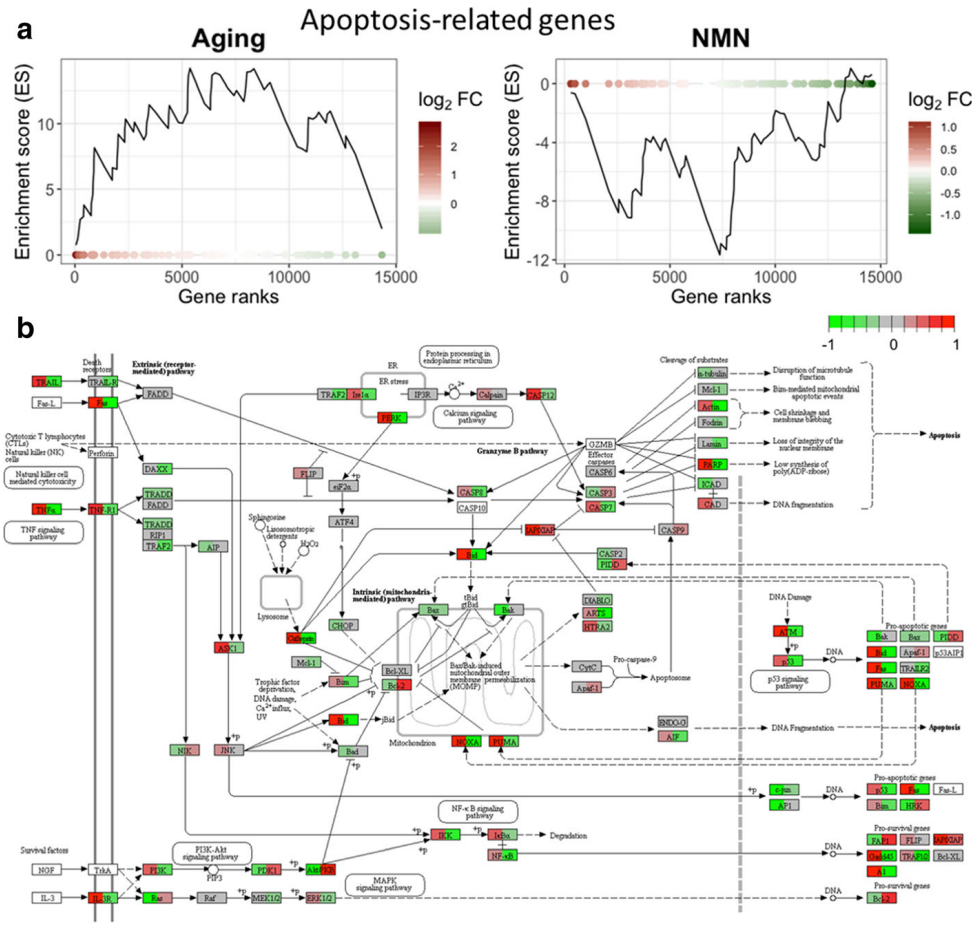

Fig. 5 NMN treatment reverses age-related changes in neurovascular expression of apoptosis-related genes. Gene Set Enrichment Analysis (GSEA) to test for enrichment of the set of pro-apoptotic genes by comparing NVU samples derived from aged (24 months old) mice with NVU samples derived from young (3 months old) mice (left, **a**) and NMN-treated aged NVU samples with untreated aged NVU samples (right, **b**). Aging-induced gene expression changes were ranked from most upregulated (left, red) to most downregulated (right, green). Dots represent identified pro-apoptotic genes. Panels **a** and **b** depict a running-sum statistic (enrichment score) based on panel **b**, increasing when a gene is a member of the apoptosis-related gene set and decreasing when it is not. Note that in aged mice, GSEA scores increased predominantly on the left indicating upregulation of pro-apoptotic genes by aging. In contrast, in NMN-treated aged mice, GSEA scores increased predominantly on the right indicating downregulation of pro-apoptotic genes by NMN treatment in aged mice. **b** Kyoto Encyclopedia of Genes and Genomes (KEGG) pathway map depicting age- and NMN treatment-related changes in the expression of genes in the apoptosis pathways. Each rectangle on the map represents a gene product in the apoptosis pathway. The rectangles are set to color by age-related (left side) and NMN treatment-induced (right side) changes in gene expression (fold-change). Red color indicates upregulation, green color indicates downregulation. Genes involved in positive regulation of apoptosis were identified based on GO classification

NMN-induced neurovascular transcriptomic changes predict anti-inflammatory effects, including inhibition of endothelial activation in aged mice

Chronic low-grade inflammation, characterized by endothelial activation, is a hallmark of vascular aging (Ungvari et al. 2018b, 2007a; Csiszar et al. 2007, 2004, 2003). To elucidate the putative anti-inflammatory effects of NMN treatment, we assessed its effect on the expression of endothelial activation–related genes. Endothelial activation–related genes were identified based on published microarray data (GEO database; GSE45880), showing mRNA expression changes after activation of cultured cerebromicrovascular endothelial cells (CMVECs) by 10 ng/mL TNFα and IFNγ (Lopez-Ramirez et al. 2013). GSEA analysis showed that aging is associated with upregulation of endothelial activation–related genes in the NVU (Fig. 6a). We found that NMN treatment exerts significant anti-inflammatory effects, downregulating endothelial activation–related genes in the NVU (Fig. 6b). The heat map shown in Fig. 6c is a graphic representation of normalized expression values

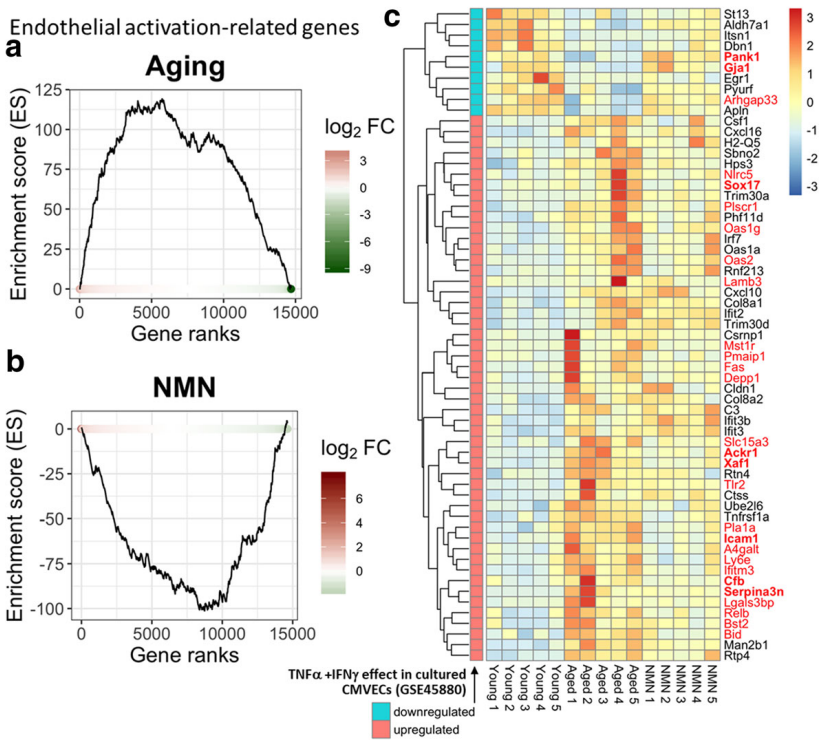

Fig. 6 NMN treatment reverses age-related changes in neurovascular expression of endothelial activation-related genes. Gene Set Enrichment Analysis (GSEA) to test for enrichment of the set of endothelial activation-related genes by comparing NVU samples derived from aged (24 months old) mice with NVU samples derived from young (3 months old) mice (**a**) and NMN-treated aged NVU samples with untreated aged NVU samples (**b**). Aging-induced gene expression changes were ranked from most upregulated (left, red) to most downregulated (right, green). Dots represent identified endothelial activation–related genes. Panels **a**, **b** depict a running-sum statistic (enrichment score) based on the upregulated endothelia activation–related genes in panel **c**, increasing when a gene is a member of the endothelial activation–related gene set and decreasing when it is not. Note that in aged mice, GSEA scores increased predominantly on the left indicating upregulation of endothelial activation–related genes by aging. In contrast, in NMN-treated aged mice, GSEA scores increased predominantly on the right indicating downregulation of endothelial activation–related genes by NMN treatment in aged mice. **c** The heat map is a graphic representation of normalized expression values of differentially expressed endothelial activation–related genes in neurovascular samples derived from young, aged, and NMN-treated aged mice. Hierarchical clustering analysis revealed the similarities on neurovascular expression profiles of endothelial activation–related genes in young and NMN-treated aged mice. Endothelial activation–related genes were identified based on published microarray data (GEO database; GSE45880), showing a distinct transcriptional signature of up and downregulated genes after activation of cultured cerebromicrovascular endothelial cells with 10 ng/mL TNFα and IFNγ (Lopez-Ramirez et al. 2013). Included in the figure are genes whose expression in aging changes similarly to the expressional changes observed in vitro upon cytokine stimulation. Discordant genes are shown in red font (bold, DE both in aging and NMN treated groups)

of differentially expressed endothelial activation–related genes in NVU samples derived from young, aged, and NMN-treated aged mice. We also found that 17 genes, which are important for blood-brain barrier integrity (Nyul-Toth et al. 2016) were significantly affected by NMN treatment (data not shown) (Fig. 7).

Discussion

Our study demonstrates that protective effects of NMN treatment on cerebromicrovascular endothelial function and neurovascular coupling responses are associated with anti-aging changes in the mRNA expression profile in the NVU in a mouse model of aging that recapitulates vascular alterations and deficits present in elderly humans at risk for vascular cognitive impairment.

To our knowledge, this is the first study to demonstrate that NMN treatment in aged mice reverses, at least in part, age-related, pro-inflammatory, pro-oxidative, pro-apoptotic, and endothelial dysfunction-promoting transcriptional alterations in the cerebral microcirculation. The results of the present study extend the findings of earlier investigations showing that treatment with NMN confers potent anti-aging neurovascular effects in aged mice, rescuing

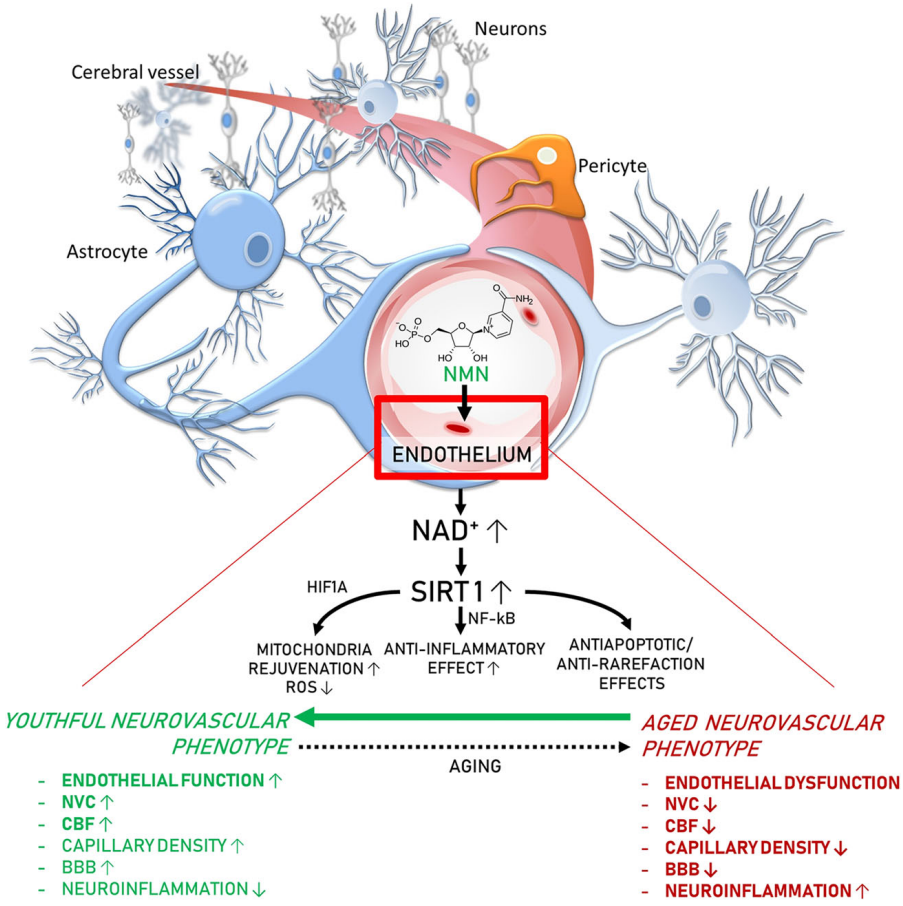

Fig. 7 Proposed scheme for the mechanisms by which restoration of NAD^+ levels in the aged neurovascular unit by NMN supplementation promotes neurovascular rejuvenation. The model, based on our present and previous findings and earlier data from the literature (Das et al. 2018; Tarantini et al. 2019a; Csiszar et al. 2019), predicts that increased NAD^+ activates sirtuin-mediated pathways, which leads to anti-aging transcriptomic changes, restores cellular energetics, and attenuates mitochondrial ROS production, rescuing a youthful neurovascular phenotype. These effects are predicted to act to improve endothelial function, increase neurovascular coupling responses, capillary density and cerebral blood flow (CBF), maintain blood-brain barrier (BBB) integrity, and inhibit neuroinflammation, protecting cognitive health (bold font, experimentally validated effects; regular fonts, predicted effects)

cerebromicrovascular endothelial dysfunction and neurovascular coupling responses, increasing cerebral blood flow, and improving cognitive performance (Yoshino et al. 2018). Demonstration of NMN-induced phenotypic and functional changes in the NVU is particularly important as neurovascular alterations (including impaired neurovascular coupling, blood-brain barrier disruption, and pro-inflammatory changes) associated with aging have been causally linked to the development of both neurodegenerative diseases and the entire spectrum of brain pathologies that contribute to vascular cognitive impairment (Iadecola 2017; Toth et al. 2017; Sweeney et al. 2019b). Endothelial protective effects of NMN have also been demonstrated in the peripheral circulation of aged mice (Das et al. 2018; Yoshino et al. 2018; de Picciotto et al. 2016), suggesting that the effects of NMN on endothelial cells in the NVU likely play a key role in NMN-induced neurovascular rejuvenation. Administration of NMN or other NAD^+ precursors (e.g., nicotinamide riboside) to aged mice was reported to increase NAD^+ levels in homogenates of complex tissues derived from multiple organs (Yoshino et al. 2018; Mills et al. 2016; Zhang et al. 2016), including the aorta (Tarantini et al. 2019a). In vitro treatment with NMN was also demonstrated to restore NAD^+ levels in aged cerebromicrovascular endothelial cells (Tarantini et al. 2019a). Future studies should determine how in vivo NMN treatment affects NAD^+ levels in each cell type constituting the NVU and elucidate the cell type–specific functional and transcriptomic effects of NMN treatment in aging.

Our study demonstrates that NMN treatment, which augments the vascular NAD^+ metabolome (Tarantini et al. 2019a), induces a neurovascular gene expression signature suggestive of SIRT1 activation. Our results expand the findings of previous studies showing that increases in NAD^+ levels induced by NMN treatment also activate SIRT1 in skeletal muscle (Gomes et al. 2013). As our recent studies demonstrate that shRNA knockdown of SIRT1 prevents the beneficial effects of NMN on aged cerebromicrovascular endothelial cells in vitro (Tarantini et al. 2019a), we posit that NMN-induced SIRT1 activation plays a critical role also in neurovascular rejuvenation in vivo. Sirtuins are known to mediate beneficial anti-aging (Cohen et al. 2004; Moroz et al. 2014; Wood et al. 2004) and vasoprotective effects (Csiszar et al. 2009a, 2013; 2014a) of caloric restriction as well. Our bioinformatics analysis also revealed a role for Hif1α signaling, confirming earlier findings (Gomes et al. 2013). Further, our recent study demonstrate that NMN treatment reverses age-related changes in miRNA expression in the aged mouse aorta (Kiss et al. 2019b). In that regard, it is significant that dysregulation of miRNA expression has been shown to significantly contribute to age-related phenotypic and functional changes in the cerebromicrovascular endothelial cells as well (Ungvari et al. 2013). These findings raise the possibility that complex changes in transcriptional and/or post-transcriptional control of expression of genes that encode critical factors determining neurovascular health contribute to the beneficial effects of treatment with NAD^+ boosters. GO enrichment analysis of discordant differentially expressed neurovascular genes identified functions in mitochondrial regulation, apoptosis, inflammation, and endothelial activation.

Mitochondrial dysfunction and increased mitochondrial oxidative stress have a critical role in the genesis of aging-induced cerebromicrovascular endothelial impairment and neurovascular dysfunction (Tarantini et al. 2018, 2019a). In support of this concept, attenuation of mitochondrial oxidative stress and restoration of mitochondrial energy metabolism in the cerebromicrovascular endothelial cells by treatment with the mitochondria-targeted antioxidants were shown to rescue neurovascular function in aged mice (Tarantini et al. 2018). Here, we report that NMN treatment rescues aging-induced changes in mitochondria-related gene expression in the NVU. Importantly, these NMN-induced changes in the mitochondria-related transcriptome are associated with attenuated mitochondrial oxidative stress and restoration of mitochondrial energy metabolism in aging cerebromicrovascular endothelial cells (Tarantini et al. 2019a; Kiss et al. 2019a). On the basis of previous findings (Gomes et al. 2013), we posit that rescue of vascular mitochondrial function by restoring the expression of ETC subunits contributes to the neurovascular protective effects of NMN. Treatment with NMN was also shown to rescue expression of mitochondrial-encoded ETC subunits in cerebral arteries of aged mice and in aged cerebromicrovascular endothelial cells (Gomes et al. 2013). It is believed that rescue of electron flow through the electron transport chain, due to the restored expression of complex I and complex III (Kwong and Sohal 2000), likely attenuates electron leak, limiting mtROS production. Treatment with NAD^+ boosters was also demonstrated to upregulate mitochondrial gene expression in the mouse skeletal muscle (Canto et al. 2012). Our recent studies provide evidence that NMN treatment exerts its mitochondrial protective effects in cerebromicrovascular endothelial cells in a SIRT1-dependent manner (Gomes et al. 2013). Our observations accord with findings from earlier studies showing that many of the health benefits conferred by SIRT1 activation are linked to improved mitochondrial function (Baur et al. 2006). In addition to sirtuin-mediated transcriptomic effects, a mitochondrial ATP production requires NAD^+ as an essential cofactor, rescuing normal cellular NAD/NADH ratio per se may also promote efficient mitochondrial function in cells of the NVU.

Analysis of the transcriptomic signature of NMN treatment predicts potent anti-apoptotic effects in the NVU. This is significant, as endothelial cell apoptosis plays a critical role in age-related cerebromicrovascular rarefaction (Ungvari et al. 2018a, b). Thus, future studies should determine how NMN treatment affects the number of apoptotic endothelial cells in the NVU as well as capillary density in the aged brain. Recent studies show that NMN also protects the integrity of the blood-brain barrier in a mouse model of brain ischemia (Wei et al. 2017). On the basis of our findings that NMN upregulates factors controlling barrier integrity, it will be also of great interest to determine whether NMN treatment can also protect against age-related disruption of the blood-brain barrier.

Our studies demonstrate that NMN treatment in aged mice reverses, at least in part, age-related, pro-inflammatory alterations in mRNA expression profile in the NVU. Our findings expand the results of recent studies demonstrating that treatment of aged mice with NMN promotes anti-inflammatory phenotypic changes in the peripheral vasculature as well (Kiss et al. 2019b). Previous studies attributed age-related endothelial activation and chronic sterile microvascular inflammation to oxidative stress-mediated activation of NF-κB and upregulation of pro-inflammatory cytokines in the vascular wall (Csiszar et al. 2003, 2008b, 2014a; Ungvari et al. 2007a). SIRT1 activation is known to attenuate cellular and mitochondrial oxidative stress, inhibit NF-κB, and attenuate microvascular inflammation (Toth et al. 2015; Csiszar et al. 2008a, 2012; Baur et al. 2012; Ungvari et al. 2009; Zhang et al. 2009; Mattison et al. 2014). Thus, it is likely that SIRT1 activation and the previously documented anti-oxidative neurovascular effects contribute significantly to the observed anti-inflammatory effects associated with NMN treatment.

Additional studies are warranted to determine the efficacy of combination treatments with NAD^+ boosters (Mitchell et al. 2018; Yoshino et al. 2018; Liu et al. 2018) and compounds that directly activate SIRT1 and/or inhibit NAD^+ overutilization for neurovascular protection. Similar to NAD^+ boosters, SIRT1-activating compounds (STACs; including resveratrol and SRT1720) were demonstrated to exert important vasoprotective effects in models of aging and accelerated vascular aging (Csiszar et al. 2008a; Ungvari et al. 2007a, b, 2011; Pearson et al. 2008; Zarzuelo et al. 2013; Chen et al. 2015; Gano et al. 2014; Minor et al. 2011). These SIRT1-mediated effects include increased mitochondrial biogenesis (Csiszar et al. 2009b), attenuation of mitochondrial oxidative stress (Ungvari et al. 2009; Csiszar et al. 2012), activation of anti-oxidative defense mechanisms (Csiszar et al. 2014b), and inhibition of apoptosis (Pearson et al. 2008). Treatment with the STAC resveratrol was shown to improve cerebromicrovascular endothelial function and rescue neurovascular coupling responses in aged mice (Toth et al. 2014; Wiedenhoeft et al. 2019). Resveratrol was also shown to increase capillary density (Oomen et al. 2009) and prevent microvascular fragility (Toth et al. 2015) in the aged mouse brain and to exert similar vasoprotective effects in non-human primate models as well (Mattison et al. 2014; Bernier et al. 2016). The molecular mechanisms contributing to age-related decline in NAD^+ in cells of the NVU are likely multifaceted. In addition to downregulation of NAMPT (nicotinamide phosphoribosyltransferase/NMN synthase; which catalyzes the rate limiting step in the biosynthesis of NAD^+) (Tarantini et al. 2019a), the increased utilization of NAD^+ by activated poly(ADP-ribose) polymerase 1 (PARP-1) (Csiszar et al. 2019; Pacher et al. 2002) also likely plays an important role in age-related decline in NAD^+ in the NVU. Accordingly, treatment with PJ-34, a potent PARP inhibitor, restores neurovascular coupling responses in aged mice, similar to the neurovascular protective effects of NMN treatment (Tarantini et al. 2019b). Thus, future studies should determine whether combination of NAD^+ boosters with STACs, mitochondria-targeted agents, and/or PARP-1 inhibitors confers greater neurovascular and cognitive health benefits as compared with NAD^+ booster treatment alone.

Conclusions

In conclusion, rescue of cerebromicrovascular endothelial function and neurovascular coupling responses in NMN-treated aged mice are accompanied by marked anti-aging changes in the neurovascular transcriptome. We hope that our findings will facilitate future endeavors to uncover the mechanistic role of neurovascular NAD^+ depletion in brain aging and the pathogenesis of VCI. The recently appreciated complex role of NVU dysfunction (ranging from impaired neurovascular coupling to blood-brain barrier disruption) in neurodegenerative diseases and VCI supports the concept that pharmacological treatments, which maintain neurovascular health, promote brain health (Kisler et al. 2017; Zlokovic 2010, 2011; Csipo et al. 2019a, b; de Montgolfier et al. 2019; Farias Quipildor et al. 2019; Fulop et al. 2019; Sorond et al. 2019; Sagare et al. 2013). Potentially, NAD^+ booster treatments (e.g., in combination with STACs) could be harnessed for development of new pharmacological approaches for neurovascular protection for the prevention and treatment of VCI and neurodegenerative diseases in older adults.

Funding information This work was supported by grants from the American Heart Association (ST), the Oklahoma Center for the Advancement of Science and Technology (to AC, AY, ZU), the National Institute on Aging (R01-AG047879; R01-AG038747; R01-AG055395), the National Institute of Neurological Disorders and Stroke (NINDS; R01-NS056218 to AC, R01-NS100782 to ZU), the National Institute of General Medical Sciences Oklahoma Shared Clinical and Translational Resources (OSCTR) (GM104938, to AY and JW) and Molecular Mechanisms and Genetics of Autoimmunity COBRE (P30-GM110766, to LG), the Presbyterian Health Foundation (to ZU, AC, AY), the NIA-supported Geroscience Training Program in Oklahoma (T32AG052363), the Oklahoma Nathan Shock Center (P30AG050911), and the Cellular and Molecular GeroScience CoBRE (1P20GM125528, sub#5337). The funding sources had no role in the study design; in the collection, analysis, and interpretation of data; in the writing of the report; and in the decision to submit the article for publication.

Compliance with ethical standards

All procedures were approved by the Institutional Animal Use and Care Committees of the University of Oklahoma Health Sciences Center. All animal experiments complied with the ARRIVE guidelines and were carried out in accordance with the National Institutes of Health guide for the care and use of Laboratory animals (NIH Publications No. 8023, revised 1978).

References

Anderson RM, Bitterman KJ, Wood JG, Medvedik O, Cohen H, Lin SS, Manchester JK, Gordon JI, Sinclair DA (2002) Manipulation of a nuclear NAD+ salvage pathway delays aging without altering steady-state NAD+ levels. J Biol Chem 277:18881–18890

Baur JA, Pearson KJ, Price NL, Jamieson HA, Lerin C, Kalra A, Prabhu VV, Allard JS, Lopez-Lluch G, Lewis K, Pistell PJ, Poosala S, Becker KG, Boss O, Gwinn D, Wang M, Ramaswamy S, Fishbein KW, Spencer RG, Lakatta EG, Le Couteur D, Shaw RJ, Navas P, Puigserver P, Ingram DK, de Cabo R, Sinclair DA (2006) Resveratrol improves health and survival of mice on a high-calorie diet. Nature. 444:337–342

Baur JA, Ungvari Z, Minor RK, Le Couteur DG, de Cabo R (2012) Are sirtuins viable targets for improving healthspan and lifespan? Nat Rev Drug Discov 11:443–461

Bernier M, Wahl D, Ali A, Allard J, Faulkner S, Wnorowski A, Sanghvi M, Moaddel R, Alfaras I, Mattison JA, Tarantini S, Tucsek Z, Ungvari Z, Csiszar A, Pearson KJ, de Cabo R (2016) Resveratrol supplementation confers neuroprotection in cortical brain tissue of nonhuman primates fed a high-fat/sucrose diet. *Aging (Albany NY)* 8:899–916

Bolger AM, Lohse M, Usadel B (2014) Trimmomatic: a flexible trimmer for Illumina sequence data. Bioinformatics. 30:2114–2120

Bray NL, Pimentel H, Melsted P, Pachter L (2016) Near-optimal probabilistic RNA-seq quantification. Nat Biotechnol 34:525–527

Canto C, Houtkooper RH, Pirinen E, Youn DY, Oosterveer MH, Cen Y, Fernandez-Marcos PJ, Yamamoto H, Andreux PA, Cettour-Rose P, Gademann K, Rinsch C, Schoonjans K, Sauve AA, Auwerx J (2012) The NAD(+) precursor nicotinamide riboside enhances oxidative metabolism and protects against high-fat diet-induced obesity. Cell Metab 15:838–847

Chen YX, Zhang M, Cai Y, Zhao Q, Dai W (2015) The Sirt1 activator SRT1720 attenuates angiotensin II-induced atherosclerosis in apoE(−)/(−) mice through inhibiting vascular inflammatory response. Biochem Biophys Res Commun 465:732–738

Cohen HY, Miller C, Bitterman KJ, Wall NR, Hekking B, Kessler B, Howitz KT, Gorospe M, de Cabo R, Sinclair DA (2004) Calorie restriction promotes mammalian cell survival by inducing the SIRT1 deacetylase. Science. 305:390–392

Csipo T, Lipecz A, Fulop GA, Hand RA, Ngo BN, Dzialendzik M, Tarantini S, Balasubramanian P, Kiss T, Yabluchanska V, Silva-Palacios F, Courtney DL, Dasari TW, Sorond F, Sonntag WE, Csiszar A, Ungvari Z, Yabluchanskiy A (2019a) Age-related decline in peripheral vascular health predicts cognitive impairment. Geroscience. 41:125–136

Csipo T, Mukli P, Lipecz A, Tarantini S, Bahadli D, Abdulhussein O, Owens C, Kiss T, Balasubramanian P, Nyul-Toth A, Hand RA, Yabluchanska V, Sorond FA, Csiszar A, Ungvari Z, Yabluchanskiy A (2019b) Assessment of age-related decline of neurovascular coupling responses by functional near-infrared spectroscopy (fNIRS) in humans. Geroscience. 41:495–509

Csiszar A, Ungvari Z, Koller A, Edwards JG, Kaley G (2003) Aging-induced proinflammatory shift in cytokine expression profile in rat coronary arteries. FASEB J 17:1183–1185

Csiszar A, Ungvari Z, Koller A, Edwards JG, Kaley G (2004) Proinflammatory phenotype of coronary arteries promotes endothelial apoptosis in aging. Physiol Genomics 17:21–30

Csiszar A, Labinskyy N, Smith K, Rivera A, Orosz Z, Ungvari Z (2007) Vasculoprotective effects of anti-TNFalfa treatment in aging. Am J Pathol 170:388–698

Csiszar A, Labinskyy N, Podlutsky A, Kaminski PM, Wolin MS, Zhang C, Mukhopadhyay P, Pacher P, Hu F, de Cabo R, Ballabh P, Ungvari Z (2008a) Vasoprotective effects of resveratrol and SIRT1: attenuation of cigarette smoke-induced oxidative stress and proinflammatory phenotypic alterations. Am J Physiol Heart Circ Physiol 294:H2721–H2735

Csiszar A, Wang M, Lakatta EG, Ungvari ZI (2008b) Inflammation and endothelial dysfunction during aging: role of NF-{kappa}B. J Appl Physiol 105:1333–1341

Csiszar A, Labinskyy N, Jimenez R, Pinto JT, Ballabh P, Losonczy G, Pearson KJ, de Cabo R, Ungvari Z (2009a) Anti-oxidative and anti-inflammatory vasoprotective effects of caloric restriction in aging: role of circulating factors and SIRT1. Mech Ageing Dev 130:518–527

Csiszar A, Labinskyy N, Pinto JT, Ballabh P, Zhang H, Losonczy G, Pearson KJ, de Cabo R, Pacher P, Zhang C, Ungvari ZI (2009b) Resveratrol induces mitochondrial biogenesis in endothelial cells. Am J Physiol Heart Circ Physiol. 2009 Jul;297(1):H13-20. https://doi.org/10.1152/ajpheart.00368.2009

Csiszar A, Sosnowska D, Wang M, Lakatta EG, Sonntag WE, Ungvari Z (2012) Age-associated proinflammatory secretory phenotype in vascular smooth muscle cells from the non-human primate Macaca mulatta: reversal by resveratrol treatment. J Gerontol A Biol Sci Med Sci 67:811–820

Csiszar A, Sosnowska D, Tucsek Z, Gautam T, Toth P, Losonczy G, Colman RJ, Weindruch R, Anderson RM, Sonntag WE, Ungvari Z (2013) Circulating factors induced by caloric restriction in the nonhuman primate Macaca mulatta activate angiogenic processes in endothelial cells. J Gerontol A Biol Sci Med Sci 68:235–249

Csiszar A, Gautam T, Sosnowska D, Tarantini S, Banki E, Tucsek Z, Toth P, Losonczy G, Koller A, Reglodi D, Giles CB, Wren JD, Sonntag WE, Ungvari Z (2014a) Caloric restriction confers persistent anti-oxidative, pro-angiogenic, and anti-inflammatory effects and promotes anti-aging miRNA expression profile in cerebromicrovascular endothelial cells of aged rats. Am J Physiol Heart Circ Physiol 307:H292–H306

Csiszar A, Pinto JT, Gautam T, Kleusch C, Hoffmann B, Tucsek Z, Toth P, Sonntag WE, Ungvari Z (2014b) Resveratrol encapsulated in novel fusogenic liposomes activates Nrf2 and attenuates oxidative stress in cerebromicrovascular endothelial cells from aged rats. J Gerontol A Biol Sci Med Sci. 2015 Mar;70(3):303-13. https://doi.org/10.1093/gerona/glu029

Csiszar A, Tarantini S, Fulop GA, Kiss T, Valcarcel-Ares MN, Galvan V, Ungvari Z, Yabluchanskiy A (2017) Hypertension impairs neurovascular coupling and promotes microvascular injury: role in exacerbation of Alzheimer's disease. GeroScience. 2017 Aug; 39(4): 359–372.

Csiszar A, Tarantini S, Yabluchanskiy A, Balasubramanian P, Kiss T, Farkas E, Baur JA, Ungvari ZI (2019) Role of endothelial NAD+ deficiency in age-related vascular dysfunction. *Am J Physiol Heart Circ Physiol*. 2019 Jun 1;316(6):H1253-H1266. https://doi.org/10.1152/ajpheart.00039.2019

Das A, Huang GX, Bonkowski MS, Longchamp A, Li C, Schultz MB, Kim LJ, Osborne B, Joshi S, Lu Y, Trevino-Villarreal JH, Kang MJ, Hung TT, Lee B, Williams EO, Igarashi M, Mitchell JR, Wu LE, Turner N, Arany Z, Guarente L, Sinclair DA (2018) Impairment of an endothelial NAD(+)-H2S signaling network is a reversible cause of vascular aging. Cell. 173:74–89 e20

de Montgolfier O, Pouliot P, Gillis MA, Ferland G, Lesage F, Thorin-Trescases N, Thorin E (2019) Systolic hypertension-induced neurovascular unit disruption magnifies vascular cognitive impairment in middle-age atherosclerotic LDLr(−/−):hApoB(+/+) mice. Geroscience. 41:511–532

de Picciotto NE, Gano LB, Johnson LC, Martens CR, Sindler AL, Mills KF, Imai S, Seals DR (2016) Nicotinamide mononucleotide supplementation reverses vascular dysfunction and oxidative stress with aging in mice. Aging Cell 15:522–530

Durinck S, Spellman PT, Birney E, Huber W (2009) Mapping identifiers for the integration of genomic datasets with the R/Bioconductor package biomaRt. Nat Protoc 4:1184–1191

Falcon S, Gentleman R (2007) Using GOstats to test gene lists for GO term association. Bioinformatics. 23:257–258

Farias Quipildor GE, Mao K, Hu Z, Novaj A, Cui MH, Gulinello M, Branch CA, Gubbi S, Patel K, Moellering DR, Tarantini S, Kiss T, Yabluchanskiy A, Ungvari Z, Sonntag WE, Huffman DM (2019) Central IGF-1 protects against features of cognitive and sensorimotor decline with aging in male mice. Geroscience. 41:185–208

Fulop GA, Ahire C, Csipo T, Tarantini S, Kiss T, Balasubramanian P, Yabluchanskiy A, Farkas E, Toth A, Nyul-Toth A, Toth P, Csiszar A, Ungvari Z (2019) Cerebral venous congestion promotes blood-brain barrier disruption and neuroinflammation, impairing cognitive function in mice. Geroscience. 41:575–589

Gano LB, Donato AJ, Pasha HM, Hearon CM Jr, Sindler AL, Seals DR (2014) The SIRT1 activator SRT1720 reverses vascular endothelial dysfunction, excessive superoxide production, and inflammation with aging in mice. Am J Physiol Heart Circ Physiol 307:H1754–H1763

Gomes AP, Price NL, Ling AJ, Moslehi JJ, Montgomery MK, Rajman L, White JP, Teodoro JS, Wrann CD, Hubbard BP, Mercken EM, Palmeira CM, de Cabo R, Rolo AP, Turner N, Bell EL, Sinclair DA (2013) Declining NAD(+) induces a pseudohypoxic state disrupting nuclear-mitochondrial communication during aging. Cell. 155:1624–1638

Hubbard BP, Gomes AP, Dai H, Li J, Case AW, Considine T, Riera TV, Lee JE, E SY, Lamming DW, Pentelute BL, Schuman ER, Stevens LA, Ling AJ, Armour SM, Michan S, Zhao H, Jiang Y, Sweitzer SM, Blum CA, Disch JS, Ng PY, Howitz KT, Rolo AP, Hamuro Y, Moss J, Perni RB, Ellis JL, Vlasuk GP, Sinclair DA (2013) Evidence for a common mechanism of SIRT1 regulation by allosteric activators. Science. 339:1216–1219

Iadecola C (2017) The neurovascular unit coming of age: a journey through neurovascular coupling in health and disease. Neuron. 96:17–42

Iliff JJ, Lee H, Yu M, Feng T, Logan J, Nedergaard M, Benveniste H (2013) Brain-wide pathway for waste clearance captured by contrast-enhanced MRI. J Clin Invest 123:1299–1309

Imai S, Guarente L (2014) NAD+ and sirtuins in aging and disease. Trends Cell Biol 24:464–471

Imperio CG, McFalls AJ, Colechio EM, Masser DR, Vrana KE, Grigson PS, Freeman WM (2016) Assessment of individual differences in the rat nucleus accumbens transcriptome following taste-heroin extended access. Brain Res Bull 123:71–80

Jessen NA, Munk AS, Lundgaard I, Nedergaard M (2015) The glymphatic system: a Beginner's guide. Neurochem Res 40:2583–2599

Kisler K, Nelson AR, Montagne A, Zlokovic BV (2017) Cerebral blood flow regulation and neurovascular dysfunction in Alzheimer disease. Nat Rev Neurosci 18:419–434

Kiss T, Balasubramanian P, Valcarcel-Ares MN, Tarantini S, Yabluchanskiy A, Csipo T, Lipecz A, Reglodi D, Zhang XA, Bari F, Farkas E, Csiszar A, Ungvari Z (2019a) Nicotinamide mononucleotide (NMN) treatment attenuates oxidative stress and rescues angiogenic capacity in aged cerebromicrovascular endothelial cells: a potential mechanism for prevention of vascular cognitive impairment. *GeroScience*. in press

Kiss T, Giles CB, Tarantini S, Yabluchanskiy A, Balasubramanian P, Gautam T, Csipo T, Nyul-Toth A, Lipecz A, Szabo C, Farkas E, Wren JD, Csiszar A, Ungvari Z (2019b) Nicotinamide mononucleotide (NMN) supplementation promotes anti-aging miRNA expression profile in the aorta of aged mice, predicting epigenetic rejuvenation and anti-atherogenic effects. Geroscience. 2019 Aug;41(4):419–439. https://doi.org/10.1007/s11357-019-00095-x. Accessed 28 Aug 2019

Kramer A, Green J, Pollard J Jr, Tugendreich S (2014) Causal analysis approaches in Ingenuity Pathway Analysis. Bioinformatics. 30:523–530

Kress BT, Iliff JJ, Xia M, Wang M, Wei HS, Zeppenfeld D, Xie L, Kang H, Xu Q, Liew JA, Plog BA, Ding F, Deane R, Nedergaard M (2014) Impairment of paravascular clearance pathways in the aging brain. Ann Neurol 76:845–861

Kwong LK, Sohal RS (2000) Age-related changes in activities of mitochondrial electron transport complexes in various tissues of the mouse. Arch Biochem Biophys 373:16–22

Libert S, Pointer K, Bell EL, Das A, Cohen DE, Asara JM, Kapur K, Bergmann S, Preisig M, Otowa T, Kendler KS, Chen X, Hettema JM, van den Oord EJ, Rubio JP, Guarente L (2011) SIRT1 activates MAO-A in the brain to mediate anxiety and exploratory drive. Cell. 147:1459–1472

Liu L, Su X, Quinn WJ 3rd, Hui S, Krukenberg K, Frederick DW, Redpath P, Zhan L, Chellappa K, White E, Migaud M, Mitchison TJ, Baur JA, Rabinowitz JD (2018) Quantitative analysis of NAD synthesis-breakdown fluxes. Cell Metab 27: 1067–1080 e5

Lopez-Ramirez MA, Male DK, Wang C, Sharrack B, Wu D, Romero IA (2013) Cytokine-induced changes in the gene expression profile of a human cerebral microvascular endothelial cell-line, hCMEC/D3. Fluids Barriers CNS 10:27

Love MI, Huber W, Anders S (2014) Moderated estimation of fold change and dispersion for RNA-seq data with DESeq2. Genome Biol 15:550

Massudi H, Grant R, Braidy N, Guest J, Farnsworth B, Guillemin GJ (2012) Age-associated changes in oxidative stress and NAD+ metabolism in human tissue. PLoS One 7:e42357

Mattison JA, Wang M, Bernier M, Zhang J, Park SS, Maudsley S, An SS, Santhanam L, Martin B, Faulkner S, Morrell C, Baur JA, Peshkin L, Sosnowska D, Csiszar A, Herbert RL, Tilmont EM, Ungvari Z, Pearson KJ, Lakatta EG, de Cabo R (2014) Resveratrol prevents high fat/sucrose diet-induced central arterial wall inflammation and stiffening in nonhuman primates. Cell Metab 20:183–190

Michan S, Li Y, Chou MM, Parrella E, Ge H, Long JM, Allard JS, Lewis K, Miller M, Xu W, Mervis RF, Chen J, Guerin KI, Smith LE, McBurney MW, Sinclair DA, Baudry M, de Cabo R, Longo VD (2010) SIRT1 is essential for normal cognitive function and synaptic plasticity. J Neurosci 30:9695–9707

Mills KF, Yoshida S, Stein LR, Grozio A, Kubota S, Sasaki Y, Redpath P, Migaud ME, Apte RS, Uchida K, Yoshino J, Imai SI (2016) Long-term administration of nicotinamide mononucleotide mitigates age-associated physiological decline in mice. Cell Metab 24:795–806

Minor RK, Baur JA, Gomes AP, Ward TM, Csiszar A, Mercken EM, Abdelmohsen K, Shin YK, Canto C, Scheibye-Knudsen M, Krawczyk M, Irusta PM, Martin-Montalvo A, Hubbard BP, Zhang Y, Lehrmann E, White AA, Price NL, Swindell WR, Pearson KJ, Becker KG, Bohr VA, Gorospe M, Egan JM, Talan MI, Auwerx J, Westphal CH, Ellis JL, Ungvari Z, Vlasuk GP, Elliott PJ, Sinclair DA, de Cabo R (2011) SRT1720 improves survival and healthspan of obese mice. *Sci Rep*. 1. https://doi.org/10.1038/srep00070

Mitchell SJ, Martin-Montalvo A, Mercken EM, Palacios HH, Ward TM, Abulwerdi G, Minor RK, Vlasuk GP, Ellis JL, Sinclair DA, Dawson J, Allison DB, Zhang Y, Becker KG, Bernier M, de Cabo R (2014) The SIRT1 activator SRT1720 extends lifespan and improves health of mice fed a standard diet. Cell Rep 6:836–843

Mitchell SJ, Bernier M, Aon MA, Cortassa S, Kim EY, Fang EF, Palacios HH, Ali A, Navas-Enamorado I, Di Francesco A, Kaiser TA, Waltz TB, Zhang N, Ellis JL, Elliott PJ, Frederick DW, Bohr VA, Schmidt MS, Brenner C, Sinclair DA, Sauve AA, Baur JA, de Cabo R (2018) Nicotinamide improves aspects of healthspan, but not lifespan, in mice. Cell Metab 27:667–676 e4

Montagne A, Zhao Z, Zlokovic BV (2017) Alzheimer's disease: a matter of blood-brain barrier dysfunction? J Exp Med 214: 3151–3169

Moroz N, Carmona JJ, Anderson E, Hart AC, Sinclair DA, Blackwell TK (2014) Dietary restriction involves NAD(+)-dependent mechanisms and a shift toward oxidative metabolism. Aging Cell 13:1075–1085

Nyul-Toth A, Suciu M, Molnar J, Fazakas C, Hasko J, Herman H, Farkas AE, Kaszaki J, Hermenean A, Wilhelm I, Krizbai IA (2016) Differences in the molecular structure of the blood-brain barrier in the cerebral cortex and white matter: an in silico, in vitro, and ex vivo study. Am J Physiol Heart Circ Physiol 310:H1702–H1714

Oomen CA, Farkas E, Roman V, van der Beek EM, Luiten PG, Meerlo P (2009) Resveratrol preserves cerebrovascular density and cognitive function in aging mice. Front Aging Neurosci 1:4

Pacher P, Mabley JG, Soriano FG, Liaudet L, Komjati K, Szabo C (2002) Endothelial dysfunction in aging animals: the role of poly(ADP-ribose) polymerase activation. Br J Pharmacol 135:1347–1350

Pearson KJ, Baur JA, Lewis KN, Peshkin L, Price NL, Labinskyy N, Swindell WR, Kamara D, Minor RK, Perez E, Jamieson HA, Zhang Y, Dunn SR, Sharma K, Pleshko N, Woollett LA, Csiszar A, Ikeno Y, Le Couteur D, Elliott PJ, Becker KG, Navas P, Ingram DK, Wolf NS, Ungvari Z, Sinclair DA, de Cabo R (2008) Resveratrol delays age-related deterioration and mimics transcriptional aspects of dietary restriction without extending life span. Cell Metab 8:157–168

Sagare AP, Bell RD, Zlokovic BV (2013) Neurovascular defects and faulty amyloid-beta vascular clearance in Alzheimer's disease. J Alzheimers Dis 33(Suppl 1):S87–S100

Solano Fonseca R, Mahesula S, Apple DM, Raghunathan R, Dugan A, Cardona A, O'Connor J, Kokovay E (2016) Neurogenic niche microglia undergo positional remodeling and progressive activation contributing to age-associated reductions in neurogenesis. Stem Cells Dev 25:542–555

Soneson C, Love MI, Robinson MD (2015) Differential analyses for RNA-seq: transcript-level estimates improve gene-level inferences. *F1000Res* 4:1521

Sorond FA, Whitehead S, Arai K, Arnold D, Carmichael ST, De Carli C, Duering M, Fornage M, Flores-Obando RE, Graff-Radford J, Hamel E, Hess DC, Ihara M, Jensen MK, Markus HS, Montagne A, Rosenberg G, Shih AY, Smith EE, Thiel A, Tse KH, Wilcock D, Barone F (2019) Proceedings from the Albert Charitable Trust Inaugural Workshop on white matter and cognition in aging. Geroscience. 2019 Dec 6. https://doi.org/10.1007/s11357-019-00141-8

Stanimirovic DB, Friedman A (2012) Pathophysiology of the neurovascular unit: disease cause or consequence? J Cereb Blood Flow Metab 32:1207–1221

Subramanian A, Tamayo P, Mootha VK, Mukherjee S, Ebert BL, Gillette MA, Paulovich A, Pomeroy SL, Golub TR, Lander ES, Mesirov JP (2005) Gene set enrichment analysis: a knowledge-based approach for interpreting genome-wide expression profiles. Proc Natl Acad Sci U S A 102:15545–15550

Sweeney MD, Sagare AP, Zlokovic BV (2018) Blood-brain barrier breakdown in Alzheimer disease and other neurodegenerative disorders. Nat Rev Neurol 14:133–150

Sweeney MD, Zhao Z, Montagne A, Nelson AR, Zlokovic BV (2019a) Blood-brain barrier: from physiology to disease and back. Physiol Rev 99:21–78

Sweeney MD, Montagne A, Sagare AP, Nation DA, Schneider LS, Chui HC, Harrington MG, Pa J, Law M, Wang DJJ, Jacobs RE, Doubal FN, Ramirez J, Black SE, Nedergaard M, Benveniste H, Dichgans M, Iadecola C, Love S, Bath PM, Markus HS, Salman RA, Allan SM, Quinn TJ, Kalaria RN, Werring DJ, Carare RO, Touyz RM, Williams SCR, Moskowitz MA, Katusic ZS, Lutz SE, Lazarov O, Minshall RD, Rehman J, Davis TP, Wellington CL, Gonzalez HM, Yuan C, Lockhart SN, Hughes TM, CLH C, Sachdev P, O'Brien JT, Skoog I, Pantoni L, Gustafson DR, Biessels GJ, Wallin A, Smith EE, Mok V, Wong A, Passmore P, Barkof F, Muller M, MMB B, Roman GC, Hamel E, Seshadri S, Gottesman RF, van Buchem MA, Arvanitakis Z, Schneider JA, Drewes LR, Hachinski V, Finch CE, Toga AW, Wardlaw JM, Zlokovic BV (2019b) Vascular dysfunction-the disregarded partner of Alzheimer's disease. *Alzheimers Dement*. 15:158–167

Tarantini S, Hertelendy P, Tucsek Z, Valcarcel-Ares MN, Smith N, Menyhart A, Farkas E, Hodges EL, Towner R, Deak F, Sonntag WE, Csiszar A, Ungvari Z, Toth P (2015) Pharmacologically induced neurovascular uncoupling is associated with cognitive impairment in mice. J Cereb Blood Flow Metab 35:1871–1881

Tarantini S, Tucsek Z, Valcarcel-Ares M, Toth P, Gautam T, Giles C, Ballabh P, Wei Y, Wren J, Ashpole N, Sonntag W, Ungvari Z, Csiszar A (2016) Circulating IGF-1 deficiency exacerbates hypertension-induced microvascular rarefaction in the mouse hippocampus and retrosplenial cortex: implications for cerebromicrovascular and brain aging. *Age (Dordr)* 38:273–289

Tarantini S, Tran CHT, Gordon GR, Ungvari Z, Csiszar A (2017a) Impaired neurovascular coupling in aging and Alzheimer's disease: contribution of astrocyte dysfunction and endothelial impairment to cognitive decline. Exp Gerontol 94:52–58

Tarantini S, Yabluchanksiy A, Fulop GA, Hertelendy P, Valcarcel-Ares MN, Kiss T, Bagwell JM, O'Connor D, Farkas E, Sorond F, Csiszar A, Ungvari Z (2017b) Pharmacologically induced impairment of neurovascular coupling responses alters gait coordination in mice. Geroscience. 39:601–614

Tarantini S, Valcarcel-Ares NM, Yabluchanskiy A, Springo Z, Fulop GA, Ashpole N, Gautam T, Giles CB, Wren JD, Sonntag WE, Csiszar A, Ungvari Z (2017c) Insulin-like growth factor 1 deficiency exacerbates hypertension-induced cerebral microhemorrhages in mice, mimicking the aging phenotype. Aging Cell 16:469–479

Tarantini S, Valcarcel-Ares NM, Yabluchanskiy A, Fulop GA, Hertelendy P, Gautam T, Farkas E, Perz A, Rabinovitch PS, Sonntag WE, Csiszar A, Ungvari Z (2018) Treatment with the mitochondrial-targeted antioxidant peptide SS-31 rescues neurovascular coupling responses and cerebrovascular endothelial function and improves cognition in aged mice. Aging Cell. 2018 Apr;17(2). https://doi.org/10.1111/acel.12731

Tarantini S, Valcarcel-Ares MN, Toth P, Yabluchanskiy A, Tucsek Z, Kiss T, Hertelendy P, Kinter M, Ballabh P, Sule Z, Farkas E, Baur JA, Sinclair DA, Csiszar A, Ungvari Z (2019a) Nicotinamide mononucleotide (NMN) supplementation rescues cerebromicrovascular endothelial function and neurovascular coupling responses and improves cognitive function in aged mice. Redox Biol 24:101192

Tarantini S, Yabluchanskiy A, Csipo T, Fulop G, Kiss T, Balasubramanian P, DelFavero J, Ahire C, Ungvari A, Nyul-Toth A, Farkas E, Benyo Z, Toth A, Csiszar A, Ungvari Z (2019b) Treatment with the poly(ADP-ribose) polymerase inhibitor PJ-34 improves cerebromicrovascular endothelial function, neurovascular coupling responses and cognitive performance in aged mice, supporting the NAD+ depletion hypothesis of neurovascular aging. Geroscience. 2019 Oct;41(5):533–542. https://doi.org/10.1007/s11357-019-00101-2

Toth P, Tarantini S, Tucsek Z, Ashpole NM, Sosnowska D, Gautam T, Ballabh P, Koller A, Sonntag WE, Csiszar A, Ungvari ZI (2014) Resveratrol treatment rescues neurovascular coupling in aged mice: role of improved cerebromicrovascular endothelial function and down-regulation of NADPH oxidas. Am J Physiol Heart Circ Physiol 306:H299–H308

Toth P, Tarantini S, Springo Z, Tucsek Z, Gautam T, Giles CB, Wren JD, Koller A, Sonntag WE, Csiszar A, Ungvari Z (2015) Aging exacerbates hypertension-induced cerebral microhemorrhages in mice: role of resveratrol treatment in vasoprotection. Aging Cell 14:400–408

Toth P, Tarantini S, Csiszar A, Ungvari Z (2017) Functional vascular contributions to cognitive impairment and dementia: mechanisms and consequences of cerebral autoregulatory dysfunction, endothelial impairment, and neurovascular uncoupling in aging. Am J Physiol Heart Circ Physiol 312: H1–H20

Tucsek Z, Toth P, Tarantini S, Sosnowska D, Gautam T, Warrington JP, Giles CB, Wren JD, Koller A, Ballabh P, Sonntag WE, Ungvari Z, Csiszar A (2014) Aging exacerbates obesity-induced cerebromicrovascular rarefaction, neurovascular uncoupling, and cognitive decline in mice. J Gerontol A Biol Sci Med Sci 69:1339–1352

Ungvari Z, Orosz Z, Labinskyy N, Rivera A, Xiangmin Z, Smith K, Csiszar A (2007a) Increased mitochondrial H2O2 production promotes endothelial NF-kappaB activation in aged rat arteries. Am J Physiol Heart Circ Physiol 293:H37–H47

Ungvari Z, Orosz Z, Rivera A, Labinskyy N, Xiangmin Z, Olson S, Podlutsky A, Csiszar A (2007b) Resveratrol increases vascular oxidative stress resistance. Am J Physiol 292: H2417–H2424

Ungvari Z, Labinskyy N, Mukhopadhyay P, Pinto JT, Bagi Z, Ballabh P, Zhang C, Pacher P, Csiszar A (2009) Resveratrol attenuates mitochondrial oxidative stress in coronary arterial endothelial cells. Am J Physiol Heart Circ Physiol 297: H1876–H1881

Ungvari Z, Sonntag WE, de Cabo R, Baur JA, Csiszar A (2011) Mitochondrial protection by resveratrol. Exerc Sport Sci Rev. 2011 Jul;39(3):128–32. https://doi.org/10.1097/JES.0b013e3182141f80.

Ungvari Z, Tucsek Z, Sosnowska D, Toth P, Gautam T, Podlutsky A, Csiszar A, Losonczy G, Valcarcel-Ares MN, Sonntag WE (2013) Aging-induced dysregulation of Dicer1-dependent MicroRNA expression impairs angiogenic capacity of rat cerebromicrovascular endothelial cells. J Gerontol A Biol Sci Med Sci 68:877–891

Ungvari Z, Tarantini S, Kirkpatrick AC, Csiszar A, Prodan CI (2017) Cerebral microhemorrhages: mechanisms, consequences, and prevention. Am J Physiol Heart Circ Physiol 312:H1128–H1143

Ungvari Z, Tarantini S, Kiss T, Wren JD, Giles CB, Griffin CT, Murfee WL, Pacher P, Csiszar A (2018a) Endothelial dysfunction and angiogenesis impairment in the ageing vasculature. Nat Rev Cardiol 15:555–565

Ungvari Z, Tarantini S, Donato AJ, Galvan V, Csiszar A (2018b) Mechanisms of vascular aging. Circ Res 123:849–867

Valcarcel-Ares MN, Tucsek Z, Kiss T, Giles CB, Tarantini S, Yabluchanskiy A, Balasubramanian P, Gautam T, Galvan V, Ballabh P, Richardson A, Freeman WM, Wren JD, Deak F, Ungvari Z, Csiszar A (2018) Obesity in aging exacerbates neuroinflammation, dysregulating synaptic function-related genes and altering eicosanoid synthesis in the mouse hippocampus: potential role in impaired synaptic plasticity and cognitive decline. J Gerontol A Biol Sci Med Sci. 2019 Feb 15;74(3):290–298. https://doi.org/10.1093/gerona/gly127.

Warrington JP, Ashpole N, Csiszar A, Lee YW, Ungvari Z, Sonntag WE (2013) Whole brain radiation-induced vascular cognitive impairment: mechanisms and implications. J Vasc Res 50:445–457

Wei CC, Kong YY, Hua X, Li GQ, Zheng SL, Cheng MH, Wang P, Miao CY (2017) NAD replenishment with nicotinamide mononucleotide protects blood-brain barrier integrity and attenuates delayed tissue plasminogen activator-induced haemorrhagic transformation after cerebral ischaemia. Br J Pharmacol 174:3823–3836

Wiedenhoeft T, Tarantini S, Nyúl-Tóth A, Yabluchanskiy A, Csipo T, Balasubramanian P, Lipecz A, Kiss T, Csiszar A, Csiszar A, Ungvari Z (2019) Fusogenic liposomes effectively deliver resveratrol to the cerebral microcirculation and improve endothelium-dependent neurovascular coupling responses in aged mice. *Geroscience*. 2019 Dec;41(6):711–725. https://doi.org/10.1007/s11357-019-00102-1

Wood JG, Rogina B, Lavu S, Howitz K, Helfand SL, Tatar M, Sinclair D (2004) Sirtuin activators mimic caloric restriction and delay ageing in metazoans. Nature. 430:686–689

Wren JD, Garner HR (2004) Shared relationship analysis: ranking set cohesion and commonalities within a literature-derived relationship network. Bioinformatics. 20:191–198

Yang H, Yang T, Baur JA, Perez E, Matsui T, Carmona JJ, Lamming DW, Souza-Pinto NC, Bohr VA, Rosenzweig A, de Cabo R, Sauve AA, Sinclair DA (2007) Nutrient-sensitive mitochondrial NAD+ levels dictate cell survival. Cell. 130:1095–1107

Yoshino J, Baur JA, Imai SI (2018) NAD(+) intermediates: the biology and therapeutic potential of NMN and NR. Cell Metab 27:513–528

Zarzuelo MJ, Lopez-Sepulveda R, Sanchez M, Romero M, Gomez-Guzman M, Ungvary Z, Perez-Vizcaino F, Jimenez R, Duarte J (2013) SIRT1 inhibits NADPH oxidase activation and protects endothelial function in the rat aorta: implications for vascular aging. Biochem Pharmacol 85:1288–1296

Zhang H, Zhang J, Ungvari Z, Zhang C (2009) Resveratrol improves endothelial function: role of TNF{alpha} and vascular oxidative stress. Arterioscler Thromb Vasc Biol 29:1164–1171

Zhang Y, Chen K, Sloan SA, Bennett ML, Scholze AR, O'Keeffe S, Phatnani HP, Guarnieri P, Caneda C, Ruderisch N, Deng S, Liddelow SA, Zhang C, Daneman R, Maniatis T, Barres BA, Wu JQ (2014) An RNA-sequencing transcriptome and splicing database of glia, neurons, and vascular cells of the cerebral cortex. J Neurosci 34:11929–11947

Zhang H, Ryu D, Wu Y, Gariani K, Wang X, Luan P, D'Amico D, Ropelle ER, Lutolf MP, Aebersold R, Schoonjans K, Menzies KJ, Auwerx J (2016) NAD(+) repletion improves mitochondrial and stem cell function and enhances life span in mice. Science. 352:1436–1443

Zlokovic BV (2008) The blood-brain barrier in health and chronic neurodegenerative disorders. Neuron. 57:178–201

Zlokovic BV (2010) Neurodegeneration and the neurovascular unit. Nat Med 16:1370–1371

Zlokovic BV (2011) Neurovascular pathways to neurodegeneration in Alzheimer's disease and other disorders. Nat Rev Neurosci 12:723–738